# THE FUNCTIONAL ROLE OF ROOT-ASSOCIATED MICROBIOME AND METABOLOME OF *MYROTHAMNUS FLABELLIFOLIA*

by

**Shandry Mmasetshaba Tebele**

(tblsha001)


Thesis Presented for the Degree of

DOCTOR OF PHILOSOPHY

In the Department of Molecular and Cell Biology

University of Cape Town

**Supervisor: Prof. Jill M. Farrant**

Department of Molecular and Cell Biology

University of Cape Town

South Africa

February 2024

# Plagiarism Declaration

I, Shandry Mmasetshaba Tebele hereby state that the composition of this PhD thesis is based on my original work, unless stated otherwise where acknowledgement is provided. All components of research presented in this study, have never been submitted to any University or higher institutions.

Signature: Signed by candidate Date: 09 February 2024

# Declaration: Inclusion of Publication in a PhD Thesis

I confirm that I have been granted permission by the University of Cape Town's Doctoral Degrees Board to include the following publication(s) in my PhD thesis, and where co-authorships are involved, my co-authors have agreed that I may include the publication:

1. Tebele, S.M., Marks, R.A. and Farrant, J.M. 2023. Exploring the root-associated microbiome of the resurrection plant *Myrothamnus flabellifolia*. Plant and Soil, pp.1-16. Doi: https://doi.org/10.1007/s11104-023-06019-1.

Signature: Signed by candidate Date: 09 February 2024

Student Name: Shandry Mmasetshaba Tebele Student Number: TBLSHA001

# Abstract

Global climate change is predicted to increase the occurrence and severity of drought, particularly in Africa, which will negatively impact crops and food production. Drought is the leading factor that adversely affects agricultural productivity and yield. Over the last four decades, extensive research on resurrection plants has yielded valuable insights into the mechanisms these plants employ to adapt during desiccation. Despite this, the role of the microbiome in desiccation tolerance, particularly in resurrection plants, remains a relatively unexplored area. *Myrothamnus flabellifolia*, a resurrection plant, stands out for its remarkable ability to endure severe desiccation, making it an ideal model for investigating the contributions of the plant microbiome to desiccation tolerance. Recognising the significance of root-associated microbes in stress tolerance opens up promising opportunities for enhancing drought resilience in crucial crops. However, the intricate dynamics of these interactions under severe water limitations have not been comprehensively investigated. Consequently, a primary objective of this study was to unravel the beneficial root-associated microbiome of *M. flabellifolia* and delineate their functions in the context of water deficit conditions.

The intricate tripartite interplay involving plant roots, soil, and microorganisms remains enigmatic and demands further exploration. This study delved into the microbiome of belowground zones—bulk soil, rhizosphere soil, and endosphere of *M. flabellifolia*. Metagenomic analysis unveiled prevalent bacterial phyla (*Acidobacteriota*, *Actinobacteriota*, *Chloroflexota*, *Planctomycetota*, and *Pseudomonadota*) and dominant fungal phyla (*Ascomycota* and *Basidiomycota*) across all zones. While the bulk soil hosted numerous beneficial root-associated microbes, it exhibited lower functional diversity than the rhizosphere, which showcased the highest diversity of bacteria and fungi. Conversely, the endosphere exhibited lower microbial abundance and diversity. These findings suggest that *M. flabellifolia* may recruits soil microbes from bulk soil to rhizosphere and subsequently to the endosphere.

Metatranscriptomic analysis has revealed crucial insights into the dynamics of plant-microbe interactions and the adaptive mechanisms employed by root-associated bacteria during desiccation in *M. flabellifolia*. The transcriptional activity of bacteria involved both monoderm and diderm lineages, consistent with the bacterial phyla identified in metagenomic analysis. However, the dominance of the *Pseudomonadota* phyla at the transcriptional activity was observed. Root-associated bacteria showed distinct transcriptional responses during dehydration and rehydration, suggesting dynamic shifts in microbial activity under fluctuating water availability. The expression of differentially expressed genes (DEGs) under dehydration conditions showcased the activation of

proteins associated with antioxidant enzymes, molecular chaperones, protein kinases, and biosynthesis of sugars and amino acids. This implies a coordinated response to counteract damage and enhance survival. Intriguingly, the upregulation of genes encoding protein kinases, antioxidant enzymes, and trehalose synthase in root-associated bacteria reflects a common strategy for surviving desiccation stress. This suggests a potential case of convergent evolution in desiccation tolerance within microbiomes. The observed upregulation of genes related to plant growth and enhanced plant-microbe interaction under rehydration conditions suggests a resumption of microbial activity.

Exploring the rhizosphere soil metabolome provided insights into the metabolic changes during drought stress in *M. flabellifolia*. Dehydrated rhizosphere soil exhibited increased levels of sugars (e.g., trehalose), organic acids (malic acid), and phytohormones (indole-3-acetic). Conversely, rehydrated rhizosphere samples showed significantly higher amino acid levels compared to desiccated samples, indicating a shift in biochemical processes in both the plant roots and rhizosphere microbiome. While rhizosphere metabolites are typically attributed to root exudates and microbial activity, this study revealed that many were possibly produced by rhizospheric bacteria. The upregulation of bacterial genes associated with metabolite biosynthesis under dehydration conditions, such as trehalose, further substantiated the the notion that drought serves as a selective pressure driving convergent evolution in species with desiccation tolerance. These findings indicates that the microbiome's adaptability under harsh environmental stress. Furthermore, inoculating maize plants with rhizospheric bacteria from *M. flabellifolia*'s rhizosphere significantly improved drought tolerance, physiological, and morphological traits. The study concludes that root-associated microbiomes play a crucial role in *M. flabellifolia*'s desiccation tolerance and plant growth-promoting microbes have a potential to be used as a biostimulant. This innovative research has implications for enhancing food security, developing resilient agricultural systems, and promoting sustainability.

Dedication

To my loving family and friends

# Acknowledgements

Firstly, I express my gratitude to the Almighty God for His mercies and for granting me the strength, wisdom, and courage to complete my doctoral degree.

I extend my deepest thanks to my supervisor, Prof. Jill Farrant, who welcomed me wholeheartedly into her research group and provided me with the opportunity to fulfil my dreams. Prof. Farrant, your unwavering support, encouragement, and innovative ideas have been invaluable to my success. Thank you for being a fantastic conduit and for propelling me forward. I appreciate your kind words and the exposure to international conferences. You are not just a supervisor but a research mother to me.

A special acknowledgment goes to Dr. Rose Marks for her exceptional mentorship and continuous academic support. Your constructive and insightful feedback has been instrumental, and I'm grateful for your guidance and friendship. I also extend my thanks to Prof. Henk Hilhorst for his encouraging and constructive comments, and Prof. Suhail Rafudeen for valuable guidance and writing supporting letters.

I want to express my sincere gratitude to Keren Cooper for her endless support and contribution to my project. Thanks to Pei-Yin for her technical support with GC-MS and extensive knowledge on its operation and data processing. My appreciation goes to the members of the Plant Stress lab for providing a conducive research environment and assisting with troubleshooting methods.

To my family, thank you for your unwavering support and nurturing throughout this journey. A special thanks to my mother, Georginah Tebele for teaching me resilience and perseverance in life, qualities that helped me complete this degree. My profound appreciation goes to my husband, Mr. Simisi Mosamane, for his emotional support and ensuring my well-being during this research journey.

Lastly, I extend my gratitude to SwebeSwebe Nature Reserve personnel for allowing me to conduct fieldwork and collect plant materials. I am also thankful for the financial support from the National Research Foundation, UCT Postgraduate financial aid, and the AOAC-International student award.

# Research Output

**Journal articles**

Tebele, S.M., Marks, R.A. and Farrant, J.M., 2025. Microbial survival strategies in desiccated roots of Myrothamnus flabellifolia. *Frontiers in Microbiology*, 16, p.1560114. Doi: 10.3389/fmicb.2025.1560114

Tebele, S.M., Marks, R.A. and Farrant, J.M. 2023. Exploring the root-associated microbiome of the resurrection plant Myrothamnus flabellifolia. *Plant and Soil*, pp.1-16. Doi: 10.1007/s11104-023-06019-1

Marks, R.A., Amézquita, E.J., Percival, S., Rougon-Cardoso, A., Chibici-Revneanu, C., Tebele, S.M., Farrant, J.M., Chitwood, D.H. and VanBuren, R. 2023. A critical analysis of plant science literature reveals ongoing inequities. *Proceedings of the National Academy of Sciences*, 120(10). Doi: 10.1073/pnas.2217564120

Tebele, S. M., Marks, R. A., and Farrant, J. M. 2021. Two Decades of Desiccation Biology. A Systematic Review of the Best Studied Angiosperm Resurrection Plants. *Plants*, 10(12), 2784. Doi: 10.3390/plants10122784

**Conferences**

Tebele, S. M., Marks, R.A., and Farrant. 2024. Deciphering the transcriptional dynamics of root-associated bacteria in a *Myrothamnus flabellifolia* during drought stress. 8th International workshop on desiccation sensitivity and tolerance across life forms. Limpopo Province, South Africa.

Tebele, S. M., Marks, R.A., and Farrant. 2023. Exploring the role of *Myrothamnus flabellifolia* microbiome in enhancing drought resistance and crop productivity for sustainable agriculture in arid environments. AOAC. New Orleans, USA.

Tebele, S. M., Marks, R.A., and Farrant. 2023. Metabolic profiling of the rhizosphere of the resurrection plant *Myrothamnus flabellifolia* under desiccated and rehydrated conditions. VIB Conference–Translational Research in Crops. Ghent, Belgium.

Tebele, S. M., Marks, R.A., and Farrant, J.M. 2022. Co-evolution of the microbiome and the iconic desiccation tolerant plant *Myrothamnus flabellifolia*: A metagenomic study. The 2nd African Microbiome Symposium. Stellenbosch University, South Africa.

Tebele, S. M., Marks, R. A., and Farrant, J. M. 2022. The microbiome of the resurrection plant *Myrothamnus flabellifolia* and its multiple- applications. The Royal Society-Anhydrobiosis Conference. London, UK (virtual).

# Table of Contents

# List of Figures

## Chapter One



## Chapter Two



## Chapter Three

## Chapter Four



## Chapter Five

## Chapter Six

# List of Tables

# Abbreviation and Acronyms

| | |
|---|---|
| ABC transport | ATP-binding cassette transport |
| ACC | Aminocyclopropane-1-carboxylate |
| AMF | Arbuscular mycorrhizal fungi |
| APX | Ascorbate peroxidase |
| ASVs | Amplicon sequence variances |
| ATP | Adenosine triphosphate |
| CAT | Catalase |
| Chl a | Chlorophyll a |
| Chl b | Chlorophyll b |
| CFU | Colony forming unit |
| FRAP | Ferric reducing antioxidant power |
| ECF | Extracytoplasmatic function |
| EPS | Exopolysaccharides |
| EMF | Ectomycorrhizal fungi |
| F0 | minimum fluorescence |
| Fm | maximum fluorescence |
| Fv/Fm | maximum quantum yield of photosystem II |
| FAD | Flavin adenine dinucleotide |
| FMN | Flavin mononucleotide |
| GC | Gas chromatography |
| GPX | Glutathione peroxidase |
| GSH | Glutathione |
| HPS20/70 | Heat shock protein |
| IAA | Indole-3-acetic acid |
| ISR | Induced systemic resistance |

| | |
|---|---|
| ITS | Internal transcribed spacers |
| KEGG | Kyoto Encyclopedia of Genes and Genomes |
| Log FC | Logarithmic fold changes |
| μM | Micromolar |
| M | Molar |
| mM | Millimolar |
| MDA | Malondialdehyde |
| MS | Mass spectrometry |
| MSTFA | N-methyl-N-(trimethylsilyl)trifluoroacetamide |
| NCBI | National Center for Biotechnology Information |
| NADH | Nicotinamide adenine dinucleotide |
| NADPH | Nicotinamide adenine dinucleotide phosphate |
| NGS | Next generation sequencing |
| NMDS | Non-metric multidimensional scaling |
| DEGs | Differentially expressed genes |
| PLS-DA | Partial least square discriminant analysis |
| PGPM | Plant growth-promoting microbes |
| PGPR | Plant growth-promoting rhizobacteria |
| ROS | Reactive oxygen species |
| RWC | Relative water content |
| SAMSA2 | Simple annotation of metatranscriptomes by sequence analysis |
| SOD | Superoxide dismutase |
| TCA | Tricarboxylic acid cycle |
| VIP | Variable importance in projection |
| VWC | Volumetric water content |

## Thesis Outline

**Chapter One** provides a literature overview of *M. flabellifolia*, detailing its natural distribution, particularly in South African countries. The chapter emphasizes the gaps in microbiome studies within resurrection plant lineages and underscores the significance of plant microbiomes in combating environmental stresses. Additionally, it introduces high-throughput technologies used in resurrection plant studies and outlines unexplored avenues, including the adoption of metatranscriptomics.

**Chapter Two** delves into the fundamental composition of plant microbiome studies using 16S rRNA and ITS sequencing. It uncovers the novel bacterial and fungal communities in the endosphere, rhizosphere, and bulk soil of *M. flabellifolia* under desiccated conditions. This chapter identifies the soil zones with diverse microbiomes and elucidates the potential functions of significant bacterial and fungal genera. Physicochemical analyses of bulk and rhizosphere soil are conducted to assess how soil factors influence the microbiome.

**Chapter Three** explores the robustness of metatranscriptomic technology and its significant contribution to understanding plant-microbe interactions under drought stress. The central focus is on the metatranscriptome of *M. flabellifolia* root-associated bacteria, aiming to unveil actively transcribed genes during both dehydration and rehydration conditions. This chapter sheds light on the defense mechanisms employed by root-associated bacteria, emphasizing their critical role and potential contribution to the overall desiccation tolerance of *M. flabellifolia*.

**Chapter Four** aims to elucidate metabolic changes in the rhizosphere soil of *M. flabellifolia* during dehydration and rehydration conditions. It explores the origin of metabolites in the rhizosphere soil, whether from root exudates or microbial sources. The difficulty of distinguishing root exudates from microbial metabolites in field setups is acknowledged, and the potential role of drought-responsive metabolites in the rhizosphere soil for *M. flabellifolia*'s desiccation tolerance is explored.

**Chapter Five** serves as a proof of concept, demonstrating that the microbiome associated with *M. flabellifolia* contributes to drought tolerance in the host plant. The isolation of rhizospheric bacteria under desiccated conditions and the subsequent microbial metabolome analysis using GC-MS are conducted. The chapter distinguishes microbial metabolites from the rhizosphere soil and explores biopriming of maize seeds with bacterial isolates to identify those most impactful in enhancing drought tolerance.

**Chapter Six** provides a summary and discussion of the key findings derived from amplicon metagenomic, metatranscriptome analysis, rhizosphere metabolome analysis, and the application of rhizospheric bacteria on maize. This chapter illustrates the integration of the various studies conducted in this thesis and underscores their significance. Additionally, it delves into future research considerations and provides recommendations for further exploration.

# Chapter One

## Introduction and Literature Review

## 1.1. Impact of climate change on food security

The world is presently undergoing climate change, primarily characterised by shifts in temperatures and rainfall patterns. Climate change manifests through the recurrent incidence of drought episodes, heatwaves, and flooding events (Vermeulen et al., 2012). The magnitude of these events poses a major challenge to agricultural systems and food security. Plants are important constituents of agriculture and serve as a source of food for humans and animals (FAO, 2017). With the growing population, particularly in Africa, food security remains a challenge (Hall et al., 2017). It is predicted that the food demand in the world will rise by 35% to 56% between 2010 and 2050, however, due to climate change the range is expected to rise by +30% to +62% (van Dijk et al., 2021). Agricultural systems encounter numerous environmental stresses, with drought being a significant threat that impacts nearly 40% of the world's landscape (Wen et al., 2021). The main question is whether agricultural systems can meet the food demands in the progressive climate change. Therefore, it is crucial to implement innovative strategies and systems to improve sustainable agriculture.

## 1.2. Resurrection plants

Water is crucial for survival and plants frequently encounter scarcities of this vital resource as a result of their sessility trait. Numerous plants have developed intricate mechanisms to withstand or endure periods of water scarcity (Farrant et al., 2003; Mundree et al., 2000). One highly effective response to severe drought conditions is desiccation tolerance, which involves the capacity to endure water loss down to 10% relative water content (RWC), corresponding to 0.1 g $H_2O$/g dry weight, and then restore full metabolic activity upon rehydration (Oliver et al., 2020). Such plants are commonly called resurrection plants (Gaff, 1971). Desiccation tolerance is prevalent in seeds and spores, but it is exceptionally uncommon in the plant's vegetative tissues, being present in only around 240 angiosperms (Marks et al., 2021). Interestingly, angiosperm resurrection plants exhibit significant diversity, spanning at least 10 families in both monocotyledon and dicotyledon lineages (Marks et al., 2021).

Resurrection plants predominantly thrive in environment characterised by growing on the rocky soil, elevated temperatures, and shortage of rainfall (Marks et al., 2021; Porembski and Barthlott, 2000).

The response to desiccation varies across species and they may employ different mechanisms. For instance, many species in the monocot lineage dismantle their chlorophyll, whereas dicotyledon species retain the photosynthetic apparatus during desiccation (Marks et al., 2021). Resurrection plant are disseminated worldwide, with occurrences present in the north and south poles. However, the greatest concentration of resurrection plants is observed in xeric and semi-arid lands, particularly in Africa, South America, and Australia (Tebele et al., 2021), yet *B. hygrometrica* and *Paraboea rufescens* are predominate in Asia, and *H. rhodopensis* and *Ramonda* species are exclusive to Europe (Georgieva et al., 2007; Mitra et al., 2013; Rakić et al., 2013). Despite the broad geographical distribution, resurrection plants have the ability to tolerate desiccation and thrive in xeric microclimatic environments where other plants perish.

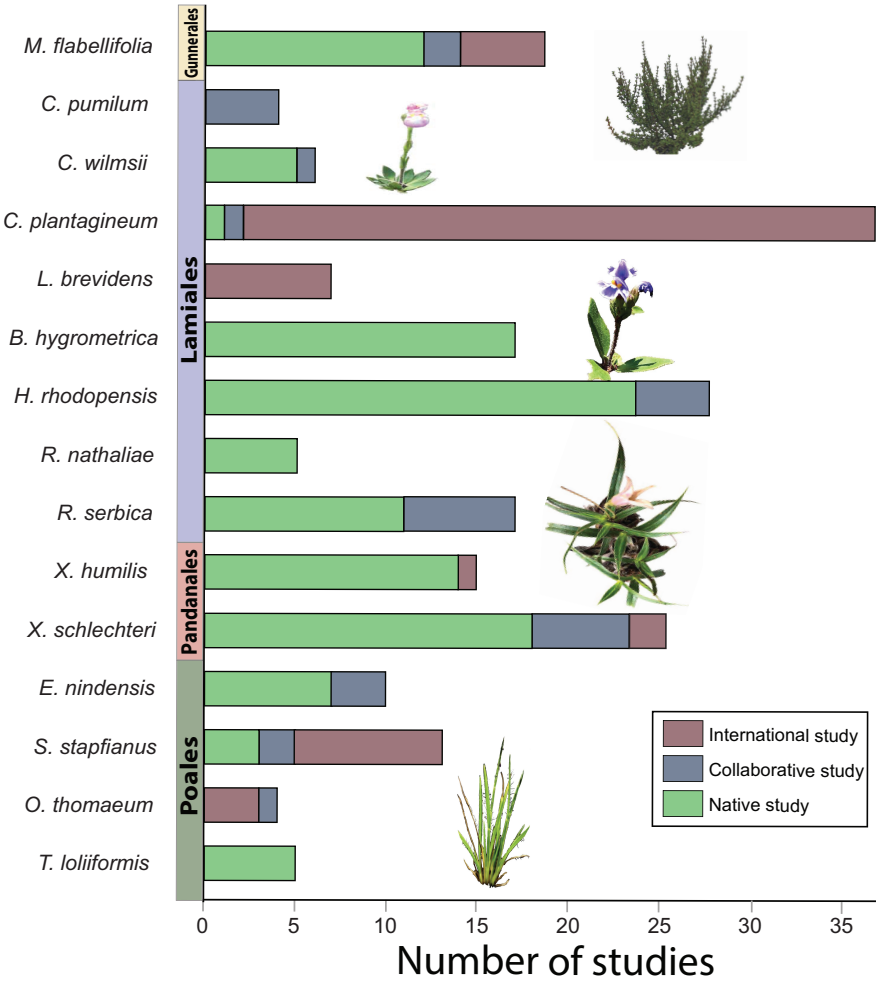


**Figure 1-1.** The sum of published research articles on each angiosperm resurrection plant species across the world. The number of articles are classified as either native, collaborative, or international study and species are ordered phylogenetically. Adapted from (Tebele et al., 2021).

Research on resurrection plants has significantly increased over the past two decades, and a few species have become notable models for studying desiccation tolerance. The most investigated models in the resurrection plant research between 2000 and 2020 are shown in Figure 1-1 (Tebele et al., 2021). Nevertheless, the majority of these investigations have focused exclusively on aboveground plant's tissues, largely neglecting the role of belowground plant's tissues. The limited number of studies on resurrection plants that delve into root functions include a physiological examination of the roots of *X. schlechteri* (Kamies et al., 2010) and *H. rhodopensis* (Péli et al., 2012), a metabolomic and transcriptomic investigation in *T. loliiformis* (Asami et al., 2019), and a study highlighting the significant involvement of plant hormones in desiccated *H. rhodopensis* (Djilianov et al., 2013). Despite their varied approaches, these investigations affirm the fundamental importance of osmolytes and antioxidants in conferring desiccation tolerance to roots. However, they also unveil distinct variations in root lifespan. In the case of *C. plantagineum*, roots do not endure desiccation, instead, new ones are regenerated after rehydration (Norwood et al., 2003). Conversely, in the other two species (*X. schlechteri* and *H. rhodopensis*), roots are preserved, and in *T. lolliformis*, senescence is actively inhibited (Asami et al., 2019).Taken together, there is a paucity of studies investigating the fundamental roles of root microbiome. This study address the knowledge gap using *Myrothamnus flabellifolia* as a model organism to elucidate the underlying functions of belowground microbiome.

## 1.3. Desiccation tolerance mechanisms of *Myrothamnus flabellifolia*

Among angiosperm resurrection plants, the family *Mythamnaceae* is iconic and includes a single genus (*Myrothamnus*). This genus was coined from the Greek words 'myron' and 'thamnos' meaning aromatic and bush, respectively (Erhabor et al., 2020; Kondlo, 2013). In South Africa, the local name of *M. flabellifolia* is typically associated with its resurrection traits: in Northern Sotho, it is called "patje ya tshwene", in Afrikaans it is "opstandingsplant", and Zulu and Ndebele populations named it "uvukakwabafile" and "umazifisi", respectively (Kondlo, 2013; Marks et al., 2022). *Myrothamnus* consists of only two species, which are *M. flabellifolia* and *M. moschatha* (Glen et al., 1999), both of which are diecious, shrubby, and xerophytic (Erhabor et al., 2020). Resurrection plants belonging to the dioecious angiosperm category are uncommon, making *Myrothamnus* even more distinctive within this group. *Myrothamnus moschatha* is indigenous in Madagascar (Rasoanaivo et al., 2012), whereas *M. flabellifolia* is distributed across southern Africa (Figure 1-2). It is a widely known large resurrection plant that grows between 0.5 and 1.5 m in height (Figure 1-3) and is often found on rock inselbergs (Moore et al., 2007). *M. flabellifolia* leaves possesses various medicinal and cosmetic applications (Bentley et al., 2019; Erhabor et al., 2020; Farrant, 2019).

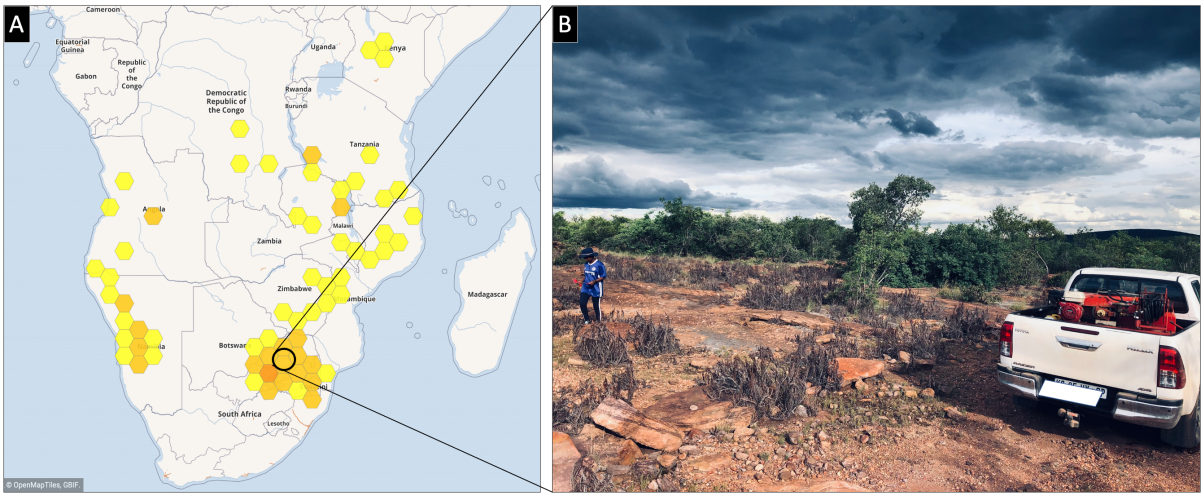


**Figure 1-.** A) Geographical distribution of *Myrothamnus flabellifolia* resurrection plant in Southern African countries. B) Ecological niche of *M. flabellifolia* at the SwebeSwebe field site.

*Myrothamnus flabellifolia* is a valuable model to study desiccation tolerance due to its ability to survive prolonged desiccation for a period of 9 to 12 months without water (Farrant and Kruger, 2001). *M. flabellifolia* retains its photosynthetic apparatus such as chlorophyll and intact thylakoids throughout dehydration and rehydration (Neeragunda Shivaraj et al., 2018; Oliver et al., 2020). It responds to desiccation by folding leaves to reduce the level of light reaching the photosystems (Farrant et al., 2003). This method reduces the production of light-induced reactive oxygen species (ROS) by shielding the photosynthetic apparatus coupled with the organised shutdown of photosynthetic processes (Farrant and Kruger, 2001). The folding of mesophyll cells during drought stress is enabled by the high content of arabinose polymers and promotes the flexibility of the cells (Moore et al., 2006). *M. flabellifolia* is not only rich in arabinose but also polyphenols and antioxidants. The most prominent compound is 3,4,5-tri-O-galloylquinic acid, which has been shown to protect liposomes during desiccation, so presumably also the cell membranes and prevents ROS production (Moore et al., 2005). Metabolomic analysis of *M. flabellifolia* has offered the understanding into the pivotal function of sugars, with a particular emphasis on trehalose and sucrose, as well as selected amino and organic acids, along with phenolic antioxidants (Bentley and Farrant, 2020; Dace et al., 2023; Moore et al., 2006; Passon et al., 2021). However, the role of rhizospheric metabolites of *M. flabellifolia* under desiccation stress remains largely unknown.

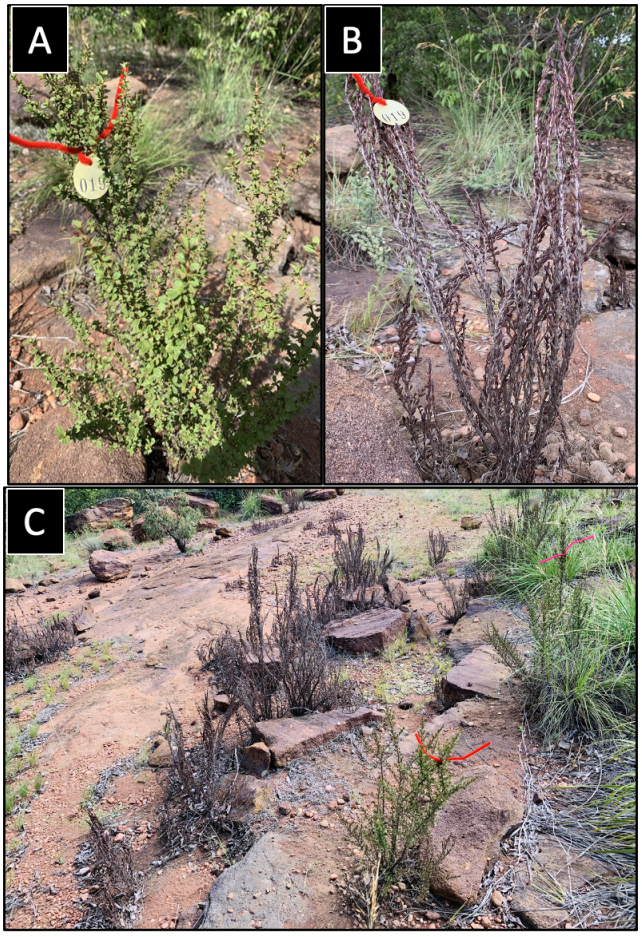


**Figure 1-2.** *Myrothamnus flabellifolia* in its natural habitat at the SwebeSwebe field site. A) *M. flabellifolia* plant at hydrated stage, B) the air-dry stage of dehydration, and C) the overview of the ecological niche of *M. flabellifolia* and co-occurring species .

## 1.4. The unexplored belowground avenues

*Myrothamnus flabellifolia* is a geophyte woody shrub with an extensive root system that spreads within the cracks of rock slopes up to ~15 cm depth, as shown in Figure 1-4 (Glen et al., 1999). As the surface of the soil dries, water may be available in deeper profiles, thus, the root system of *M. flabellifolia* extends across and into rocks to access this water (Glen et al., 1999). In most plants that possess a woody stem, the hydraulic refilling in roots fails during rehydration due to the xylem being susceptible to cavitation (Comas et al., 2013). However, water transportation in *M. flabellifolia* is assisted by the presence of lipids in the narrow xylem, enabling recovery from extreme drought episodes (Moore et al., 2007; Sherwin et al., 1998).

**Figure 1-3.** *Myrothamnus flabellifolia* root system with multiple lateral roots under desiccated conditions.

The ecological niche of *M. flabellifolia* makes this plant an important model to explore the belowground desiccation tolerance strategies. *Myrothamnus flabellifolia* is classified as an initial rock slope coloniser and it may even nurture the growth of other species such as grass and moss (Figure 1-3C) (Moore et al., 2007; Porembski and Barthlott, 2000). For that reason, *M. flabellifolia* has potential applications for improving survival in water-limited habitats for neighbouring species. Consequently, root system is a very important part of drought responses due to its fundamental function of water absorption and transportation. This study hypothesise(s) that *M. flabellifolia* is associated with a desiccation-tolerant microbiome, potentially enhancing the plant's ability to withstand desiccation. However, the specific role of the *M. flabellifolia* microbiome under drought stress has not been investigated.

## 1.5. Plant-microbe interactions

Microorganisms are ubiquitous, found nearly everywhere in the world, from the surfaces of objects to intracellular spaces, and are prominent actors within the bodies of humans, animals, and plants. Plants naturally form associations with diverse bacterial and fungal communities (Compant et al., 2019). The belowground zones of plant root systems within the soil microenvironment are conventionally classified into four zones based on their proximity to the plant roots: bulk soil,

rhizosphere, rhizoplane, and endosphere, as illustrated in Figure 1-5. Bulk soil refers to the soil infiltrated but unaffected by plant root systems (Bashir et al., 2016). The rhizosphere constitutes a dynamic zone surrounding the plant root, typically hosting various microbes and influenced by root exudates (Kennedy and De Luna, 2004). A thin layer of the soil adhering to the root is referred as the rhizosphere, whereas microbes that are found on the root surface are called rhizoplane microbiomes (Bashir et al., 2016). Root exudates play a pivotal role in shaping the soil microbiome, influencing microbial composition and diversity. These exudates are conveyed into the rhizosphere soil through symplastic and apoplastic pathways, with casparian strips precluding the apoplastic pathway at the root's differentiation zone (Canarini et al., 2019). As a result, a significant content of root exudates is released at the transition and meristem zones of roots, utilising both pathways. Metabolites present in the rhizosphere soil are commonly termed rhizodeposits and can influence microbial behavior by functioning as chemoattractants, thereby facilitating plant–microbe interactions (Bornø et al., 2022). As yet, the fundamental role of rhizosphere metabolites in resurrection plants has never been explored. This represents a promising avenue to shed light on the desiccation tolerance mechanisms involved in *M. flabellifolia*.

The rhizosphere soil is a hotspot for diverse bacterial and fungal communities. This root–soil interface harbors a rich array of microorganisms (Figure 1-5). Microbial colonization is influenced by factors such as the secretion of exopolysaccharides, which support chemotaxis and biofilm formation on root surfaces (Mwajita et al., 2013). Many microbes adhere to the root surface using flagella and gain entry through natural openings such as stomata, lenticels, hydathodes, or physical wounds (Lata et al., 2018). Once inside, certain microbes colonize plant tissues intercellularly or intracellularly and are classified as endophytes (Schulz and Boyle, 2006). These endophytes can inhabit not only the roots but also the stems and leaves. Together, rhizosphere and root-associated microbial communities significantly influence plant health and development. Previous studies have shown that these microbes enhance host resilience to environmental stresses, particularly by promoting drought tolerance (Aslam et al., 2022; Mathur and Roy, 2021; Poudel et al., 2021). However, key questions remain: What specific bacterial and fungal taxa are associated with *M. flabellifolia*, and what roles do they play in its desiccation tolerance?

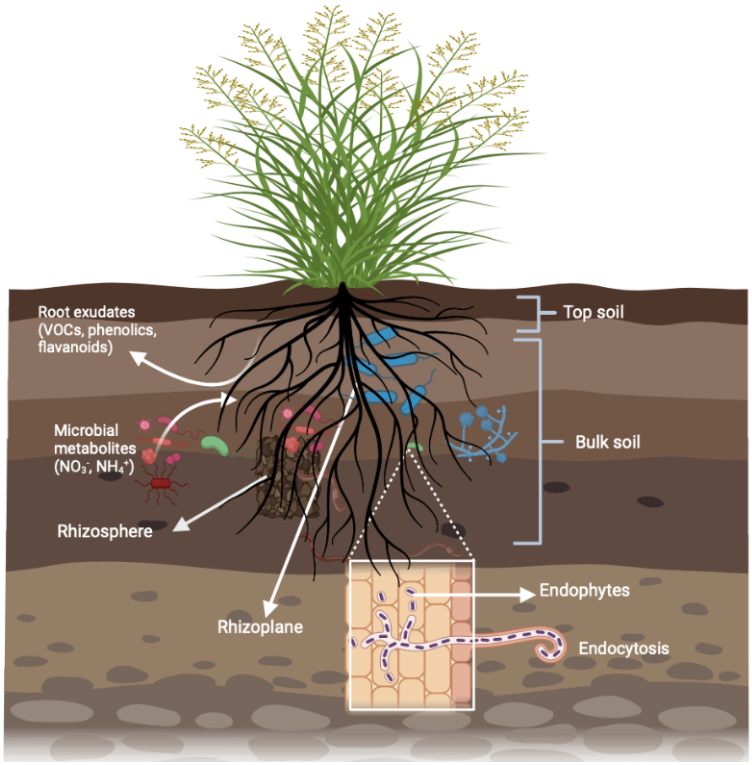


**Figure 1-4.** The soil microbiome zones are typically categorised into three zones based on their respective proximity to the plant roots.

Microbial diversity and composition are influenced by various factors such as plant species, environmental conditions and ecological niche. A paucity of microbiome investigations in resurrection plants has been highlighted in a comprehensive review of the most extensively studied angiosperm resurrection plants (Tebele et al., 2021). Although bacterial communities in the soil of *Ramonda* species were examined, those analysis did not specifically address mechanisms related to drought tolerance (Rakić et al., 2013). Interest in plant microbiome research is increasing, particularly due to findings that associate microbial communities with improved stress resilience in crops. For instance, a recent study demonstrated that plant growth-promoting bacteria (PGPB) isolated from the resurrection plants of the *Ramonda* species improved drought tolerance in wheat (Lozo et al., 2023). Consequently, there is a value of further investigating the microbiomes of resurrection plants, which may contribute to improving drought resilience in host plants and have potential applications in sustainable agriculture.

## 1.6. How microbiomes confer drought tolerance

Periodic soil drying results in a temporary nutrient shortages, which ultimately impede plant growth. Managing plant root systems often involves substantial costs for soil supplementation with fertilizers

(Schroth and Sinclair, 2003). Consequently, chemical fertilizers, are widely employed to enhance plant yield, but they come with significant expenses. The extensive use of chemical fertilizers in agriculture is not considered sustainable due to its adverse environmental effects (Souza et al., 2015). Understanding the plant-microbiota interactions, particularly how microbial communities shift under environmental stress, is increasingly important. As mentioned earlier, plants encounter numerous environmental stresses, and current literature indicates that root-associated microbiota can influence plant response to such stressors through physiological and molecular mechansisms.

The ability of microorganisms to withstand significant changes in environmental conditions is determined by specific response traits that provide protection against desiccation. Examples of such traits include the presence of a thick peptidoglycan cell wall in monoderm (gram-positive) lineages, osmolyte production, sporulation, and dormancy (Xu and Coleman-Derr, 2019). Similar characteristics have independently evolved in various organisms, particularly in fungi and the gram-negative bacteria (diderm lineage). These organisms are classified as stress-tolerant microbes and hold a potential to confer an increased drought tolerance in the host plant. Although microbial composition is influenced by plant species, shift in community structure are often associated with environmental stress factors. For instance, drought-tolerant microbes such as arbuscular mycorrhizal fungi (AMF), *Actinomycetota*, and *Bacillota*, tend to increase in abundance under water deficit conditions (de Vries et al., 2020; Liu et al., 2021; Xu and Coleman-Derr, 2019), whereas the abundance of *Pseudomonadota* (*Proteobacteria*) and *Bacteriodota* phyla is known to decrease under drought stress. AMF improves nutrient uptake, growth, physiological attributes and RWC of plants under drought stress (Gholamhoseini et al., 2013; Xiao et al., 2023). Although the microbial defence mechanisms vary among species, certain microbial communities traits may contribute to mitigating the effects of drought stress on plants.

It is important to comprehend the molecular mechanisms involved in the intricate plant-microbe interactions, particular under drought stress. At the transcriptional level, PGPM can induced drought tolerance in the sorghum, soybean, *Arabidopsis* and tobacco plants through the expression of genes associated with indole alkaloid, exopolysaccharides (EPS), glycine betaine, ATP synthase, NADH dehydrogenase, glutamine biosynthesis and secondary metabolites (Nishu et al., 2022; Xu et al., 2022, 2018). Another example of microbial facilitation of drought tolerance is related to indirectly enhance osmolyte biosynthesis such as carbohydrates and amino acids within the host plant (Pande et al., 2023). Plant growth-promoting microbes synthesize 1-aminocyclopropane-1-carboxylate (ACC) deaminase that regulates ethylene levels in water deficit conditions, which ultimately promotes drought stress tolerance of the plant (Kielak et al., 2016). Under drought conditions, beneficial microbes exhibit physiological and molecular mechanisms that may support survival. Conversely,

microbial defense systems may indirectly or directly contribute to the overall drought tolerance of the host plants under water deficit conditions.

The application of PGPM in mitigating plant abiotic stress has been investigated in various plants such as *Arabidopsis* (Zolla et al., 2013), wild barley (Timmusk et al., 2009), soybean (Asaf et al., 2017), tomato (Khan et al., 2014), white clover (Zhang et al., 2020), and wheat (Yandigeri et al., 2012) among others. Microbes facilitate the uptake of water, nutrients, and trace elements such as iron by exuding siderophores (Pecoraro et al., 2022). In addition, PGPM secrete plant regulators such as auxins, cytokines, gibberellins, and other volatile organic compounds that directly enhance plant growth (Khan et al., 2014). The production of phytohormones enhances plant resilience during drought conditions and promotes plant-microbe communication. These microbial traits play a key role in modulating plant response to drought stress and the involvement of bacteria and fungi in improving drought-sensitive plants is well document.

There is a limited research focusing on the microbial communities associated with resurrection plants, although the significance of plant microbiota in influencing plant host performance gains increasing recognition. Many of these symbiotic microbes perform multiple functions including nitrogen-fixation, phosphate solubilisation, promoting plant growth, inhibit pathogens and improving soil quality (Abdelaal et al., 2021; Khan et al., 2014; Ojuederie et al., 2019; Souza et al., 2015; Wang et al., 2016). It is probable that microbes may play a significant role in resurrection plants. Consequently, numerous questions remain about the role of the soil microbiome in resurrection plants, and this study was designed to address these research gaps. With the use of high-throughput technologies, this study provides a comprehensive overview of nature and potential functions of the root microbiome of *M. flabellifolia*, and their potential contribution towards desiccation tolerance in this species.

## 1.7. Omics technologies

In the last twenty years, "omics" techniques have been a growing application in the study of resurrection plants, providing valuable insights into the biochemical processes and molecular mechanisms underlying desiccation tolerance (Gechev et al., 2021). Advanced sequencing technologies have played a pivotal role in exploring the tripartite interaction. A summary of the major research conducted on model resurrection plants between 2000 to 2020 shows that multiple physiological/biochemical (29,1%), transcriptomic (22.7%), proteomic (18.6%), metabolomic (16.1%), genomic (13.2%), and metagenomic (0.3%) methods have been employed to characterise the physiology, transcripts, proteins, metabolites and novel genes that play a role in desiccation tolerance (Tebele et al., 2021)(Figure 1-6). The vast majority of these studies investigated the leaves (97.3%) and

belowground studies lag behind. Therefore, this study highlights the need of using high-throughput technologies to delve in microbiome of resurrection plants and elucidate how they contribute to the desiccation tolerance mechanisms.

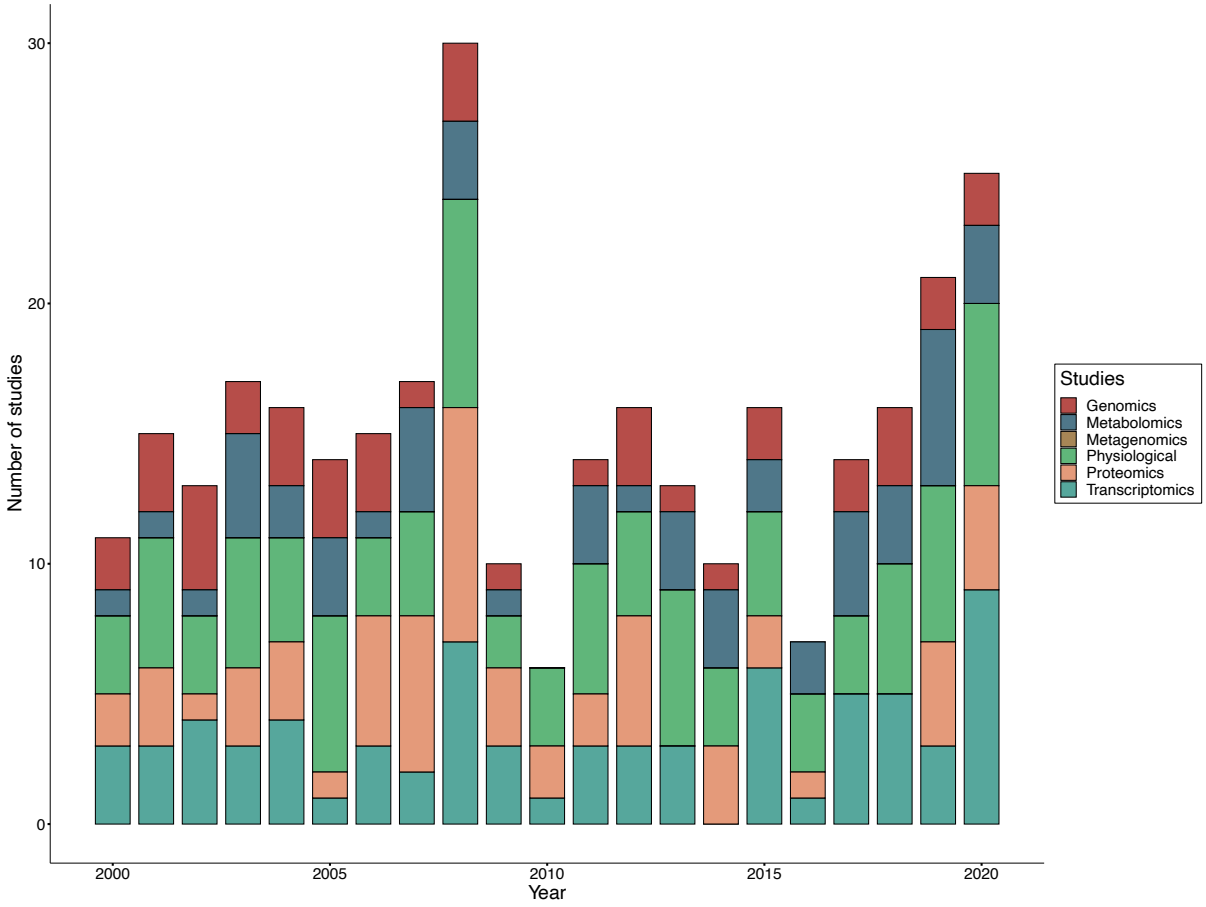


**Figure 1-5.** Application of omics technologies in resurrection plants studies. The total number of studies investigating desiccation tolerance mechanisms of resurrection plants between the year 2000 and 2020 using genomic, metabolomic, metagenomic, proteomic, and physiological techniques. Adapted from (Tebele et al., 2021).

### 1.7.1. Application of metagenomics on plant-associated microbiota

The interaction between microbes and other living organisms is intricate, involving competition over nutrients, secretion of metabolites, pathogen attacks, and maintaining a healthy environment within the host (Abdelaal et al., 2021). Metagenomic techniques analyse the whole microbial community within samples including uncultured microbes. Several high-throughput techniques have been developed to understand plant and soil microbiomes, including the amplicon and shot-gun metagenomic sequencing. Although amplicon metagenome sequencing often lacks the accuracy of

identification at the species level, it characterises the microbial community and can provide estimates of taxon abundance and diversity.

Currently, only two metagenomic studies have explored the resurrection plant microbiomes, and these studies were based on *Ramonda* species only. For instance, Djokic et al. (2010) described the rhizospheric bacterial communities of *Ramonda* species, but microbial function under drought stress was not investigated. On the other hand, Rakić et al. (2013) also explored the function of mycorrhizal fungi found in association with the roots of *Ramonda nathaliae* in aiding mineral stress linked to serpentine soils. However, this aspect was not directly connected to the desiccation tolerance of the plant. Only recently, researchers have delved into the rhizosphere microbiome of *Ramonda* species to investigate their drought tolerance, and plant growth-promoting microbes were subsequently tested on wheat cultivars (Lozo et al., 2023). Therefore, more investigations are sorely required to determine the role of microorganisms in desiccation tolerance, understand their functions within resurrection plants, and test how environmental factors influence microbial composition.

### 1.7.2. Metatranscriptomic analysis of root microbiome

Metatranscriptomics is an emerging and promising technology in the research of plant microbiomes. This approach provides a snapshot of the expressed genes (mRNA) and active processes of microbial communities during drought stress (Hayden et al., 2018). Metatranscriptomics is not subjected to PCR primer biases, as result, it provides various taxonomic levels (Choma et al., 2016). This high-throughput technique enables the investigation of vast microbial communities without culturing. This is achieved by directly sequencing actively transcribed genes via RNA-seq. However, there are several obstacles encountered in metatranscriptomics studies and workflow pipelines to analyse genes of microbial communities. For instance, the isolation of high-quality RNA is a prerequisite for molecular biology techniques and mRNA is notoriously unstable. Bacterial RNA lacks a 3' polyA tail similar to archaeal species, thus, polyA tagging is not applicable for removing rRNA (Pastor et al., 2022). Alternatively, rRNA is depleted though enzymatic digestion, which is mostly applied in metatranscriptomic analysis.

Metatranscriptomics has been used to identify and characterise the functional profiles of microbial communities in environmental samples (Marcelino et al., 2019), and this technology has been employed in studies of agricultural crop models. For instance, metatranscriptomics analysis of ectomycorrhizal fungi (EMF) *Piloderma* genus in *Pinus taeda* roots revealed the upregulation of gibberellin precursor genes, which suggests that EMF promote plant growth during the development stage (Liao et al., 2014). Based on the systematic literature review, there were no metatranscriptomic

studies conducted on resurrection plants over the past two decades (Tebele et al., 2021). Utilising metatranscriptomics on resurrection plants could offer valuable understanding into the functional roles of bacteria and fungi during desiccation stress.

### 1.7.3. Metabolomics approach

Metabolomic techniques provide a comprehensive analysis of metabolites present in organisms or within the environment. The quantification of metabolites can follow either targeted or untargeted methods using a combination of chromatography techniques (gas or liquid chromatography) and detection techniques such as mass spectrometry (MS) and nuclear magnetic resonance (NMR) (Aguiar-Pulido et al., 2016; Moco et al., 2007). Metabolites provide essential knowledge about the attributes of the microbiome as well as the interaction of the microbial community with the host plant. This technique provides information on numerous biological pathways in plant and microbes, and can be used to identify enriched metabolites during drought stress. The usage of metabolomics in resurrection plant research has been sufficiently expanding, particularly in the past two decades, but few studies have investigated the metabolome of rhizosphere soil and microbiomes.

Metabolomes of *M. flabellifolia* leaves have been comprehensively investigated over the past years, to understand the functions of primary and secondary metabolites during desiccation conditions. A South African population and Namibian population of *M. flabellifolia* have disparate secondary metabolite composition, with higher content of the membrane protectant and antioxidant (3,4,5-tri-O-galloylquinic acid) found in Namibian plants (Bentley et al., 2019; Moore et al., 2005). As indicated before, multiple environmental factors may influence the metabolome of the plant, but Bentley et al. (2019) indicated that increased drought stress in Namibian populations could modulate plant metabolomics. Despite the thorough characterisation of the *M. flabellifolia* leaf metabolome, little is known about the rhizospheric or root metabolites. Consequently, this study sought to characterise the rhizosphere metabolome of *M. flabellifolia* and root-associated microbes. With the use of high-throughput technologies, this study may elucidate key markers within the rhizosphere soil and microbial metabolites that contribute to the desiccation tolerance of plants.

## 1.8. Aims and Objectives

This study aims to elucidate the functional roles and mechanistic interplay between the root microbiome, metabolome, and root system of the resurrection plant *M. flabellifolia* under extreme water loss and recovery conditions

The objectives of this study were to:

- Identify the bacterial and fungal communities in the bulk soil, rhizosphere, and endosphere of the *M. flabellifolia* under extreme drought stress using amplicon metagenome sequencing.
- To investigate the transcriptional responses of root-associated microbial communities to desiccation stress using metatranscriptomic analysis.
- Quantify the rhizosphere soil metabolites of *M. flabellifolia* under drought stress and rehydration using gas chromatography-mass spectrometry (GC-MS).
- Isolate the plant-growth-promoting microbes from the rhizosphere soil of *M. flabellifolia* during desiccation and analyse the effects of these species on maize plants germination and drought tolerance.

## 1.9. References


Abdelaal, K., AlKahtani, M., Attia, K., Hafez, Y., Király, L., and Künstler, A. 2021. The Role of Plant Growth-Promoting Bacteria in Alleviating the Adverse Effects of Drought on Plants. *Biology,* 10, p. 520.

Aguiar-Pulido, V., Huang, W., Suarez-Ulloa, V., Cickovski, T., Mathee, K., and Narasimhan, G. 2016. Metagenomics, metatranscriptomics, and metabolomics approaches for microbiome analysis: supplementary issue: bioinformatics methods and applications for big metagenomics data. *Evolutionary Bioinformatics*, 12, EBO-S36436.

Asaf, S., Khan, A.L., Khan, M.A., Imran, Q.M., Yun, B.W., and Lee, I.J. 2017. Osmoprotective functions conferred to soybean plants via inoculation with Sphingomonas sp. LK11 and exogenous trehalose. *Microbiological research*, 205, pp.135-145.

Asami, P., Rupasinghe, T., Moghaddam, L., Njaci, I., Roessner, U., Mundree, S., and Williams, B. 2019. Roots of the Resurrection Plant Tripogon loliiformis Survive Desiccation Without the Activation of Autophagy Pathways by Maintaining Energy Reserves. *Frontiers in Plant Science*, 10, p. 459.

Aslam, M.M., IDRIS, A.L., Zhang, Q.I.A.N., Weifeng, X.U., KARANJA, J.K. and Wei, Y.U.A.N. 2022. Rhizosphere microbiomes can regulate plant drought tolerance. *Pedosphere*, 32(1), pp.61-74.

Bashir, O., Kamran, K., Hekeem, K. R., Mir, N. A., Rather, G. H., and Mohiuddin, R. 2016. Soil microbe diversity and root exudates as important aspects of the rhizosphere ecosystem. In Hakeem, K. R. and Akhtar, M. S. (eds) *Plant, Soil, and Microbes*. Switzerland: Springer Nature, pp.337-357.

Bentley, J., Moore, J. P., and Farrant, J. M. 2019. Metabolomic profiling of the desiccation-tolerant medicinal shrub Myrothamnus flabellifolia indicates phenolic variability across its natural habitat: Implications for tea and cosmetics production. *Molecules*, 24(7), p. 1240.

Bentley, J., and Farrant, J. 2020. Field and acclimated metabolomes of a resurrection plant suggest strong environmental regulation in the extreme end of the species' range. *South African Journal of Botany*, 135, pp. 127–136.

Bornø, M.L., Mueller-Stoever, D.S. and Liu, F. 2022. Biochar modifies the content of primary metabolites in the rhizosphere of well-watered and drought-stressed Zea mays L.(maize). *Biology and Fertility of Soils*, 58(6), pp.633-647.

Canarini, A., Kaiser, C., Merchant, A., Richter, A. and Wanek, W. 2019. Root exudation of primary metabolites: mechanisms and their roles in plant responses to environmental stimuli. *Frontiers in Plant Science*, 10, p.157.

Choma, M., Bárta, J., Šantrůčková, H., and Urich, T. 2016. Low abundance of Archaeorhizomycetes among fungi in soil metatranscriptomes. *Scientific reports*, 6(1), p. 38455.

Comas, L. H., Becker, S. R., Cruz, V. M. V., Byrne, P. F., and Dierig, D. A. 2013. Root traits contributing to plant productivity under drought. *Frontiers in plant science*, 4, p. 442.

Compant, S., Samad, A., Faist, H., and Sessitsch, A. 2019. A review on the plant microbiome: Ecology, functions, and emerging trends in a microbial application. *Journal of Advanced Research*, 19, pp.29-37.

Dace, H.J., Reus, R., Ricco, C.R., Hall, R., Farrant, J.M. and Hilhorst, H.W. 2023. A horizontal view of primary metabolomes in vegetative desiccation tolerance. *Physiologia Plantarum*, 175(6), p.e14109.

de Vries, F.T., Griffiths, R.I., Knight, C.G., Nicolitch, O. and Williams, A. 2020. Harnessing rhizosphere microbiomes for drought-resilient crop production. *Science*, 368(6488), pp.270-274.

Djilianov, D.L., Dobrev, P.I., Moyankova, D.P., Vankova, R., Georgieva, D.T., Gajdošová, S., and Motyka, V. 2013. Dynamics of Endogenous Phytohormones during Desiccation and Recovery of the Resurrection Plant Species Haberlea rhodopensis. *Journal of Plant Growth Regulation*, 32, pp. 564–574.

Đokić, L., Savić, M., Naranc̆ić, T., and Vasiljević, B. 2010. Metagenomic analysis of soil microbial communities. *Archives of Biological Sciences*, 62, pp. 559–564.

Erhabor, J., Komakech, R., Kang, Y., Tang, M., and Matsabisa, M. 2020. Ethnopharmacological importance and medical applications of Myrothamnus flabellifolius Welw. (Myrothamnaceae)-A review. *Journal of Ethnopharmacology*, 252(112576), pp.1-10.

FAO. 2017. The Future of Food and Agriculture: Trends and Challenges. Food and Agriculture Organization of the United Nations, Rome, Italy. Available at: http://www.fao.org/3/a-i6583e.pdf. [Accessed on 15 April 2020].

Farrant, J. M., and Kruger, L. A. 2001. The longevity of dry Myrothamnus flabellifolius in simulated field conditions. *Plant Growth Regulation*, 35(2), pp.109-120.

Farrant, J.M., Vander Willigen, C., Loffell, D.A., Bartsch, S., and Whittaker, A. 2003. An investigation into the role of light during desiccation of three angiosperm resurrection plants. *Plant Cell Environment*, 26, pp. 1275–1286.

Farrant, J.M., Cooper, K., Hilgart, A., Abdalla, K.O., Bentley, J., Thomson, J.A., Dace, H.J.W., Peton, N., Mundree, S.G., and Rafudeen, M.S. 2015. A molecular physiological review of vegetative desiccation tolerance in the resurrection plant Xerophyta viscosa (Baker). *Planta*, 242, pp. 407–426.

Farrant, J.M. 2019. Plants that Rise from the Dead Breathe Life into Research. Available online: https://lagenceodyc.com/wpcontent/uploads/2019/02/Brand_content_Nature_Armani_20190207-compressed.pdf (accessed on 5 December 2021).

Gaff, D.F. 1971. Desiccation-tolerant flowering plants in southern Africa. *Science*. 174, pp. 1033–1034.

Gechev, T., Lyall, R., Petrov, V., and Bartels, D. 2021. Systems biology of resurrection plants. *Cellular and Molecular Life Sciences*, 78(19-20), pp. 6365-6394.

Georgieva, K., Szigeti, Z., Sarvari, E., Gaspar, L., Maslenkova, L., Peeva, V., Peli, E., and Tuba, Z. 2007. Photosynthetic activity of homoiochlorophyllous desiccation tolerant plant Haberlea rhodopensis during dehydration and rehydration. *Planta* 2007, 225, pp. 955–964.

Gholamhoseini, M., Ghalavand, A., Dolatabadian, A., Jamshidi, E. and Khodaei-Joghan, A. 2013. Effects of arbuscular mycorrhizal inoculation on growth, yield, nutrient uptake and irrigation water productivity of sunflowers grown under drought stress. *Agricultural Water Management*, 117, pp.106-114.

Glen, H. F., Sherwin, H. W., and Condy, G. 1999. Myrothamnus flabellifolia. In: *Flowering plants of Africa*. Pretoria: NBI Publications, 56, pp.62–68.

Hall, C., Dawson, T., Macdiarmid, J., Matthews, R., and Smith, P. 2017. The impact of population growth and climate change on food security in Africa: looking ahead to 2050. *International Journal of Agricultural Sustainability*, 15(2), pp.124-135.

Hayden, H. L., Savin, K. W., Wadeson, J., Gupta, V. V., and Mele, P. M. 2018. Comparative metatranscriptomics of wheat rhizosphere microbiomes in disease suppressive and non-suppressive soils for Rhizoctonia solani AG8. *Frontiers in microbiology*, 9, p. 859.

Hilhorst, H.W., Costa, M.-C.D., and Farrant, J.M. 2018. A footprint of plant desiccation tolerance. Does it exist? *Molecular Plant*, 11, pp. 1003–1005.

Kennedy, A.C., and Luna, L. Z. 2005. Rhizosphere. In Encyclopedia of Soils in the Environment. Hillel, D. and Hatfield, J.L. eds., 2005. (Vol. 3). Amsterdam: Elsevier.

Khan, A.L., Waqas, M., Kang, S.M., Al-Harrasi, A., Hussain, J., Al-Rawahi, A., Al-Khiziri, S., Ullah, I., Ali, L., Jung, H.Y., and Lee, I.J. 2014. Bacterial endophyte Sphingomonas sp. LK11 produces gibberellins and IAA and promotes tomato plant growth. *Journal of Microbiology*, 52, pp.689-695.

Khan, N., Bano, A., Rahman, M.A., Guo, J., Kang, Z., and Babar, M.A. 2019. Comparative Physiological and Metabolic Analysis Reveals a Complex Mechanism Involved in Drought Tolerance in Chickpea (Cicer arietinum L.) Induced by PGPR and PGRs. *Scientific Reports*, 9, p. 2097.

Kamies, R., Rafudeen, M., and Farrant, J. 2010. The use of aeroponics to investigate antioxidant activity in the roots of Xerophyta viscosa. *Plant Growth Regulation*, 62, 203–211.

Kielak, A.M., Cipriano, M.A., and Kuramae, E.E. 2016. Acidobacteria strains from subdivision 1 act as plant growth-promoting bacteria. *Archives of microbiology*, 198, pp.987-993.

Kondlo, M. 2013. Myrothamnus flabellifolius welw. Available at: http://pza.sanbi.org/myrothamnus-flabellifolius Accessed [December 2022].

Lata, R., Chowdhury, S., Gond, S., and White, J. 2018. Induction of abiotic stress tolerance in plants by endophytic microbes. *Letters in Applied Microbiology*, 66(4), pp.268-276.

Liao, H.L., Chen, Y., Bruns, T.D., Peay, K.G., Taylor, J.W., Branco, S., Talbot, J.M., and Vilgalys, R. 2014. Metatranscriptomic analysis of ectomycorrhizal roots reveals genes associated with Piloderma Pinus symbiosis: improved methodologies for assessing gene expression in situ. *Environmental microbiology*, 16(12), pp.3730-3742.

Liu, J., Moyankova, D., Djilianov, D., and Deng, X. 2019. Common and Specific Mechanisms of Desiccation Tolerance in Two Gesneriaceae Resurrection Plants. Multiomics Evidences. *Frontiers in Plant Science*, 10, p. 1067.

Liu, Q., Zhao, X., Liu, Y., Xie, S., Xing, Y., Dao, J., Wei, B., Peng, Y., Duan, W. and Wang, Z. 2021. Response of sugarcane rhizosphere bacterial community to drought stress. *Frontiers in microbiology*, 12, p.716196.

Lozo, J., Ristović, N., Kungulovski, G., Jovanović, Ž., Rakić, T., Stanković, S. and Radović, S. 2023. Rhizosphere microbiomes of resurrection plants Ramonda serbica and R. nathaliae: comparative analysis and search for bacteria mitigating drought stress in wheat (Triticum aestivum L.). *World Journal of Microbiology and Biotechnology*, 39(10), p.256.

Majidi, M., and Bahmani, Y. 2017. Isolation of high-quality RNA from a wide range of woody plants. *Journal of Plant Molecular Breeding*, 5(2), pp. 50-59.

Marcelino, V.R., Irinyi, L., Eden, J.S., Meyer, W., Holmes, E.C., and Sorrell, T.C. 2019. Metatranscriptomics as a tool to identify fungal species and subspecies in mixed communities–a proof of concept under laboratory conditions. *IMA Fungus: The Global Mycological Journal*, 10, pp.1-10.

Marks, R.A., Farrant, J.M., Nicholas McLetchie, D., and Van Buren, R. 2021. Unexplored dimensions of variability in vegetative desiccation tolerance. *American Journal of Botany*, 108, pp. 346–358.

Marks, R.A., Mbobe, M., Greyling, M., Pretorius, J., McLetchie, D.N., VanBuren, R., and Farrant, J.M. 2022. Variability in Functional Traits along an Environmental Gradient in the South African Resurrection Plant Myrothamnus flabellifolia. *Plants*, 11(10), p.1332.

Mathur, P. and Roy, S. 2021. Insights into the plant responses to drought and decoding the potential of root associated microbiome for inducing drought tolerance. *Physiologia Plantarum*, 172(2), pp.1016-1029.

Mitra, J., Xu, G., Wang, B., Li, M., and Deng, X. 2013. Understanding desiccation tolerance using the resurrection plant Boea hygrometrica as a model system. *Frontiers in Plant Science*, 4, p. 446.

Moco, S., Vervoort, J., Bino, R. J., De Vos, R. C., and Bino, R. 2007. Metabolomics technologies and metabolite identification. *Trends in Analytical Chemistry*, 26(9), pp. 855-866.

Moore, J.P., Farrant, J.M., Lindsey, G.G., and Brandt, W.F. 2005. The South African and Namibian populations of the resurrection plant Myrothamnus flabellifolius are genetically distinct and display variation in their galloylquinic acid composition. *Journal of Chemical Ecology*. 31 (12), pp. 2823–2834.

Moore, J.P., Nguema-Ona, E., Chevalier, L., Lindsey, G.G., Brandt, W.F., Lerouge, P., Farrant, J.M., and Driouich, A. 2006. Response of the leaf cell wall to desiccation in the resurrection plant Myrothamnus flabellifolius. *Plant Physiology*, 141(2), pp.651-662.

Moore, J.P., Lindsey, G.G., Farrant, J.M., and Brandt, W.F. 2007. An overview of the biology of the desiccation-tolerant resurrection plant Myrothamnus flabellifolia. *Annals of botany*, 99(2), pp.211-217.

Mundree, S., Whittaker, A., Thomson, J., and Farrant, J. 2000. An aldose reductase homolog from the resurrection plant Xerophyta viscosa Baker. *Planta*, 211, pp. 693–700.

Mwajita, M.R., Murage, H., Tani, A. and Kahangi, E.M. 2013. Evaluation of rhizosphere, rhizoplane and phyllosphere bacteria and fungi isolated from rice in Kenya for plant growth promoters. *SpringerPlus*, 2(1), pp.1-9.

Neeragunda, S. Y., Barbara, P., Gugi, B., Vicré-Gibouin, M., Driouich, A., Ramasandra Govind, S., Devaraja, A., and Kambalagere, Y. 2018. Perspectives on Structural, Physiological, Cellular, and Molecular Responses to Desiccation in Resurrection Plants. *Scientifica*, pp.1-18.

Nilsson, R. H., Tedersoo, L., Ryberg, M., Kristiansson, E., Hartmann, M., Unterseher, M., and Abarenkov, K. 2015. A comprehensive, automatically updated fungal ITS sequence dataset for reference-based chimera control in environmental sequencing efforts. *Microbes and environments*, 30(2), pp. 145-150.

Nishu, S.D., No, J.H. and Lee, T.K. 2022. Transcriptional response and plant growth promoting activity of Pseudomonas fluorescens DR397 under drought stress conditions. *Microbiology Spectrum*, 10(4), pp.00979-22.

Norwood, M., Toldi, O., Richter A., and Scott, P. 2003. Investigation into the ability of roots of the poikilohydric plant Craterostigma plantagineum to survive dehydration stress. *Journal of Experimental Botany*, 54, pp. 2313–2321.

Ojuederie, O., Olanrewaju, O., and Babalola, O. 2019. Plant Growth Promoting Rhizobacterial Mitigation of Drought Stress in Crop Plants: Implications for Sustainable Agriculture. *Agronomy*, 9(11), p.712.

Oliver, J.M., Farrant, M.J., Hilhorst, W.M.H., Mundree, S., Williams, B., and Bewley, D.J. 2020. Desiccation Tolerance: Avoiding Cellular Damage During Drying and Rehydration. *Annual Review of Plant Biology*. 2020, 71, pp. 435–460.

Pande, P.M., Azarbad, H., Tremblay, J., St-Arnaud, M. and Yergeau, E. 2023. Metatranscriptomic response of the wheat holobiont to decreasing soil water content. *Journal of the International Society for Microbial Ecology communications*, 3(1), p.30.

Passon Née Gleichenhagen, M., Weber, F., Jung, N., and Bartels, D. 2020. Profiling of phenolic compounds in desiccation-tolerant and non-desiccation-tolerant Linderniaceae. *Phytochemical Analysis*, 32, pp. 521–529.

Pastor, M.M., Sakrikar, S., Rodriguez, D.N. and Schmid, A.K. 2022. Comparative Analysis of rRNA Removal Methods for RNA-Seq Differential Expression in Halophilic Archaea. *Biomolecules*, 12(5), p.682.

Péli, E.R., Mihailova, G., Petkova, S., Tuba, Z., and Georgieva, K. 2012. Differences in physiological adaptation of Haberlea rhodopensis Friv. leaves and roots during dehydration–rehydration cycle. Acta Physiol. *Plant*, 34, pp. 947–955.

Pecoraro, L., Wang, X., Shah, D., Song, X., Kumar, V., Shakoor, A., Tripathi, K., Ramteke, P.W., and Rani, R. 2021. Biosynthesis pathways, transport mechanisms and biotechnological applications of fungal siderophores. *Journal of Fungi*, 8(1), p.21.

Pieterse, C.M., Zamioudis, C., Berendsen, R.L., Weller, D.M., Van Wees, S.C. and Bakker, P.A. 2014. Induced systemic resistance by beneficial microbes. *Annual review of phytopathology*, 52, pp.347-375.

Porembski, S., and Barthlott, W. 2000. Granitic and gneissic outcrops (inselbergs) as centers of diversity for desiccation-tolerant vascular plants. *Plant Ecology*. 151, pp. 19–28.

Poudel, M., Mendes, R., Costa, L.A., Bueno, C.G., Meng, Y., Folimonova, S.Y., Garrett, K.A. and Martins, S.J. 2021. The role of plant-associated bacteria, fungi, and viruses in drought stress mitigation. *Frontiers in microbiology*, 12, p.3058.

Radermacher, A.L., du Toit, S.F., and Farrant, J.M. 2019. Desiccation-Driven Senescence in the Resurrection Plant Xerophyta schlechteri (Baker) N.L. Menezes: Comparison of Anatomical, Ultrastructural, and Metabolic Responses Between Senescent and Non- Senescent Tissues. *Frontiers in Plant Science*, 10, p.1396.

Rakic, T., Ilijevic, K., Lazarevic, M., Grzetic, I., Stevanovic, V., and Stevanovic, B. 2013. The resurrection flowering plant Ramonda nathaliae on serpentine soil–coping with extreme mineral element stress. Flora-Morphol. Distrib. Funct. Plant Ecology, 208, pp. 618–625.

Rasoanaivo, P., Ralaibia, E., Maggi, F., Papa, F., Vittori, S., and Nicoletti, M. 2012. Phytochemical investigation of the essential oil from the ‘resurrection plant’Myrothamnus moschatus

(Baillon) Niedenzu endemic to Madagascar. *Journal of Essential Oil Research*, 24(3), pp.299-304.

Sheibani-Tezerji, R., Rattei, T., Sessitsch, A., Trognitz, F. and Mitter, B. 2015. Transcriptome profiling of the endophyte Burkholderia phytofirmans PsJN indicates sensing of the plant environment and drought stress. *The Journal of Microbiology*, 6(5), pp.10-1128.

Souza, R.D., Ambrosini, A., and Passaglia, L.M. 2015. Plant growth-promoting bacteria as inoculants in agricultural soils. *Genetics and molecular biology*, 38(4), pp.401-419.

Tebele, S.M., Marks, R.A. and Farrant, J.M. 2021. Two decades of desiccation biology: A systematic review of the best studied angiosperm resurrection plants. *Plants*, 10(12), p.2784.

Timmusk, S., Paalme, V., Lagercrantz, U., and Nevo, E. 2009. Detection and quantification of Paenibacillus polymyxa in the rhizosphere of wild barley (Hordeum spontaneum) with real-time PCR. Journal of applied microbiology, 107(3), pp.736-745.

VanBuren, R., Pardo, J., Man Wai, C., Evans, S., and Bartels, D. 2019. Massive tandem proliferation of ELIPs supports convergent evolution of desiccation tolerance across land plants. *Plant physiology*, 179(3), pp.1040-1049.

Van Dijk, M., Morley, T., Rau, M.L. and Saghai, Y. 2021. A meta-analysis of projected global food demand and population at risk of hunger for the period 2010–2050. *Nature Food*, 2(7), pp.494-501.

Vermeulen, S.J., Aggarwal, P.K., Ainslie, A., Angelone, C., Campbell, B.M., Challinor, A.J., Hansen, J.W., Ingram, J.S., Jarvis, A., Kristjanson, P. and Lau, C. 2012. Options for support to agriculture and food security under climate change. *Environmental Science & Policy*, 15(1), pp.136-144.

Wang, W., Zhai, Y., Cao, L., Tan, H., and Zhang, R. 2016. Endophytic bacterial and fungal microbiota in sprouts , roots and stems of rice ( Oryza sativa L .). *Microbiological Research*, pp.188–189.

Wen, W., Timmermans, J., Chen, Q. and van Bodegom, P.M. 2020. A review of remote sensing challenges for food security with respect to salinity and drought threats. *Remote Sensing*, 13(1), p.6.

Xiao, X., Liao, X., Yan, Q., Xie, Y., Chen, J., Liang, G., Chen, M., Xiao, S., Chen, Y. and Liu, J. 2023. Arbuscular mycorrhizal fungi improve the growth, water status, and nutrient uptake of

cinnamomum migao and the soil nutrient stoichiometry under drought stress and recovery. *Journal of Fungi*, 9(3), p.321.

Xu, H., Gao, J., Portieles, R., Du, L., Gao, X. and Borras-Hidalgo, O. 2022. Endophytic bacterium Bacillus aryabhattai induces novel transcriptomic changes to stimulate plant growth. *Public Library of Science*, 17(8), p.e0272500.

Xu, L. and Coleman-Derr, D. 2019. Causes and consequences of a conserved bacterial root microbiome response to drought stress. *Current Opinion in Microbiology*, 49, pp.1-6.

Xu, L., Naylor, D., Dong, Z., Simmons, T., Pierroz, G., Hixson, K.K., Kim, Y.M., Zink, E.M., Engbrecht, K.M., Wang, Y.I. and Gao, C. 2018. Drought delays development of the sorghum root microbiome and enriches for monoderm bacteria. *Proceedings of the National Academy of Sciences*, 115(18), pp.E4284-E4293.

Yandigeri, M.S., Meena, K.K., Singh, D., Malviya, N., Singh, D.P., Solanki, M.K., Yadav, A.K., and Arora, D.K. 2012. Drought-tolerant endophytic actinobacteria promote growth of wheat (Triticum aestivum) under water stress conditions. *Plant Growth Regulation*, 68, pp.411-420.

Yu, Y., Gui, Y., Li, Z., Jiang, C., Guo, J. and Niu, D. 2022. Induced systemic resistance for improving plant immunity by beneficial microbes. *Plants*, 11(3), p.386.

Zhang, Y., Li, Y., Hassan, M.J., Li, Z., and Peng, Y. 2020. Indole-3-acetic acid improves drought tolerance of white clover via activating auxin, abscisic acid and jasmonic acid related genes and inhibiting senescence genes. *BMC plant biology*, 20(1), pp.1-12.

Zolla, G., Bakker, M.G., Badri, D.V., Chaparro, J.M., Sheflin, A.M., Manter, D.K., and Vivanco, J. 2013. Understanding root–microbiome interactions. In: *Plant microbiome: stress response*, 1, pp.743-754.

# Chapter Two

## Exploring the root-associated microbiome of the resurrection plant *Myrothamnus flabellifolia*

## 2.1. Summary

Aims and background: The resurrection plant *Myrothamnus flabellifolia* tolerates complete desiccation and is a great model for studying how plants cope with extreme drought. Root-associated microbes play a major role in stress tolerance and are an attractive target for enhancing drought tolerance in staple crops. However, how these dynamics play out under the most extreme water limitation remains underexplored. This study aimed to identify bacterial and fungal communities that tolerate extreme drought stress in the bulk soil, rhizosphere, and endosphere of *M. flabellifolia*. Methods: High-throughput amplicon sequencing was used to characterise the microbial communities associated with *M. flabellifolia*. Results: The bacterial phyla that were most abundant across all zones were *Acidobacteriota, Actinobacteriota, Chloroflexota, Planctomycetota,* and *Pseudomonadota*, while the most abundant fungal phyla were *Ascomycota* and *Basidiomycota*. Although the bulk soil hosted multiple beneficial root-associated microbes, the rhizosphere zone showed the highest functional diversity of bacteria and fungi. In contrast, the endosphere exhibited a low abundance and diversity of microbes. These findings share consistent with the theory that *M. flabellifolia* recruits soil microbes from the bulk to the rhizosphere and finally to the endosphere. Conclusion: We find that zones act as the major driver of microbial diversity, but the soil physicochemical factors also influence microbial composition. These results suggest that the root-associated microbiome of *M. flabellifolia* is highly structured.

## 2.2. Introduction

Many plants are threatened by climate change and fluctuating rainfall patterns (Lizumi and Ramankutty, 2016). Although plants have evolved mechanisms to cope with periods of drought, the extreme weather patterns brought on by global change are likely to push some species beyond the limits of their tolerance. However, some unique plants that evolved in habitats with seasonal aridity have developed the ability to tolerate complete desiccation of their vegetative tissues. These species, commonly called resurrection plants, may provide critical insight into how organisms survive the extreme drought that can be used to protect vulnerable species and mitigate drought induced losses (Bewley, 1979; Gaff, 1989; Hilhorst and Farrant, 2018).

Most of the research on *M. flabellifolia* has focused on its leaf phytochemical properties, medicinal value, and the physiological and biochemical mechanisms of vegetative desiccation tolerance (Bentley et al., 2019; Erhabor et al., 2020; Marks et al., 2022; Moore et al., 2005, 2006, 2011; Sherwin et al., 1998). However, the belowground mechanisms associated with desiccation tolerance in *M. flabellifolia* remain largely unknown (Tebele et al., 2021). Processes happening in the soil and roots play a major role in sensing and responding to drought stress. The occurrence of root elongation, branching, and rhizogenesis are drought-adaptive traits in multiple models and crop species (Kato and Okami, 2011). However, little is known about parallel processes in resurrection plants, and they may respond to water deficit in a very different way as a result of their unique adaptations to extreme environmental stresses.

The roots of nearly all plants support a vast community of microorganisms internally and on their external surfaces, which could aid during environmental stresses. In fact, under drought stress, root microbes not only protect themselves but also minimise drought induced damage to the plant host (Hartman and Tringe, 2019). The mechanisms by which microbes improve plant drought tolerance are complex but likely involve reactive oxygen species (ROS) scavenging systems. For example, the upregulation of ROS genes in *Burkholderia phytofirmans* associated with *Solanum tuberosum* roots was observed under drought stress (Sheibani-Tezerji et al., 2015). Additionally, wheat primed with a *Paenibacillus polymyxa* mutant greatly improved water use efficiency, water relative content, and increased the activity of antioxidant enzyme activities (Timmusk et al., 2015). The antioxidant enzymes such as superoxide dismutase, glutathione reductase, catalase, and monodehydroascorbate reductase play a significant role in scavenging ROS caused by drought and this defense mechanism enhances drought tolerance in plants. Resurrection plants have robust antioxidant systems, in which there is high activity of ascorbate, catalase, glutathione (GSH), peroxidase (POD), superoxide dismutase (SOD) and that scavenge ROS to combat drought effects (Kranner et al., 2002). How host and microbiome ROS scavenging systems interact to improve drought tolerance is not known, but differences in the ability to recruit and retain beneficial microorganisms can have major impacts on holobiont performance and survival.

Soil microbiomes have multiple functions that are significant to plant health, including nutrient cycling, breakdown of soil organic matter, defense against plant pathogens, and enhancing abiotic stress tolerance (Hartman and Tringe, 2019; Yadav et al., 2021). A consortium of microbes is more efficient in enhancing a crop's drought tolerance than one inoculum. A recent study showed that co-inoculation of soybean with *Bacillus amyloliquefaciens* and AMF alleviated drought stress by increasing the production of sugars such as sucrose, fructose, and stachyose, as well as increased protein content compared to non- inoculated plants (Sheteiwy et al., 2021a). Microbes influence plant physiological

and biochemical metabolism under water deficit conditions, leading to metabolic changes and increased accumulation of primary metabolites in inoculated compared to non-inoculated plants under drought stress.

A substantial amount of research has gone into studying these interactions in model and crop species, but the interaction between root and soil microbiomes in resurrection plants remains largely unknown. Therefore, exploring the interaction of bacteria and fungi associated with the roots of the resurrection plant *M. flabellifolia* provides novel insight into how plant-microbe interactions function in the most extreme drought events. *M. flabellifolia* occurs in shallow rocky soil and high-temperature environments with limited rainfall in summer only. It is thus highly likely to harbour diverse microbial communities that possess desiccation tolerance traits.

The soil microbiome is typically divided into multiple zones based on its proximity to the host plant from bulk soil to rhizosphere to endosphere (Figure 2-1). To better understand the role of the soil microbiome in extreme drought stress, we quantified the bacterial and fungal communities in the bulk soil, rhizosphere, and endosphere of *M. flabellifolia*. The aims of this study were to (1) identify the microbial taxa associated with *M. flabellifolia* under extreme drought stress, (2) quantify the differential abundance of microbial clades and explore the ecological function of the microbiome based on previous characterisations of the specific microbiota in each zone.

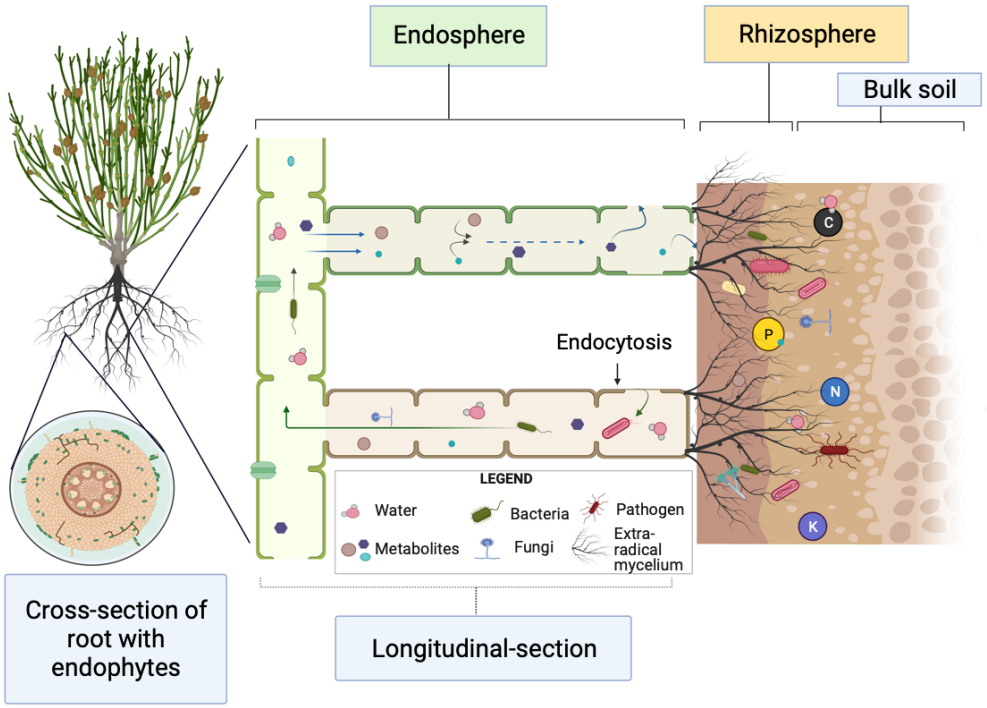


**Figure 2-1.** Plant-microbe interaction belowground. Soil microbiome zones are typically categorised into three zones based on their respective proximity to the plant roots. The rhizosphere is the region around the roots into which the lateral roots extend. The rhizoplane is a narrow area on the root's surface, and the endosphere is the area inside the roots. Plants actively recruit beneficial bacterial and fungal species into these zones, with increasing specificity from rhizosphere to endosphere. The upper root shows the secretion of metabolites, and the bottom root shows the uptake of nutrients, water, and the process of microbes entering the root endosphere.

## 2.3. Materials and methods

Five *Myrothamnus flabellifolia* plants were collected from Swebeswebe Nature Reserve in the Waterberg, Limpopo Province, South Africa in the autumn of 2021. Individual *M. flabellifolia* plants and surrounding native soil (~2 kg) were harvested from five discrete locations (within two metres of one another) and placed in a air-tight plastic. These plants were in the state of desiccation (Fig. 2-S1A). These plants were transported to the University of Cape Town for experimental procedures. Each plant's root system was gently pulled out of the ground to avoid tissue damage. Loose soil attached to the roots was removed by vigorously shaking the plant, and it was classified as bulk soil. Additionally, three replicates of bulk soil were used for soil physicochemical and DNA analysis. Next, a sterilised scissor was used to cut ~5 cm roots with rhizosphere soil attached from the shoot-root joint. Five replicates of the rhizosphere were collected for soil physicochemical analysis by vigorously

shaking to dislodge the rhizosphere from the roots. To prepare samples for microbial DNA extraction, five replicates of roots with rhizosphere soil attached were placed in a 50 mL conical centrifuge tube containing 15 mL of autoclaved phosphate-buffered saline (PBS). The rhizosphere soil, which was firmly attached to the root system, was removed according to Edwards et al. (2018). Briefly, tubes were vortexed at the maximum speed for 20 seconds to dislodge the rhizosphere soil from the roots (Fig. 2-S1B). The roots were transferred using a sterile tweezer into a new 50 ml falcon tube with 25 ml PBS. The rhizosphere soil was briefly centrifuged, and the PBS buffer was discarded. Roots were washed with 20 ml of PBS before isolating the endosphere zone and vortexed at maximum speed for 20–30 seconds. The PBS buffer was discarded, and another 20 ml of PBS was added and vortexed for 20–30 seconds. This step was repeated until there were no soil residues at the bottom of the tube. A fresh 20 ml PBS buffer was added to the root tissues, and they were cleaned by sonicating at 40 Hz for 30 seconds, and this step was repeated twice. Root tissues with no traces of soil were pulverised in liquid nitrogen using a sterile pestle and mortar. All samples were stored at -80°C for DNA extraction and 4°C soil physicochemical analysis, respectively.

#### 2.3.1. Physicochemical soil analysis

Soil samples (0.5 g) were prepared in microwave-assisted acid digestion (Mars 6 Microwave Digester) using concentrated boric, hydrofluoric, and nitric acid (AlHarahsheh et al., 2009). Before the elemental analysis, the method was validated using certified reference materials (CRMs), and calibration curves for each analyte were constructed. The targeted elements of, calcium (Ca), copper (Cu), iron (Fe), potassium (K), magnesium, manganese (Mn), sodium (Na), phosphorus (P), and zinc (Zn) were analysed using Varian ES730 inductively coupled plasma-optical emission spectroscopy (Agilent Technologies, Inc). The organic carbon (OC) and organic matter (OM) measurements/analysis of the soil were performed based on the established Walkley Black protocol (Walker-Black, 1934). The soil pH, moisture content, exchangeable acidity, and aluminium ions were also determined according to (Robertson et al., 1999). We used a one-way analysis of variance (ANOVA) with Turkey's pairwise comparison test to test for differences in physicochemical soil analysis between bulk and rhizosphere soil zones.

#### 2.3.2. DNA extraction, PCR amplification, library preparation, and sequencing

Total DNA was extracted from the bulk soil, rhizosphere, and endosphere samples using DNeasy PowerSoil (QIAGEN, 12888–50) kit following the manufacturer's protocol. The purity and quantity of the extracted DNA were assessed using gel electrophoresis and a Nanodrop ND-2000 UV-Vis spectrophotometer (Thermo Fisher Scientific, USA). The V3-V4 hypervariable region of the 16S rRNA

gene from each sample was amplified using the 341F (5'-TCGTCGGCAGCGTCAGATGTGTATAAG AGACAG-3') and the 505R (5-GTCTCGTGGGCTCGGAGATGTGTATAAGAGACAG-3') primers. The mitochondrial peptide nucleic acid (mPNA, 5-GGCAAGTGTTCTTCGGA-3) and plastid peptide nucleic acid (pPNA, 5-GGCTCAACCCTG GACAG-3) clamps (PNA Bio, Newbury Park, CA, USA) were included to minimise the amplification of host plant DNA in the PCR reaction (Fitzpatrick et al., 2018b). Each 25 µL PCR reaction consisted of the following ingredients: 12.5 µL of 2x KAPA HiFi HotStart mix, 1.25 µL of 0.25 µ*M* mPNA, 1.25 µL of 0.25 µ*M* pPNA, 5 µL of 1 µ*M* forward primer, 5 µL of 1 µ*M* forward reverse, and 2.5 µL microbial genomic DNA. The reaction mixture was placed in the thermocycler for PCR program: denature at 95°C for 3 min, followed by 25 cycles of 95°C for 30 sec denaturation, 75°C for 10 sec PNAs annealing, 55°C for 30 sec primer annealing, 72°C for one min elongation, and 72°C for five min final extension before holding at 4°C. The ITS1 and ITS2 regions were amplified using the NSA3 (5'-AAACTCTGTCGTGCTGGGGATA- 3') and NLC2 (5'-GAGCTGCATTCCCAAACA ACTC-3') primers. These *Dikaryomycota*-specific primers were developed to reduce the amplification of host plant DNA (Martin and Rygiewicz, 2005). All reactions, including negative (sterile $H_2O$) and positive (ZymoBIOMICS standard) controls, were performed in duplicates. The PCR amplicons of both bacterial and fungal species were purified using Agencourt AMPure XP beads (Beckman Coulter) to remove free primers and primer-dimers molecules. The PCR amplicons were analysed using an Agilent D1000 ScreenTape. Libraries were generated using the Illumina 16S rRNA and fungal metagenomic protocol. For library preparations, the 16S rRNA and ITS1 regions were amplified using a pool of nested primers modified to include the binding site for the sequencing primer and regions for index binding. Similar PCR conditions were used for the index PCR. The ITS1 amplicon varied in length relative to taxa. Library quantification, normalisation, and pooling were performed prior to Illumina sequencing. The 16S V3-V4 libraries were sequenced on an Illumina MiSeq sequencing instrument (Illumina, Inc) using a MiSeq reagent v2 kit (500 cycles) with 2 × 250 bp paired-end reads. The ITS1 libraries were sequenced using a MiSeq reagent nano v2 kit (500 cycles) with 2 × 250 bp paired-end reads.

### 2.3.3. Bioinformatics analysis of 16S rRNA and ITS data

The resulting fastq files were processed using R for mac OS X GUI version 4.1.2 (Urbanek, 2022). Raw sequencing paired-end reads were imported to RStudio for pre-processing steps. The quality profile of the reads was inspected using the DADA2 version 1.22.0 (Callahan et al., 2016), and the raw sequence reads with poor quality average scores (< 30) were discarded. The bacterial and fungal reads were filtered and trimmed using DADA2 to eliminate primer and adaptor sequences. In addition, error rates for each consensus quality score were evaluated. Samples were processed independently after sharing information between samples using pool 'pseudo'. The denoised forward and reverse reads

longer than ten bp were merged into a multiple sequence alignment using DECIPHER package, and amplicon sequence variances (ASVs) were obtained. Chimeric sequences were identified and removed using DADA2. Taxonomic annotation was performed using the most updated and extensive SILVA and UNITE databases for bacteria and fungi, respectively (Nilsson et al., 2019; Quast et al., 2012).

The bacterial and fungal alpha-diversity were calculated based on the pairwise Wilcoxon test metric at the ASV level and was measured using phyloseq, picante, and stat R packages. The beta-diversity of bacterial and fungal communities was assessed by computing Bray-Curtis distance across different microbial taxa of three zones. The ordination was performed using non-metric multidimensional scaling (NMDS). The differences in microbial composition between zones were transformed with total sum scaling (Nilsson et al., 2019) from 16S rRNA and ITS data. A non-parametric paired samples Wilcoxon test was performed to evaluate the alpha-diversity and taxonomic differences among various zones. The microbiome dissimilarity distance metrics were also analysed by the multivariate permutation analysis of variance (PERMANOVA), together with the nonparametric statistical Adonis test (vegan package) to establish the homogeneity of dispersion among three zones. The PERMANOVA test was performed using 999 permutations. A Dirichlet-Multinomial distribution test was used for relative abundance using the HMP package and this test is analogous to a paired sample t-test. However, it evaluates whether taxa frequencies observed in all groups of metagenomic samples are equal. Differentially abundant ASVs were identified using the DESeq2 package and a pseudo count was added to bypass the errors in the logarithm transformation. Taxa on the heatmap were selected from the annotation table fitted to a negative binomial generalised linear model (nbFLM) using analysis of deviance (alpha = 0.05) at the genus level.

## 2.4. Results

### 2.4.1. Soil physicochemical analysis

There were significant physiochemical and elemental differences between bulk and rhizosphere soil (Table 2-1). The bulk soil had significantly lower moisture content than the rhizosphere soil ($P < 0.01$), and exchangeable hydrogen ions were significantly ($P < 0.05$) lower in the rhizosphere than the bulk soil. Thus the bulk soil was more acidic compared to the rhizosphere. In general, with the exception of Fe and Mn, the rhizosphere had higher concentrations of elements tested.

**Table 2-1**. Physicochemical factors and abundance of elements (µg/g) in the bulk and rhizosphere soil of *M. flabellifolia*.

| | **Bulk soil** | **Rhizosphere soil** |
|---|---|---|
| **pH** | 4.1±0.06 | 4.3±0.11 |
| **OC (g/kg)** | 2.1±0.08 | 2.0±0.39 |
| **OM (g/kg)** | 3.6±0.15 | 3.5±0.69 |
| **Moisture(%)** | 3.5±0.95** | 5.4±1.45** |
| **Exch Al (cmol/kg)** | 0.26±0.12 | 0.26±0.076 |
| **Exch H (cmol/kg)** | 0.77±0.04* | 0.58±0.12* |
| **Ca** | 2492.3±1189.1 | 2903.6±1676.4 |
| **Cu** | 6.967±6.0 | 27.7±25.4 |
| **Fe** | 78530±26473.6 | 67331±22833.2 |
| **K** | 2733.7±769.2 | 3047.4±715.5 |
| **Mg** | 428±87.9 | 652.8±202.7 |
| **Mn** | 155.3±16.2 | 148.1±36.4 |
| **Na** | 746±206.2 | 1002.2±130.1 |
| **P** | 283±32.8 | 376.8±74.3 |
| **Zn** | 88.6±75.3 | 176.1±104.8 |

NB: Mean ± standard error (n=5). The asterisk on the same column indicates significantly different values (*$P < 0.05$, **$P < 0.01$) based on Tukey's pairwise significantly different test. Organic carbon (OC), organic matter (OM), exchangeable acidity (Exch acidity), exchangeable aluminium ion (Exch Al) and exchangeable hydrogen (Exch H), calcium (Ca), copper (Cu), iron (Fe), potassium (K), magnesium, manganese (Mn), sodium (Na), phosphorus (P) and zinc (Zn).

### 2.4.2. Amplicon 16S rRNA and ITS sequencing data

A total of 21,871 bacterial ASVs and 1332 fungal ASVs were retained after filtering across all zones. The Venn diagrams of bacteria and fungi were constructed by creating a presence/absence matrix summarising the total number of ASVs in all samples for each zone. The ASVs that were present in the bulk soil, rhizosphere, and endosphere were compared. We identified unique and common taxa across the different soil zones (Figure 2-2A and B). The majority of bacterial and fungal taxa were specific to the different soil zones. A total of 5584 ASVs of bacterial taxa were shared across all three zones

(Figure 2-2A). The bulk soil, rhizosphere, and endosphere each harboured 3215, 5833, and 2899 unique ASVs, respectively. The rhizosphere had the richest diversity of bacterial taxa compared to other zones and the rhizosphere and bulk soil shared 2751 ASVs. Similarly, with the fungal communities, the rhizosphere had greater unique ASVs (699) compared to other zones (Figure 2-2B). The shared ASVs across all zones, and between the rhizosphere and endosphere were the same (22). However, the fungal bulk and rhizosphere soil shared higher ASVs (132) relative to other shared ASVs between zones. Furthermore, the bulk soil and endosphere showed lower overlap in bacterial (275) and fungal (4) ASVs. There was a high overlap of bacterial and fungal taxa between bulk soil and rhizosphere, and the endosphere had the least unique ASVs.

### 2.4.3. Alpha and Beta-diversity

To understand the community diversity of *M. flabellifolia's* root microbiome, we characterised the alpha (within the community) and beta (across the communities) diversity of the bulk soil, rhizosphere, and endosphere zones. Rarefaction curves at the ASV level show the sequencing depth of both bacterial and fungal community diversity (Figure 2-S2A and S2B). Alpha-diversity, both in terms of species richness using Shannon's index and species evenness using Simpson was measured. In bacterial communities, species richness was significantly higher in bulk and rhizosphere soil compared to the endosphere (Wilcoxon test, $P$=0.05) (Figure 2-2C). Similarly, fungal richness was significantly higher ($P$=0.02) in bulk and rhizosphere soil than in the endosphere (Figure 2-2D). There was no significant difference between bulk and rhizosphere soil for bacteria ($P$=0.39) or fungi ($P$=0.25). Moreover, the bulk and rhizosphere soil exhibited a high degree of evenness in their bacterial and fungal communities, whereas there was more variability in the endosphere (Figure 2-2C-D). The bulk and rhizosphere soil had a greater diversity of bacteria and fungi compared to the endosphere compared.

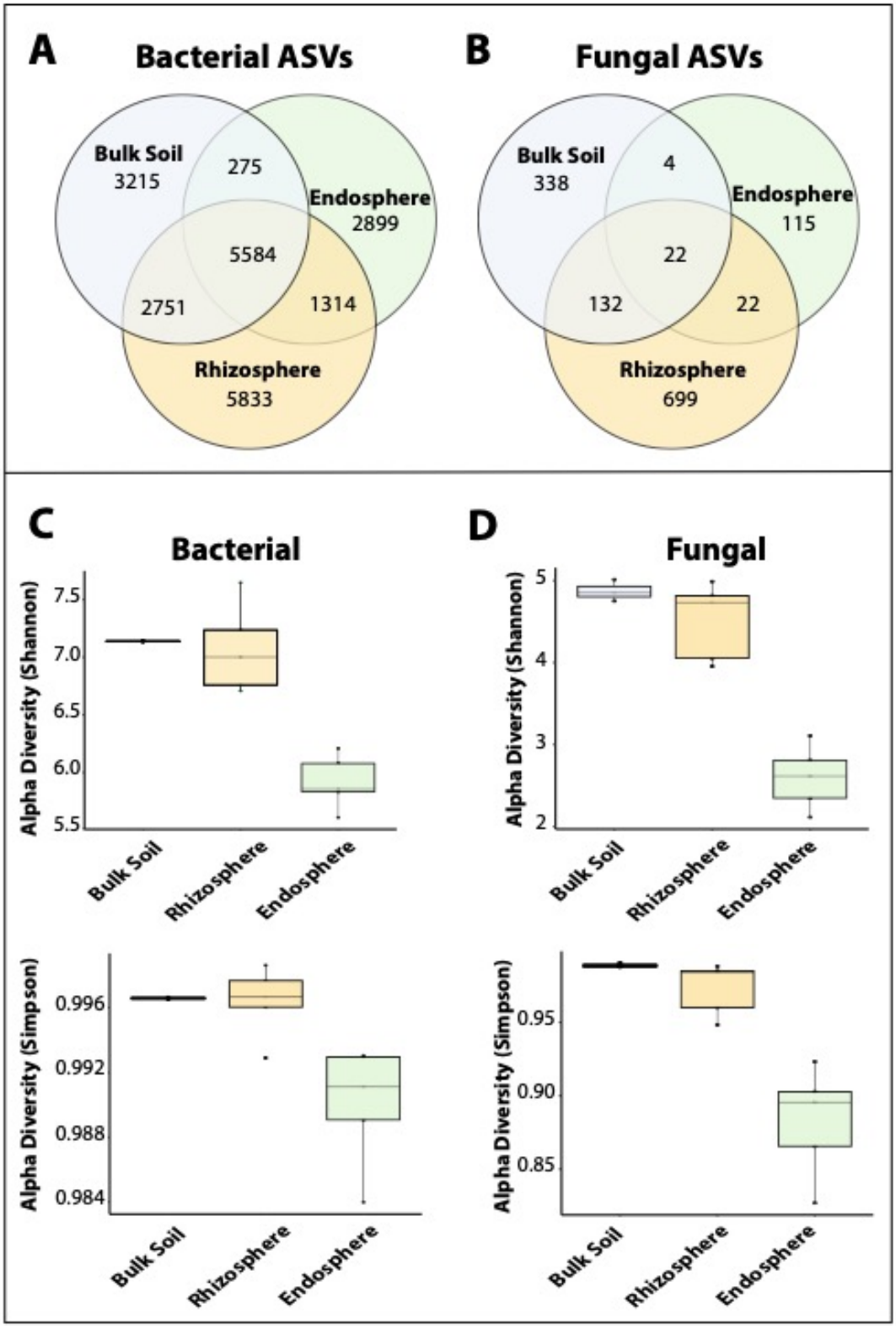


**Figure 2-2.** Venn diagram and alpha-diversity shows the number of A) bacterial and B) fungal amplicon sequence variants (ASVs) that are unique and shared across the three soil zones. Alpha-diversity of C) bacterial and D) fungal communities in the three zones. A Shannon diversity index was used to measure species richness (number of different ASVs in the sample). Simpson diversity index

measures the evenness of the microbial community (abundance of ASVs relative to each other) within each zone.

Next, we calculated beta-diversity–a measure of variation in species diversity between zones (Figure 2-3A and B). The PERMANOVA indicated significant variation in bacterial and fungal communities across zones. The separation between the groups was statistically significant (PERMANOVA, *P*=0.01), providing strong evidence for a difference in bacterial composition between soil zones and endosphere. (Figure 2-3A). There was an overlap in bacterial ASVs between the rhizosphere and bulk soil zones, which was further observed in hierarchical clustering. The fungal community showed substantial variation in species diversity between zones with a high statistical difference (PERMANOVA, *P*=0.001) in variation between three zones (Figure 2-3B). Moreover, hierarchical cluster analysis further confirmed the clustering of zones with Bray-Curtis dissimilarity distances ranging from 0.1 to 1 distance across zones for both bacterial (Figure 2-3C) and fungal ASVs (Figure 2-3D). However, the fungal dissimilarity distance between the zones was one, indicating that observations were well clustered and had distinct taxa compared to bacterial hierarchy. Taken together, the endosphere microbiome was more distinct compared to the bulk and rhizosphere soil for both bacteria and fungi clustering.

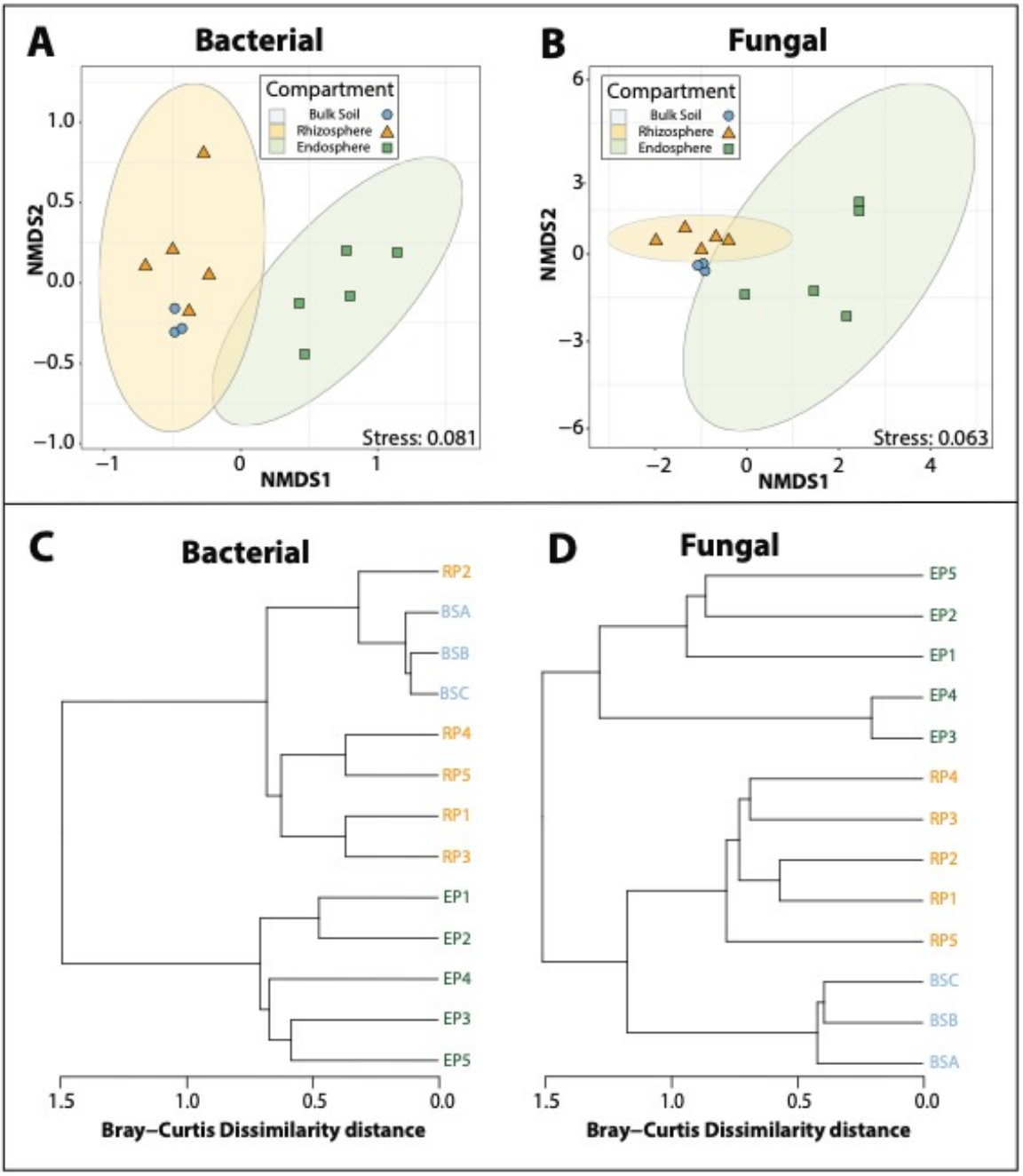


**Figure 2-3.** Differences in microbial composition between endosphere, bulk, and rhizosphere soil.Beta-diversity analysis using non-metric multidimensional scaling (NMDS) based on the PERMANOVA test. A) Bacterial and B) fungal community composition in different zones were analysed at the amplicon sequence variant (ASV) level. C) Bacterial and D) fungal hierarchical cluster analysis of taxa using Bray-Curtis dissimilarity.

### 2.4.4. Relative and differential abundance

To better understand the possible functional impact of the root microbiome, relative abundances of different taxa were evaluated (Figure 2-4). Not only were different taxa present in different zones, but the abundance of these bacterial and fungal taxa differed significantly. The top six most abundant bacterial phyla across all zones were *Acidobacteriota, Actinobacteriota, Chloroflexota, Planctomycetota, Pseudomonadota, and WPS-2* (Figure 2-4A). The relative abundance of *Chloroflexota, Crenarchaeota, Cyanophyta, Gemmatimonadota, RCP2–54,* and *WPS-2* was more enriched in bulk soil (Figure 2-4A). In contrast, the rhizosphere had a high abundance of *Bdellovibrionota, Dependentiae, Bacillota, GAL-15, Spirochaetota,* and *Verrucomicrobiota.* Furthermore, we observed an enrichment of *Acidobacteriota, Actinobacteriota, Elusimicrobiota, Myxococcota, Patescibacteria, Planctomycetota,* and *Pseudomonadota* in the endosphere. Interestingly, the relative abundance of *Chloroflexota* decreased from bulk-rhizosphere soil to endosphere, whereas *Actinobacteriota* increased from bulk-rhizosphere to endosphere. Interestingly there was no significant difference in the relative abundance of bacterial taxa between the rhizosphere and endosphere, but we found that the bacterial microbiome composition was significantly different between the soil zones (bulk and rhizosphere soil) and endosphere ($P$=0.00054). The most dominant fungal phyla found across all zones were *Ascomycota* and *Basidiomycota* (Figure 2-4B), but the fungal microbiome differed significantly between the three zones ($P$=0.01). The rhizosphere harboured a more diverse fungal microbiome than the endosphere and bulk soil, and the significantly enriched phyla were *Chytridiomycota*, *Mortierellomycota*, *Mucoromycota*, *Rozellomycota,* and *Zoopagomycota*. The endosphere and rhizosphere had a similar composition of the dominant bacterial phyla, while fungal composition across zones was dominated by *Ascomycota*.

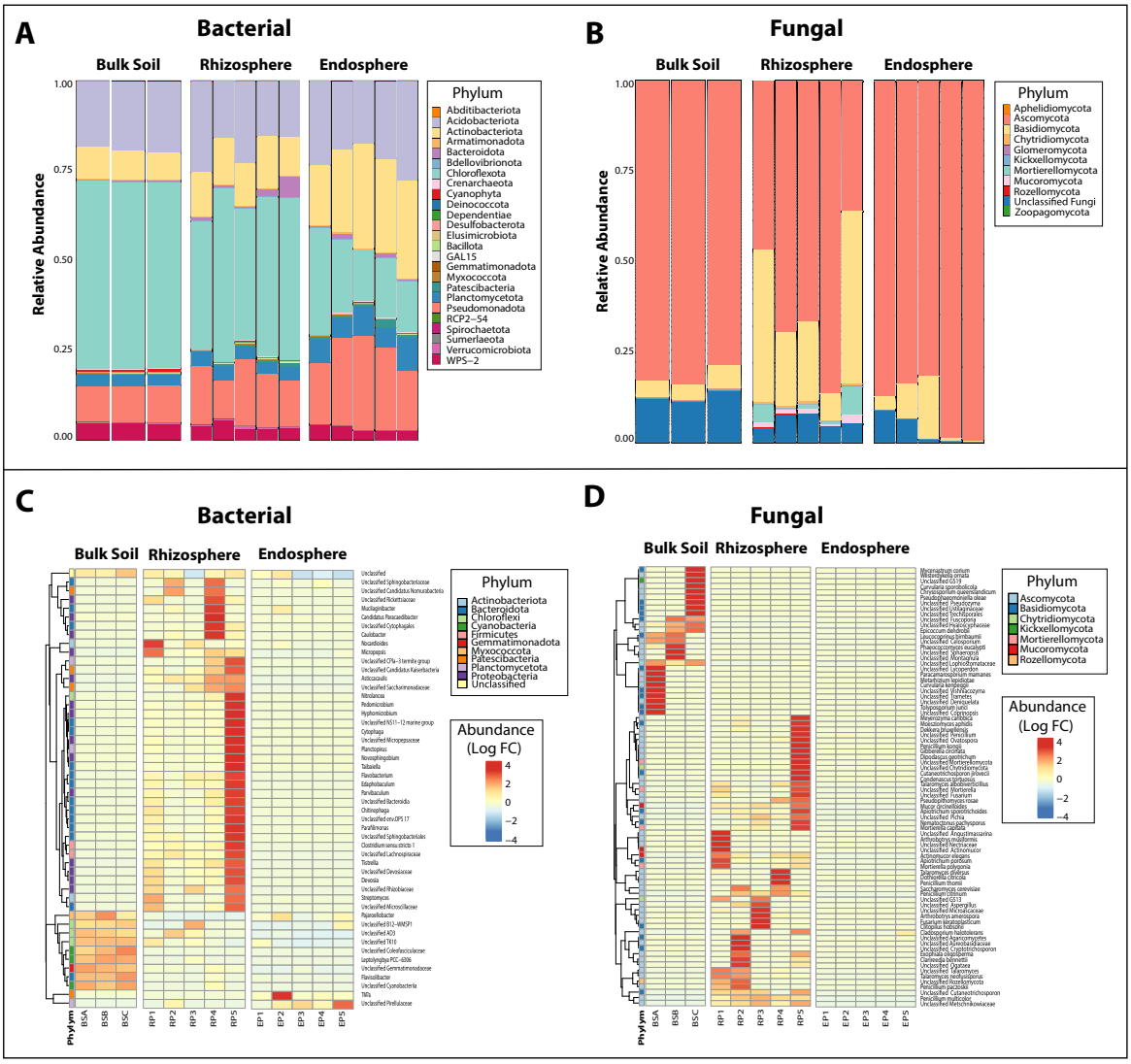


**Figure 2-4. .** Relative abundance of A) bacterial B) fungal microbial community composition of bulk soil, rhizosphere, and endosphere zones at phylum level during extreme drought stress. Significant differences ($P < 0.01$) in the Dirichlet-multinomial distribution of bacterial and fungal phyla between bulk and rhizosphere soil, and bulk soil and endosphere. C) Bacterial and D) fungal heatmap plots of the abundance of taxa differing significantly between three soil zones. Presented data are centred and scaled to the average of each taxon abundance, and each vertical bar corresponds to a sample. The $\log_2$ fold change shows the abundance of different taxa in the sample.

To identify the bacterial and fungal lineages enriched within the root relative to the rhizosphere and bulk soil, a negative binomial model was used to test for the differential abundance of ASVs across zones. Many bacterial and fungal genera were more abundant in the rhizosphere compared to other zones. A total of 84 bacterial ASVs were significantly enriched (nbGLM, $P < 0.01$) across all zones

(Figure 2-4C). The most significantly enriched taxa in bulk soil were *Leptolyngbya, Flavisolibacter, Cyanophyta,* and unclassified genera (*B12-WMSP1, AD3, TK10, Coleofasciculaceae, Gemmatimonadaceae*). There was high variability within rhizosphere samples for both bacterial and fungal communities (Figure 2-4C and D). The enriched taxa in the rhizosphere were *Asticcacaulis, Nitrolancea, Pedomicrobium, Hyphomicrobium, Cytophaga, Micropepsis, Nocardioides, Planctopirus, Novosphingobium, Tailbaiella, Flavobacterium, Edaphobaculum, Parvibaculum, Chitinophaga, Parafilimonas, Clostridium, Tistrella, Caulobacter, Candidatus paracaedibacter, Mucilaginibacter, Devosia, Streptomyces* and unclassified genera (*Sphingobacteriaceae*, *Rickettsiaceae, Cytophagales, CPIa-3termite group, Saccharimonadaceae, Micropepsaceae, Bacterioidia, Lachnospiraceae, Rhizobiaceae, Devosiaceae* and *Microscillaceae*). In the endosphere, we detected only *Pirellulaceae, TM7a, Mucilagnibacter, Pajaroellobacter*, and an unclassified genus (*B12*-WMSP1). A total of 71 fungal ASVs were significantly different (*P*=0.01) across the three zones. The most significantly enriched fungal genera in bulk soil were *Chrysosporium, Epicoccum, Leucucuprinus, Pseudophaeomoniella, Westerdykella, Metarhizium, Tolyposporium, Paracamarosporium,* and *Sphaeropsis* (Figure 2-4D). Some fungal genera were significantly enriched in the rhizosphere including *Apiotrichum sporotrichoides, Clitopilus hobsonii, Nematoctonus pachysporus, Meyerozyma caribbica, Mortierella capitata, Penicillin kongi,* and *Talaromyces diversus*. In contrast, the endosphere zone hosts only a small number of fungal genera namely *Cladosporium* and *Penicillium*. Taken together, the most significantly different phyla in the bulk soil were *Cyanophyta* and *Chloroflexota* for bacteria, *Ascomycota,* and *Basidiomycota* for fungi relative to other zones. Although the rhizosphere showed high variability, this zone had a higher number of significantly enriched taxa compared to other zones.

### 2.4.5. Environmental factors influencing the microbial composition

To explore the effects of edaphic factors on the microbial composition of bulk and rhizosphere soil of *M. flabellifolia*, we performed a redundancy analysis (RDA) to relate elemental soil variables to microbiome composition for both bacteria (Figure 2-5A and C) and fungi (Figure 2-2-5B and D). Bulk soil samples clustered together more than the rhizosphere samples, indicating a higher variability within the rhizosphere compared to the bulk soil zone. The soil physicochemical factors pH, moisture, organic carbon and matter, and soil elements positively correlated with a high abundance of bacterial and fungal species in the rhizosphere zone. Furthermore, the soil elements Ca, K, Mg, Na, P, and Zn were associated with the enrichment of bacterial genera *Gordonia, Taonella,* and *Rhodobacter* (Figure 2-S3A), whereas Ca, Fe, and Mn were significantly associated with the enrichment of fungal genera *Spegazzinia, Dothideales* and *Vishniacozyma* in both bulk and rhizosphere soil (Figure 2-S3B). There was a strong correlation between the rhizosphere microbiome and soil physicochemical factors.

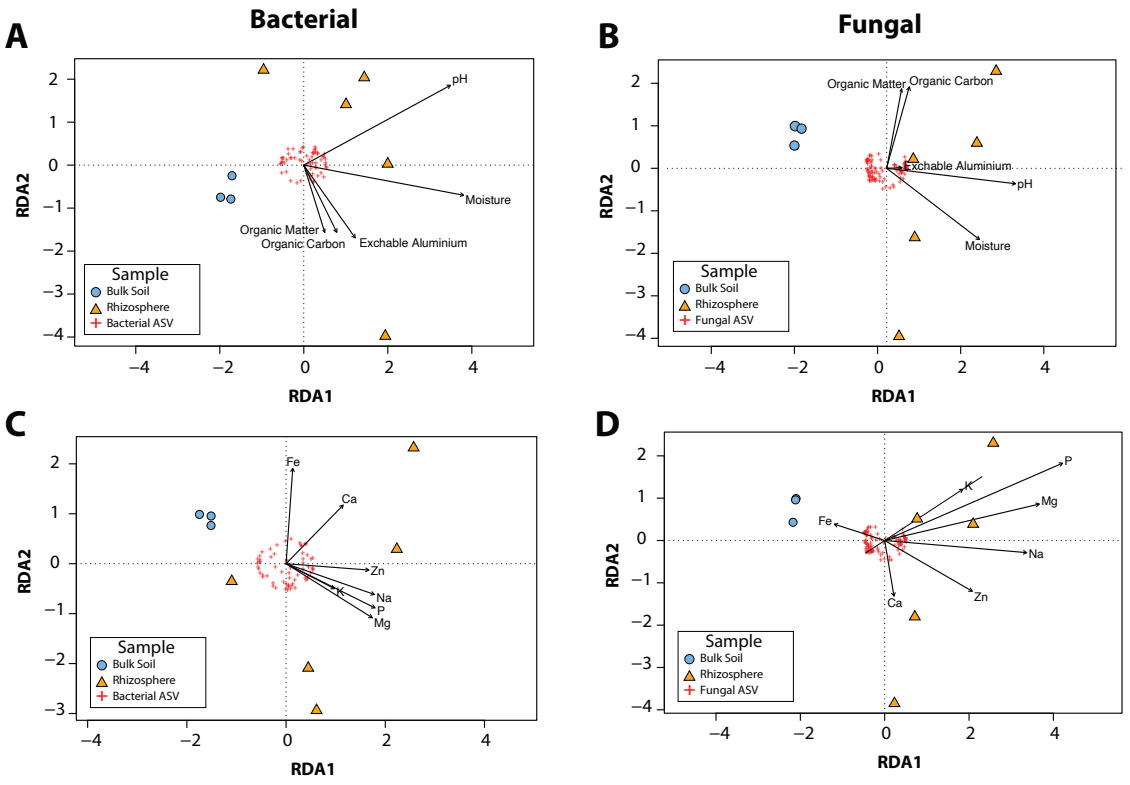


**Figure 2-5.** Redundancy analysis of soil physicochemical parameters of bulk and rhizosphere soil and their influence on bacterial (A and C) and fungal communities (B and D).

## 2.5. Discussion

Plant-microbe interactions play an important role in plant growth, health, and productivity. Despite the importance of plant growth-promoting microbes in plants, particularly in the rhizosphere, microbial species associated with resurrection plants have not been explored (Tebele et al., 2021). Our study provides one of the first high-resolution characterisations of the root microbiome of a resurrection plant. We described the bacterial and fungal microbiomes associated with the resurrection plant *M. flabellifolia* under air-dry conditions and investigated how the microbial community composition varied across zones from bulk soil to the rhizosphere, to the endosphere. While this provided only a snapshot of communities present under extreme conditions, providing a full understanding of progressive changes in community dynamics during dehydration, this study does allow speculation on the role of these communities and their contribution to the unique resilience of *M. flabellifolia.* Bacterial ASVs were significantly more abundant than fungal ASVs in both soil and root samples, which was expected given the generally higher species richness of soil bacterial communities. Our analyses revealed substantial differences in the microbiome of the bulk soil, rhizosphere, and

endosphere zones. Species richness and microbial diversity were observed in the bulk soil and, to a higher degree, in the rhizosphere samples. In contrast, the endosphere microbiome was notably reduced in such properties, with only a few select species being present, suggesting that strong filtering occurs at the soil-to-root interface. These findings suggest that regardless of extreme drought conditions, *M. flabellifolia* harbours a diverse microbial community and may actively regulate microbial assemblages in different zones.

The most dominant bacterial phyla across all zones were *Acidobacteriota, Actinobacteriota, Chloroflexota, Planctomycetota, Pseudomonadota,* and *WPS-2*, whereas the most dominant fungal phyla were *Ascomycota*, *Basidiomycota*, *Mortierellomycota* and *Mucoromycota*. These results are parallel to previous studies that also reported the presence of *Actinobacteriota*, *Chloroflexota,* and *Planctomycetota* in the resurrection plant *Ramonda* as well as in chickpea, sorghum, and other plant hosts (Ahkami et al., 2017; Đokić et al., 2010; Xu et al., 2018; Yadav et al., 2021). However, there are notable differences between the findings on *Ramonda spp.* and the current study. Most importantly, the presence of *Flavobacterium*, *Mucilaginibacter,* and *Nocardioides* in *M. flabellifolia* but absent in the *Ramonda* species' rhizosphere, suggests that these microbes could be environmentally or geographically determined (*M. flabellifolia* occurs in southern Africa whereas *Ramonda spp*. occurs in Eurasia). In desiccation sensitive species, such as sorghum, Xu et al. (2018) have a low abundance of *Acidobacteriota* in roots under drought stress. In contrast, our study shows a high enrichment of *Acidobacteriota* in the endosphere of *M. flabellifolia* suggesting a possible role for these taxa in coping with soil with lower pH. The abundance of these distinctive microbial strains in *M. flabellifolia* demonstrates that extreme environmental stress may restructure the plant microbiome. It is worth mentioning that there are other factors such as nutrient availability and environmental conditions that may contribute microbiome differences between the rhizosphere and bulk soil. Additionally, microbial communities in the rhizosphere is also shaped and regulated by root exudates and this may be due to *M. flabellifolia* is rich with phenolics and flavonoids. Drought stress induces a range of physiological, metabolic, and genetic responses while also impacting nutrient availability in both the plant host and its associated microbiome. Bulk soil samples were clustered together more strongly compared to the rhizosphere zone (Figure 2-3; 2-5). There was variability in the rhizosphere samples, suggesting that the rhizosphere of each plant hosts a slightly different microbial composition and this could be due to the landscape topography of the natural environment.

We identified differences in soil physicochemical factors that were associated with changing microbiome composition across soil zones. The concentration of micronutrients such as Ca, Cu, Mg, Mn, Na, and Zn in the soil of *M. flabellifolia* was positively correlated with the abundance of both bacterial and fungal communities in rhizosphere and bulk soil samples (Figure 2-5). Previous studies

have conclusively shown that arbuscular mycorrhizal enhances plant growth by increasing root access to immobile mineral ions and binding to heavy metals and transporting them from roots to shoot tissues (Srinivasagam et al., 2013). These findings showed a diverse and co-occurrence of bacterial and fungal communities across soil and root zones under desiccation conditions. The content of soil moisture and exchangeable $H^+$ were significantly correlated with bacterial and fungal communities in the rhizosphere zone. A high concentration of acidic cations, particularly hydrogen ions, contributes to soil acidity, with exchangeable $H^+$ being the primary factor influencing soil pH (Zheng et al., 2020). Although the difference in soil pH between bulk and rhizosphere soils was not statistically significant, the results suggest that rhizosphere soil tends to be less acidic compared to bulk soil. Taken together, the rhizosphere soil had higher moisture content and micronutrients and it was less acidic compared to bulk soil, which could attract diverse and beneficial microbial communities.

The enrichment of certain bacteria and fungi under extreme drought conditions may reflect inherent microbial adaptations to arid environments. Several taxa that were uniquely enriched in different zones of *M. flabellifolia*. These patterns suggest potential ecological associations between enriched microbes and different zones affected by drought. The *M. flabellifolia* microbiome is extremely complex consisting of over 900 unique bacterial and fungal taxa in each zone. To summarise this complexity, we highlight selected taxa from each zone and discuss their possible role in mitigating drought stress.

This study found a significant enrichment of monoderm (*Actinobacteriota, Chloroflexota* and *Bacillota*) and diderm (*Acidobacteriota, Bacteriodota,* and *Pseudomonadota*) lineages in rhizosphere and endosphere compared to the bulk soil, except for *Chloroflexota,* which showed high enrichment in bulk soil. The bulk soil zone of the *M. flabellifolia* microbiome hosted an abundance of bacterial taxa in *Coleofascicus*, *Flavisolibacter,* and *Leptolyngbya*. These bacterial genera are known to be resistant to drought stress and can improve the physical and biological conditions of rhizosheath soil (Liu et al., 2021; Moreira et al., 2021). The finding of *Cyanophyta* in bulk soil is significant, as these species are normally restricted to the upper surface of soil crusts (due to their photosynthetic ability). Such species have been shown to play a significant role in soil stabilisation and the addition of organic carbon (Gao et al., 2020b) and their role in the bulk soil could be significant. Interestingly, our study revealed that the bulk soil zone hosts unique, beneficial bacterial and fungal taxa, and this might be due to the ecological niche of *M. flabellifolia.*

The significantly enriched fungal taxa in bulk soil were *Epicoccum dendrobii*, *Metarhizium lepidiotae,* and *Mycenastrum.* These enriched fungal taxa also have multiple functions related to resilience. For instance, *Epicoccum dendrobii* is an antifungal agent that enters the plant tissue through stomatal cells

and secretes compounds that inhibit anthracnose lesion development caused by pathogens (Bian et al., 2021). *Metarhizium spp.* is an endophyte that proliferates propagule levels in the rhizosphere (Steinwender et al., 2015). Remarkably, *Metarhizium spp.* was found in the bulk soil of *M. flabellifolia*, instead of the endosphere compared to previous studies. These findings indicate the co-occurrence of that both bacteria and fungi in *M. flabellifolia*, which is in accordance with the study by Sheteiwy et al. (2021b) reported the co-inoculation of soybean seedlings with AMF and *Bradyrhizobium* improved root length and dry weight of the plant as compared to the controls. The microbial diversity in the bulk soil depends on the plant species and habitat, and the bulk soil zone of *M. flabellifolia* hosted a high relative abundance of *Chloroflexota* and *Cyanophyta* compared to other zones.

A plethora of bacterial and fungal taxa were significantly enriched in the rhizosphere compared to other zones. The bacterial genera include *Flavobacterium*, *Nocardioides,* and *Streptomyces.* These bacterial genera produce indoleacetic acid (IAA) which improves xylem and phloem formation in roots and further increases the formation of lateral and adventitious roots to mitigate drought effects (Khan et al., 2014). This suggests that these species play a vital role in *M. flabellifolia*, because a large root system plays a significant role in sourcing water in the deeper soil profiles. A recent study reported the upregulation of the TaIAA15-1A gene is enhanced by exogenous abscisic acid (ABA) treatment and overexpression of TaIAA15-1A in *Brachypodium* improved drought tolerance through the regulation of antioxidant pathways and ABA signalling, which further reduces ROS and decreased malondialdehyde content (Su et al., 2023). Moreover, the high amounts of iron in the rhizosphere soil may be associated with the increased abundance of *Acidicapsa* species (Fig. S3A), which have been reported to produce induce IAA (Kielak et al., 2016). Interestingly maize primed with *Pseudomonas* species enhanced the upregulation of protein kinases (SnRKs), which are positive regulators of ABA receptors (SkZ et al., 2018). This may suggest that the activity of diverse protein kinases involved in the desiccation tolerance of *M. flabellifolia* (Ma et al., 2015) could be influenced by the presence of *Pseudomonatota*. Water limitation and nutrient starvation in plants stimulate the transcription of multiple drought-responsive genes that ameliorate drought stress effects.

The enriched fungal taxa in the rhizosphere included *Actinomucor*, *Aspergillus,* and *Penicillium spp*. *Actinomucor spp*. has been shown to produce abundant quantities of proteases, lipases, and amylases that hydrolyse the components of sorghum seeds (Gao et al., 2020a). Therefore, the presence of hydrolytic-enzyme-producing species under drought conditions in the rhizosphere suggests that they might be involved in the rearrangement of metabolism through the selective degradation of short-lived proteins (Vaseva et al., 2012). A recent study by Sheteiwy et al. (2021b) reported high antioxidant activity and upregulation of catalase and peroxidase gene expression in the soybean seedling under drought stress was enhanced by *Bradyrhizobium* and mycorrhizal co-inoculant. The presence of

trehalose in *M. flabellifolia's* leaves has been related to fungal species, and trehalose is a desiccation-induced osmoticum in resurrection plants (Farrant 2000; Moore et al., 2011). Although there was variation in the rhizosphere microbiome, this zone hosted diverse microbial communities that may confer drought tolerance and promote plant growth to the host.

The endosphere of *M. flabellifolia* was significantly less diverse in microbial taxa than the other two zones, suggesting that stringent filtering occurs at the soil-root interface. Bacterial genera significantly enriched in the endosphere were *Mucilaginibacter*, TMa7, and unclassified *Pirellulaceae,* and fungal taxa were *Cladosporium* and *Penicillium*. The *Mucilaginibacter* and *Cladosporium* genera are known to produce exopolysaccharides which form biofilms and adhere to root surfaces (Fan et al., 2018; Kielak et al., 2016; Mahapatra and Banerjee, 2013). Exopolysaccharides facilitate biofilm formation around the root, which helps maintain a hydrated microenvironment and limits water loss (Morcillo and Manzanera, 2021). As the rhizosphere soil moisture was significantly greater than bulk soil, it is possible that the presence of exopolysaccharide-producing microbes may slow water loss and microbial mobility. These results provide further support for the hypothesis that root-associated microorganisms confer drought tolerance to their host plant.

## 2.6. Conclusion

*Myrothamnus flabellifolia* hosts a diverse microbiome that may assist the plant in surviving extreme drought stress. Understanding the microbial composition and the distribution across three zones and characterising the core taxa in the bulk soil, rhizosphere, and endosphere provides a great opportunity to identify the drought tolerant microbes associated with *M. flabellifolia*. Taken together, this study demonstrated that the most dominant bacterial phyla across all zones were *Acidobacteriota, Actinobacteriota, Chloroflexota, Planctomycetota, Pseudomonadota,* and *WPS-2*, and fungal phyla were *Ascomycota*, *Basidiomycota*, *Mortierellomycota* and *Mucoromycota*. Additionally, the rhizosphere hosted a high level of bacterial and fungal diversity compared to other zones. Future studies should consider investigating *M. flabellifolia* under rehydration and dehydration conditions using metatranscriptomic and metabolomic approaches to explore the expressed microbial genes and responsive metabolites under extreme drought conditions. The identified microbial communities associated with *M. flabellifolia* roots could have the potential to improve plant resilience and well-being.

## 2.7. Supplementary

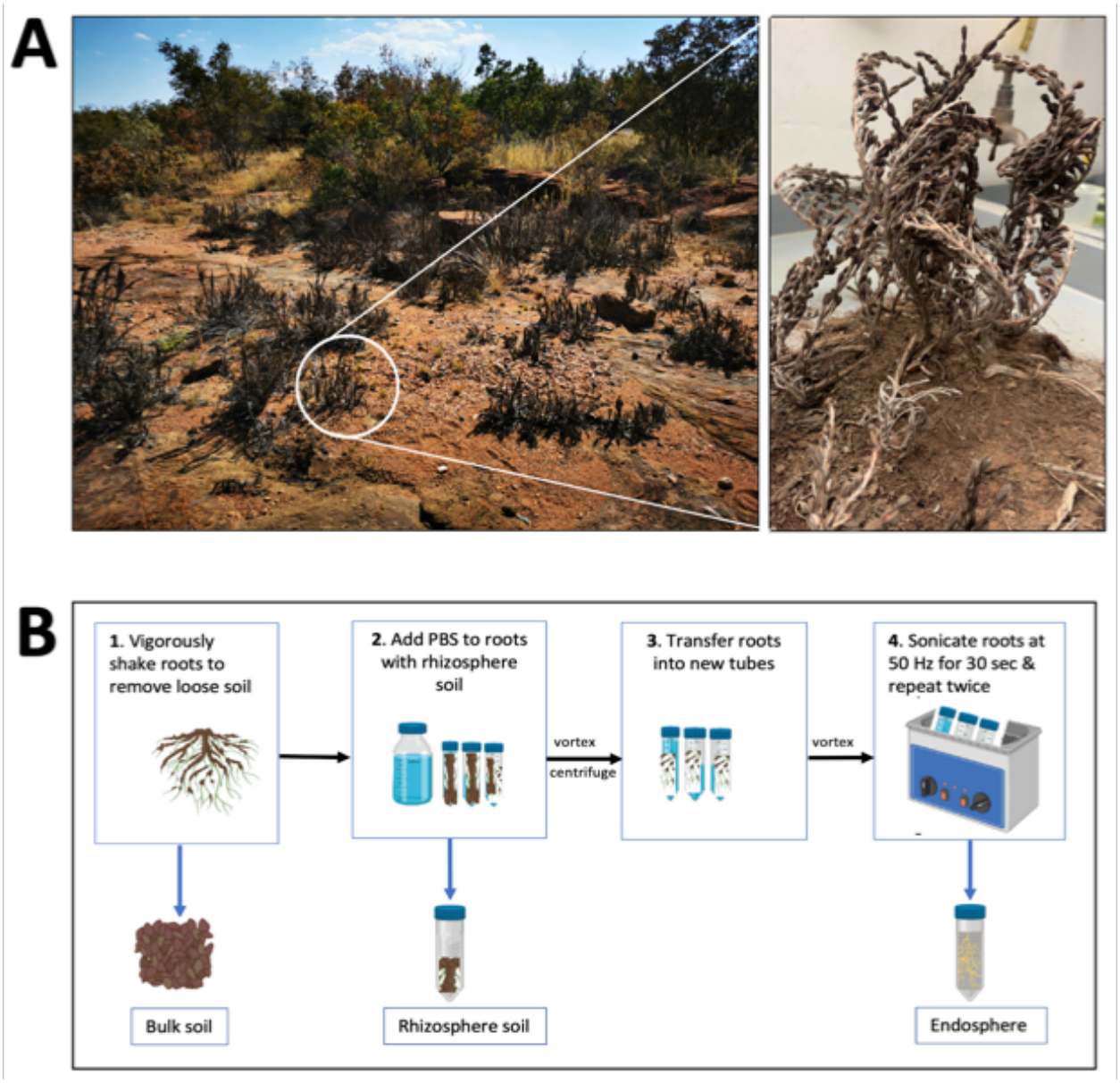


**Figure 2-S1**. Overview of experimental design and sample processing. A) *Myrothamnus flabellifolia* at Swebeswebe Nature Reserve. The bulk soil, rhizosphere and roots were collected at the desiccated state of *M. flabellifolia*. Briefly, plants were harvested from the field with their native soil and transported to the University of Cape Town. B) The bulk soil, rhizosphere, and endosphere zones were separated.

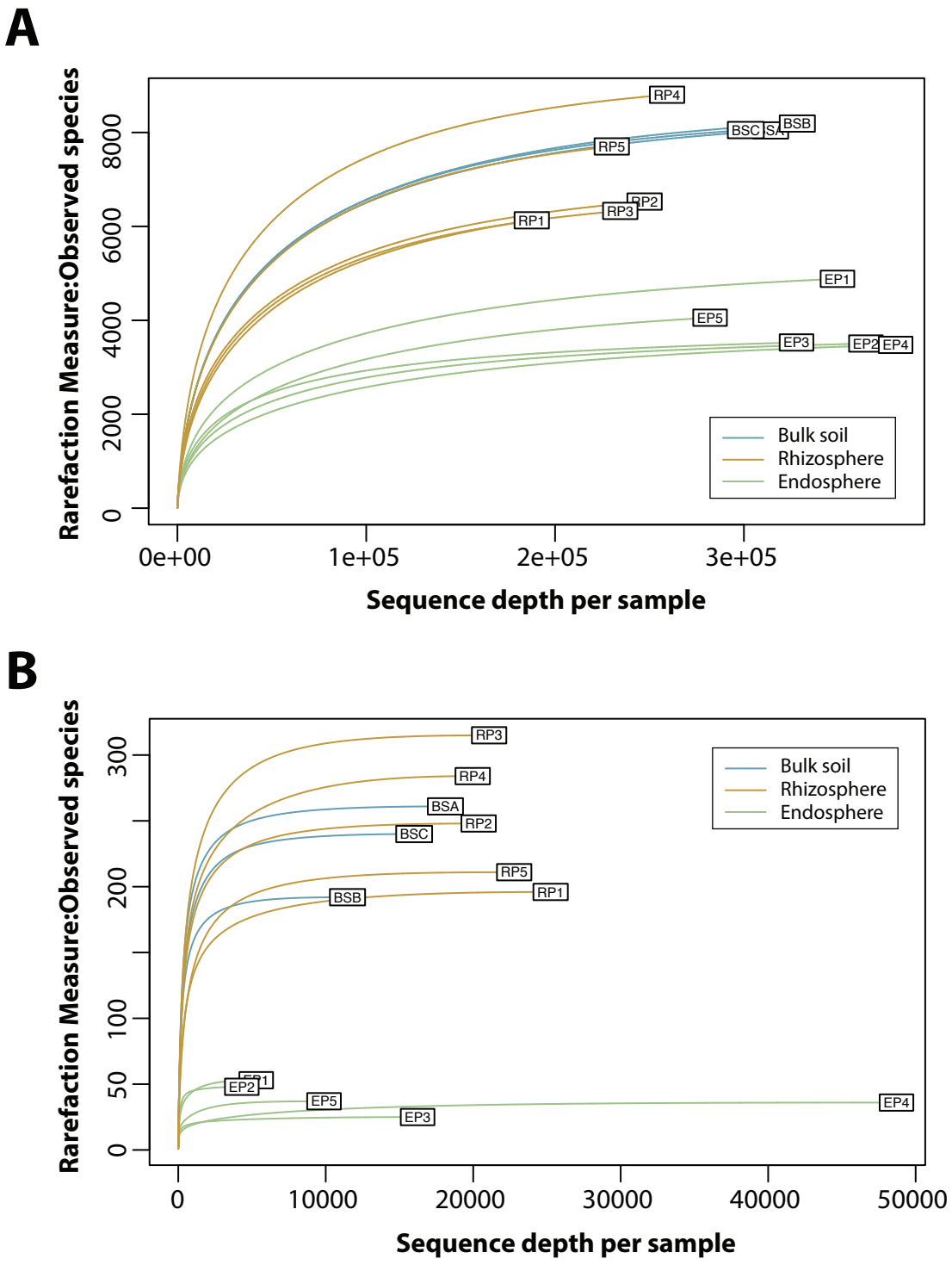


**Figure 2-S2**. Rarefaction curves show the number of amplicon sequence variants (ASVs) from A) bacteria and B) fungi sequencing data. Observed species from bulk soil, rhizosphere and endosphere of *M. flabellifolia* resurrection plant.

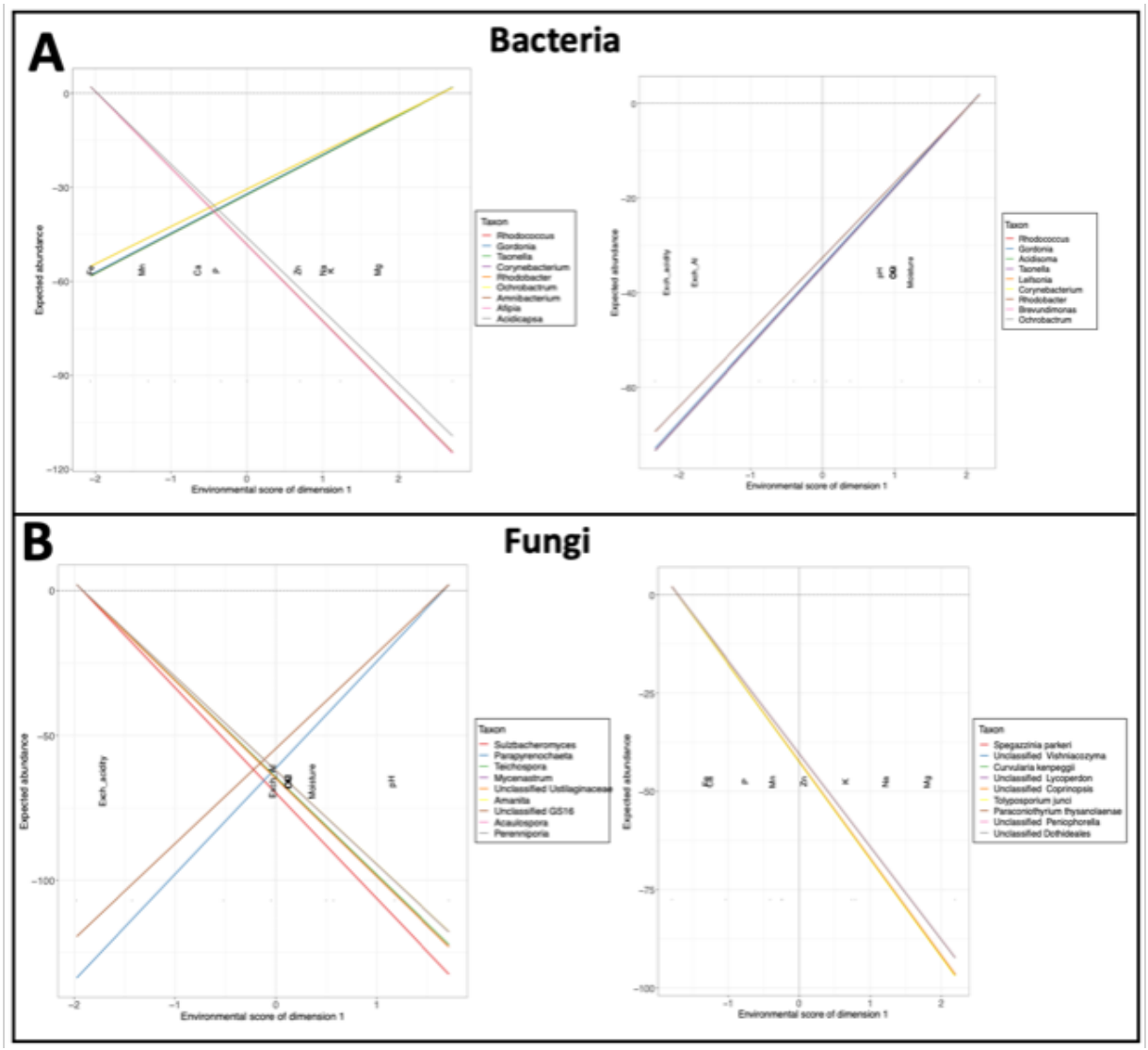


**Figure 2-S3**. Non-parametric analysis of soil factors. A) The influence of soil factors and elements on bacterial abundance, and B) fungi abundance at the genus level.

**Table 2-S1**. Alpha-diversity adjusted p-values of three zones using pairwise Wilcox-test

| | Bacteria | | Fungi | |
|---|---|---|---|---|
| | **Shannon p-value** | **Simpson p-value** | **Shannon p-value** | **Simpson p-value** |
| Bulk soil vs rhizosphere | 0.39 | 0.78 | 0.25 | 0.14 |
| Bulk soil vs endosphere | 0.05 | 0.05 | 0.05 | 0.05 |
| Rhizosphere vs endosphere | 0.02 | 0.05 | 0.02 | 0.02 |

## 2.8. References


Ahkami, A. H., White Iii, R. A., Handakumbura, P. P. and Jansson, C. 2017. Rhizosphere engineering: enhancing sustainable plant ecosystem productivity. *Rhizosphere*, 3, pp. 233-243.

Al-Harahsheh, M., Kingman, S., Somerfield, C. and Ababneh, F. 2009. Microwave-assisted total digestion of sulphide ores for multi-element analysis. *Analytica chimica acta*, 638, pp. 101-105.

Anahid, S., Yaghmaei, S. and Ghobadinejad, Z. 2011. Heavy metal tolerance of fungi. *Scientia Iranica*, 18, pp. 502-508.

Bentley, J., Moore, J. P. and Farrant, J. M. 2019. Metabolomics as a complement to phylogenetics for assessing intraspecific boundaries in the desiccation-tolerant medicinal shrub Myrothamnus flabellifolia (Myrothamnaceae). *Phytochemistry*, 159, pp. 127-136.

Bewley, J. D. 1979. Physiological aspects of desiccation tolerance. Annual review of plant physiology, 30, pp. 195-238.

Bian, J.Y., Fang, Y.L., Song, Q., Sun, M.L., Yang, J.Y., Ju, Y.-W., Li, D.W. and Huang, L. 2021. The Fungal Endophyte Epicoccum dendrobii as a Potential Biocontrol Agent Against Colletotrichum gloeosporioides. *Phytopathology*, 111, 2 pp. 93-303.

Callahan, B. J., Mcmurdie, P. J., Rosen, M. J., Han, A. W., Johnson, A. J. A. and Holmes, S. P. 2016. DADA2: High-resolution sample inference from Illumina amplicon data. *Nature methods*, 13, pp. 581-583.

Đokić, L., Savić, M., Narančić, T. and Vasiljević, B. 2010. Metagenomic analysis of soil microbial communities. *Archives of Biological Sciences*, 62, pp. 559-564.

Edwards, J. A., Santos-Medellín, C. M., Liechty, Z. S., Nguyen, B., Lurie, E., Eason, S., Phillips, G. and Sundaresan, V. 2018. Compositional shifts in root-associated bacterial and archaeal microbiota track the plant life cycle in field-grown rice. *Public Library of Science biology*, 16, pp. 2003862.

Erhabor, J., Komakech, R., Kang, Y., Tang, M. and Matsabisa, M. 2020. Ethnopharmacological importance and medical applications of Myrothamnus flabellifolius Welw.(Myrothamnaceae)-A review. *Journal of ethnopharmacology*, 252, pp. 112576.

Fan, X., Tang, J., Nie, L., Huang, J. and Wang, G. 2018. High-quality-draft genome sequence of the heavy metal resistant and exopolysaccharides producing bacterium Mucilaginibacter pedocola TBZ30T. *Standards in Genomic Sciences*, 13, pp. 1-8.

Farrant, J. M. 2000. A comparison of mechanisms of desiccation tolerance among three angiosperm resurrection plant species. *Plant Ecology*, 151, pp. 29-39.

Farrant, J. M. and Kruger, L. 2001. Longevity of dry Myrothamnus flabellifolius in simulated field conditions. *Plant Growth Regulation*, 35, pp. 109-120.

Fitzpatrick, C. R., Copeland, J., Wang, P. W., Guttman, D. S., Kotanen, P. M. and Johnson, M. T. 2018a. Assembly and ecological function of the root microbiome across angiosperm plant species. *Proceedings of the National Academy of Sciences*, 115, pp. 1157-1165.

Fitzpatrick, C. R., Lu-Irving, P., Copeland, J., Guttman, D. S., Wang, P. W., Baltrus, D. A., Dlugosch, K. M. and Johnson, M. T. 2018b. Chloroplast sequence variation and the efficacy of peptide nucleic acids for blocking host amplification in plant microbiome studies. *Microbiome*, 6, pp. 1-10.

Gaff, D. F. 1989. Responses of desiccation tolerant 'resurrection'plants to water stress. In Structural and functional responses to environmental stresses, pp. 255-268.

Gao, C., Montoya, L., Xu, L., Madera, M., Hollingsworth, J., Purdom, E., Singan, V., Vogel, J., Hutmacher, R. B. and Dahlberg, J. A. 2020a. Fungal community assembly in drought-stressed sorghum shows stochasticity, selection, and universal ecological dynamics. *Nature communications*, 11, pp. 1-14.

Gao, L., Sun, H., Xu, M. and Zhao, Y. 2020b. Biocrusts resist runoff erosion through direct physical protection and indirect modification of soil properties. *Journal of Soils and Sediments*, 20, pp. 133-142.

Hartman, K. and Tringe, S. G. 2019. Interactions between plants and soil shaping the root microbiome under abiotic stress. *Biochemical Journal*, 476, pp. 2705-2724.

Hilhorst, H. W. and Farrant, J. M. 2018. Plant desiccation tolerance: a survival strategy with exceptional prospects for climate-smart agriculture. *Annual Plant Reviews Online*, pp. 327-354.

Kato, Y. and Okami, M. 2011. Root morphology, hydraulic conductivity and plant water relations of high-yielding rice grown under aerobic conditions. *Annals of Botany*, 108, pp. 575-583.

Kennedy, A. C. and De Luna, L. Z. 2005. Rhizosphere. In: Hillel, D. (ed) Encyclopedia of Soils in the Environment. Elsevier, Oxford, pp. 2200.

Khan, A. L., Waqas, M., Kang, S.-M., Al-Harrasi, A., Hussain, J., Al-Rawahi, A., Al-Khiziri, S., Ullah, I., Ali, L. and Jung, H.-Y. 2014. Bacterial endophyte Sphingomonas sp. LK11 produces gibberellins and IAA and promotes tomato plant growth. *Journal of Microbiology*, 52, pp. 689-695.

Kielak, A. M., Cipriano, M. A. and Kuramae, E. E. 2016. Acidobacteria strains from subdivision 1 act as plant growth-promoting bacteria. *Archives of microbiology*, 198, pp. 987-993.

Kranner, I., Beckett, R. P., Wornik, S., Zorn, M. and Pfeifhofer, H. W. 2002. Revival of a resurrection plant correlates with its antioxidant status. *The Plant Journal*, 31, pp. 13-24.

Leborgne-Castel, N., Adam, T. and Bouhidel, K. 2010. Endocytosis in plant–microbe interactions. *Protoplasma*, 247, pp. 177-193.

Liu, T.-Y., Ye, N., Wang, X., Das, D., Tan, Y., You, X., Long, M., Hu, T., Dai, L., Zhang, J. and Chen, M.-X. 2021. Drought stress and plant ecotype drive microbiome recruitment in switchgrass rhizosheath. *Journal of Integrative Plant Biology*, 63, pp. 1753-1774.

Lizumi, T. and Ramankutty, N. 2016. Changes in yield variability of major crops for 1981–2010 explained by climate change. *Environmental research letters*, 11, pp. 034003.

Ma, C., Wang, H., Macnish, A. J., Estrada-Melo, A. C., Lin, J., Chang, Y., Reid, M. S. and Jiang, C.-Z. 2015. Transcriptomic analysis reveals numerous diverse protein kinases and transcription factors involved in desiccation tolerance in the resurrection plant Myrothamnus flabellifolia. *Horticulture Research*, 2, pp. 15034.

Mahapatra, S. and Banerjee, D. 2013. Fungal exopolysaccharide: production, composition and applications. *Microbiology Insights*, 6, pp. 1-16.

Marks, R., Mbobe, M., Greyling, M., Pretorius, J., Mcletchie, D., Vanburen, R. and Farrant, J. 2022. Variability in Functional Traits along an Environmental Gradient in the South African Resurrection Plant Myrothamnus flabellifolia. *Plants*, 11, pp. 1332.

Martin, K. J. and Rygiewicz, P. T. 2005. Fungal-specific PCR primers developed for analysis of the ITS region of environmental DNA extracts. *BMC microbiology,* 5, pp. 1-11.

Moore, J., Waldron, M., Lindsey, G., Farrant, J. and Brandt, W. 2011. An ultrastructural investigation of the surface microbiota present on the leaves and reproductive structures of the resurrection plant Myrothamnus flabellifolia. *South African Journal of Botany*, 77, pp. 485-491.

Moore, J. P., Nguema-Ona, E., Chevalier, L., Lindsey, G. G., Brandt, W. F., Lerouge, P., Farrant, J. M. and Driouich, A. 2006. Response of the leaf cell wall to desiccation in the resurrection plant Myrothamnus flabellifolius. *Plant Physiology,* 141, pp. 651-662.

Moore, J. P., Westall, K. L., Ravenscroft, N., Farrant, J. M., Lindsey, G. G. and Brandt, W. F. 2005. The predominant polyphenol in the leaves of the resurrection plant Myrothamnus flabellifolius, 3, 4, 5 tri-O-galloylquinic acid, protects membranes against desiccation and free radical-induced oxidation. *Biochemical Journal*, 385, pp. 301-308.

Morcillo, R. J. and Manzanera, M. 2021. The effects of plant-associated bacterial exopolysaccharides on plant abiotic stress tolerance. *Metabolites,* 11, pp. 337.

Moreira, F., Giraldo-Silva, A., Roush, D. and Garcia-Pichel, F. 2021. Coleofasciculaceae, a monophyletic home for the Microcoleus steenstrupii complex and other desiccation-tolerant filamentous cyanobacteria*. Journal of Phycology*, 57, pp. 1563-1579.

Naylor, D., Degraaf, S., Purdom, E. and Coleman-Derr, D. 2017. Drought and host selection influence bacterial community dynamics in the grass root microbiome. *The international society for microbial ecology journal*, 11, 2691-2704.

Nilsson, R. H., Larsson, K. H., Taylor, A. F. S., Bengtsson-Palme, J., Jeppesen, T. S., Schigel, D., Kennedy, P., Picard, K., Glöckner, F. O., Tedersoo, L., Saar, I., Kõljalg, U. and Abarenkov, K. 2019. The UNITE database for molecular identification of fungi: handling dark taxa and parallel taxonomic classifications. *Nucleic Acids Research*, 47, pp. D259-d264.

Quast, C., Pruesse, E., Yilmaz, P., Gerken, J., Schweer, T., Yarza, P., Peplies, J. and Glöckner, F. O. 2012. The SILVA ribosomal RNA gene database project: improved data processing and web-based tools. *Nucleic Acids Research*, 41, pp. D590-D596.

Robertson, G. P., Sollins, P., Ellis, B. G. and Lajtha, K. 1999. Exchangeable ions, pH, and cation exchange capacity. In: Sollins, P. (ed) Standard soil methods for long-term ecological research. Oxford University Press, New York, 2, pp. 462.

Sheibani-Tezerji, R., Rattei, T., Sessitsch, A., Trognitz, F. and Mitter, B. 2015. Transcriptome Profiling of the Endophyte Burkholderia phytofirmans PsJN Indicates Sensing of the Plant Environment and Drought Stress. *American Society for Microbiology*, 6, pp. e00621-00615.

Sherwin, H. W., Pammenter, N., February, E., Vander Willigen, C. and Farrant, J. M. 1998. Xylem hydraulic characteristics, water relations and wood anatomy of the resurrection plant Myrothamnus flabellifolius Welw. *Annals of Botany*, 81, pp. 567-575.

Sheteiwy, M. S., Abd Elgawad, H., Xiong, Y. C., Macovei, A., Brestic, M., Skalicky, M., Shaghaleh, H., Alhaj Hamoud, Y. and El-Sawah, A. M. 2021a. Inoculation with Bacillus amyloliquefaciens and mycorrhiza confers tolerance to drought stress and improve seed yield and quality of soybean plant. *Physiologia Plantarum*, 172, pp. 2153-2169.

Sheteiwy, M. S., Ali, D. F. I., Xiong, Y.-C., Brestic, M., Skalicky, M., Hamoud, Y. A., Ulhassan, Z., Shaghaleh, H., Abdelgawad, H. and Farooq, M. 2021b. Physiological and biochemical responses of soybean plants inoculated with Arbuscular mycorrhizal fungi and Bradyrhizobium under drought stress. *BMC plant biology*, 21, pp. 1-21.

Skz, A., Vardharajula, S. and Vurukonda, S. S. K. P. 2018. Transcriptomic profiling of maize (Zea mays L.) seedlings in response to Pseudomonas putida stain FBKV2 inoculation under drought stress. *Annals of Microbiology*, 68, pp. 331-349.

Srinivasagam, K., Natarajan, B., Raju, M. and Selvan, R. K. 2013. Myth and mystery of soil mycorrhiza: a review. *African Journal of Agricultural Research*, 8, pp. 4706-4717.

Steinwender, B. M., Enkerli, J., Widmer, F., Eilenberg, J., Kristensen, H. L., Bidochka, M. J. and Meyling, N. V. 2015. Root isolations of Metarhizium spp. from crops reflect diversity in the soil and indicate no plant specificity. *Journal of invertebrate pathology*, 132, pp. 142-148.

Su, P., Sui, C., Li, J., Wan, K., Sun, H., Wang, S., Liu, X. and Guo, S. 2023. The Aux/IAA protein TaIAA15-1A confers drought tolerance in Brachypodium by regulating abscisic acid signal pathway. *Plant Cell Reports*, 42, pp. 385-394.

Tebele, S. M., Marks, R. A. and Farrant, J. M. 2021. Two Decades of Desiccation Biology: A Systematic Review of the Best Studied Angiosperm Resurrection Plants. *Plants*, 10, pp. 2784.

Timmusk, S., Kim, S.-B., Nevo, E., Abd El Daim, I., Ek, B., Bergquist, J. and Behers, L. 2015. Sfp-type PPTase inactivation promotes bacterial biofilm formation and ability to enhance wheat drought tolerance. *Frontiers in Microbiology*, 6, pp. 387.

Tomer, S., Suyal, D.C., Goel, R. 2016. Biofertilizers: A Timely Approach for Sustainable Agriculture. In: Choudhary, D., Varma, A., Tuteja, N. (eds) Plant-Microbe Interaction: *An Approach to Sustainable Agricultur*e. Springer, Singapore.

Urbanek, S. 2022. R for macOS [Online]. Cran.R-project. Available: https://cran.r-project.org/bin/macosx/ [Accessed 02 February 2022].

Vaseva, I., Sabotič, J., Šuštar-Vozlič, J., Meglič, V., Kidrič, M., Demirevska, K. and Simova-Stoilova, L. 2012. The response of plants to drought stress: the role of dehydrins, chaperones, proteases and protease inhibitors in maintaining cellular protein function. *Droughts: new research*, 1, pp. 1-45.

Walker-Black, I. 1934. An examination of the Degtajareff method for soil organic matter determination and a proposed modification of the chronic acid titration. *Soil Science*, 37, pp. 29-38.

Xu, L., Naylor, D., Dong, Z., Simmons, T., Pierroz, G., Hixson, K. K., Kim, Y.-M., Zink, E. M., Engbrecht, K. M. and Wang, Y. 2018. Drought delays development of the sorghum root microbiome and enriches for monoderm bacteria. *Proceedings of the National Academy of Sciences*, 115, pp. E4284-E4293.

Yadav, A. N., Kour, D., Kaur, T., Devi, R., Yadav, A., Dikilitas, M., Abdel-Azeem, A. M., Ahluwalia, A. S. and Saxena, A. K. 2021. Biodiversity, and biotechnological contribution of beneficial soil microbiomes for nutrient cycling, plant growth improvement and nutrient uptake. *Biocatalysis and Agricultural Biotechnology*, 33, pp. 102009.

Zheng, X., Song, W., Guan, E., Wang, Y., Hu, X., Liang, H. and Dong, J. 2020. Response in physicochemical properties of tobacco-growing soils and N/P/K accumulation in tobacco plant to tobacco straw biochar. *Journal of Soil Science and Plant Nutrition*, 20, pp. 293-305.

# Chapter Three

## Metatranscriptomic analysis reveals microbial survival strategies in desiccated roots of *Myrothamnus flabellifolia*

### 3.1. Summary

Plant microbiome studies have demonstrated that microorganisms increase drought tolerance in the host plant. However, the adaptation mechanisms used by root-associated bacteria of resurrection plants remain poorly explored. Here, metatranscriptomics was used to analyse bacterial gene expression in the microbiome of the resurrection plant *Myrothamnus flabellifolia* roots. This study aimed to characterise the functional response of the microbial communities within the roots and on the rhizoplane of *M. flabellifolia* under dehydration and rehydration conditions in the field. Drought stress resulted in a shift in bacterial taxonomy and gene expression. These results showed that most expressed genes were derived from *Pseudomonadota* and *Bacillota* phyla. Whereas, *Bacillot*a and *Actinomycetota* also exhibited an increased abundance upon rehydration. Analysis of differentially expressed genes showed an upregulation of transcripts mainly involved in respiration (cytochrome oxidase, ATP synthases), drought stress response (Dnak, HSP20, antioxidant, kinases and osmolytes), and photosynthesis (PsbB and Ycf9) in response to drought stress. Interestingly, transcripts belonging to regulation and cell signalling metabolism (anti-sigma regulatory factor) were only highly expressed in dehydrated roots, but not in rehydrated roots. In the rehydrated roots, several abundant transcripts were related to protein synthesis metabolism such as carbohydrate transporter proteins, phosphatase, polysaccharides and ECF sigma factor enzymes. Overall, dehydration was associated with the induction of genes potentially involved in stress response, while rehydration led to the expression of genes related to symbiotic interactions and plant growth promotion. Root-associated bacteria of *M. flabellifolia* showed stress-responsive transcriptional patterns analogous to those reported in desiccation tolerance, suggesting that drought may drive convergent evolutionary adaptations in both plant and microbial lineages.

## 3.2. Introduction

Within soil microenvironments, a diverse array of belowground microbiomes exists, with some specifically selected to reside in proximity to root systems. The diversity and composition of microbial communities in the rhizosphere are contingent upon the plant species and prevailing environmental conditions. Functioning as a reservoir, rhizosphere soil host beneficial microbes that colonise the root surface (rhizoplane) and exert influence over the root-associated microbiome (Frank et al., 2017). Previous studies have demonstrated that introducing root-associated bacteria and fungi in agricultural settings enhances plant growth and improves resilience against both abiotic and biotic stresses (Adeleke et al., 2021). Undoubtedly, the root-associated microbiome plays a pivotal role in the plant life cycle under diverse environmental conditions. However, the intricate interaction between plant roots and microbes requires further investigation.

The functional dynamics of root-associated microbes under drought stress, particularly in resurrection plants, are intricate and remains unknown. Undoubtedly, root-associated microbes (on the rhizoplane or within plant tissues) encounter severe drought stress (Byregowda et al., 2022). The scarcity of information regarding the microbiome of resurrection plants gives rise to several research questions. Does the microbiome employ drought-responsive mechanisms, analogous to plants? And to what extent do the defense mechanisms of bacteria influence the plant host at the transcriptional level? Addressing these questions is crucial, requiring the use of robust, sensitive, and pertinent investigative methods. While culture-dependent techniques have their merits, they come with limitations, particularly in identifying uncultivable microorganisms. Despite this drawback, these methods remain contributory in ultimate characterisation of novel species and have enabled industrial applications for enhancing the growth and resilience of agricultural crops (Hayden et al., 2018). Conversely, the application of next-generation sequencing (NGS) techniques offers different advantages such as minimal bias in microbial identification, the ability to detect unculturable taxa and high resolution quantification of changes in taxa abundance and gene expression, making it a preferred choice for discerning plant-microbe interactions (Hinsu et al., 2021). Hence, it is imperative to explore and utilise both culture-independent and culture-based techniques for a comprehensive understanding of root-associated microbes under drought stress.

A previous transcriptomics study on the leaves of *Myrothamnus flabellifolia* showed that desiccation is associated with the upregulation of late embryogenesis abundant (LEA) proteins and sucrose phosphate synthase genes, among other stress-responsive pathways (Ma et al., 2015). However, the root and soil microbiomes also respond to the stress of desiccation and may even play a role in improving the resilience of the host plant. For instance, a recent rhizosphere metatranscriptome study

revealed the upregulation of oxidative, osmotic and heat stress-related genes in *Burkholderiales* and *Rhodospirillales* under stressful conditions (Tartaglia et al., 2023). Presumably, the upregulation of microbial genes are known to combat their osmotic stress, however, it is also possible that these microbial defense mechanisms might also enhance the drought tolerance of the host plant. For instance, *Actinomycetota* within sorghum roots are thought to improve drought tolerance of the host plant by modulating secondary metabolite biosynthesis, carbohydrate and amino acid transporters, which improved drought tolerance (Xu et al., 2018). In this and other examples the interaction with root-associated microbes positively impacts plant growth and resilience of plant against drought stress.

Metatranscriptomics provides a snapshot of transcript abundance (mRNA) and associated metabolic processes within microbial communities (Hayden et al., 2018; Yergeau et al., 2018). An illustration of its efficacy lies in the detection of upregulated microbial genes encoding plant growth hormones, such as indole-3-acetate, which enhances mutualistic interactions within seagrasses (Crump et al., 2018). While metatranscriptomics has been applied to elucidate the functional role of active microbes within plants under drought stress, its utilisation in resurrection plants remains limited (Shakya et al., 2019). Exploring this technology in the context of resurrection plants, specifically to understand how their microbiomes respond to severe drought conditions, holds promise for revealing instances where microbes may mirror or enhance response of the host plant. The diversity of microbial communities harboured by *M. flabellifolia*, as indicated in Chapter Two (Tebele et al., 2023), suggests that these bacteria may express drought-responsive genes contributing to overall desiccation tolerance. In light of these considerations, this study hypothesizes that drought stress may reshape microbial composition, and root-associated bacteria may respond to drought through the expression of relevant genes. The aim of this study was to characterise gene expression changes in the root-associated bacterial microbiome of *M. flabellifolia* under drought stress and upon rehydration, in order to understand the functional dynamics of bacteria.

## 3.3. Materials and Methods

### 3.3.1. Sampling Procedure

The roots and rhizosphere soil of *Myrothamnus flabellifolia* were collected in the Swebeswebe field site between the 7$^{th}$ and 18$^{th}$ of January 2022. Plants were selected based on health status, an equal number of males and females, and similar height and size. The sampling procedure was designed in a way to minimise damage to the plant. Sampling was conducted during a natural dehydration event at two time points: 0 hours (when leaves appeared partially dry) and 48 hours (when plants were visibly

desiccated), as shown in Figure 3-1A. After collecting the desiccated samples at 48 hours, a simulated rehydration was applied 24 hours later. Water was applied directly to the plant base using a hosepipe connected to a portable fire water tank (see Supplementary Figure 3-S1). Following this rehydration treatment, additional samples were collected at two recovery intervals: 12 and 24 hours post-rehydration (Figure 3-1D, E). The relative water content (RWC) of leaves and roots was measured according to Ginbot and Farrant (2011) for each sampling point and RWC was calculated using Equation 1. Root samples were collected at four-time points: 1) partially dry (39,78 ± 6.55 % RWC), 2) desiccated (10.86 ± 0.64 % RWC), 3) partially rehydrated (43 ± 7.72 % RWC), and 4) fully rehydrated (81.25 ± 3.77 % RWC) as shown in Figure 3-1B-E.

$$RWC(\%) = [FW - DW]/(TW - DW)] \times 100 \quad \text{(Equation 1)}$$

Six biological plant replicates were sampled at each time point. A sterilised shovel was used to excavate around the roots to a depth of ~ 10-15 cm deep and the exposed roots with rhizosphere soil were carefully cut from the mother plant and removed. These root tissues were shaken gently to remove bulk soil and then vigorously to obtain the rhizosphere soil. Ribonucleic acid (RNA) molecules are unstable and rapidly degrade, therefore, no further sterilisation was applied. Samples were immediately flash-frozen in liquid nitrogen. Roots with small particles of soil (rhizoplane and endosphere) were further used for metatranscriptomic analysis of root-associated bacteria. Therefore, the identified bacterial communities emanate from the endosphere (root tissue) and rhizoplane (root surface). The rhizosphere soil was sieved to remove small root hairs. All samples were immediately placed into liquid nitrogen to prevent degradation and stored in a -80$^{o}$ C freezer for further analysis.

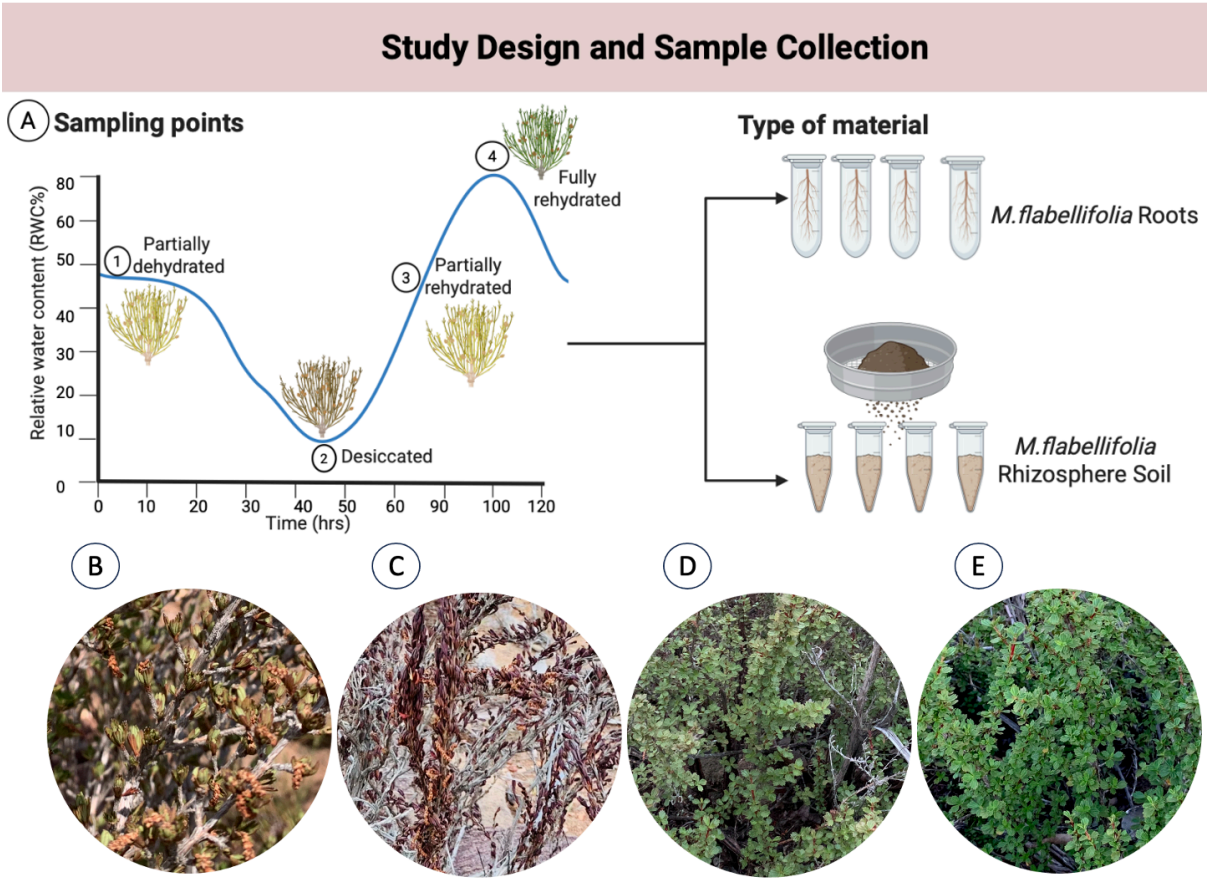


**Figure 3-1.** A) Roots and rhizosphere soil of *Myrothamnus flabellifolia* were sampled at different hours during dehydration and rehydration in the Swebeswebe Nature Reserve. B) *M. flabellifolia* under partial dehydration, C) desiccated, D) partially rehydrated, and E) fully rehydrated in the field.

### 3.3.2. RNA isolation and metatranscriptomic sequencing

The frozen roots (24) and rhizosphere soil (24) were ground in liquid nitrogen using a sterile pestle and mortar, followed by a Retsch mixer mill MM 400 to break down rigid cell walls via rigorous oscillation for 10 minutes at a frequency of 28 Hz. Total RNA from roots and soil samples was isolated according to Majidi and Bahmani (2017) with minor modifications. A Cetyltrimethylammonium bromide (CTAB) buffer was used due to high contents of polyphenols, polysaccharides, tannins and polyquinanes in *M. flabellifolia* (Bentley et al., 2019). Briefly, fine powder of roots was placed in a 1 mL heated CTAB extraction buffer [100 mM Tris-HCl (pH=8), 25 mM $Na_2EDTA$ (pH=8), 3% CTAB (w/v), 2 M NaCl, 3% PVP (MW: 40000) and 1 M sodium citrate] with 50 mL beta-mercaptoethanol and samples were vortexed for 20 sec and incubated at 65°C for 30 mins in the heating block. Samples were vigorously mixed every 10 min, then cooled at room temperature in the fume hood and 50 mL helper buffers were added sequentially. After mixing, 600 mL of chloroform-isoamyl alcohol (24:1, ice cold) was added, mixed and centrifuged at 12 000 rpm for 10 mins at 4°C. The upper phase was transferred into a new 2 mL Eppendorf, 1000 mL of chloroform-isoamyl-alcohol was added, and

samples were centrifuged as previously described. The supernatant was transferred into a new 1.5 mL tube, then 600 mL of 10 M LiCl (ice cold) was added, and samples were placed on ice and stored in the 4°C refrigerator for 24 hours. Then, samples were centrifuged at 12 000 rpm for 30 mins at 4°C and the pellet was washed with 70% ethanol (ice cold). Lastly, RNA samples were treated with DNase I (Thermo Fisher Scientific, USA) and then, RNA was eluted with 40 mL of sterile nuclease-free (DNase and RNase) water.

The quantity and purity of isolated RNA were measured by absorbance at 230, 260 and 280 nm using a NanoDrop ND-1000 UV-Vis Spectrophotometer (Thermo Fisher Scientific, USA). The integrity of RNA was visualised on 2% agarose gel to evaluate the 28S, 18S and 5.8S/5S bands and any degradation. It is worth noting that relatively poor RNA quality was generated from the rhizosphere soil samples (24) even after multiple attempts and troubleshooting a variety of extraction methods. The low yield of RNA was likely due to several factors such as the high content of humic substances, carbohydrates, and RNases in soil, which degrade RNA molecules (Wang et al., 2012). Therefore, rhizosphere soil samples were removed from this study. Out of 24 root samples only 18 passed the quality checks and they were sent for metatranscriptomic sequencing at the Centre for Proteomic and Genomic Research (CPGR). The RNA quality was further analysed using a Qubit 4.0 Fluorometer with fluorescent-based Qubit RNA Broad Range Assay Kit (Thermo Fisher Scientific). The RNA integrity was assessed using Agilent TapeStation 4200. Libraries for 18 samples were prepared using the Illumina Stranded Total RNA Prep kit and ribodepleted by Ribo-Zero Plus. Libraries were sequenced on a NovaSeq 6000 platform with a paired-end run of 2 x 100 bp by CPGR.

### 3.3.3. Bioinformatic and statistical analysis

Metatranscriptome data analysis is a rapidly progressing and emerging technology with pipeline challenges (Shakya et al., 2019). This study adopted the read-based pipelines for prepossessing sequenced data. The Simple Annotation of Metatranscriptomes by Sequence Analysis (SAMSA2) tool, known for quantifying complex microbial gene expression in environmental samples (Westreich et al., 2018), was employed with modifications for RNA-seq data analysis as illustrated in Figure 3-2.

RNAseq of the 18 root-associated bacterial metatranscriptomes generated 981.64 gigabytes (GB) of sequence data. The raw data initially contained both prokaryotic and eukaryotic mRNA. However, the distinction between prokaryotic mRNA and eukaryotic mRNA (from plant roots and fungi) became crucial during annotation, leading to the exclusion of eukaryotic mRNA. Initially, all fastq files for each sample were merged to join forward and reverse reads using PEAR (Zhang et al., 2014). The BBTool package's bbduk.sh component (https://jgi.doe.gov/data-and-tools/software-tools/bbtools/bb-tools-

user-guide/bbduk-guide/) was employed for k-mer matching, quality trimming, removal of adaptor sequences and low-quality reads below a 35 phred score. FastQC assessed the quality of the trimmed reads, and quality reporting for all samples was generated from MultiQC (https://multiqc.info). The riboDetector tool (Deng et al., 2022) was used to eliminate ribosomal RNA (rRNA) sequence residues not depleted by the Ribo-Zero Plus kit.

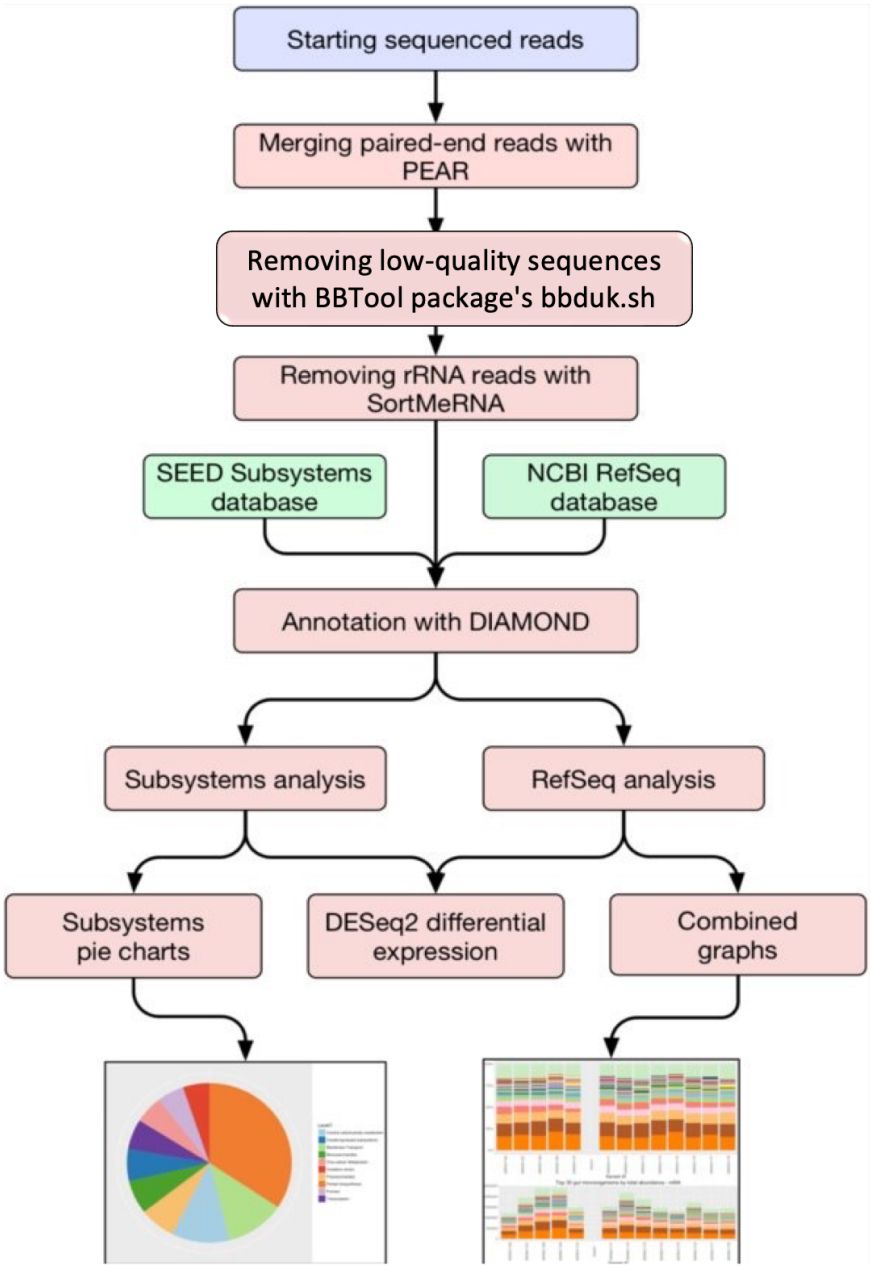


**Figure 3-2**. Metatranscriptome analysis using SAMSA2 pipeline adopted from Westreich et al., (2018).

Reads were annotated using the DIAMOND tool with the National Center for Biotechnology Information (NCBI) prokaryotic reference sequence (RefSeq) database at various taxa for functional annotation(https://www.ncbi.nlm.nih.gov/assembly/?term=(Bacteria%5Borgn%5D+OR+Archaea%5B

orgn%5D)+AND+(latest_refseq%5Bfilter%5D). The NCBI RefSeq database facilitated the annotation of transcripts against bacterial genomes, generating ID for the expressed genes (Figure 3-2). The unmapped sequences were classified as eukaryotic mRNA and subsequently discarded. Therefore, utilising a prokaryotic reference sequence database for transcript annotation allowed the exclusion of eukaryotic and aberrant protein sequences. Additionally, SEED Subsystems were employed to identify upregulated biological processes or pathways through the analysis of the predicted prokaryotic protein sequences (Figure 3-2). The SEED Subsystems is developed as a tool to assign functional roles to the microbiome, its utilises an integrated database from various sources and is predominantly employed in metatranscriptomics and shotgun sequencing studies (OverBeek et al., 2014).

Statistical analysis was performed using RStudio. A Principal Component analysis (PCA) of bacterial taxonomy and total gene expression was used to determine the overall consistency across replicates and variation of the expressed transcripts between nine dehydrated and nine rehydrated samples. DESeq2 R package was used to identify differentially expressed transcripts and taxonomic abundances through Wald test ($p$-value < 0.05) and negative binomial linear models such $\log_2$ fold change with a cut-off of 2 as a threshold between dehydrated and rehydrated conditions. Subsequently, a maximum-likelihood estimates (MLE) plot was constructed using the normalised gene expression counts and $\log_2$ fold change, and volcano and heatmap plots were generated from adjusted $p$-values. One-way analysis of variance (ANOVA) test was used to determine the statistical difference ($P$ < 0.001) between the sampling conditions.

## 3.4. Results

### 3.4.1. Relative water content

Drought stress significantly reduced the RWC of leaves and roots of *M. flabellifolia* in the field setup. Specifically, the RWC of leaves and roots across the four sampling time points showed statistically significant differences ($P$ < 0.001), paralleling the process of de- and re-hydration (Figure 3-3). Although this study is largely focused on the root metatranscriptome, leaf RWC was measured to corroborate the rate of water loss in the shoot tissue and complement measurements of root RWC. These data showed that roots lost water more rapidly compared to leaves. However, at the desiccated state, both plant tissues reached a similarly low RWC of < 11%. Variation in the rate of rehydration was observed in leaves, but the RWC of both leaves and roots after 24 hours stabilised at > 75% RWC. Overall, the rate of water loss in roots was faster than in leaves, but both tissues went through the full cycle of hydrated to desiccated to rehydrated.

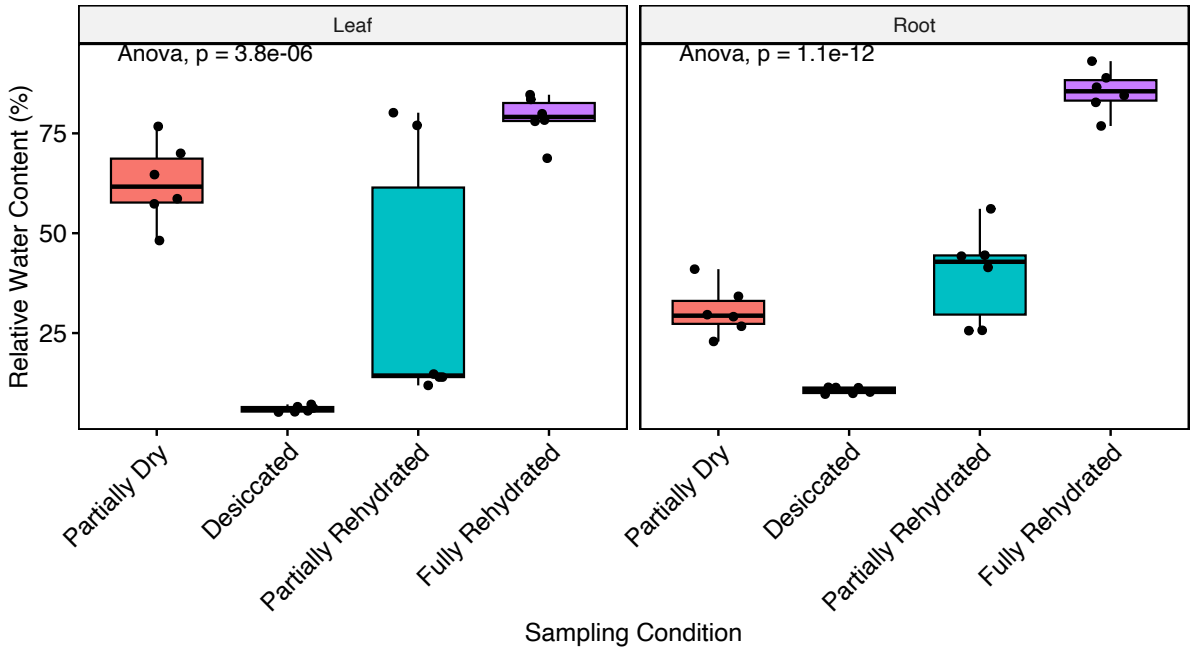


**Figure 3-3.** Effects of dehydration and rehydration on the relative water content (RWC) of leaf and root tissues of *Myrothamnus flabellifolia* in Swebeswebe field site. Plants were sampled at four-time points during the process of dehydration and rehydration.

### 3.4.2. Multivariate analysis of the global metatranscriptome

Sequencing of bacterial RNA from roots of *M. flabellifolia* collected at each of the sampling time points generated 147 996 445 clean reads (mean: 8 222 024, max: 13 116 483, min 867 317). A PCA was used to assess broad patterns of bacterial diversity and gene expression across dehydrated and rehydrated *M. flabellifolia* roots. Dehydrated (partially and desiccated) and rehydrated (partially and fully) samples formed two distinct clusters in PCA plots (Figure 3-4). Consequently, downstream analyses focused on the primary comparison between the two broad categories of dehydration and rehydration. PCA explained a large proportion of the variability in the dataset and separated samples clearly by hydration status for both abundant taxa and gene expression. The first principal component accounted for 44% of the variability in the dataset and the second principal component accounted for 24% of the variability (Figure 3-4A). Similar trends were observed for expressed genes, with PC1 accounting for 61% of the variability and PC2 accounting for another 15% and clear separation between dehydrating and rehydrating samples (Figure 3-4B). These findings suggest that distinct bacterial species were active during dehydration compared to rehydration, despite the similar RWC of partially-dry and rehydrated roots.

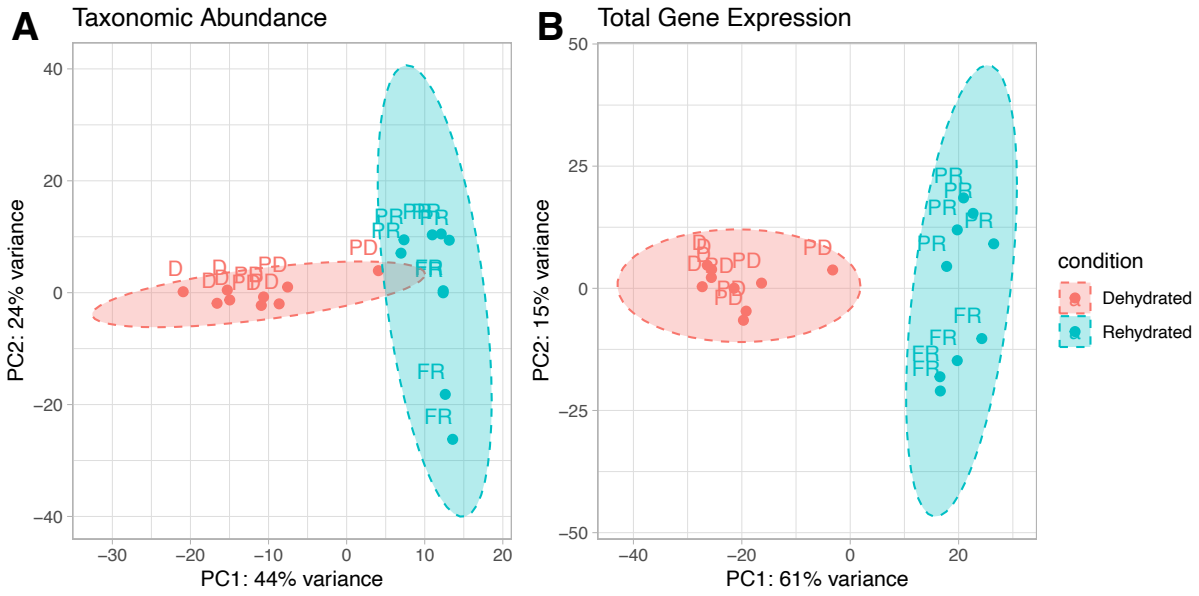


**Figure 3-4.** Principal Component Analysis (PCA) of bacterial transcripts showing A) taxonomic abundance and B) total gene expression. Dehydrated conditions include, partially dehydrated (PD) and desiccated (D). The dehydration condition is colour-coded with a red colour for both species and functional analysis. Rehydrated samples were labelled as partially rehydrated (PR) and fully rehydrated (FR) as indicated with blue colour for species and functional analysis.

### 3.4.3. Taxonomic profiling

Bacterial taxa were classified at the phylum and species level based on the sequenced transcripts. The most abundant transcripts detected in dehydrated and rehydrated conditions were assigned to *Actinomycetota*, *Bacilliota*, *Bacteriota*, *Cyanophyta* (*Cyanobacteriota*) and *Pseudomonadota* (Figure 3-5A). At the species level, a high abundance of *Acinetobacter* species (*Pseudomonadota*) was exhibited across all sampling points (Figure 3-5B). On the other hand, *Conexibacter* species belonging to *Actinomycetota* phyla were highly enriched in the rehydrated condition compared to dehydrated (Figure 3-5B). In desiccated root samples, the most abundant transcripts were assigned to *Pseudomonadota* (14%) and *Bacillota* (7%). Interestingly, *Cyanophyta* was another diderm lineage that exhibited high abundance in desiccated roots. This is further observed at the species level showing enrichment of *Leptolyngbya* species in dehydrated roots. The abundance reduction in monoderm lineages such as *Actinomycetota* and *Bacillota* was observed in dehydrated roots. Both monoderm and diderm lineages were transcriptionally active under drought stress.

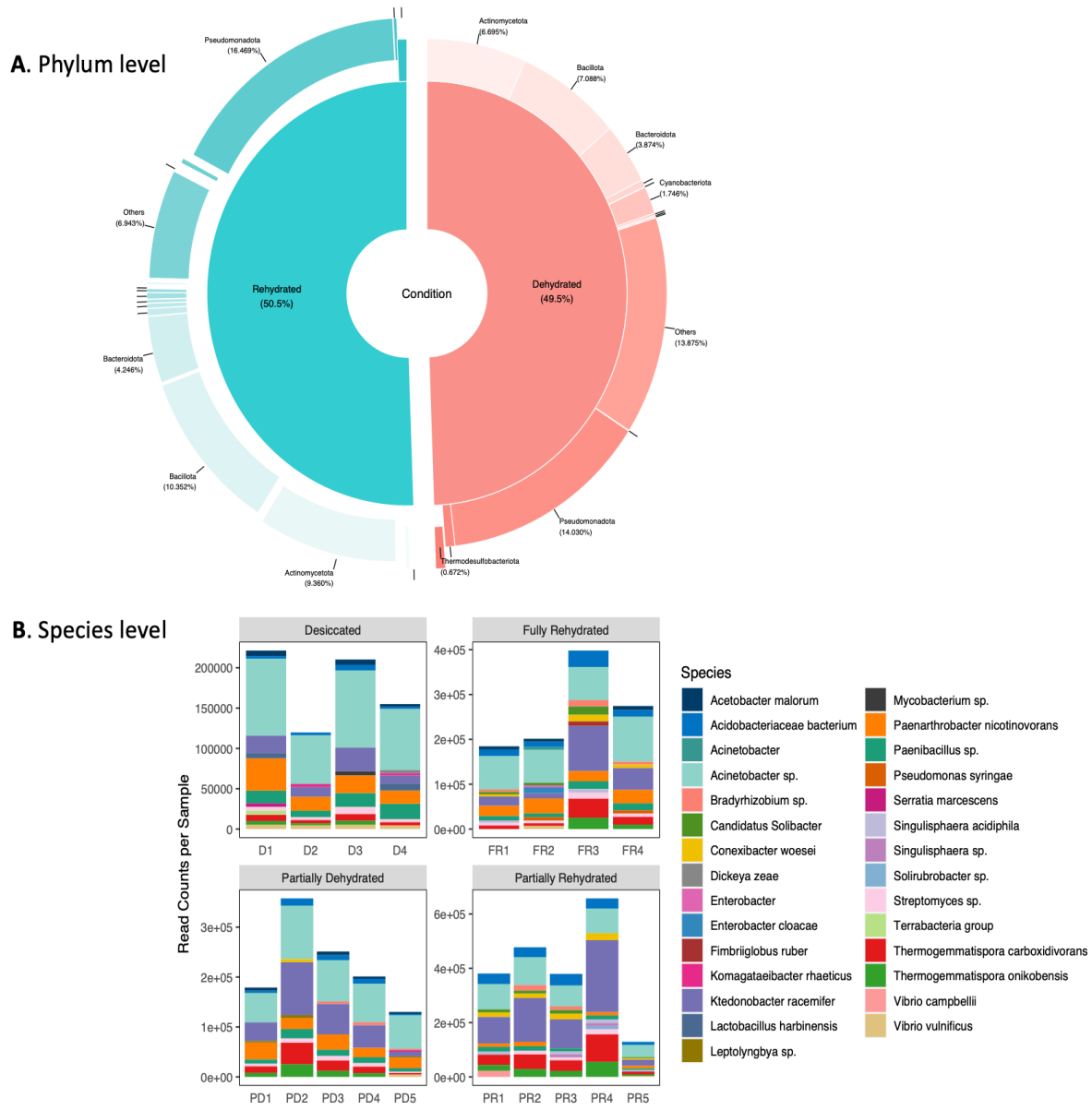


**Figure 3-5.** Taxonomic profiling of A) transcriptionally active bacterial phyla and B) a subset of the most abundant species under dehydration and rehydration. The x-axis on bar plots represents the number of biological replicates.

This study revealed a total of 1764 differentially abundant species and 859 (9,5%) were differentially abundant ($P$ < 0.05) in dehydrated roots, whereas 906 (10%) were differentially abundant in rehydrated samples (Figure 3-S2A). At the species level, under dehydrated conditions the most significantly active species were *Azospirillum halopraeferens*, *Amycolatopsis benzoatilytica*, *Chryseobacterium*, *Eggerthellaceae spp.*, *Ehrlichia ruminantium*, *Kibdelosporagium spp.*, *Myroides odoratus*, *Nostoc spp.*, *Rhizobium anhuiense*, *Rickettsiales spp.*, *Saccharomonospora marina*, *Tolypothrix spp.*, and *Streptoalloteichus hindustanus* (Figure 3-6). Most of these species are plant growth-promoting bacteria (PGPB) that have drought-tolerance traits (Glick, 2012). During the

rehydration phase, the metatranscriptomic analysis revealed active transcription by specific bacterial taxa. These included *Acidobacteriaceae*, *Caulobacter*, *Enterobacter*, *Fimbriiglobus ruber*, *Gemmata obscuriglobus*, *Isosphaera pallida*, *Novosphingobium malaysiense*, *Phenylobacterium*, *Singulisphaera*, and others (Figure 3-6), which mostly belonged to diderm lineage. The transcripts from these bacterial groups have a potential contribution during the rehydration process.

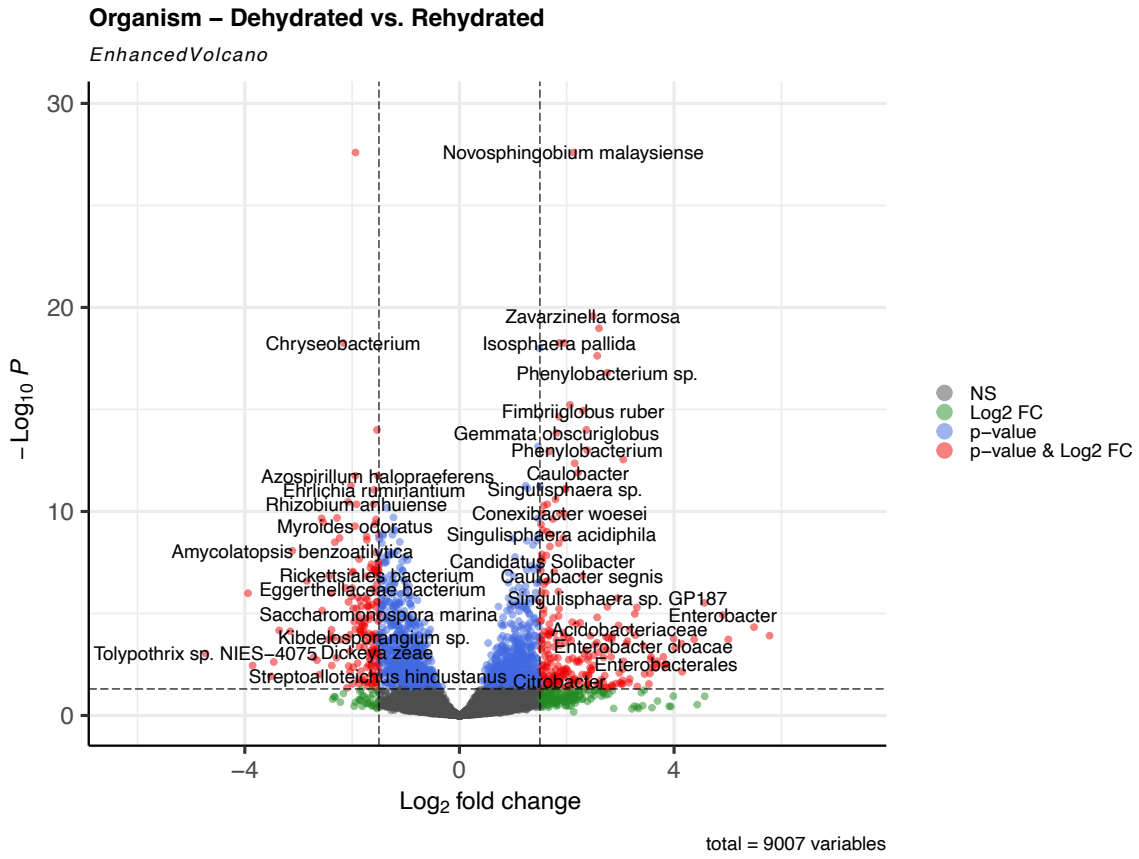


**Figure 3-6.** Volcano plot of top 30 transcriptionally active bacterial species under dehydrated (left side) and rehydrated (right side of the plot) conditions.

### 3.4.4. Functions of differentially abundant transcripts and biological metabolisms

The transcripts were functionally annotated with the NCBI RNA-Seq and SEED subsystems database for expressed genes. Out of 28 290 annotated transcripts, this study identified 2948 differentially expressed genes (DEGs) across both conditions (Figure 3-S2B), with 3.7% (1041) of genes being upregulated under drought stress, and 6.9% (1945) of genes were upregulated under rehydration. Rehydrated root samples had substantially more DEGs relative to dehydrated samples, indicating the resumption of bacterial biochemical processes. DEGs encoding molecular chaperone Dnak, DNA starvation, cytochrome oxidase, ATP synthase, and NADH dehydrogenase were highly abundant in

dehydrated samples (Figure 3-7, 3-S3). In contrast, RNA polymerase and molecular chaperone GroeL genes were only detected in rehydrated samples (Figure 3-S3). These genes encode proteins that are essential in biological pathways involved in abiotic and biotic stress.

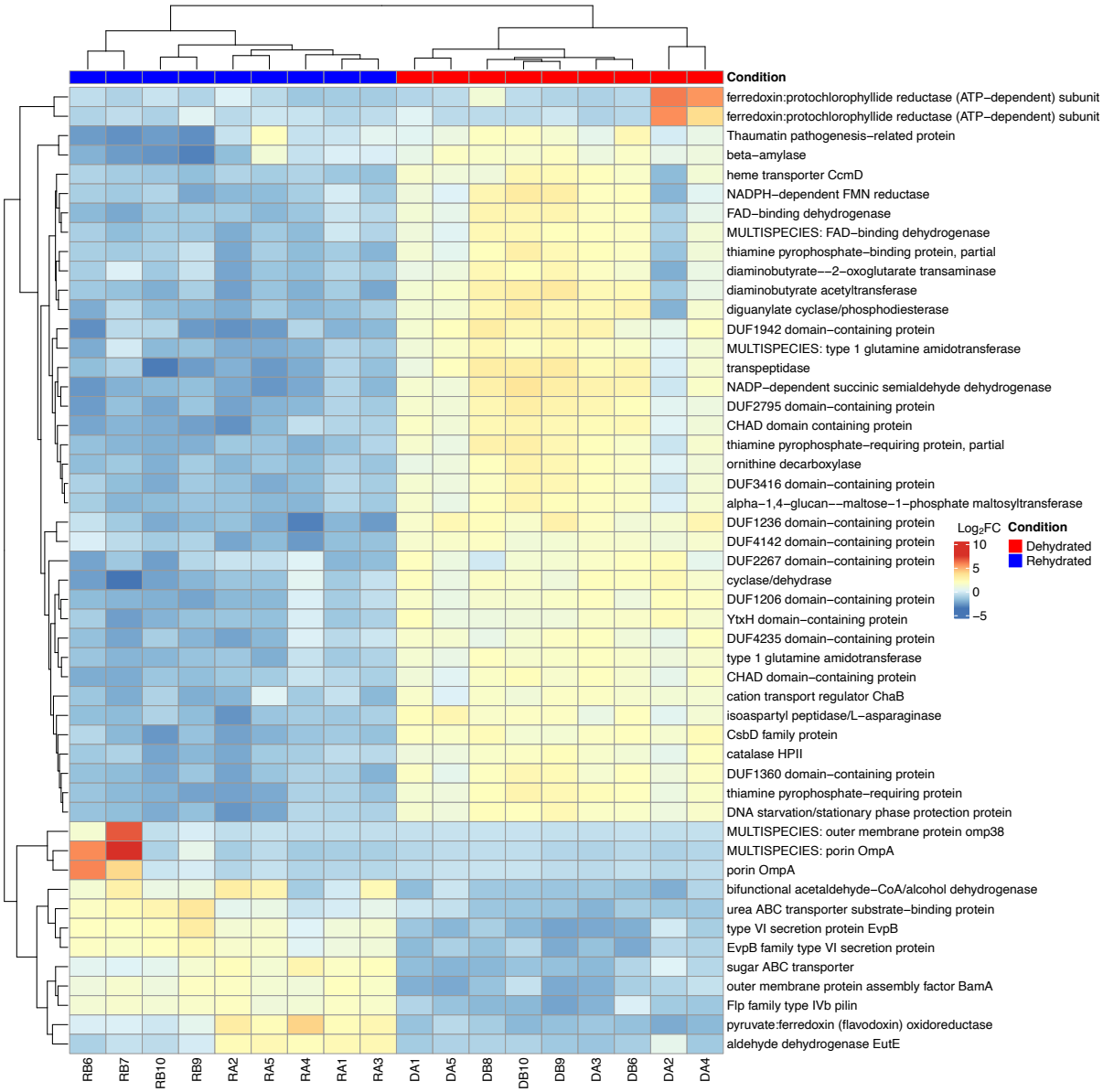


**Figure 3-7.** A heatmap of the top 40 differentially expressed genes (DEGs) of bacteria in roots of *Myrothamnus flabellifolia* under dehydration (red) and rehydration (blue) conditions. The x-axis shows the sample ID.

The functional diversity of bacteria within the roots of *M. flabellifolia* under dehydration and rehydration was further explored using SEED hierarchical subsystems. The most highly transcribed genes were associated with protein biosynthesis metabolism. During dehydration, many of the DEG (24.32%) were also assigned to respiratory metabolism including genes encoding respiratory-chain

NADH dehydrogenase subunit 1, pyruvate oxidase, NAD (+)/NADH kinase, photosystem I P700 chlorophyll and apoprotein A2, and cytochrome oxidase proteins (Figure 3-7, 3-8). Interestingly, under dehydrated conditions transcripts assigned to protein metabolism were associated with a wide range of proteins namely kinases, transcription factors, phosphatases, hydrolases, oxidoreductase, transferase, isomerase, and ligases (Figure 3-8, Table 3-S1). In contrast, rehydration induced the expression of transcripts involved in protein metabolism (23.75%) including genes encoding for electron transfer flavoprotein-ubiquinone oxidoreductase, ATP synthase, phosphoenolpyruvate carboxykinase and pyruvate dehydrogenase genes (Table 3-S1). Although dehydrated roots exhibited lower protein biosynthesis transcripts compared to rehydrated, most transcripts were related to drought-responsive mechanisms. Rehydration condition showed DEGs that encode fatty acid hydrolase, desaturase, complex subunit alpha FadB, long-chain fatty acid acyl-CoA, CoA-ligase were associated with fatty acid biosynthetic pathway.

Many of the DEGs that were elevated under drought stress were related to carbohydrate metabolism, including glycogen synthase, 6-phosphogluconate dehydrogenase, gluconate transporter, stress response protein ysnF, glucosyl-3-phosphoglycerate synthase, sucrose-phosphate synthase, malto-oligosyltrehalose synthase, trehalose-6-phosphate synthase and trehalose synthase genes (Figure 3-8, Table 3-S1). In contrast, carbohydrate metabolism under rehydrated conditions was linked to genes encoding trehalose utilisation, glutamine-fructose-6-phosphate transaminase, polysaccharides biosynthesis and carbohydrate transporter proteins. As expected, stress response metabolism was higher in dehydrated samples relative to rehydrated samples (Figure 3-8). This was likely facilitated by the upregulation of molecular chaperone DnaK, molecular chaperone HtpG, HSP20, proline/glycine betaine ABC transporters, glutamate decarboxylase, superoxide dismutase, peroxidase and NAD-glutamate dehydrogenase genes (Figure 3-7, 3-S3). A significant upregulation of drought-related genes such as catalase-peroxidase, FMN-binding glutamate synthase family protein, HSP70 and glutamate synthase was also observed in rehydrated samples (Figure 3-7, Table 3-S1). The least upregulated metabolism under both conditions were virulence, disease and defense pathways (Figure 3-7). The upregulation of secondary metabolism in rehydrated samples involved many DEGs related to polyhydroxyalkanoate-related proteins and poly(R)-hydroxyalkanoic acid synthase.

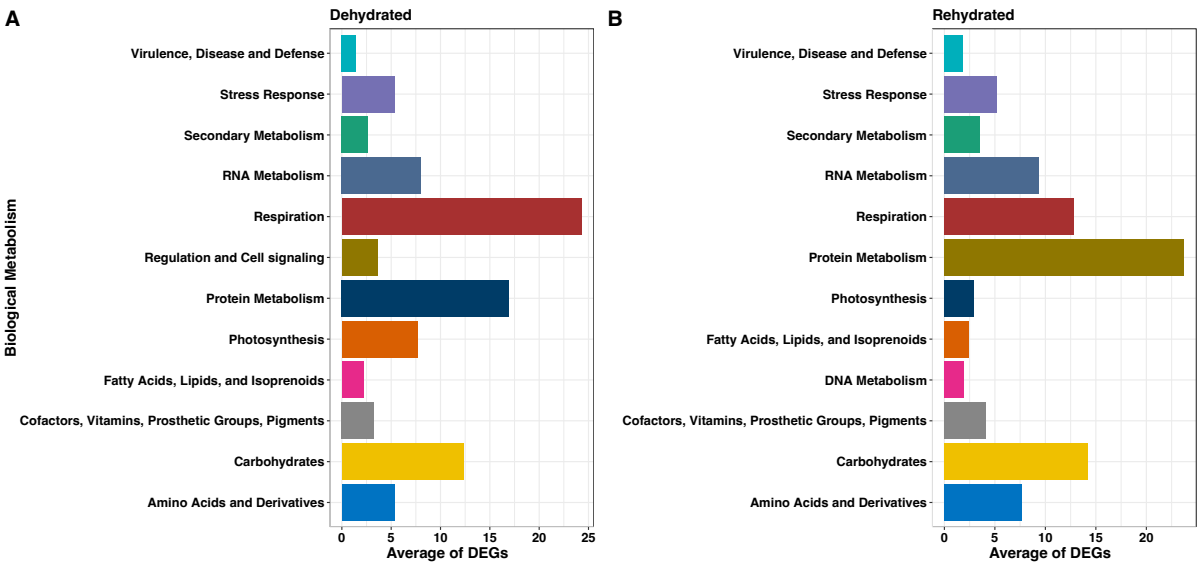


**Figure 3-8.** Functional assignment of bacterial transcripts. A) The proportion of DEGs under drought stress and B) rehydration conditions.

Transcripts related to regulation and cell signalling were only detected in dehydrated samples. These DEGs were related to anti-sigma regulatory factors, iron-related proteins, calcium-translocating P-type ATPase, ferredoxin, sensor histidine protein and serine/threonine kinases (Table 3-S1). The number of transcripts affiliated with photosynthesis under dehydration was significantly higher relative to the rehydration condition (Figure 3-8). Those DEGs were linked to iron-sulfur center protein PsaC, photosystem-related proteins, assembly protein Ycf3, chlorophyll-binding protein CP47 and biogenesis protein Psp29 (Table 3-S1). Additionally, these photosynthesis metabolism transcripts were associated with cyanobacteria lineages including *Tolypothrichaceae*, *Nostocales* cyanobacterium HT-58-2, *Oscillatoriales* cyanobacterium and *Cyanothece* (Figure 3-5, 3-6) and transcripts from these cyanobionts showed increased abundance in dehydrated tissue compared to rehydrated samples, as mentioned previously.

There was an upregulation of DEGs involved in nitrogen metabolism, under rehydrated conditions compared to dehydrated conditions. For instance, an upregulation of nitrate reductase, ammonium transporter, NarK/NasA family nitrate transporter, ammonia channel protein, partial, nitrogen regulation protein NR(I) and nitronate monooxygenase genes were observed (Table 3-S1). In comparison, a DEG of ferredoxin-nitrite reductase was only detected under drought stress conditions (Table 3-S1). Interestingly, DEG of indolepyruvate decarboxylase, which is associated with auxin metabolism, was upregulated in dehydrated samples. Rehydration enriched DEGs that regulate salicylic and jasmonic acids such as salicylaldehyde dehydrogenase and PAP2 family protein,

respectively, were evident. Overall, root-associated bacteria were affected by drought stress resulting in higher expression of genes related to defense mechanisms.

## 3.5. Discussion

This study was designed to test the effects of drought stress on microbiome function on the surface of and within the roots of *M. flabellifolia* using transcriptional profiling of bacterial communities. It is essential to note that different aspects of microbiome function can be investigated at the transcriptional level compared to taxonomic profiling using amplicon-metagenomic techniques (e.g., 16S rRNA and ITS amplicon sequencing, see Chapter Two). Metatranscriptomic analysis provides a high-resolution characterisation of active bacteria and their gene expression. This study sought to understand the responses of root-associated bacteria within *M. flabellifolia* during desiccation and rehydration. While bacteria in the rhizosphere soil could not be analysed, the assumption was made that bacterial transcripts isolated from the roots might include some tightly adhering rhizoplane bacteria. In this study, distinct signatures of desiccation tolerance were identified in the bacterial community during dehydration and characteristic responses to rehydration were evident. In addition, this study detected changes in the expression of critical drought-responsive genes including superoxide dismutase, and other antioxidants that likely play important roles in enhancing desiccation tolerance (Rais et al., 2017) of both the microbiome and host plant, *M. flabellifolia*.

### 3.5.1. Taxonomic profiling

The composition of the bacterial community depends on numerous factors such as plant species, abiotic stresses, biotic interactors, and stochastic events. The effect of drought stress on the root microbiome of resurrection plants is an emerging area of research (Chapter Two; Tebele et al., 2023) and the current results provide new insight into the role of the microbiome in desiccation tolerance. Monoderm bacteria are typically characterised by a thicker peptidoglycan layer and are predominantly classified as gram-positive, whereas diderm bacteria have a thinner peptidoglycan layer and are primarily gram-negative (Xu et al., 2017). While the presence of both monoderm and diderm bacterial groups is not unexpected, a substantial number of transcripts under drought stress were assigned to *Pseudomonadota* (diderm), *Actinomycetota*, and *Bacillota* (monoderm), indicating that these lineages were transcriptionally active and potentially involved in microbial drought responses. The current results align with the observed increase in relative abundance of bacterial lineages characterised in both the rhizosphere soil and endosphere of *M. flabellifolia* during desiccated conditions (Chapter Two; Tebele et al., 2023). At the genus level, this study characterised the transcriptional activity of

*Pseudomonadota* such as *Azospririllium sp, Caulobacter sp*, *Leptolyngbya sp*, *Nostoc sp, Pseudomonas sp, Rhizobium sp*, and others, which were also reported in the desiccated rhizosphere soil and endosphere, as illustrated in Figure 2-4 (Chapter Two; Tebele et al., 2023). Taken together, these findings suggest that desiccation has remarkable effects on root-associated microbiome and leads to shift in microbial composition shift.

*Actinomycetota* species produce antimicrobial compounds (Costa and Amoroso, 2014) and confer drought tolerance to the host plant by expressing hydrolase genes (Wang et al., 2019). This study showed an increased abundance of *Kibdelosporangium*, *Paenarthrobacter, Streptomyces, Saccharomonospora*, and *Streptoalloteichus* species in dehydrated roots, which are known for promoting plant growth and antibiotic biosynthesis (Qin et al., 2015; Salimi et al., 2023; Tao et al., 2007). *Paenibacillus spp*. (another monoderm) was significantly abundant under dehydrated conditions and rapidly decreased in the rehydrated conditions. This finding is consistent with previous studies demonstrating that these species are plant growth-promoting rhizobacteria and facilitate drought tolerance (de Albuquerque et al., 2022; Timmusk and Wagner, 1999). These results suggest that diderm and monoderm lineages that were present in the rhizosphere soil or root surface have successfully colonised the roots of *M. flabellifolia*. Overall, monoderm lineages may play a significant role within the roots under drought stress.

The enrichment of transcripts associated with *Azospirillum* and *Rhizobium* genera under desiccation was remarkable (Figure 3-6), which indicates their transcriptional activity during drought stress. These species are primarily known as PGPR that enhance drought tolerance of the host plant (Glick , 2012). This finding was also reported by (Tartaglia et al., 2023), indicating high transcriptional activity of diderm lineages under drought stress. Interestingly, another diderm lineage, *Cyanophyta* phylum was enriched under dehydrated conditions. This includes various species such as *Leptolyngbya* and *Nostoc spp.*, which were also characterised in the desiccated roots of *M. flabellifolia* (Chapter Two, Tebele et al., 2023). These results are in agreement with a study by Liu et al. (2021) who found the enrichment of *Cyanophyta* under drought stress in rhizosheath soil of switchgrass. Cyanobacteria possess valuable traits, including water retention through exopolysaccharide secretion, enhancement of soil stability, and active involvement in carbon and nitrogen cycling (Adams and Duggan, 2008; Lebre et al., 2017; Sneha et al., 2021). These characteristics make them valuable contributors to mitigating drought stress and promoting sustainable agriculture. Overall, it is plausible that environmental stress led to microbiome plasticity, causing a shift towards bacteria responsible for enhancing drought stress.

### 3.5.2. Functional analysis of expressed genes

Water deficit conditions impair the biological and metabolic processes of microbes and plant, causing osmotic stress, loss of integrity of cell membranes and an efflux of reactive oxygen species (ROS) (Farrant et al., 2009; Malik and Bouskill, 2022). Therefore, bacteria residing within the plant tissue are inevitably exposed to plant ROS. This study found that desiccation stress was associated with the upregulation of bacterial genes linked to cell signalling and environmental stress response pathways. The root-associated microbiome showed a widespread response to drought. Regulation and cell signalling processes were detected under drought stress and not in rehydrated samples. The cell signalling process involved the upregulation of genes encoding anti-sigma factors. These findings were consistent with a previous study of the transcriptome of *Burkholderia phytofirmans* showing the activation of signal transduction systems under drought stress (Sheibani-Tezerji et al., 2015). Signal transduction systems are crucial for detecting water-limiting conditions and initiating regulatory cascades that facilitate gene expression responsible for environmental stresses responses (Kocharunchitt et al., 2012). Overall, these findings indicate that bacterial gene expression patterns shift in response to drought stress, potentially contributing to both microbial resilience and may support plant root survival under desiccation conditions.

Most of the upregulated genes under drought stress were related to respiration metabolism. This metabolism is linked with several pathways such as glycolysis, glyoxylate shunt and oxidative phosphorylation and is essential for generating energy (Ahn et al., 2006). This study revealed the constitutive upregulation of ATP-related genes across drought and rehydration time points. However, the SEED subsystem level 1 (Figure 3-S4) showed that ATPase and electron transport and phosphorylation pathways were two-fold greater in dehydrated samples relative to rehydrated roots. This also accords with a study by Sheibani-Tezerji et al. (2015) who also found the activation of oxidative phosphorylation in *B*. *phytofirmans* under water deficit conditions. Another important finding was the upregulation of genes encoding for NAD (+)/NADH kinases (NADKs) only under drought stress. NADKs function in antioxidant systems, which modulate ROS homeostasis and they are the only enzymes that catalyse the phosphorylation of NADH to generate NADPH in almost all living organisms (Li et al., 2018; Wang et al., 2020). The expression of bacterial genes associated with energy generation may be linked to reactive oxygen species (ROS) scavenging processes in the soil and around the root system.

Under rehydrated conditions, there was an increase in the expression of genes related to protein metabolism broadly, whereas only protein kinases such as DUF-related and leucine-rich repeat kinases were observed under drought stress. Interestingly, these receptor-like kinases were also upregulated

in leaves of *M. flabellifolia* under drought stress (Ma et al., 2015) and they are known to transmit osmotic signals in plants (Chen et al., 2021). This demonstrates that root-associated bacteria employ similar mechanisms as the host plant to survive drying and rehydration cycles. The activation of these defense mechanisms suggests that drought has driven the convergent evolution of desiccation tolerance. Many molecular chaperones, HSP20, CsbD, antioxidant, auxin synthesis and oxidative stress genes were elevated under drought relative to rehydration (Figure 3-8, Table 3-S1). The expression of indole-pyruvate dehydrogenase genes indicates that bacteria have an ability to synthesize indole-3-acetic acid (IAA), which may enhance the root growth of the *M. flabellifolia* under drought stress to source water in deeper soil profiles. These findings are similar to previous studies that reported activation of drought stress genes in plant growth-promoting bacteria such as *Azospirillum spp., Enterobacter cloacae, Corynebacterium, Cyanobacteria*, *Bacillus, Pseudomonas,* and *Rhizobium spp.* (Akbar et al., 1999; Kim et al., 2019; Xu et al., 2020, Zhang et al., 2021; Zhu et al., 2022). The upregulated genes under drought included a wide spectrum of ROS scavenging systems (NAD-glutamate dehydrogenase, superoxide dismutase and manganese catalase and peroxidase) which are critical for sustaining homoeostasis within the bacterial cells. Although bacterial gene expression under drought conditions may primarily support microbial survival, these stress-related responses could also enhance host plant fitness.

Desiccation triggered the expression of genes involved in carbohydrate metabolism, particularly those encoding for glycogen and trehalose biosynthesis. The latter consists of three distinct bacterial enzymes, namely malto-oligosyltrehalose synthase, trehalose synthase, and trehalose-6-phosphate synthase, whereas only glycogen synthase was detected for glycogen biosynthesis. Trehalose is a non-reducing disaccharide that stabilises proteins and cell membranes, replaces water molecules, and facilitates vitrification to prevent cell damage (Yobi et al., 2013). The accumulation of trehalose is characteristic of several desiccation tolerant organisms and was previously detected in tardigrades, microorganisms and resurrection plants such as *M. flabellifolia* and *Selaginella lepidophylla* under desiccation (Avonce et al., 2006; Drennan et al., 1993; Farrant et al., 2009; Moore et al., 2007; Nguyen et al., 2022; Yobi et al., 2012). Mechanisms of convergent evolution under extreme drought stress were further evidenced by the upregulation of bacterial genes (TPS, TS and TreY) involved in trehalose biosynthesis. It is possible that the expression of trehalose biosynthesis and proline/glycine betaine ABC transporter ATP-binding genes might result in the accumulation of highly water-soluble osmolytes, which protect bacterial cellular processes under drought stress. Glycogen has been postulated to function in drought stress by reinstating cell size and acting as carbon storage in bacterial cells (Sekar et al., 2020) and is expressed in *Psedomonadota spp.* under drought stress (Cytryn et al., 2007). In contrast, genes that encode trehalose hydrolysis proteins and sucrose synthase were

upregulated under rehydrated conditions, suggesting that trehalose is no longer required and sucrose might serve as a carbon source. It is worth mentioning that genes from carbohydrate metabolism were greater in the rehydrated root microbiome compared to dehydrated samples. Most of the genes were involved in lipopolysaccharides, exopolysaccharide synthesis and carbohydrate transportation. Taken together, carbohydrate metabolism plays a crucial role both in bacteria and plants by enhancing drought tolerance.

It was remarkable to detect proteins associated with photosynthesis under drought stress. Photosynthesis does not occur in the plant root system, therefore, it is certain that these genes emanate from photosynthetic bacteria. Furthermore, it is striking that the photosynthetic genes were expressed at the partially dehydrated state of 25% root RWC. Anoxygenic phototrophic bacteria were only enriched in rehydrated samples. These include genes encoding for photosystem II core protein (Ycf9), chlorophyll biosynthesis (ChlG), chlorophyll cytochrome b6f complex unit (PetG) and regulatory chloroplast proteins (Ycf3 and Ycf4). These results align with a previous study that revealed cyanobacteria have distinct photosynthetic genes compared to the anoxygenic phototrophic bacteria (Mulkidjanian et al., 2006). The expression of molecular chaperone DnaK genes may have the potential to synthesize proteins for repairing PSII under drought stress (Xu et al., 2020). This might have led to the upregulation of photosynthetic genes in preparation for rehydration condition. Furthermore, the expression of photosynthetic genes under partial drought stress has also been reported in a previous transcriptomic analysis of *M. flabellifolia* (Ma et al., 2015).

Genes encoding for various transporters, nitrogen-fixation, exopolysaccharides, phosphatase and ECF sigma factor enzymes were prevalent in rehydrated roots compared to dehydrated roots. These enzymes play a crucial role in phosphorus (P) mobilization and constitutive expression of nitrogen reductase, indicating that root-associated bacteria may improve nutrient acquisition within the roots of *M. flabellifolia*. This finding agrees with a previous study indicating that bacterial phosphate enhances P availability in forest trees (Cabugao et al., 2017) and bacterial nitrate reductase reduces nitrite to ammonia and nitrogen, which is utilised by plant metabolism (Berger et al., 2020). Polysaccharide synthesis and transporter genes were upregulated in bacterial cells during rehydration, indicating microbial responses aimed at maintaining cellular hydration and structural integrity during fluctuating moisture conditions. Overall, dehydration induced drought-responsive genes to combat the stress, whereas rehydration expressed genes were involved in initiated symbiotic interaction and promoting plant growth.

## 3.6. Conclusion

In summary, the interaction between plants and bacteria is an enigmatic phenomenon which remains poorly understood. Notwithstanding, the utilisation of root-associated bacteria is a promising strategy to improve plant tolerance against abiotic and biotic stresses. The application of bacteria in agricultural systems requires a clear understanding of these intricate interactions. This study used metatranscriptomics to characterise the actively transcribed genes of bacteria associated with the roots of *M. flabellifolia* and explore their influence on desiccation stress. Water stress induced many desiccation-responsive genes. These include genes that encodes the cell signalling, molecular chaperone activity, kinases, antioxidant enzymes, trehalose synthase and transporters proteins within the bacterial cells. These findings suggest that root-associated bacteria may express specific genes, pointing to the possibility of convergent evolution driven by drought stress. The association reflects microbial adaptations that support survival under desiccation stress in the root environment of *M. flabellifolia*. Therefore, future studies should consider culture-dependent techniques to screen bacterial species and the application of potential isolates on drought-sensitive plants. Taken together, this study shows that root-associated bacteria of *M. flabellifolia* exhibit functional adaptations to drought stress, including the expression of genes associated with desiccation tolerance, suggesting convergent responses to extreme environmental conditions.

## 3.7. Supplementary

**Figure 3-S1**. Simulation of rainfall using a hose pipe connected to the portable fire water tank and a generator to rehydrate *Myrothamnus flabellifolia* plants in the Swebeswebe field site.

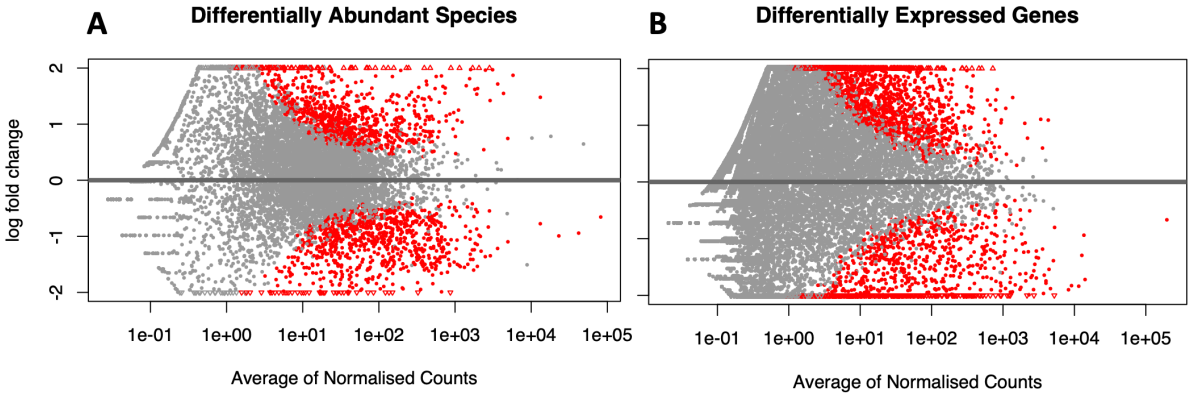


**Figure 3-S2**. Maximum-likelihood estimates (MLE) plot showing A) differentially abundant bacterial species, and B) differentially expressed genes. The significantly different transcripts are highlighted in red with an application of adjusted p-value < 0.05 and log fold change cut-off = 2. The small triangles at the top and bottom of the plot show that points would be outside of the plot.


**Figure 3-S3**. Absolute read counts for the most abundant genes during dehydration and rehydration.

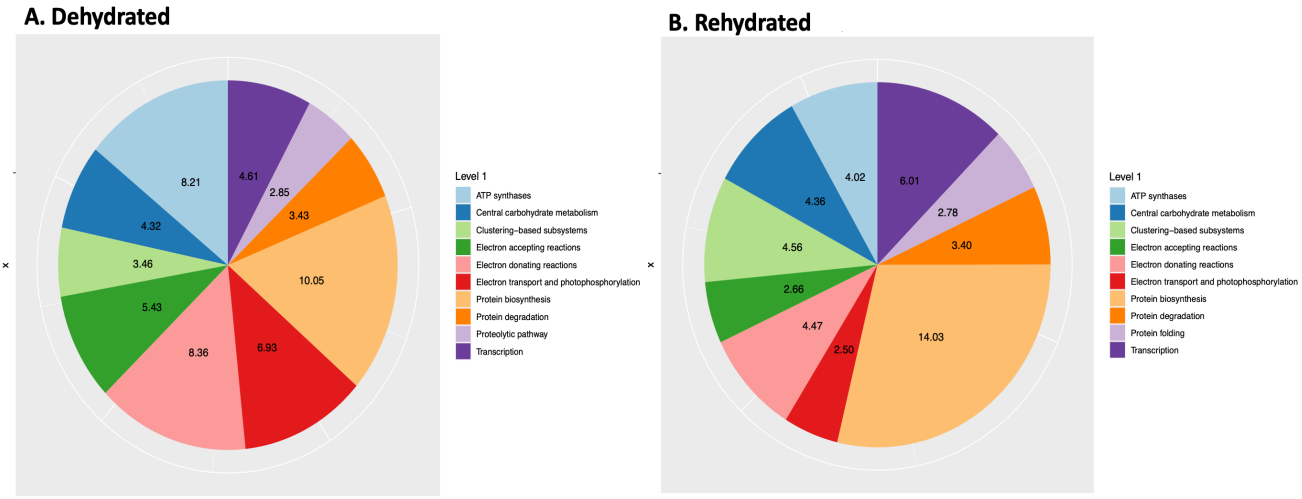


**Figure 3-S4**. Pie chart showing the percentage distribution of bacterial transcripts assigned to the functional metabolism at SEED level 1 under A) drought stress and B) rehydration conditions.

**Table 3-S1**. The functional process of key differentially expressed genes of root-associated bacteria of *Myrothamnus flabellifolia* under dehydration and rehydration.

| Type | Dehydration | Rehydration |
|---|---|---|
| **Kinases** | polyphosphate glucokinase, | ATP synthase |
| | serine/threonine protein | phosphoenolpyruvate carboxykinase (ATP) |
| | acetylglutamate | pyruvate dehydrogenase |
| | sphingosine | two-component system sensor histidine kinase |
| | diacylglycerol kinase catalytic region | signal transduction histidine kinase |
| | phosphoribulokinase | rhamnulokinase |
| | selenide | adenylate kinase |
| | ABC1 family kinase-like protein | adenylyl-sulfate kinase |
| | maltokinase | dihydroxyacetone kinase subunit DhaK |
| | sensor histidine kinase | protein arginine kinase |
| | NAD(+)/NADH kinase | serine protein kinase PrkA |
| | phosphoglycerate kinase | lysine-sensitive aspartokinase 3 |
| | adenylate kinase | GHMP kinase |
| | putative unusual protein kinase | Ser protein kinase |
| | uridine kinase | acetate kinase |
| | acetylaminoadipate kinase | signal transduction histidine kinase |
| | S-methyl-5-thioribose kinase | polyphosphate kinase 1 |
| | hydroxyethylthiazole kinase | bifunctional isocitrate dehydrogenase kinase/phosphatase |
| | ubiquinone biosynthesis regulatory protein kinase UbiB | dTMP kinase |
| | leucine-rich repeat domain-containing protein | pyruvate, phosphate dikinase |
| | ATP synthase subunit C | dihydroxyacetone kinase subunit L |
| | | protein tyrosine kinase |
| | | guanylate kinase |
| | | secretory protein kinase |
| | | carbohydrate kinase family protein |
| | | xylulokinase |
| | | anhydro-N-acetylmuramic acid kinase |
| | | 6-phosphofructokinase |
| | | cytidylate kinase |
| | | protein-tyrosine kinase |

| | | |
|---|---|---|
| **Stress response/Antioxidant** | Peroxidase | catalase-peroxidase<br><br>catalase/hydroperoxidase HPI(I) |
| | Peroxiredoxin<br><br>bifunctional folylpolyglutamate synthase | FMN-binding glutamate synthase family protein |
| | glutamate--cysteine ligase | glutamate synthase |
| | NAD-glutamate dehydrogenase | glutamate formimidoyltransferase |
| | manganese catalase | formimidoylglutamate deiminase |
| | glutamate decarboxylase | glutamate--ammonia ligase |
| | molecular chaperone DnaK | peroxiredoxin |
| | molecular chaperone HtpG | HSP70 |
| | HSP20 | |
| | superoxide dismutase | |
| | peroxidase, peroxiredoxin | |
| | indolepyruvate decarboxylase | |
| | stress response protein ysnF | |
| | catalase HPII | |
| **Carbohydrates** | glycogen debranching enzyme | trehalose utilization protein |
| | trehalose synthase | glutamine--fructose-6-phosphate transaminase |
| | trehalose-6-phosphate synthase | polysaccharide biosynthesis protein |
| | malto-oligosyltrehalose synthase | polysaccharide export protein |
| | sucrose-phosphate synthase | exopolysaccharide biosynthesis protein |
| | glucosyl-3-phosphoglycerate synthase | fructose 2,6-bisphosphatase |
| | Glycogen synthase | 1, 6-phosphofructokinase |
| | gluconate transporter | PTS fructose transporter subunit IIA |
| | 6-phosphogluconate dehydrogenase | polysaccharide ABC transporter ATP-binding protein |
| | maltose alpha-D-glucosyltransferase | GDP-mannose 4,6-dehydratase |
| | glycogen debranching protein | exoglucanase |
| | alpha-1,4-glucan--maltose-1-phosphate maltosyltransferase | glucan endo-1,6-beta-glucosidase |
| | 1,4-alpha-glucan branching enzyme | alpha-glucan family phosphorylase |
| | 4-alpha-glucanotransferase | Sucrose synthase |
| | glucan 1,3-beta-glucosidase | lipopolysaccharide biosynthesis protein RfbH |
| | phosphoglycolate phosphatase | lipopolysaccharide heptosyltransferase II |
| **Essential Elements/Regulation and signalling** | calcium-translocating P-type ATPase | ATP-dependent zinc metalloprotease FtsH 1 |
| | PMCA-type | deacetylase family metallohydrolase |

| | | |
|---|---|---|
| | calcium/proton exchanger | metalloprotease |
| | calcium-transporting P-type ATPase | zinc metalloprotease HtpX |
| | PMR1-type | subclass B3 metallo-beta-lactamase |
| | photosystem I iron-sulfur center protein PsaC | metalloprotease TldD |
| | iron-sulfur cluster scaffold-like protein | metalloendopeptidase-like membrane protein |
| | succinate dehydrogenase iron-sulfur subunit | chemotaxis response regulator protein-glutamate methylesterase |
| | iron-containing redox enzyme family protein | NAD(P)H:quinone oxidoreductase |
| | iron-sulfur cluster biosynthesis protein | |
| | zinc-dependent metalloprotease | |
| | ATP-dependent metalloprotease FtsH | |
| | metallophosphoesterase | |
| | | |
| **Photosynthesis** | iron-sulfur center protein PsaC | photosystem I iron-sulfur center protein PsaC |
| | phosphoglycolate phosphatase | |
| | photosystem reaction center subunit H | |
| | photosystem II D2 protein | |
| | photosystem I core protein PsaA | |
| | photosystem I P700 chlorophyll a apoprotein A1 | |
| | photosystem II core protein PsbZ | |
| | photosystem II 44 kDa subunit reaction center protein | |
| | photosystem I assembly protein Ycf3/4 | |
| | photosystem I iron-sulfur center protein PsaC | |
| | photosystem II chlorophyll-binding protein CP47 | |
| | photosystem II biogenesis protein Psp29 | |
| | chlorophyll synthase ChlG | |
| | cytochrome b6-f complex subunit PetG | |
| **Fatty acids/isoprenoids** | MULTISPECIES: fatty acid desaturase | long-chain-fatty-acyl-CoA reductase |
| | bifunctional demethylmenaquinone methyltransferase/2-methoxy-6-polyprenyl-1,4-benzoquinol methylase | long-chain fatty acid--CoA ligase |
| | c-type cytochrome biogenesis protein CcsB | fatty acid hydroxylase |
| | cytochrome b559 subunit beta | fatty acid desaturase |
| | isopentenyl-diphosphate delta-isomerase | fatty acid oxidation complex subunit alpha FadB |
| | | isoprenyl transferase |

| | | |
|---|---|---|
| | | polyisoprenoid-binding protein |
| | | 3-octaprenyl-4-hydroxybenzoate carboxy-lyase |
| | | undecaprenyl-diphosphate phosphatase |
| | | polyprenyl glycosylphosphotransferase |
| **Transporter** | folate/biopterin family MFS transporter | oxalate/formate MFS antiporter |
| | sugar porter family MFS transporter | BMP family ABC transporter substrate-binding protein |
| | ABC-1 domain-containing protein | glucose/galactose MFS transporter |
| | hydroxyectoine ABC transporter substrate-binding protein EhuB | urea ABC transporter substrate-binding protein |
| | ABC1 family kinase-like protein | sugar ABC transporter |
| | phosphate ABC transporter ATP-binding protein | ABC transporter permease |
| | proline/glycine betaine ABC transporter ATP-binding protein | rhamnose ABC transporter substrate-binding protein |
| | methionine ABC transporter ATP-binding protein | nitrate ABC transporter substrate-binding protein |
| | heme ABC transporter permease | sugar ABC transporter ATP-binding protein |
| | ectoine/hydroxyectoine ABC transporter permease subunit EhuC | branched-chain amino acid ABC transporter permease |
| | secreted chitinase | phosphate ABC transporter substrate-binding protein PstS |
| | ADP/ATP carrier protein | polysaccharide ABC transporter ATP-binding protein |
| | | BMP family ABC transporter substrate-binding protein |
| | | phosphate ABC transporter permease |
| | | D-xylose ABC transporter substrate-binding protein |
| | | arginine ABC transporter substrate-binding protein |
| | | LPS export ABC transporter permease LptG |
| | | molybdate ABC transporter substrate-binding protein |
| | | multidrug ABC transporter substrate-binding protein |
| | | spermidine/putrescine ABC transporter substrate-binding protein |
| | | efflux ABC transporter inner membrane protein |
| **Secondary metabolism** | alkaline and neutral invertase | polyhydroxyalkanoate depolymerase |
| | neutral/alkaline nonlysosomal ceramidase | class I poly(R)-hydroxyalkanoic acid synthase |
| | alkaline ceramidase | polyhydroxyalkanoate synthesis repressor PhaR |

| | | |
|---|---|---|
| | alkaline invertase | epoxyalkane--coenzyme M transferase |
| | YggS family pyridoxal phosphate enzyme | poly(R)-hydroxyalkanoic acid synthase |
| | hemerythrin | pyridoxal phosphate-dependent aminotransferase |
| | | pyridoxine 5'-phosphate synthase |
| | | 12-oxophytodienoate reductase |
| | | Jasmonic acid |
| **Nitrogen and phosphate metabolism** | allantoate amidohydrolase | allantoinase PuuE |
| | threonine ammonia-lyase | ammonium transporter |
| | ferredoxin--nitrite reductase | type I glutamate--ammonia ligase, partial |
| | nitrite reductase | ethanolamine ammonia-lyase |
| | divergent PAP2 family protein (2 phosphatidic acid phosphatase (PAP2)) | ammonia channel protein, partial |
| | phosphatase PAP2 family protein | nitrate ABC transporter substrate-binding protein |
| | | nitrate reductase subunit alpha |
| | | nitrate reductase |
| | | NarK/NasA family nitrate transporter |
| | | nitric-oxide reductase large subunit |
| | | nitrile hydratase subunit beta |
| | | nitric oxide reductase |
| | | nitrilase/cyanide hydratase |
| | | nitrogen regulation protein NR(I) |
| | | NAD(P)H nitroreductase |
| | | nitroreductase family deazaflavin-dependent oxidoreductase |
| | | nitronate monooxygenase |
| | | TAT-dependent nitrous-oxide reductase |

## 3.8. References


Adams, D.G. and Duggan, P.S. 2008. Cyanobacteria–bryophyte symbioses. *Journal of experimental botany*, 59(5), pp.1047-1058.

Adeleke, B.S., Babalola, O.O. and Glick, B.R. 2021. Plant growth-promoting root-colonizing bacterial endophytes. *Rhizosphere*, 20, p.100433.

Ahn, S., Jung, J., Jang, I.A., Madsen, E.L. and Park, W. 2016. Role of glyoxylate shunt in oxidative stress response. *Journal of Biological Chemistry*, 291(22), pp.11928-11938.

Akbar, S., Lee, S.Y., Boylan, S.A. and Price, C.W. 1999. Two genes from bacillus subtilis under the sole control of the general stress transcription factor σb'. *Microbiology*, 145(5), pp. 1069–1078. doi:10.1099/13500872-145-5-1069.

Armada, E., Leite, M.F., Medina, A., Azcón, R. and Kuramae, E.E. 2018. Native bacteria promote plant growth under drought stress condition without impacting the rhizomicrobiome. *Federation of European Microbiological Societies Microbiology Reviews*, 94(7), p.92.

Avonce, N., Mendoza-Vargas, A., Morett, E. and Iturriaga, G. 2006. Insights on the evolution of trehalose biosynthesis. *BMC evolutionary biology*, 6(1) pp.1-15.

Bentley, J., Moore, J.P. and Farrant, J.M. 2019. Metabolomics as a complement to phylogenetics for assessing intraspecific boundaries in the desiccation-tolerant medicinal shrub Myrothamnus flabellifolia (Myrothamnaceae). *Phytochemistry*, 159, pp.127-136.

Berger, A., Boscari, A., Horta Araujo, N., Maucourt, M., Hanchi, M., Bernillon, S., Rolin, D., Puppo, A. and Brouquisse, R. 2020. Plant nitrate reductases regulate nitric oxide production and nitrogen-fixing metabolism during the Medicago truncatula–Sinorhizobium meliloti symbiosis. *Frontiers in plant science*, 11, p.535004.

Byregowda, R., Prasad, S.R., Oelmüller, R., Nataraja, K.N. and Prasanna Kumar, M.K. 2022. Is endophytic colonization of host plants a method of alleviating drought stress? Conceptualizing the hidden world of endophytes. *International Journal of Molecular Sciences*, 23(16), p.9194.

Cabugao, K.G., Timm, C.M., Carrell, A.A., Childs, J., Lu, T.Y.S., Pelletier, D.A., Weston, D.J. and Norby, R.J. 2017. Root and rhizosphere bacterial phosphatase activity varies with tree species and soil phosphorus availability in Puerto Rico tropical forest. *Frontiers in Plant Science*, 8, p.1834.

Carvalhais, L.C., Dennis, P.G., Fan, B., Fedoseyenko, D., Kierul, K., Becker, A., von Wiren, N. and Borriss, R. 2013. Linking plant nutritional status to plant-microbe interactions. Public Library of Science one, 8(7), p.e68555.

Chen, X., Ding, Y., Yang, Y., Song, C., Wang, B., Yang, S., Guo, Y. and Gong, Z. 2021. Protein kinases in plant responses to drought, salt, and cold stress. *Journal of integrative plant biology*, 63(1), pp.53-78.

Compant, S., Cambon, M.C., Vacher, C., Mitter, B., Samad, A. and Sessitsch, A. 2021. The plant endosphere world–bacterial life within plants. *Environmental Microbiology*, 23(4), pp.1812-1829.

Costa, J.S. and Amoroso, M.J. 2014. Current biotechnological applications of the genus Amycolatopsis. *World Journal of Microbiology and Biotechnology*, 30, pp.1919-1926.

Cytryn, E.J., Sangurdekar, D.P., Streeter, J.G., Franck, W.L., Chang, W.S., Stacey, G., Emerich, D.W., Joshi, T., Xu, D. and Sadowsky, M.J. 2007. Transcriptional and physiological responses of Bradyrhizobium japonicum to desiccation-induced stress. *Journal of bacteriology*, 189(19), pp.6751-6762.

Deng, Z.L., Münch, P.C., Mreches, R. and McHardy, A.C. 2022. Rapid and accurate identification of ribosomal RNA sequences via deep learning. *Nucleic acids research*, 50(10), pp.e60-e60.

de Albuquerque, T.M., Mendes, L.W., Rocha, S.M.B., Antunes, J.E.L., Oliveira, L.M.D.S., Melo, V.M.M., Oliveira, F.A.S., Pereira, A.P.D.A., da Silva, V.B., Gomes, R.L.F. and de Alcantara Neto, F. 2022. Genetically related genotypes of cowpea present similar bacterial community in the rhizosphere. *Scientific Reports*, 12(1), p.3472.

Drennan, P.M., Smith, M.T., Goldsworthy, D. and Van Staden, J. 1993. The occurrence of trehalose in the leaves of the desiccation-tolerant angiosperm Myrothamnus flabellifolius Welw. *Journal of plant physiology*, 142(4), pp.493-496.

du Toit, S.F., Farrant, J.M., Faigon, L., Neta-Sharir, I. and Reich, Z. 2021. Physiological characterisation of tissue differentiation in response to desiccation in the homoiochlorophyllous dicot resurrection plant Craterostigma pumilum Hochst. *Environmental and Experimental Botany*, 192, p.104650.

Farrant, J.M. and Kruger, L.A. 2001. Longevity of dry Myrothamnus flabellifolius in simulated field conditions. *Plant Growth Regulation*, 35, pp.109-120.

Farrant, J.M., Lehner, A., Cooper, K. and Wiswedel, S. 2009. Desiccation tolerance in the vegetative tissues of the fern Mohria caffrorum is seasonally regulated. *The Plant Journal*, 57(1), pp.65-79.

Glick, B.R. 2012. Plant growth-promoting bacteria: mechanisms and applications. *Scientifica*, 2012.

Frank, A., Saldierna Guzmán, J. and Shay, J. 2017. 'Transmission of bacterial endophytes', *Microorganisms*, 5(4), p. 70.

Hayden, H.L., Savin, K.W., Wadeson, J., Gupta, V.V. and Mele, P.M. 2018. Comparative metatranscriptomics of wheat rhizosphere microbiomes in disease suppressive and non-suppressive soils for Rhizoctonia solani AG8. *Frontiers in microbiology*, 9, p.859.

Hinsu, A., Dumadiya, A., Joshi, A., Kotadiya, R., Andharia, K., Koringa, P. and Kothari, R. 2021. To culture or not to culture: a snapshot of culture-dependent and culture-independent bacterial diversity from peanut rhizosphere. *Journal of Life & Environmental Sciences*, 9, p.e12035.

Kibido, T., Kunert, K., Makgopa, M., Greve, M. and Vorster, J. 2020. Improvement of rhizobium-soybean symbiosis and nitrogen fixation under drought. *Food and Energy Security*, 9(1), p.177.

Kim, Y.M., Kwak, M.H., Kim, H.S. and Lee, J.H. 2019. Production of Indole-3-acetate in Corynebacterium glutamicum by Heterologous Expression of the Indole-3-pyruvate Pathway Genes. *Microbiology and Biotechnology Letters*, 47(2), pp.242-249.

Kocharunchitt, C., King, T., Gobius, K., Bowman, J.P. and Ross, T. 2012. Integrated transcriptomic and proteomic analysis of the physiological response of Escherichia coli O157: H7 Sakai to steady-state conditions of cold and water activity stress. *Molecular & Cellular Proteomics*, 11(1).

Li, B.B., Wang, X., Tai, L., Ma, T.T., Shalmani, A., Liu, W.T., Li, W.Q. and Chen, K.M. 2018. NAD kinases: metabolic targets controlling redox co-enzymes and reducing power partitioning in plant stress and development. *Frontiers in Plant Science*, 9, p.379.

Liu, T.Y., Ye, N., Wang, X., Das, D., Tan, Y., You, X., Long, M., Hu, T., Dai, L., Zhang, J. and Chen, M.X. 2021. Drought stress and plant ecotype drive microbiome recruitment in switchgrass rhizosheath. *Journal of Integrative Plant Biology*, 63(10), pp.1753-1774.

Ma, C., Wang, H., Macnish, A.J., Estrada-Melo, A.C., Lin, J., Chang, Y., Reid, M.S. and Jiang, C.Z. 2015. Transcriptomic analysis reveals numerous diverse protein kinases and transcription factors involved in desiccation tolerance in the resurrection plant Myrothamnus flabellifolia. *Horticulture research*, 15034 (2), pp.1-12.

Malik, A.A. and Bouskill, N.J. 2022. Drought impacts on microbial trait distribution and feedback to soil carbon cycling. *Functional Ecology*, *36*(6), pp.1442-1456.

Moore, J.P., Hearshaw, M., Ravenscroft, N., Lindsey, G.G., Farrant, J.M. and Brandt, W.F. 2007. Desiccation-induced ultrastructural and biochemical changes in the leaves of the resurrection plant Myrothamnus flabellifolia. *Australian Journal of Botany*, 55(4), pp.482-491.

Moore, J.P., Lindsey, G.G., Farrant, J.M. and Brandt, W.F. 2007a. An overview of the biology of the desiccation-tolerant resurrection plant Myrothamnus flabellifolia. *Annals of botany*, 99(2), pp.211-217.

Monciardini, P., Cavaletti, L., Schumann, P., Rohde, M. and Donadio, S. 2003. Conexibacter woesei gen. nov., sp. nov., a novel representative of a deep evolutionary line of descent within the class Actinobacteria. *International journal of systematic and evolutionary microbiology*, 53(2), pp.569-576.

Naylor, D., DeGraaf, S., Purdom, E. and Coleman-Derr, D. 2017. Drought and host selection influence bacterial community dynamics in the grass root microbiome. *The International Society for Microbial Ecology journal*, 11(12), pp.2691-2704.

Naver, H., Boudreau, E. and Rochaix, J.D. 2001. Functional studies of Ycf3: its role in assembly of photosystem I and interactions with some of its subunits. *The Plant Cell*, 13(12), pp.2731-2745.

Nguyen, K., Kc, S., Gonzalez, T., Tapia, H. and Boothby, T.C. 2022. Trehalose and tardigrade CAHS proteins work synergistically to promote desiccation tolerance. *Communications Biology*, 5(1), p.1046.

Overbeek, R., Olson, R., Pusch, G.D., Olsen, G.J., Davis, J.J., Disz, T., Edwards, R.A., Gerdes, S., Parrello, B., Shukla, M. and Vonstein, V. 2014. The SEED and the Rapid Annotation of microbial genomes using Subsystems Technology (RAST). *Nucleic acids research*, 42(D1), pp. D206-D214.

Qin, S., Feng, W.W., Xing, K., Bai, J.L., Yuan, B., Liu, W.J. and Jiang, J.H. 2015. Complete genome sequence of Kibdelosporangium phytohabitans KLBMP 1111T, a plant growth promoting

endophytic actinomycete isolated from oil-seed plant Jatropha curcas L. *Journal of Biotechnology*, 216, pp.129-130.

Raghavan, V., Kraft, L., Mesny, F. and Rigerte, L. 2022. A simple guide to de novo transcriptome assembly and annotation. *Briefings in bioinformatics*, 23(2), p.563.

Rais, A., Jabeen, Z., Shair, F., Hafeez, F.Y. and Hassan, M.N. 2017. Bacillus spp., a bio-control agent enhances the activity of antioxidant defense enzymes in rice against Pyricularia oryzae. *Public Library of Science one*, 12(11), p.e0187412.

Refai, M.Y., Abulfaraj, A.A., Hakeem, I.J., Shaer, N.A., Alqahtani, M.D., Alomran, M.M., Alotaibi, N.M., Sonbol, H.S., Alhashimi, A.M., Al-Abbas, N.S. and Ashy, R.A. 2023. Rhizobiome Signature and Its Alteration Due to Watering in the Wild Plant Moringa oleifera. *Sustainability,* 15(3), p.2745.

Reinhold, B., Hurek, T., Fendrik, I., Pot, B., Gillis, M., Kersters, K., Thielemans, S. and De Ley, J. 1987. Azospirillum halopraeferens sp. nov., a nitrogen-fixing organism associated with roots of Kallar grass (Leptochloa fusca (L.) Kunth). *International Journal of Systematic and Evolutionary Microbiology*, 37(1), pp.43-51.

Ruprecht, J.J., King, M.S., Zögg, T., Aleksandrova, A.A., Pardon, E., Crichton, P.G., Steyaert, J. and Kunji, E.R. 2019. The molecular mechanism of transport by the mitochondrial ADP/ATP carrier. *Cell*, 176(3), pp.435-447.

Salimi, F., Khorshidi, M., Amirahmadi, F. and Amirahmadi, A. 2023. Effectiveness of Phosphate and Zinc Solubilizing Paenarthrobacter nitroguajacolicus P1 as Halotolerant Rhizobacterium with Growth-Promoting Activity on Pistacia vera L. *Current Microbiology*, 80(10), p.336.

Schneider, S.A., Erro, R. and Bhatia, K.P. 2017. DYT8, Paroxysmal Non-kinesigenic Dyskinesia—PNKD. In *Reference Module in Neuroscience and Biobehavioral Psychology*, Elsevier, pp 579-584.

Sekar, K., Linker, S.M., Nguyen, J., Grünhagen, A., Stocker, R. and Sauer, U. 2020. Bacterial glycogen provides short-term benefits in changing environments. *Applied and environmental microbiology*, 86(9), pp.e00049-20.

Shakya, M., Lo, C.C. and Chain, P.S. 2019. Advances and challenges in metatranscriptomic analysis. *Frontiers in genetics*, 10, p.904.

Sheibani-Tezerji, R., Rattei, T., Sessitsch, A., Trognitz, F. and Mitter, B. 2015. Transcriptome profiling of the endophyte Burkholderia phytofirmans PsJN indicates sensing of the plant environment and drought stress. *Journal of the American Society for Microbiology*., 6(5), pp.10-1128.

Sneha, G.r., Yadav, R.K., Chatrath, A., Gerard, M., Tripathi, K., Govindsamy, V. and Abraham, G. 2021. Perspectives on the potential application of cyanobacteria in the alleviation of drought and salinity stress in crop plants. *Journal of Applied Phycology*, pp.1-18.

Steiner, F.A.B.I.O., da Silva Oliveira, C.E., Zoz, T.I.A.G.O., Zuffo, A.M. and de Freitas, R.S. 2020. Co-Inoculation of common bean with Rhizobium and Azospirillum enhance the drought tolerance. *Russian Journal of Plant Physiology*, 67, pp.923-932.

Tao, M., Wang, L., Wendt-Pienkowski, E., George, N.P., Galm, U., Zhang, G., Coughlin, J.M. and Shen, B. 2007. The tallysomycin biosynthetic gene cluster from Streptoalloteichus hindustanus E465-94 ATCC 31158 unveiling new insights into the biosynthesis of the bleomycin family of antitumor antibiotics. *Molecular BioSystems*, 3(1), pp.60-74.

Tartaglia, M., Ranauda, M.A., Falzarano, A., Maisto, M., Postiglione, A., Prigioniero, A., Scarano, P., Zuzolo, D., Sciarrillo, R. and Guarino, C. 2023. Metatranscriptomics of pastures under drought stress show a rhizospheric meta-organism reshape. *Rhizosphere*, 26, p.100687.

Timm, C.M., Carter, K.R., Carrell, A.A., Jun, S.R., Jawdy, S.S., Vélez, J.M., Gunter, L.E., Yang, Z., Nookaew, I., Engle, N.L. and Lu, T.Y.S. 2018. Abiotic stresses shift belowground Populus-associated bacteria toward a core stress microbiome. *Journal of Microbial Cell Biology*, 3(1), pp.10-1128.

Timmusk, S. and Wagner, E.G.H. 1999. The plant-growth-promoting rhizobacterium Paenibacillus polymyxa induces changes in Arabidopsis thaliana gene expression: a possible connection between biotic and abiotic stress responses. *Molecular plant-microbe interactions*, *12*(11), pp.951-959.

Xu, H.F., Dai, G.Z., Ye, D.M., Shang, J.L., Song, W.Y., Shi, H. and Qiu, B.S. 2020. Dehydration-induced DnaK2 chaperone is involved in PSII repair of a desiccation-tolerant cyanobacterium. *Plant physiology*, 182(4), pp.1991-2005.

Wang, Y., Hayatsu, M. and Fujii, T. 2012. Extraction of bacterial RNA from soil: challenges and solutions. *Microbes and environments*, 27(2), pp.111-121.

Wang, X., Li, B.B., Ma, T.T., Sun, L.Y., Tai, L., Hu, C.H., Liu, W.T., Li, W.Q. and Chen, K.M. 2020. The NAD kinase OsNADK1 affects the intracellular redox balance and enhances the tolerance of rice to drought. *BMC Plant Biology*, 20(1), pp.1-19.

Wang, Z., Solanki, M.K., Yu, Z.X., Yang, L.T., An, Q.L., Dong, D.F. and Li, Y.R. 2019. Draft genome analysis offers insights into the mechanism by which Streptomyces chartreusis WZS021 increases drought tolerance in sugarcane. *Frontiers in microbiology*, 9, p.3262.

Westreich, S.T., Treiber, M.L., Mills, D.A., Korf, I. and Lemay, D.G. 2018. SAMSA2: a standalone metatranscriptome analysis pipeline. *BMC Bioinformatics*, 19(1), pp.1-11.

Xu, L., Naylor, D., Dong, Z., Simmons, T., Pierroz, G., Hixson, K.K., Kim, Y.M., Zink, E.M., Engbrecht, K.M., Wang, Y.I. and Gao, C. 2018. Drought delays development of the sorghum root microbiome and enriches for monoderm bacteria. *Proceedings of the National Academy of Sciences*, 115(18), pp.4284-4293.

Xu, H.F., Dai, G.Z., Ye, D.M., Shang, J.L., Song, W.Y., Shi, H. and Qiu, B.S. 2020. Dehydration-induced DnaK2 chaperone is involved in PSII repair of a desiccation-tolerant cyanobacterium. *Plant Physiology*, 182(4), pp.1991-2005.

Yergeau, E., Tremblay, J., Joly, S., Labrecque, M., Maynard, C., Pitre, F.E., St-Arnaud, M. and Greer, C.W. 2018. Soil contamination alters the willow root and rhizosphere metatranscriptome and the root–rhizosphere interactome. *The International society for microbial ecology journal*, 12(3), pp.869-884.

Yobi, A., Wone, B.W., Xu, W., Alexander, D.C., Guo, L., Ryals, J.A., Oliver, M.J. and Cushman, J.C. 2013. Metabolomic profiling in Selaginella lepidophylla at various hydration states provides new insights into the mechanistic basis of desiccation tolerance. *Molecular Plant*, 6(2), pp.369-385.

Zhang, J., Kobert, K., Flouri, T. and Stamatakis, A. 2014. PEAR: a fast and accurate Illumina Paired-End reAd mergeR. *Bioinformatics*, 30(5), pp.614-620.

Yobi, A., Wone, B. W. M., Xu, W., Alexander, D. C., Guo, L., Ryals, J. A., Oliver, M. J. and Cushman, J. C. 2012. Comparative metabolic profiling between desiccation-sensitive and desiccation-tolerant species of Selaginella reveals insights into the resurrection trait. *The Plant Journal,* 72**,** 983-999.

Zhang, B.X., Li, P.S., Wang, Y.Y., Wang, J.J., Liu, X.L., Wang, X.Y. and Hu, X.M. 2021. Characterization and synthesis of indole-3-acetic acid in plant growth promoting Enterobacter sp. *Royal Society of Chemistry Advances*, 11(50), pp.31601-31607.

Zhu, J., Jiang, X., Guan, D., Kang, Y., Li, L., Cao, F., Zhao, B., Ma, M., Zhao, J. and Li, J. 2022. Effects of rehydration on physiological and transcriptional responses of a water-stressed rhizobium. *Journal of Microbiology*, 60, pp.31-46.

# Chapter Four

## Metabolic profiling of the rhizosphere of the resurrection plant *Myrothamnus flabellifolia* under dehydrated and rehydrated conditions

## 4.1. Summary

Global warming is predicted to increase the occurrence and severity of drought, particularly in Africa, which will negatively impact crops and food production. In order to mitigate negative consequences, it is essential to understand the impact of drought on soil, plant root systems, and associated microorganisms. Water deficit perturbs biochemical, morphological, and physiological activities in plants and microorganisms. This study focuses on gaining a fundamental understanding of the role of root-associated microbes in the desiccation response of the iconic medicinal resurrection plant *Myrothamnus flabellifolia*. The present study aimed to characterise the metabolic responses within the rhizosphere soil of *M. flabellifolia* during desiccation stress and subsequent rehydration. Non-targeted metabolic profiles of the rhizosphere soils of *M. flabellifolia* were generated using gas chromatography-mass spectrometry (GC-MS). Dehydration caused a significant shift in the rhizosphere metabolome, resulting in an accumulation of often reported drought- and desiccation-responsive metabolites. Importantly, dehydrated samples exhibited an accumulation of sugars, organic acids and phytohormones in the rhizosphere soil, relative to rehydrating samples. Rehydrated samples exhibited significantly higher levels of amino acids compared to desiccated samples, possibly due to root cellular leakage as the roots of *M. flabellifolia* adjust to more favorable conditions. The accumulation of solutes secreted by roots and microorganisms in the desiccated rhizosphere, many of which have been reported to function in osmotic adjustment associated with water deficit stress, may protect the roots of host plant from damages associated with the frequent cycles of desiccation and rehydration of its natural environment.

## 4.2. Introduction

Water deficit negatively affects multiple processes and perturbs biochemical, morphological, and physiological activities in plants. Water limitation can prevent growth and lead to nutrient deficiency (Guo et al., 2018). Plants counteract drought stress through multiple mechanisms, including a massive reprogramming of their transcriptional, proteomic, and metabolic pathways to help in protecting cells from osmotic and mechanical damage. The plant root system acts as a critical junction of nutrients and water exchange between the plant and soil (Pan et al., 2022). In particular, root exudates modulate the interaction between the plant and the soil microbiome in the rhizosphere. Additionally, certain function as antioxidants that scavenge reactive oxidative species (ROS) and thereby mitigating damage associated with oxidative stress induced by the impairment of the photosynthetic electron transport chain (Ghanbarzadeh et al., 2021). The accumulation of metabolites in the rhizosphere soil under environmental stresses provides information about changes in enzymatic and biochemical reactions within the plant and microbiome (Bornø et al., 2022).

It is essential to understand the root exudation process, particularly during drought stress. These root exudates consist mainly of metabolites such as sugars, amino acids, organic acids, proteins, and phenolic acids (Canarini et al., 2019). Roots consist of the undifferentiated root tip and the differentiation zone where root formation occurs. The endodermis in the differentiation zone has a casparian strip that restricts the efflux of solutes out of the roots (Canarini et al., 2019; Salas-González et al., 2021). Root exudates reach the soil environment through apoplastic and symplastic pathways in the undifferentiated root tip. The apoplastic pathway is halted by casparian strips in the root differentiation zone, but both the apoplastic and symplastic pathways are active at the undifferentiated root tip due to the lack of a casparian strip. Solutes can be transported through either active transport using ABC and MATE transporters, or passive transport using diffusion mechanisms (Canarini et al., 2019). Passive transport is a major contributor to root exudation, roots actively restrict the efflux of metabolites into the rhizosphere through apoplastic diffusion barriers (Meyer et al., 2010). Drought alters root exudates produced by plants and consequently influences the soil properties as well as the microbial community in the soil (Bornø et al., 2022).

Metabolomics is emerging in plant science as a complementary methodology to pair with other omics technologies to better understand stress tolerance mechanisms. In the current study a metabolomic approach was used to provide an understanding of changes in rhizospheric metabolites under desiccation stress. Nutrient deficiency in soil is often mitigated by rhizospheric microbes through mineralisation and nitrification (Igiehon and Babalola, 2018). The interaction between roots and rhizospheric microbial communities is significantly impacted by drought stress. For instance, root

metabolites can act as a chemoattractant for microbes that confer drought tolerance to the host plant (Bornø et al., 2022) and promote plant-microbe interaction. The rhizosphere soil hosts a wide range of microbes from bacteria to fungi and algae (Mendes et al., 2013). Metabolites in the rhizosphere soil can either emanate from root exudation or from the microbial community. The difficulty of distinguishing the origin of metabolites has been previously reported by Oburger and Jones (2018). Despite the challenges, it is essential to comprehend the holistic metabolic changes occurring in the rhizosphere soil under desiccation and elucidate the interplay between plants and microbes in their natural habitat.

Drought stress induces the synthesis and secretion of various stress-responsive metabolites in *M. flabellifolia* (Bentley et al., 2019). Both plant and microbial processes may contribute to changes in the rhizosphere environment under water-limited conditions. For example, previous studies showed that plants primed with rhizobacteria such as *Pseudomonas sp*. can produce auxins (Indole-3-acetic acid), which promote root and shoot growth under drought stress and may also play a role in the distribution of heavy metals (Uzma et al., 2022). Growth promotion leading to an enlarged root system could enable plants to access additional water and nutrient resources under drought stress. Furthermore, the rhizosphere metabolites have been shown to induce a moist environment for root system to mitigate drought stress and modulate the physiological pathways of tomato through external influence, which impacts the overall plant metabolome (Akram et al., 2019). However, little is known about the metabolites secreted by the *M. flabellifolia* root and rhizospheric microorganisms.

Despite the intricate and tripartite interactions between plant roots, soil, and microbes, a well-functioning and healthy soil environment is pivotal for plant health. A holistic understanding of soil microbiome, physicochemical properties, and root and soil metabolites is required to optimise management in both natural and agricultural settings. The dynamics of rhizosphere and root metabolites remain under-explored in resurrection plants. This study aimed to (i) investigate the influence of water deficit stress on the metabolite profile of the rhizosphere soil of *M. flabellifolia* (ii) assess the chemical diversity in the rhizosphere soil during dehydration and rehydration, and (iii) characterise the active biochemical pathways associated with the host plant and microbes in the dehydration stages.

## 4.3. Material and methods

### 4.3.1. Sampling and metabolite extraction

The sampling of rhizosphere soil was performed as described in Chapter 3, section 3.1 and a total of 6 individual plants were used for this experiment. Samples were categorised into four time points as described in Chapter Three (Figure 3-1). Soil moisture was assessed with an EM50 moisture soil probe (Meter, USA) placed at the base of the root system. Six replicates per sampling point were included in this analysis. The rhizosphere soil samples were flash frozen in liquid nitrogen immediately after collection, weighed to approximately 250 mg. The extraction of metabolites from the rhizosphere was performed as shown in Figure 4-1 (Swenson et al., 2019) and extraction buffer was spiked with the internal standard (ribitol). Quality control (QC) samples were prepared by pooling biological samples, created by aliquoting 20 µL from each individual sample. A total of 500 µL of filtrate, blanks, sample quality controls, and 100 µL of 72 standards was dried in the speedvac. The dried pellets were derivatized according to Salem et al. (2020). Samples were transferred into 2 mL vials and immediately analysed with GC-MS.

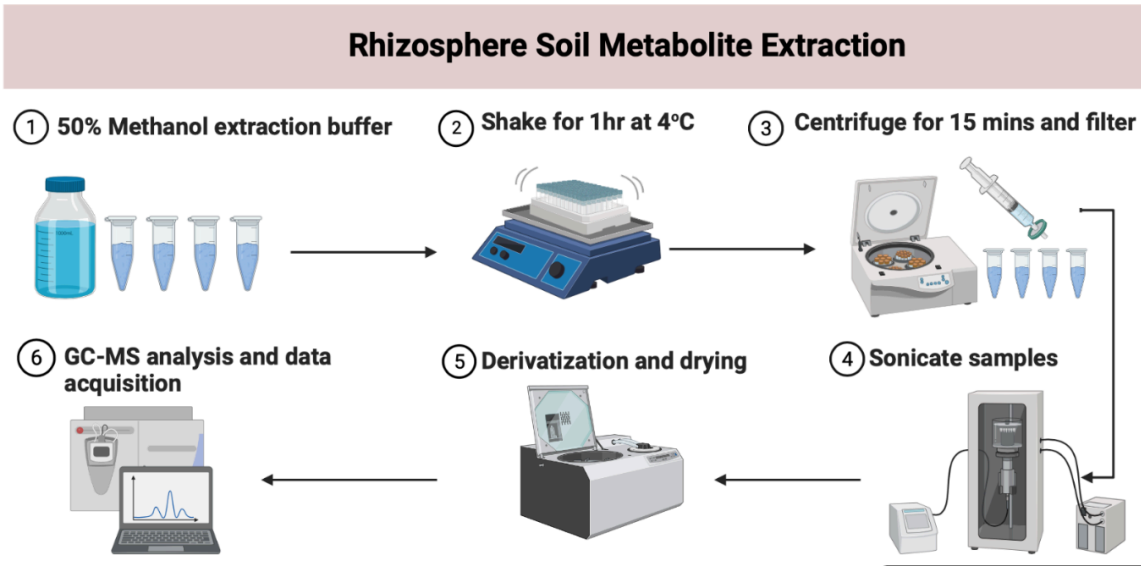


**Figure 4-1.** A schematic diagram of metabolites extraction from the rhizosphere soil of *Myrothamnus flabellifolia.*

### 4.3.2. Gas chromatography-mass spectrometry analysis and data pre-processing

The derivatised samples were auto-injected (1 µL) into an Agilent 7890A gas chromatograph system coupled with the Agilent 7000C triple quad mass spectrometry. The separation of compounds was executed on a J&W 122-5532G DB-5ms+DG column and 1 mL of the sample was auto-injected with an autosampler. The temperature settings of the injector were as follows: the inlet was 240°C, the

transfer line was 280°C, and the ion source was 230°C. The column was operated with a helium carrier gas and the constant ultrapure helium flow rate was 1 mL $min^{-1}$. The oven temperature program was initiated at 80°C and maintained for 1 min, then the temperature was raised to 320°C at a rate of 8°C/min and held for 2 min. The injector syringe was rinsed twice with isopropanol (5 µL) and the slit ratio was 14:1 (15 times dilution). The mass spectrometer scanned the mass range between 70 and 500 m/z in electron impact (EI) mode at 70 eV. The total run time for each sample was 33 min.

For pre-processing data, the Agilent MassHunter qualitative analysis software was used for compound identification and peak annotation and compounds. Peaks that were present in the blanks and samples were eliminated and classified as a contaminant or derivatization by-products. Quality control samples were included to evaluate both extraction and instrumental variability, and to ensure the reliability of the overall rhizosphere metabolome data (Fiehn, 2016). A total of 44 (sugars, sugar alcohol, organic acids) and 28 amino acids standards were quantified via GC-MS to obtain the retention time (RT) of each compound prior to sample analysis. Therefore, peak spectra and RT of each metabolite were used to search for compounds in the National Institute of Standards and Technology (NIST14) software, Fiehn and Golm metabolome (http://gmd.mpimp-golm.mpg.de) libraries. Identified compounds were confirmed by corresponding mass spectral data of the standard, chromatographic RI, and matching factor ≥ 80% (see Table A4, Annexure). Due to derivatisation which enables polar compounds to be accessible for GC-MS, each spectrum was analysed individually for the presence of trimethylsilyl (TMS) groups (Fiehn, 2016).

A one-way analysis of variance (ANOVA) test was used to determine the statistical difference ($P < 0.001$) between the sampling conditions (Figure 4-1). Detected compounds were normalised by the dry mass of the sample and the internal standard (ribitol) peak intensity. It is worth mentioning that variation was expected due to several environmental parameters such as landscape, *M. flabellifolia* growing in shallow rocks, and differences in age. Therefore, raw data were scaled by the sum of squares to standardise variances and outliers were removed in the MetaboAnalyst (Nagler et al., 2018). Principal component analysis (PCA) was performed to reduce the dimensions of variation in the dataset. Chemometric analysis was conducted using partial least square discriminant analysis (PLS-DA) modelling to validate the PCA and visualise group separation based on dehydration and rehydration conditions. Furthermore, the variable importance in projection (VIP) score plot was constructed to show the discriminant metabolites. The compounds having VIP ≥ 1 were classified as accountable for separation in the PLS-DA and were defined as discriminating metabolites. The ANOVA was used to identify metabolites with significant differences across the four conditions. Multiple comparisons were corrected by using false discovery rate (FDR) and log2 fold change was applied on a volcano plot to identify the most differentially abundant metabolites between partially dehydrated

(PD) and fully rehydrated (FR) and desiccated (D) and FR samples. Hierarchical clustering using Euclidean distance was used to identify metabolites with similar abundances through the time course on heatmaps. Metabolic pathway enrichment analysis was conducted using metabolites detected in the partially dehydrated, desiccated, partially rehydrated and fully rehydrated rhizosphere soil of *M. flabellifolia*. The pathway analysis used a hypergeometric test to analyse significant pathways for each condition. The rhizosphere metabolome may emanate from either root, bacteria, fungi, or a combination of all three. As a result, *Arabidopsis thaliana*, *Escherichia coli,* and *Saccharomyces cerevisiae* pathway libraries were used together with Kyoto Encyclopedia of Genes and Genomes (KEGG) database (see Table 4-S1, Table A5).

## 4.4. Results

### 4.4.1. Soil moisture

The moisture content of the soil adjacent to *M. flabellifolia* roots decreased only slightly from the partially dry (0 hrs) to desiccated condition (48 hrs) (Figure 4-2). This may be attributed to the high temperatures at the Swebeswebe field site during the sampling period (T0–T48), where the average temperature exceeded 28°C (Figure 4-S1). Additionally, the soil probe was unable to penetrate deeper soil profiles due to the rocky landscape. In contrast, upon rehydration after 12 hours (partially rehydrated) soil moisture content increased to 20% (Figure 4-2). Interestingly, the leaves were turning green, which indicates that the roots had absorbed water in the past 12 hours. Furthermore, soil moisture content rapidly declined 24 hours after rehydration. As previously mentioned, this reduction may be due to the weather conditions at the field site (Figure 4-S1), where the average temperature on T96 reached 30 °C and relative humidity remained low at 50%.

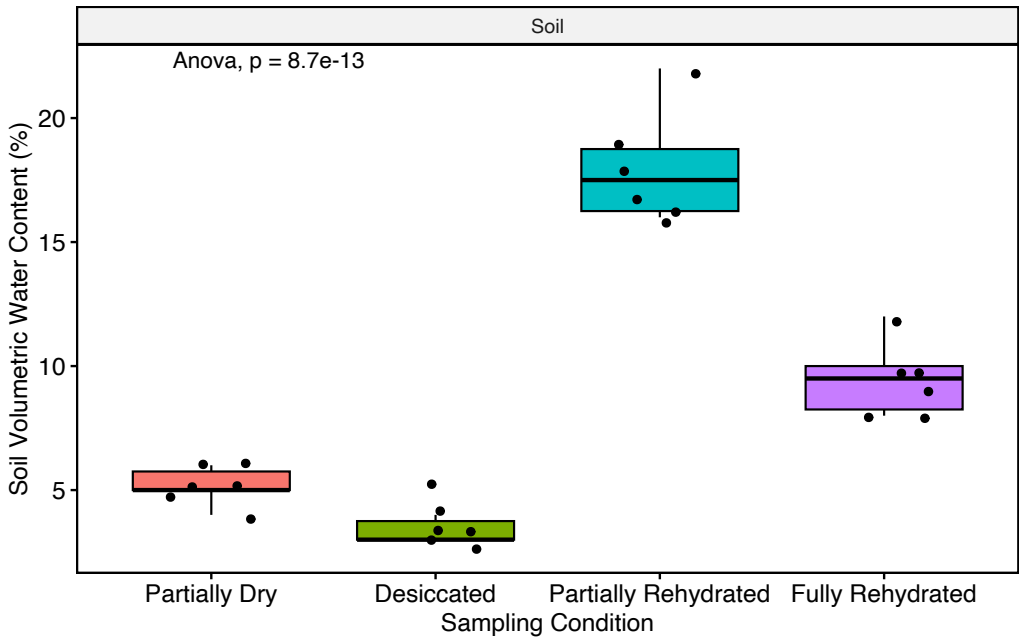


**Figure 4-2.** Soil moisture was measured in terms of volumetric water content (VWC) during partially dry (PD), desiccated (d), partially rehydrated (PR) and fully rehydrated (FR).

### 4.4.2. Multivariate analysis of rhizosphere metabolome

Rhizosphere metabolites varied considerably across the desiccation and rehydration time points. Principal Component Analysis (PCA) was used initially as an unsupervised statistical method to visualise differences in the metabolome between the treatments. PCA showed clustering of biological replicates by dehydration status. PC1 accounted for 15% and PC2 explained 13.7% of the variation in metabolite profile variation between the samples (Figure 4-3A). There was more variability in the metabolic profiles of partially dehydrated and desiccated samples relative to rehydrating samples, possibly due to higher variation in RWC within dehydrating samples. There was a clear separation between the partially dehydrated and the rehydrated samples. These results indicate global metabolic shifts occurred between drought and rehydration stages within the rhizosphere of *M. flabellifolia*. Furthermore, a multivariate analysis was conducted to validate sample relationships indicated by PCA. A supervised partial least square discriminant analysis (PLS-DA) was used to further discern metabolomic patterns and concentration changes across the dehydration-rehydration time course (Figure 4-3B). These analyses showed a clear separation between the four groups with metabolites in the partially rehydrated and fully rehydrated samples exhibiting lower variation.

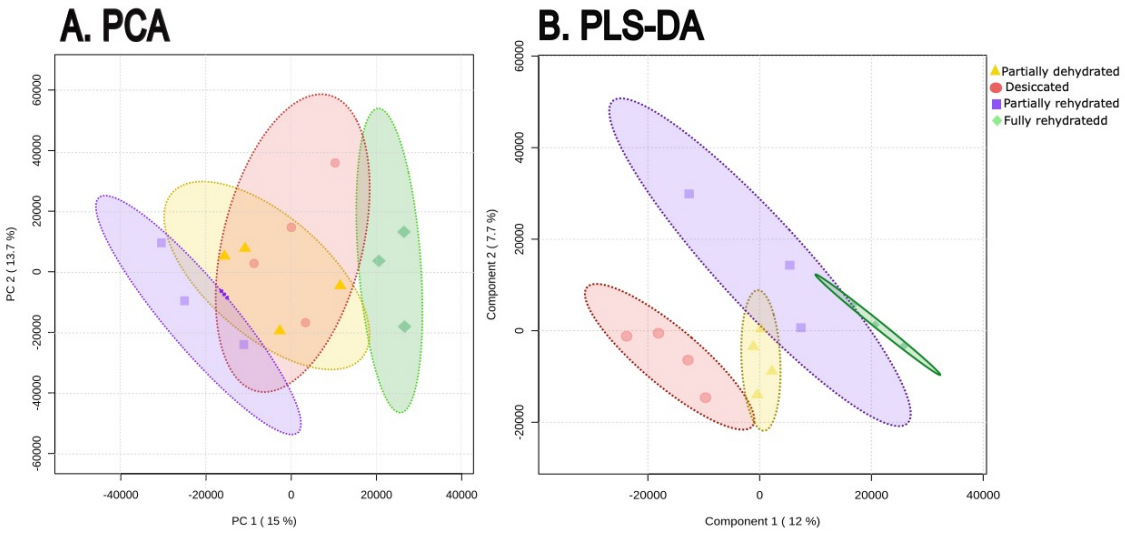


**Figure 4-3.** Multivariate analysis of metabolites of the rhizosphere soil of *Myrothamnus flabellifolia* A) PCA and B) PLS-DA plot under partially dehydrated, desiccated, partially rehydrated, and fully rehydrated conditions.

### 4.4.3. The impact of drought stress and rehydration on the rhizosphere soil metabolome

A total of 84 metabolites were identified in the rhizosphere soil of the resurrection plant *M. flabellifolia* using an untargeted metabolomic profiling approach. In order to discern metabolites that varied significantly across dehydration and rehydration stages, a univariate analysis (one-way ANOVA) was performed. Additionally, variance important projection (VIP) scores were used for identifying specific metabolic changes in the four groups. The VIP scores are essential in selecting up and downregulated metabolites and indicate the metabolic differences between stages. Metabolites with $P < 0.05$ and VIP score > 1 were considered as the most distinct between dehydration and rehydration stages.

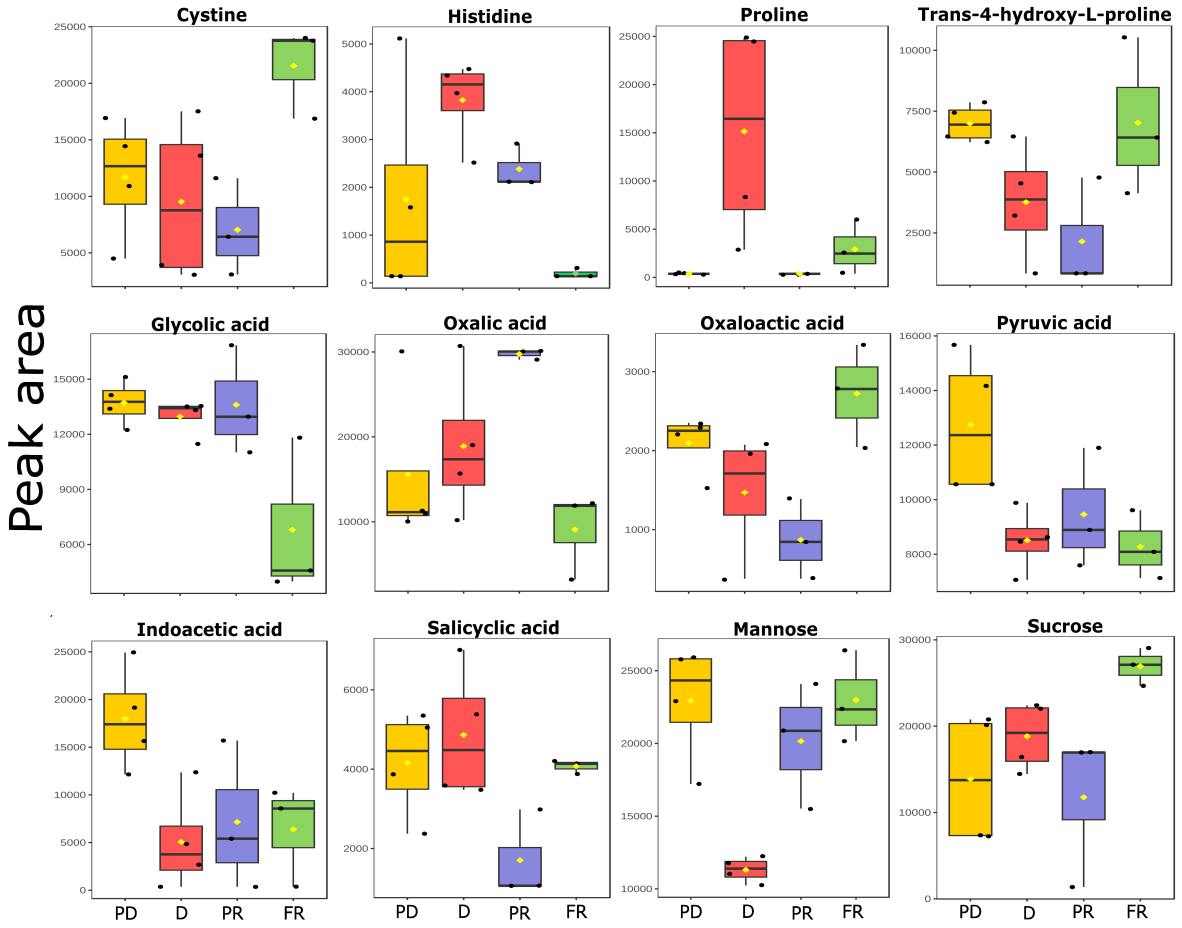


**Figure 4-4.** Significantly different metabolites across partially dehydrated (PD), desiccated (D), partially rehydrated (PR), and fully rehydrated rhizosphere soil of *Myrothamnus flabellifolia* using ANOVA ($P < 0.05$).

There was a high peak area of glycerol, gallic acid, trehalose, sucrose, and sorbitol in the quality control samples (Figure 4-S2). A total of 12 metabolites were significantly different across four stages and nine metabolites had a VIP score > 1 across all groups (Figure 4-4). Partial drought stress significantly increased the concentration of indole-3-acetic acid (IAA), glycolic acid, malic acid, maltose, pyruvic acid, and trans-4-hydro-proline in the rhizosphere soil. Under extreme drought stress (desiccated) an increase in galactose, glucose, histidine, proline, and trehalose was observed in the rhizosphere soil compared to hydrated samples (Figure 4-5). A few metabolites, such as xylitol and oxalic acid, were found at higher concentrations in partially rehydrated soil samples (Figure 4-5). In fully hydrated samples cystine, glutamic acid, galactitol, gallic acid, mannose, lactic acid, oxaloacetic acid, phosphoric acid, pyroglutamic acid, and sucrose were significantly upregulated.

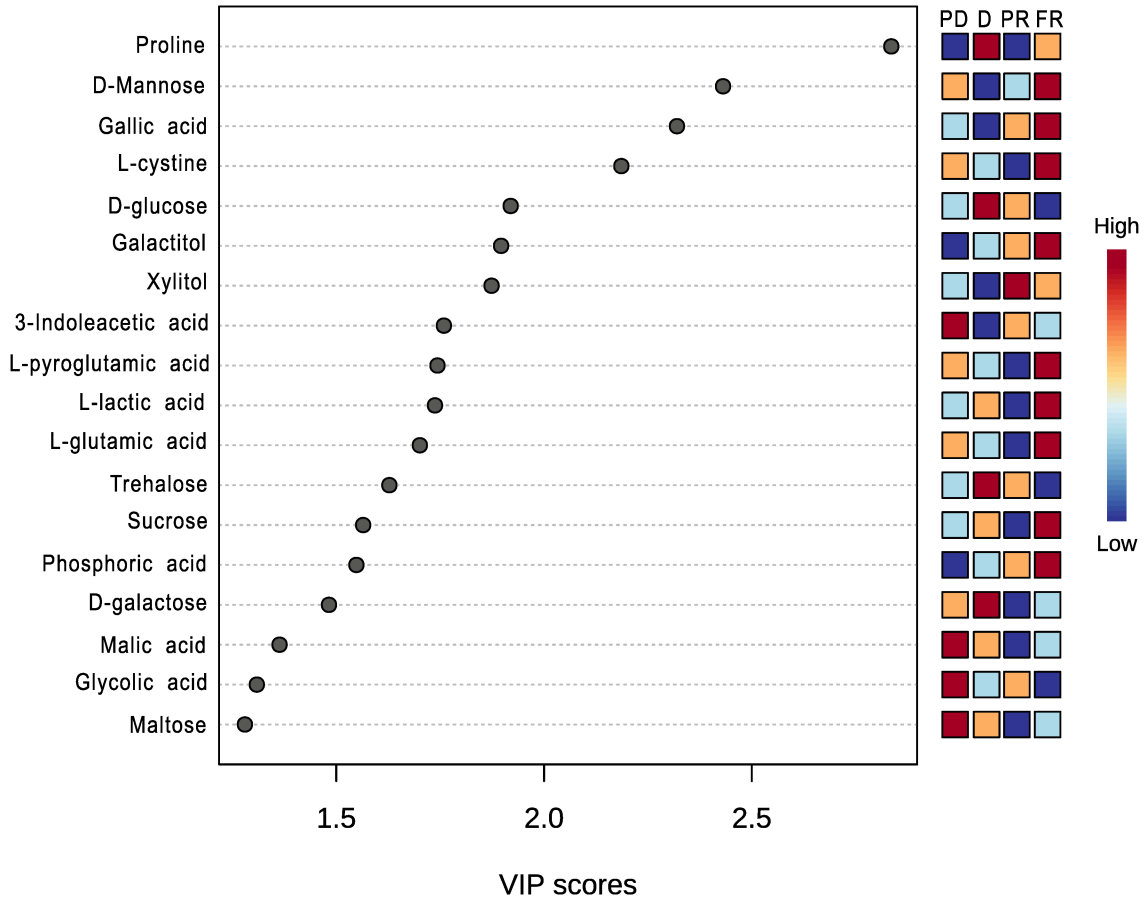


**Figure 4-5.** The variance importance in projection (VIP) score plot of discriminant metabolites. The VIP plot displays discriminant metabolites with a VIP score >1 for partially dehydrated (PD), desiccated (D), partially rehydrated (PR), and fully rehydrated (FR) rhizosphere soil samples of *Myrothamnus flabellifolia*.

Hierarchically clustering of metabolite abundances using group average showed substantial shifts in metabolite profiles across dehydration and rehydration stages in the rhizosphere soil (Figure 4-6). In general, sugars and organic acids were prominent in the dehydration stages whereas the rehydrated samples had elevated amino acids. For instance, the TCA cycle compounds such as malic, pyruvic, α-ketoglutaric and glycolic acid were enriched in dehydrated conditions. Whereas rehydrated conditions exhibited high content of oxaloacetic acid and succinic acid in the rehydrated rhizosphere soil, although it was not significant. Additionally, a large proportion of the amino acids that were accumulated in the rehydrated samples are also involved in nitrogen metabolism.

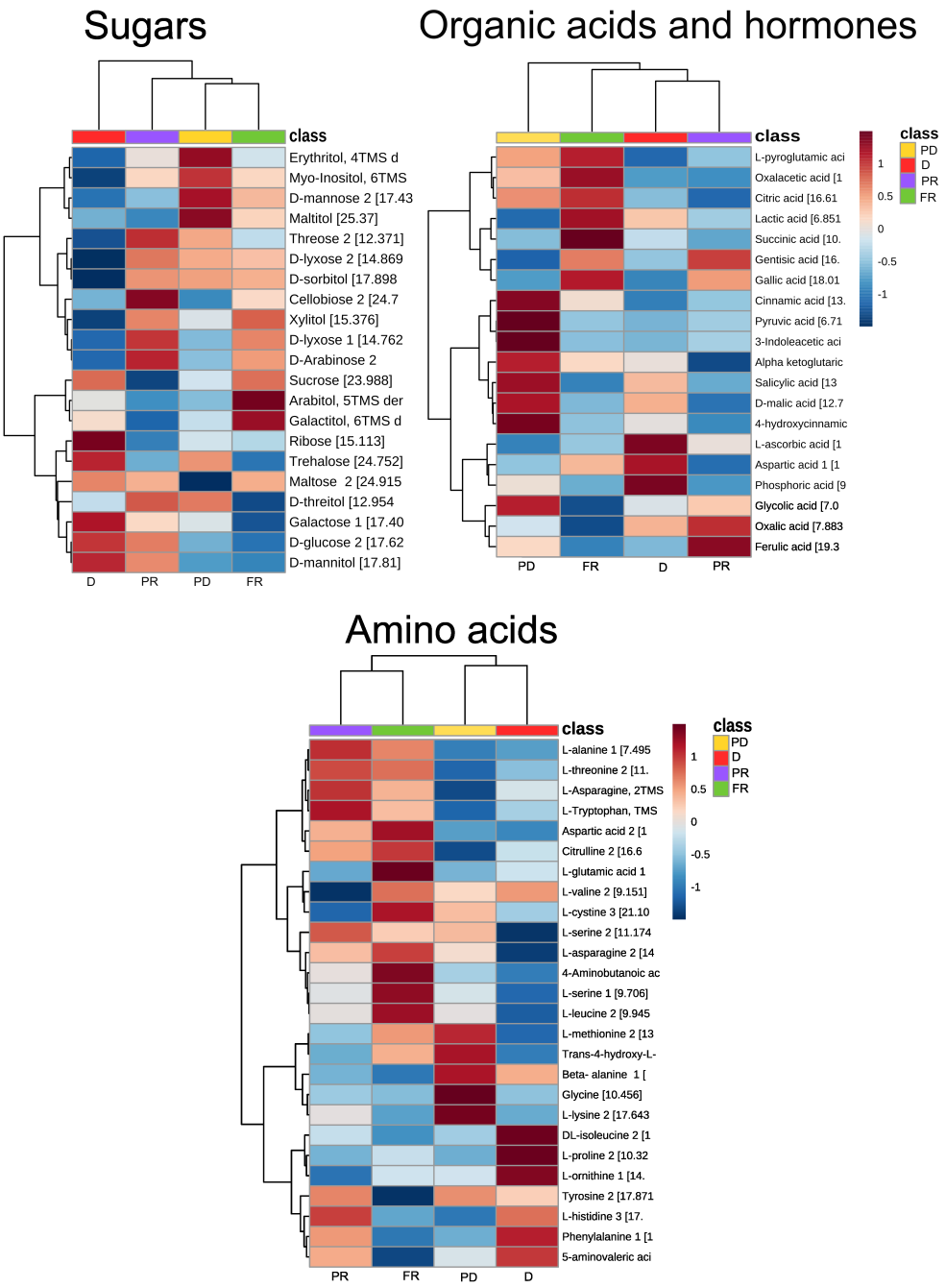


**Figure 4-6.** Hierarchical clustering of primary metabolite abundance in partially dehydrated (PD), desiccated (D), partially rehydrated (PR), and fully rehydrated (FR) rhizosphere soils of *Myrothamnus flabellifolia*.

### 4.4.4. Pairwise statistical comparison between the dehydrated and rehydrated rhizosphere soil

Targeted pairwise comparisons were made between desiccated and fully rehydrated samples, and partially dehydrated and fully rehydrated samples as shown in the volcanic plots (Figure 4-7). There were 11 significantly different metabolites between desiccated and fully rehydrated rhizosphere soils,

eight of which were significantly elevated in the desiccated rhizosphere soil, and two that were significantly elevated in the hydrated rhizosphere soil. Extreme drought stress increased the abundance of galactose, glucose, histidine, mannitol, phenylalanine, oxalic acid, trehalose, and tyrosine in the rhizosphere soil of *M. flabellifolia* (Figure 4-7A). Upon rehydration, the rhizosphere soil showed a significant elevation of myo-inositol and leucine content (Figure 4-7A). The pairwise comparison between partially dehydrated and fully rehydrated rhizosphere samples revealed that an abundance of α-ketoglutaric acid, indole-3-acetic acid, cellobiose, arabinose, erythritol, glycolic acid, and threitol in the rhizosphere soil was influenced by drought stress (Figure 4-7B). In contrast, only two amino acids namely 4-aminobutanoic acid and tryptophan exhibited higher abundance in fully rehydrated rhizosphere soil.

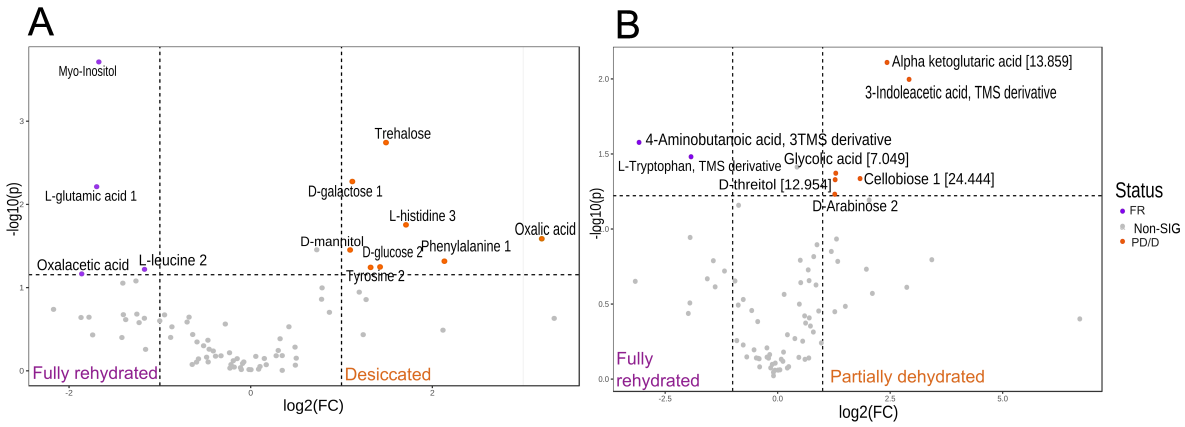


**Figure 4-7.** Volcano plot of the $\log_2$ fold changes by log abundance of metabolites between A) fully rehydrated (FR) and desiccated (D) samples, and B) FR and partially dehydrated (PD) rhizosphere soil samples of *Myrothamnus flabellifolia*.

### 4.4.5. Metabolic enrichment pathway analysis

Pathway enrichment analysis was performed to identify specific changes in soil metabolic processes. Using KEGG IDs from putatively annotated metabolites, significantly impacted pathways ($P < 0.05$) were reconstructed. The tricarboxylic acid (TCA) cycle emerged as the most significantly enriched and dominant pathway in partially dehydrated rhizosphere soil. This finding was supported by the accumulation of key intermediate metabolites, such as organic acids (Figure 4-8), which aligns with the observed upregulation of the TCA cycle in microbial species present in the rhizosphere. In contrast, phenylalanine, tyrosine, and tryptophan biosynthesis was the most enriched pathway in fully desiccated soils. Rehydrated samples showed a strong upregulation of various amino acid metabolic pathways, likely due to the elevated amino acid concentrations detected in the rhizosphere. This may result from membrane leakage in roots during rehydration and increased microbial turnover.

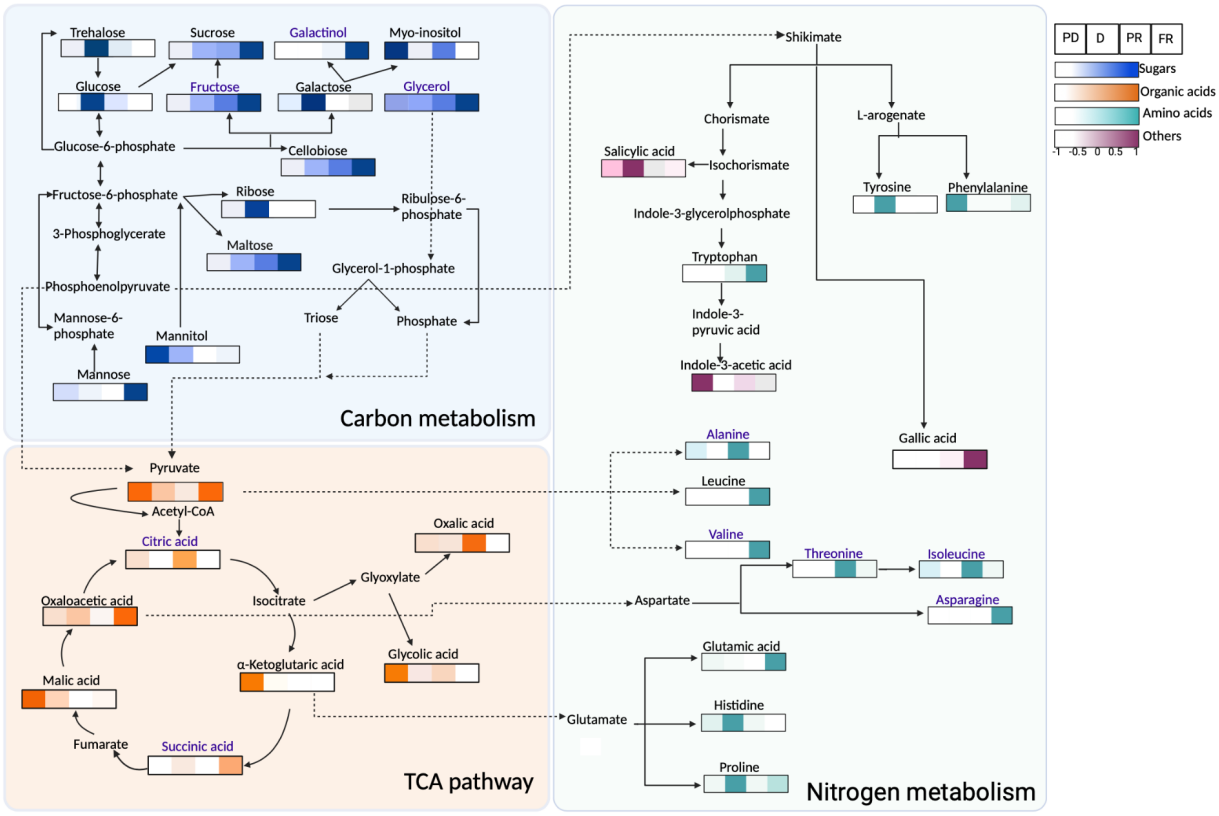


**Figure 4-8.** Metabolic pathway analysis of the quantified metabolites in the rhizosphere soil of *Myrothamnus flabellifolia* under partially dehydrated (PD), desiccated (D, partially rehydrated (PR), and fully rehydrated (FR) conditions. Metabolites were categorised into sugars (blue), organic acids (orange), amino acids (green), and others (purple). Metabolite peak intensity is indicated in the bars. Metabolites with no significant changes during the dehydration and rehydration stages of the rhizosphere soil are indicated with purple letters.

## 4.5. Discussion

An untargeted metabolomics approach was used to evaluate the effects of desiccation on the rhizosphere soil of *M. flabellifolia*. This is the first study to explore and quantify the rhizosphere metabolome of *M. flabellifolia*. Plants interact with the soil environment through root exudation, however, the interplay between roots, microbes, and soil remains largely unknown (Canarini et al., 2019). Drought represents significant stress to plants and microorganisms and disrupts numerous biochemical and physiological processes (Ghanbarzadeh et al., 2021). Therefore, plants and microbes have evolved defense mechanisms to mitigate the negative effects of drought. These include osmoregulatory activities to protect membrane integrity through the accumulation of amino acids, fatty acids, lipids, hormones, phenolics, sugars, and sugar alcohol (Bentley et al., 2019; Guo et al., 2018; Moore et al., 2011). This study identified distinct metabolite signatures associated with changes

in water content in the rhizosphere soils of *M. flabellifolia*. *M. flabellifolia* hosts a range of microorganisms from bulk soil through the rhizosphere and into the root endodermis (Chapter Two; Tebele et al., 2023). This study also found evidence of primary metabolite accumulation in the rhizosphere, which may contribute to shaping microbial community composition by serving as potential chemoattractants.

### 4.5.1. Drought-responsive sugar alcohols

The constitutive high levels of glycerol found in the rhizosphere, particularly more pronounced in rehydrated conditions (Figure 4-S2), may contribute to reducing the rate of water loss in the rhizosphere. This result aligns with the findings of Yobi et al. (2012), who similarly observed the presence of glycerol in the hydrated leaves of *Selaginella lepidophylla*. A previous (unpublished) study describes an abundance of glycerol in the roots of *M. flabellifolia* (Klamer, 2022), suggesting that the glycerol identified here in the rhizosphere soil could be due to root exudation. Because glycerol is a small molecule that can pass through plasma membranes (Canarini et al., 2019), it could easily be secreted by roots into the rhizosphere soils. This could potentially explain the higher moisture content observed in the rhizosphere soil compared to the bulk soil, as reported by Tebele et al. (2023). Glycerol has a strong water-binding ability, minimises water surface tension, and restores biochemical activities during osmoregulation (Nevoigt and Stahl, 1997; Yobi et al., 2012). Other polyols such as threitol and erythritol were highest in the partially dehydrated rhizosphere, which could enhance drought tolerance in *M. flabellifolia*. Interestingly, Klamer (2022) reported a high abundance of myo-inositol as a precursor of sucrose and oligosaccharides in the dehydrated roots of *M. flabellifolia*. This differs from the finding presented here, in which elevated myo-inositol was detected in the rehydrated rhizosphere soil. However, these findings are consistent with those of Gabier et al. (2021) who also found that *Xerophyta schlechteri* leaf tissue exhibited high myo-inositol in the partially hydrated stage. The presence of this and other polyols in the rhizosphere during dehydration and rehydration stages may be associated with osmoprotection or stress mitigation processes within the soil microenvironment.

### 4.5.2. Reprogramming of sugars in desiccation and rehydrated rhizosphere

The accumulation of various sugars in plants under drought stress is well established, but the specific types of sugar accumulated depend on the species (Dace et al., 2023). Altered carbohydrate metabolism leading to an accumulation of small non-reducing sugars plays a pivotal role in desiccation tolerance and functioning in osmo-protection, membrane structure maintenance, and antioxidant activity enhancement (Kumar et al., 2021). Here, moderate dehydration stress was associated with

the accumulation of cellobiose, arabinose, and mannose in the rhizosphere soil, which may facilitate tolerance to drought stress. The leaf cell wall of *M. flabellifolia* is rich in arabinose, which is a key component of surviving desiccation by maintaining cell wall flexibility (Moore et al., 2008). Interestingly, arabinose was not detected in the roots of *M. flabellifolia* (Klamer, 2022, unpublished). Therefore, this finding suggests that its presence in the rhizosphere may derive from microbes and act as a carbon source for microbial activity. The presence of cellobiose and mannose is thought to contribute to the overall drought tolerance of *M. flabellifolia* by enhancing osmotic adjustment, maintaining energy, enhancing plant growth, and providing substrates for antioxidant metabolism (Li et al., 2017; Schellenberger et al., 2011; Zhou et al., 2019). The accumulation of sugars might be associated with the upregulation of pentose and glucuronate metabolism in bacterial lineages. In the current study, desiccated rhizosphere soil exhibited a greater content of trehalose, glucose, galactose, and ribose, which may help to preserve tissues in a desiccated state. Although a substantial amount of trehalose was quantified in the leaves and roots of *M. flabellifolia* (Farrant, 2007), indicating endogenous production, this finding suggests that rhizospheric microbes may also contribute to the abundance of trehalose in the rhizosphere soil through exogenous secretion. This theory was indeed confirmed by the detection of bacterial expression of genes involved in trehalose biosynthesis, such as TreY, TS, and TPS genes (Chapter Three). Trehalose plays a significant role in enhancing desiccation tolerance, as reported in *Saccharomyces cerevisiae*, where it was found to confer greater desiccation tolerance compared to other disaccharides (Tapia et al., 2015). These findings indicate that rhizospheric sugars may be associated with osmotic adjustment and stress mitigation processes in the root zone and surrounding microbial communities under water deficit conditions.

Sucrose levels were significantly elevated throughout all dehydration and rehydration stages in the rhizosphere soil, with the most noticeable increase observed in the rehydrated samples. This discovery contradicts the recent study by Klamer (2022), which reported elevated sucrose only in desiccated roots of *M. flabellifolia*. However, this finding aligns with the upregulation of sucrose synthase genes in root-associated bacteria under rehydrated conditions, as discussed in Chapter Three. Another study by Yobi et al. (2012) reported similar results, showing constitutively elevated sucrose levels in drying and rehydrating *Sporobolus stapfianus*. It is possible that the abundance of sucrose in the fully rehydrated rhizosphere is due to the upregulation of galactose metabolism, which results in the abundance of fructose-6-phosphate and further converted into sucrose. Sucrose helps to form a gel-like matrix leading to intracellular glasses, which maintain cellular stability and prevent membrane fusion under desiccation (Farrant et al., 2007; Kumar et al., 2021; Moore et al., 2007; Oliver et al., 2020; Yobi et al., 2012). The presence of sucrose in the rhizosphere soil of *M. flabellifolia* may result from root exudation via passive transport mediated by SWEET transporters. In the rhizosphere, the

presence of sucrose plays an important role as a carbon source for rhizospheric microbes and may be a chemoattractant for plant-growth-promoting microbes. Additionally, the accumulation of sucrose might be due to the interaction of trehalose intermediate (Trep6P) and SnRK1 which enhances sucrose accumulation (Oliver et al., 2020; Radermacher et al., 2019). In general, sugars exhibited a greater abundance in drying and desiccated rhizosphere soils relative to rehydrated soils, suggesting that sugar accumulation is an important mechanism of protection for plants and microbes during desiccation.

### 4.5.3. Accumulation of phytohormones

This study showed an accumulation of indole-3-acetic acid (IAA) under partially dehydrated conditions followed by elevated salicylic acid (SA) in desiccated conditions in the rhizosphere soil. A recent study reported that salicylic-mediated regulation in *Arabidopsis* roots depended on the interaction with other signalling molecules such as auxin (Tran et al., 2023). These findings of an accumulation of IAA and salicylic acid during dehydration stages are in line with the findings of Tran et al. (2023) and indicate that these hormones function in conjunction, which is likely to improve the resilience of *M. flabellifolia* against drought stress. Interestingly, genes encoding a key enzyme (indolepyruvate decarboxylase) in the biosynthesis of IAA were differentially expressed in root-associated bacteria under drought stress (Chapter Three). This supports the hypothesis that IAA may emanate from rhizospheric microbes and improve plant growth. These phytohormones were not detected in the roots of *M. flabellifolia* (Klamer, 2022), indicating that their presence in the rhizosphere soil was associated with microbial activity. A possible mechanism for the protective function is that salicylic acid increases the activity of superoxide dismutase (SOD) and ascorbate peroxidase (APX) in drought-stressed plants (González-Villagra et al., 2022), which helps to mitigate oxidative stress in dry tissues.

IAA is a naturally occurring plant growth hormone that regulates cell division and many other processes. Under drought stress, IAA enhances the formation of lateral roots to absorb more water (Fu et al., 2015; Zhang et al., 2020). Interestingly, based on observation during sampling, *M. flabellifolia* roots were long with multiple root hairs (Figure 1-4). It is possible that the phytohormones in the rhizosphere soil may contribute to enhanced root length and enable the plant to reach deep soil profiles. The biosynthesis of these phytohormones uses shikimate in the plastid of the plant cell (Pérez-Llorca et al., 2019; Wenz et al., 2019) (Figure 4-8). IAA production has been shown to increase in acidic environment (Fu et al., 2015), which aligns with the measured pH 4.3 of the rhizosphere soil of *M. flabellifolia* (Chapter Two; Tebele et al., 2023). This study suggests that IAA in the rhizosphere is mostly produced by microbes, perhaps as a signalling molecule to promote plant-microbe interaction

under drought stress. A recent study reported that *Pseudomonas aeruginosa* improved drought tolerance of *Vigna radiata* through the production of IAA, siderophores, nitrogen fixation, and phosphate solubilisation (Uzma et al., 2022). These findings suggest that the presence of phytohormones in the rhizosphere soil promotes plant-microbe interactions and may potentially enhances root growth of *M. flabellifolia*.

### 4.5.4. Organic acids in the rhizosphere soil

*Myrothamnus flabellifolia* inhabits a harsh ecological niche, where soil acidity is one of the key environmental constraints. Tebele et al. (2023) revealed that the rhizosphere soil of *M. flabellifolia* was acidic (pH = 4.3) and the rhizosphere metabolome indicates that it might be due to the presence of organic acids. The detection of organic acids in the rhizosphere was not surprising, because *M. flabellifolia* is known to grow on rocks and thus may produce acids to dissolve elements and obtain nutrients (Berner, 1992). Here, drought stress significantly increased specific organic compounds namely, glycolic, malic, pyruvic, and α-ketoglutaric acids (Figure 4-6). These findings are in accordance with the study by Guo et al. (2018). Interestingly, malic acid was detected here and also found in the dehydrated roots of *M. flabellifolia* (Klamer, 2022) suggesting that malic acid is secreted by roots of *M. flabellifolia* into the rhizosphere through malate and citrate transporters using $H^+$ coupled antiport activity (Bornø et al., 2022; Canarini et al., 2019). In plants, malic acid regulates the stomatal opening and closing in leaves and an increased content of malic acid is proportional to potassium ion intake (Yao et al., 2020). In fact, malic acid is also secreted by bacteria to dissolve aluminium potassium and absorb potassium (Si et al., 2022). These findings could explain the high amount of potassium detected in the rhizosphere soil (Tebele et al., 2023).

Gallic acid mitigates $H_2O_2$ production and increases antioxidant activity in the leaves of *Lepidium sativum* under salt stress (Babaei et al., 2022). The abundance of gallic acid in the rehydrated rhizosphere soil suggests that gallic acid may play a similar role in regulating ion intake and mitigating $H_2O_2$ accumulation during recovery state in *M. flabellifolia.* Additionally, anhydrobiosis induces the accumulation of 3,4,5-tri-O-galloylquinic acid in *M. flabellifolia* leaves (Moore et al., 2004), as a result, it is plausible that the concentrated gallic acid in the rhizosphere soil may be due to the hydrolysis of this polyphenol. These organic and phenolic acids may contribute to drought tolerance and may also regulate soil pH and promote microbial colonisation with *Acidobacteria* species. The accumulation of α-ketoglutaric acid in the partially dehydrated rhizosphere soil corroborates the findings of Chmielewska et al. (2016) which reported α-ketoglutaric acid in the roots and leaves of barley under drought stress. Most of these organic acids participate in nutrient acquisition and may form ionic liquids that facilitate and sustain macromolecule solubility under water deficit (Bornø et al., 2022;

Farrant et al., 2015). For instance, clustered roots secrete a high content of carboxylic acid anions and protons into the soil to diffuse inaccessible nutrients and allow efficient phosphorus solubilisation (Playsted et al., 2006).

The tricarboxylic acid (TCA) cycle is an essential pathway in plants for the generation of ATP that is utilised to establish cellular resilience against desiccation and is involved in the synthesis of some amino acids (Tran et al., 2023; Yobi et al., 2017). TCA intermediates induced by drought stress could be attributed to other pathways such as pentose, glycolysis, and oxalate cycle. The presence of oxaloacetic acid in the rehydrated rhizosphere soil indicates the possibility of initiation of photosynthesis. In plants, oxaloacetic acid is a substrate for the TCA pathway and assimilation of $CO_2$ during photosynthesis, and oxaloacetic acid is rapidly converted into malate or aspartate (Ludwig, 2016). Significant upregulation of the TCA cycle in desiccated rhizosphere, indicates the expansion of amino acids biosynthesis pathways, generation of energy, and intermediates that improve plant growth and defend against pathogens. Additionally, TCA cycle is interconnected with other pathway such as pentose and butanoate metabolism through shared intermediate such as Acetyl-CoA (Petushkova et al., 2021). The butanoate metabolism is coupled with lipid-related pathways (Dace et al., 2023), therefore, constitutive upregulation of butanoate metabolism in partially dehydrated and fully rehydrated rhizosphere soil may provide sufficient protection of phospholipids membrane in both main root and root hairs.

### 4.5.5. Amino acids

The accumulation of amino acids in the rehydrated rhizosphere indicates the plants and microbes rapidly return to the normal state subsequent to desiccation. The initiation of protein synthesis occurs to supplement the proteins compromised during desiccation. Farrant. (2007) postulated that the accumulation of amino acids during dehydration is due to degraded proteins and these amino acids act as water-replacement solutes. Here, the abundances of proline, histidine, phenylalanine, and tyrosine reported were highest in the desiccated rhizosphere soil and these findings were in accordance with the study by You et al. (2019). Proline is an osmolyte that accumulates under drought stress, acts as a signalling molecule, stabilises proteins, and scavenges radical species (Tran et al., 2023). This finding aligns with the upregulation of genes encoding proline/glycine betaine ABC transporter ATP-binding protein in root-associated bacteria under drought stress (Chapter Three). The other aromatic amino acids such as tyrosine and phenylalanine were regulated via the phenylalanine, tyrosine, and tryptophan metabolic pathway (Table 4-S1). An upregulation of aminoacyl-tRNA biosynthesis is associated with the disruption of the biochemical process (Khan et al., 2019), therefore, this suggests that desiccation affected these metabolic processes. Anhydrobiosis in *M. flabellifolia*

results in the augmentation of polyphenols (Moore et al., 2005), therefore, it is plausible that aromatic amino acids act as precursors for secondary metabolites, auxin, alkaloids, and cell membrane components (Yobi et al., 2012). Tryptophan was most abundant in the rehydrated samples, suggesting that it may function as an intermediate for IAA biosynthesis during drought (Figure 4-8). The abundance of amino acids in the rehydrated rhizosphere soil may result from root leakage and microbial activities (Svennerstam et al., 2011).

## 4.6. Conclusion

A healthy soil environment is crucial to survival under drought stress. It is essential to understand the effects of drought stress on rhizospheric microorganisms and how they contribute to drought tolerance in plants. Understanding the impacts of desiccation on the rhizosphere soil could provide insights into additional defense mechanisms occurring belowground in the proximity of *M. flabellifolia* root system. This study provides evidence of comprehensive metabolic reprogramming in the rhizosphere soil during extreme drought stress. A significant increase of sugars, organic acids, and phytohormones in the dehydration stages was detected and likely plays a critical role in establishing desiccation tolerance in *M. flabellifolia*. The accumulation of these solutes in the rhizosphere soil may protect the root cell membrane and act as signalling molecules to promote plant-microbe communication under desiccation. The enrichment of TCA cycle intermediates in the desiccated rhizosphere soil suggests ongoing microbial metabolic activity and root exudation. These processes may influence contribute the rhizosphere microenvironment. The rehydrated rhizosphere soil exhibited a high efflux of amino acids, which may originate from root cellular leakage and the renewed activity of the microbial community following rehydration. Taken together, this study demonstrated that the majority of rhizosphere soil metabolites are likely produced by microbes and may aid in the desiccation tolerance of *M. flabellifolia* due to the presence of osmotolerant solutes that reduce rates of water loss and protect cell membranes.

## 4.7. Supplementary

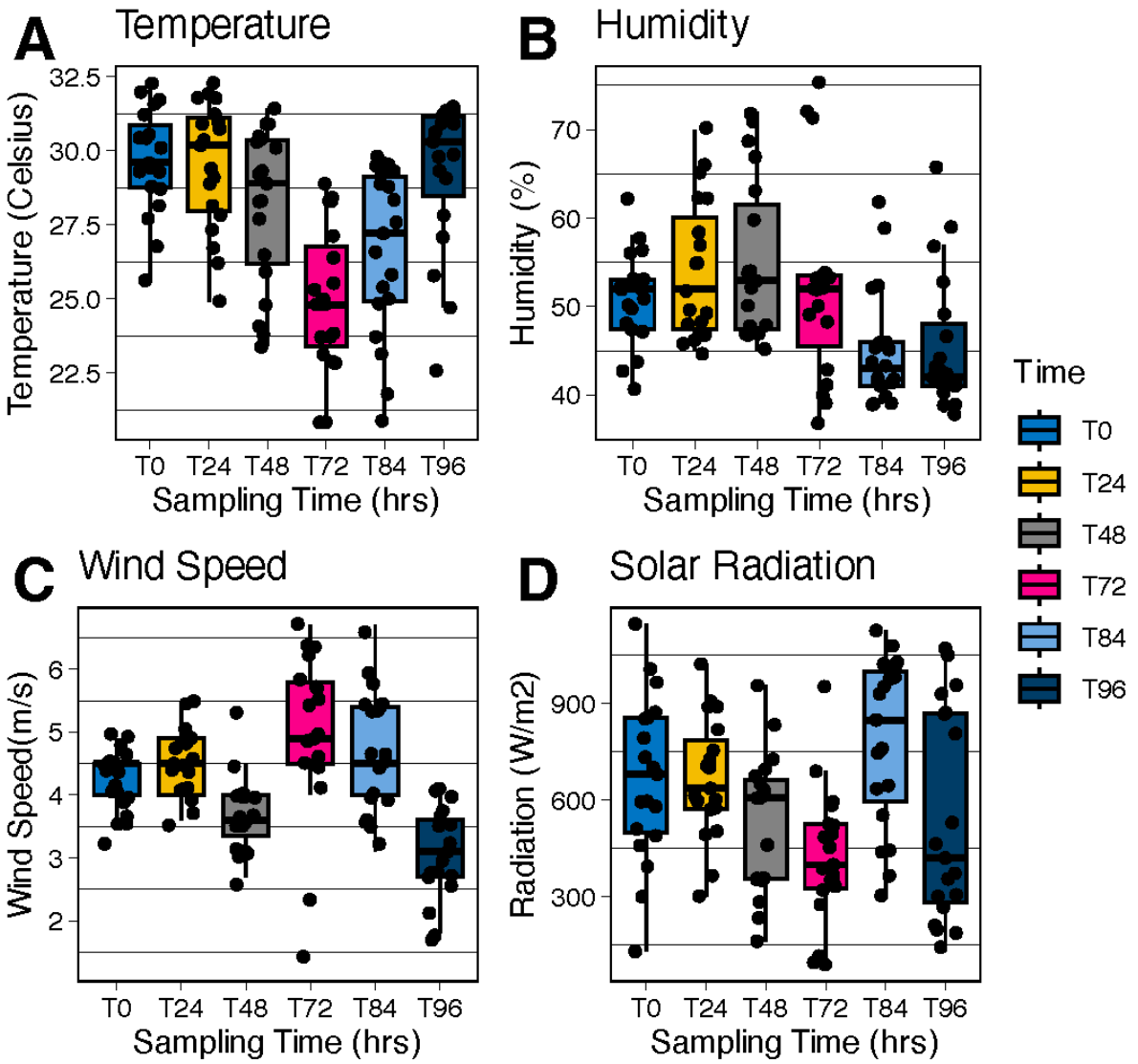


**Figure 4-S1**. Weather parameters were recorded throughout the sampling period, with data collected every 30 minutes between 12:00 PM and 9:00 PM. Sampling was conducted at 17:00 pm. A) Temperature, B) Humidity, C) Wind speed, and D) Solar radiation. The sampling points were T0, T48, T84 and T96. Data were obtained from a weather station located 0.5 km from the plant sampling site.

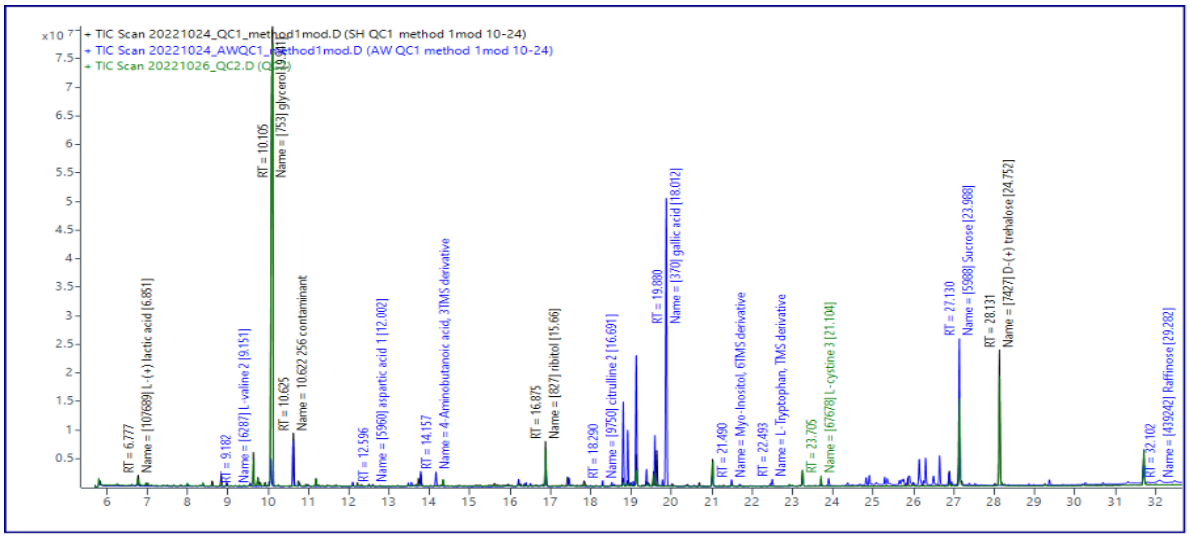


**Figure 4-S2**. The chromatogram of the quality control of the rhizosphere soil of the resurrection plant *Myrothamnus flabellifolia* under dehydration and rehydration stages. The most abundant metabolites with a greater peak area in the rhizosphere soil across all conditions were glycerol, gallic acid, trehalose, sucrose, sorbitol, and ribose.

**Table 4-S1**. Enrichment pathway analysis of significant metabolites ($P < 0.05$) which were accumulated in the rhizosphere soil of *Myrothamnus flabellifolia* under partially dehydrated, desiccated and fully rehydrated conditions. The pathway analysis in plants (*Arabidopsis thaliana*) and microbes (*E. coli* and *S. cerevisiae*) KEGG data bases were used to determine the most significant pathways. Pathway analyses were conducted in MetaboAnalyst platform.

| | **Partially dehydrated** | **Desiccated** | **Hydrated** |
|---|---|---|---|
| **Plant** | Butanoate metabolism | Aminoacyl-tRNA biosynthesis | Alanine, aspartate and glutamate metabolism |
| | Citrate cycle (TCA cycle) | Phenylalanine, tyrosine and tryptophan biosynthesis | Arginine and proline metabolism |
| | Alanine, aspartate and glutamate metabolism | Isoquinoline alkaloid biosynthesis | Aminoacyl-tRNA biosynthesis |
| | C5-Branched dibasic acid metabolism | Tropane, piperidine and pyridine alkaloid biosynthesis | Butanoate metabolism |
| | Monobactam biosynthesis | | Galactose metabolism |
| | Tyrosine metabolism | | Glyoxylate and dicarboxylate metabolism |
| | Arginine biosynthesis | | Indole alkaloid biosynthesis |
| | | | Glucosinolate biosynthesis |
| **Yeast** | Citrate cycle (TCA cycle) | Aminoacyl-tRNA biosynthesis | Alanine, aspartate and glutamate metabolism |
| | Alanine, aspartate and glutamate metabolism | Phenylalanine, tyrosine and tryptophan biosynthesis | Arginine and proline metabolism |
| | C5-Branched dibasic acid metabolism | Ubiquinone and other terpenoid-quinone biosynthesis | Butanoate metabolism |

| | | | |
|---|---|---|---|
| | Taurine and hypotaurine metabolism | | Aminoacyl-tRNA biosynthesis |
| | Butanoate metabolism | | Glyoxylate and dicarboxylate metabolism |
| | Lysine biosynthesis | | Carbapenem biosynthesis |
| | | | Nitrogen metabolism |
| **Bacteria** | Citrate cycle (TCA cycle) | Aminoacyl-tRNA biosynthesis | Alanine, aspartate and glutamate metabolism |
| | Alanine, aspartate and glutamate metabolism | Phenylalanine, tyrosine and tryptophan biosynthesis | Arginine and proline metabolism |
| | Dioxin degradation | Novobiocin biosynthesis | Aminoacyl-tRNA biosynthesis |
| | Taurine and hypotaurine metabolism | | Butanoate metabolism |
| | Pentose and glucuronate interconversions | | Carbapenem biosynthesis |
| | C5-Branched dibasic acid metabolism | | Glyoxylate and dicarboxylate metabolism |
| | Ascorbate and adorate metabolism | | Galactose metabolism |
| | Monobactam biosynthesis | | |
| | Xylene degradation | | |
| | Terpenoid backbone biosynthesis | | |
| | Arginine biosynthesis | | |
| | Lysine degradation | | |
| | Pantothenate and CoA biosynthesis | | |

## 4.8. References


Ahkami, A. H., White Iii, R. A., Handakumbura, P. P. and Jansson, C. 2017. Rhizosphere engineering: enhancing sustainable plant ecosystem productivity. *Rhizosphere,* 3**,** pp. 233-243.

Akram, W., Aslam, H., Ahmad, S. R., Anjum, T., Yasin, N. A., Khan, W. U., Ahmad, A., Guo, J., Wu, T. and Luo, W. 2019. Bacillus megaterium strain A12 ameliorates salinity stress in tomato plants through multiple mechanisms. *Journal of Plant Interactions,* 14**,** pp. 506-518.

Babaei, M., Shabani, L. and Hashemi-Shahraki, S. 2022. Improving the effects of salt stress by β-carotene and gallic acid using increasing antioxidant activity and regulating ion uptake in Lepidium sativum L. *Botanical Studies,* 63**,** p. 22.

Bentley, J. and Farrant, J. M. 2020. Field and acclimated metabolomes of a resurrection plant suggest strong environmental regulation in the extreme end of the species' range. *South African Journal of Botany,* 135**,** pp. 127-136.

Bentley, J., Moore, J. P. and Farrant, J. M. 2019. Metabolomics as a complement to phylogenetics for assessing intraspecific boundaries in the desiccation-tolerant medicinal shrub Myrothamnus flabellifolia (Myrothamnaceae). *Phytochemistry,* 159**,** pp. 127-136.

Berner, R.A. 1992. Weathering, plants, and the long-term carbon cycle Geochim. *Cosmochimica et Acta*, 56), pp. 3225-3231.

Bornø, M. L., Mueller-Stoever, D. S. and Liu, F. 2022. Biochar modifies the content of primary metabolites in the rhizosphere of well-watered and drought-stressed Zea mays L.(maize). *Biology and Fertility of Soils,* 58**,** pp. 633-647.

Canarini, A., Kaiser, C., Merchant, A., Richter, A. and Wanek, W. 2019. Root Exudation of Primary Metabolites: Mechanisms and Their Roles in Plant Responses to Environmental Stimuli. *Frontiers in plant science,* p. 10.

Chen, H. Y., Huh, J. H., Yu, Y. C., Ho, L. H., Chen, L. Q., Tholl, D., Frommer, W. B. and Guo, W. J. 2015. The Arabidopsis vacuolar sugar transporter SWEET 2 limits carbon sequestration from roots and restricts Pythium infection. *The Plant Journal,* 83**,** pp. 1046-1058.

Chen, Z., Li, X. and Zhang, L. 2014. Effect of salicylic acid pretreatment on drought stress responses of zoysiagrass (Zoysia japonica). *Russian Journal of Plant Physiology,* 61**,** pp. 619-625.

Chmielewska, K., Rodziewicz, P., Swarcewicz, B., Sawikowska, A., Krajewski, P., Marczak, Ł., Ciesiołka, D., Kuczyńska, A., Mikołajczak, K. and Ogrodowicz, P. 2016. Analysis of drought-induced proteomic and metabolomic changes in barley (Hordeum vulgare L.) leaves and roots unravel some aspects of biochemical mechanisms involved in drought tolerance. *Frontiers in plant science,* 7**,** p. 1108.

Dace, H.J., Reus, R., Ricco, C.R., Hall, R., Farrant, J.M. and Hilhorst, H.W. 2023. A horizontal view of primary metabolomes in vegetative desiccation tolerance. *Physiologia Plantarum*, 175(6), p.e14109.

Farrant, J. M. 2000. A comparison of mechanisms of desiccation tolerance among three angiosperm resurrection plant species. *Plant Ecology,* 151**,** pp. 29-39.

Farrant, J. M. 2007. Mechanisms of desiccation tolerance in angiosperm resurrection plants. *Plant desiccation tolerance***,** pp. 51-90.

Farrant, J. M., Cooper, K., Hilgart, A., Abdalla, K. O., Bentley, J., Thomson, J. A., Dace, H. J., Peton, N., Mundree, S. G. and Rafudeen, M. S. 2015. A molecular physiological review of vegetative desiccation tolerance in the resurrection plant *Xerophyta viscosa* (Baker). *Planta,* 242**,** pp. 407-426.

Fiehn, O. 2016. Metabolomics by gas chromatography–mass spectrometry: Combined targeted and untargeted profiling. *Current protocols in molecular biology*, 114(1), pp.30-34.

Fu, S.-F., Wei, J.-Y., Chen, H.-W., Liu, Y.-Y., Lu, H.-Y. and Chou, J.-Y. 2015. Indole-3-acetic acid: A widespread physiological code in interactions of fungi with other organisms. *Plant Signaling & Behavior,* 10**,** p. e1048052.

Gabier, H., Tabb, D. L., Farrant, J. M. and Rafudeen, M. S. 2021. A Label-Free Proteomic and Complementary Metabolomic Analysis of Leaves of the Resurrection Plant Xerophyta schlechteri during Dehydration. *Life,* 11**,** p. 1242.

Ghanbarzadeh, Z., Zamani, H., Mohsenzadeh, S., Marczak, Ł., Stobiecki, M. and Zarei, M. 2021. Rhizosphere symbionts improve water stress tolerance in Moldavian balm through modulation of osmolytes. *Rhizosphere,* 19**,** p. 100367.

Ginbot, Z.G. and Farrant, J.M. 2011. Physiological response of selected Eragrostis species to water-deficit stress. *African Journal of Biotechnology*, *10*(51), pp.10405-10417.

González-Villagra, J., Reyes-Díaz, M. M., Tighe-Neira, R., Inostroza-Blancheteau, C., Escobar, A. L. and Bravo, L. A. 2022. Salicylic acid improves antioxidant defense system and photosynthetic performance in Aristotelia chilensis plants subjected to moderate drought stress. *Plants,* 11**,** p.639.

Guo, R., Shi, L., Jiao, Y., Li, M., Zhong, X., Gu, F., Liu, Q., Xia, X. and Li, H. 2018. Metabolic responses to drought stress in the tissues of drought-tolerant and drought-sensitive wheat genotype seedlings. *Agronomy & Botany Plants,* 10**,** p. 016.

Igiehon, N.O. and Babalola, O.O. 2018. Rhizosphere microbiome modulators: contributions of nitrogen fixing bacteria towards sustainable agriculture. *International journal of environmental research and public health*, 15(4), p.574.

Khan, N., Bano, A. and Babar, M.A. 2019. Metabolic and physiological changes induced by plant growth regulators and plant growth promoting rhizobacteria and their impact on drought tolerance in Cicer arietinum L. *Public Library of Science one*, *14*(3), p.e0213040.

Khan, M. I. R., Fatma, M., Per, T. S., Anjum, N. A. and Khan, N. A. 2015. Salicylic acid-induced abiotic stress tolerance and underlying mechanisms in plants. *Frontiers in plant science,* 6**,** p.462.

Klamer, R. 2022. MSc dissertation: Descending below the surface: root metabolomics of the South African resurrection plant Myrothamnus Flabellifolius (unpublished). Wageningen University & Research, pp. 20-45.

Kranner, I., Beckett, R. P., Wornik, S., Zorn, M. and Pfeiffer, H. W. 2002. Revival of a resurrection plant correlates with its antioxidant status. *The Plant Journal,* 31**,** pp.13-24.

Li, Z., Yu, J., Peng, Y. and Huang, B. 2017. Metabolic pathways regulated by abscisic acid, salicylic acid and γ-aminobutyric acid in association with improved drought tolerance in creeping bentgrass (Agrostis stolonifera). *Physiologia Plantarum,* 159**,** pp.42-58.

Ludwig, M. 2016. The roles of organic acids in C4 photosynthesis. *Frontiers in plant science,* 7**,** p.647.

Mendes, R., Garbeva, P. and Raaijmakers, J.M. 2013. The rhizosphere microbiome: significance of plant beneficial, plant pathogenic, and human pathogenic microorganisms. *Federation of European Microbiological Societies Microbiology Reviews*, 37(5), pp. 634-663.

Meyer, S., De Angeli, A., Fernie, A. R. and Martinoia, E. 2010. Intra-and extra-cellular excretion of carboxylates. *Trends in plant science,* 15**,** pp. 40-47.

Moore, J., Ravenscroft, N., Lindsey, G., Farrant, J. and Brandt, W. 2004. Galloylquinate ester: anthocyanin complexes in the leaves of the desiccated resurrection plant Myrothamnus flabellifolius. Polyphenols Communications: XXII *International Conference on Polyphenols*, pp. 25-28.

Moore, J., Waldron, M., Lindsey, G., Farrant, J. and Brandt, W. 2011. An ultrastructural investigation of the surface microbiota present on the leaves and reproductive structures of the resurrection plant Myrothamnus flabellifolia. *South African Journal of Botany,* 77**,** pp.485-491.

Moore, J. P., Farrant, J. M. and Driouich, A. 2008. A role for pectin-associated arabinans in maintaining the flexibility of the plant cell wall during water deficit stress. *Plant Signaling & Behavior,* 3**,** pp.102-104.

Moore, J. P., Lindsey, G. G., Farrant, J. M. and Brandt, W. F. 2007. An Overview of the Biology of the Desiccation-tolerant Resurrection Plant Myrothamnus flabellifolia. *Annals of Botany,* 99**,** pp.211-217.

Nagler, M., Nägele, T., Gilli, C., Fragner, L., Korte, A., Platzer, A., Farlow, A., Nordborg, M. and Weckwerth, W. 2018. Eco-metabolomics and metabolic modeling: making the leap from model systems in the lab to native populations in the field. *Frontiers in Plant Science*, *9*, p.1556.

Nevoigt, E. and Stahl, U. 1997. Osmoregulation and glycerol metabolism in the yeast Saccharomyces cerevisiae. *Federation of European Microbiological Societies Microbiology Reviews,* 21**,** pp. 231-241.

Oburger, E. and Jones, D. 2018. Sampling root exudates–Mission impossible. *Rhizosphere*, 6, pp. 116–133.

Oliver, M. J., Farrant, J. M., Hilhorst, H. W., Mundree, S., Williams, B. and Bewley, J. D. 2020. Desiccation tolerance: avoiding cellular damage during drying and rehydration. *Annual review of plant biology,* 71**,** pp. 435-460.

Pan, Y., Kang, P., Tan, M., Hu, J., Zhang, Y., Zhang, J., Song, N. and Li, X. 2022. Root exudates and rhizosphere soil bacterial relationships of Nitraria tangutorum are linked to k-strategists bacterial community under salt stress. *Frontiers in plant science,* p. 13.

Passon, M., Weber, F., Jung, N. U. and Bartels, D. 2021. Profiling of phenolic compounds in desiccation-tolerant and non-desiccation-tolerant Linderniaceae. *Phytochemical Analysis,* 32**,** pp. 521-529.

Pérez-Llorca, M., Muñoz, P., Müller, M. and Munné-Bosch, S. 2019. Biosynthesis, Metabolism and Function of Auxin, Salicylic Acid and Melatonin in Climacteric and Non-climacteric Fruits. *Frontiers in plant science,* p. 10.

Pétriacq, P., Williams, A., Cotton, A., Mcfarlane, A. E., Rolfe, S. A. and Ton, J. 2017. Metabolite profiling of non-sterile rhizosphere soil. *The Plant Journal,* 92**,** pp. 147-162.

Petushkova, E., Mayorova, E. and Tsygankov, A. 2021. TCA cycle replenishing pathways in photosynthetic purple non-sulfur bacteria growing with acetate. *Life*, 11(7), p.711.

Playsted, C. W. S., Johnston, M. E., Ramage, C. M., Edwards, D. G., Cawthray, G. R. and Lambers, H. 2006. Functional significance of dauciform roots: exudation of carboxylates and acid phosphatase under phosphorus deficiency in Caustis blakei (Cyperaceae). *New Phytologist,* 170**,** pp. 491-500.

Radermacher, A. L., Du Toit, S. F. and Farrant, J. M. 2019. Desiccation-driven senescence in the resurrection plant Xerophyta schlechteri (Baker) NL Menezes: Comparison of anatomical, ultrastructural, and metabolic responses between senescent and non-senescent tissues. *Frontiers in plant science,* 10**,** p. 1396.

Salas-González, I., Reyt, G., Flis, P., Custódio, V., Gopaulchan, D., Bakhoum, N., Dew, T. P., Suresh, K., Franke, R. B., Dangl, J. L., Salt, D. E. and Castrillo, G. 2021. Coordination between microbiota and root endodermis supports plant mineral nutrient homeostasis. *Science,* 371**,** p. eabd0695.

Salem, M.A., Yoshida, T., Perez de Souza, L., Alseekh, S., Bajdzienko, K., Fernie, A.R. and Giavalisco, P. 2020. An improved extraction method enables the comprehensive analysis of lipids, proteins, metabolites and phytohormones from a single sample of leaf tissue under water-deficit stress. *The Plant Journal*, *103*(4), pp.1614-1632.

Schellenberger, S., Drake, H. L. and Kolb, S. 2011. Functionally redundant cellobiose-degrading soil bacteria respond differentially to oxygen. *Applied and Environmental Microbiology,* 77**,** pp. 6043-6048.

Sgherri, C., Cecconami, S., Pinzino, C., Navari-Izzo, F. and Izzo, R. 2010. Levels of antioxidants and nutraceuticals in basil grown in hydroponics and soil. *Food chemistry,* 123**,** pp. 416-422.

Sherwin, H. W., Pammenter, N., February, E., Vander Willigen, C. and Farrant, J. M. 1998. Xylem hydraulic characteristics, water relations and wood anatomy of the resurrection plant Myrothamnus flabellifolius Welw. *Annals of Botany,* 81**,** pp. 567-575.

Si, P., Shao, W., Yu, H., Xu, G. and Du, G. 2022. Differences in microbial communities stimulated by malic acid have the potential to improve nutrient absorption and fruit quality of grapes. *Frontiers in Microbiology,* p. 13.

Svennerstam, H., Jämtgård, S., Ahmad, I., Huss-Danell, K., Näsholm, T. and Ganeteg, U. 2011. Transporters in Arabidopsis roots mediating uptake of amino acids at naturally occurring concentrations. *New Phytologist*, 191(2), pp.459-467.

Swenson, T.L. and Northen, T.R. 2019. Untargeted soil metabolomics using liquid chromatography–mass spectrometry and gas chromatography–mass spectrometry: In E. K. Edward (ed.) Microbial Metabolomics. New York: Springer, pp. 97-109.

Tapia, H., Young, L., Fox, D., Bertozzi, C. R. and Koshland, D. 2015. Increasing intracellular trehalose is sufficient to confer desiccation tolerance to Saccharomyces cerevisiae. *Proceedings of the National Academy of Sciences,* 112**,** pp. 6122-6127.

Tebele, S.M., Marks, R.A. and Farrant, J.M. 2023. Exploring the root-associated microbiome of the resurrection plant Myrothamnus flabellifolia. *Plant and Soil*, pp.1-16.

Tran, T. L. C., Callahan, D. L., Islam, M. T., Wang, Y., Arioli, T. and Cahill, D. 2023. Comparative metabolomic profiling of Arabidopsis thaliana roots and leaves reveals complex response mechanisms induced by a seaweed extract. *Frontiers in plant science,* 14**,** p. 699.

Uzma, M., Iqbal, A. and Hasnain, S. 2022. Drought tolerance induction and growth promotion by indole acetic acid producing Pseudomonas aeruginosa in Vigna radiata. *Public Library of Science one,* 17**,** p. e0262932.

Wei, F., Fanella, B., Guo, L. and Wang, X. 2016. Membrane glycerolipidome of soybean root hairs and its response to nitrogen and phosphate availability. *Scientific Reports*, *6*(1), pp.1-11.

Wenz, J., Davis, J. G. and Storteboom, H. 2019. Influence of light on endogenous phytohormone concentrations of a nitrogen-fixing Anabaena sp. cyanobacterium culture in open raceways for use as fertilizer for horticultural crops. *Journal of Applied Phycology,* 31**,** pp. 3371-3384.

Yao, H., Zhang, S., Zhou, W., Liu, Y., Liu, Y. and Wu, Y. 2020. The effects of exogenous malic acid in relieving aluminum toxicity in Pinus massoniana. *International Journal of Phytoremediation,* 22**,** pp. 669-678.

Yobi, A., Schlauch, K. A., Tillett, R. L., Yim, W. C., Espinoza, C., Wone, B. W., Cushman, J. C. and Oliver, M. J. 2017. Sporobolus stapfianus: Insights into desiccation tolerance in the resurrection grasses from linking transcriptomics to metabolomics. *BMC plant biology,* 17**,** pp. 1-30.

Yobi, A., Wone, B. W. M., Xu, W., Alexander, D. C., Guo, L., Ryals, J. A., Oliver, M. J. and Cushman, J. C. 2012. Comparative metabolic profiling between desiccation-sensitive and desiccation-tolerant species of Selaginella reveals insights into the resurrection trait. *The Plant Journal,* 72**,** pp. 983-999.

You, J., Zhang, Y., Liu, A., Li, D., Wang, X., Dossa, K., Zhou, R., Yu, J., Zhang, Y., Wang, L. and Zhang, X. 2019. Transcriptomic and metabolomic profiling of drought-tolerant and susceptible sesame genotypes in response to drought stress. *BMC plant biology,* 19**,** p. 267.

Zhang, Y., Li, Y., Hassan, M. J., Li, Z. and Peng, Y. 2020. Indole-3-acetic acid improves drought tolerance of white clover via activating auxin, abscisic acid and jasmonic acid related genes and inhibiting senescence genes. *BMC plant biology,* 20**,** pp. 1-12.

Zhou, L., Peng, Y., Yin, S. and Han, L. 2019. Effects of exogenous mannose application on drought tolerance, sugars, and sugar alcohol accumulation in white clover. *Acta Prataculturae Sinica,* 28**,** pp. 85-93.

Zhou, Y., Yang, Z., Xu, Y., Sun, H., Sun, Z., Lin, B., Sun, W. and You, J. 2018. Soybean NADP-Malic Enzyme Functions in Malate and Citrate Metabolism and Contributes to Their Efflux under Al Stress. *Frontiers in plant science,* p.8.

# Chapter Five

## Rhizospheric bacteria of *Myrothamnus flabellifolia* improve plant growth and drought tolerance of maize

## 5.1. Summary

Plant growth-promoting bacteria can improve growth and enhance various biotic and abiotic stress tolerances in host plants. The application of rhizospheric bacteria in agricultural settings is a promising avenue for improving crop performance and offsetting the use of chemical fertilizers. *Myrothamnus flabellifolia* hosts diverse microbes in its rhizosphere. However, the effects of rhizospheric bacteria from resurrection plants on staple crops, and how these microbes can improve drought tolerance, remain understudied. Therefore, this study aimed to isolate bacteria from dry rhizosphere soil of *M. flabellifolia* and evaluate their impact on maize. The performance of primed maize plants with rhizospheric bacteria was measured under moderate drought stress using physiological, and metabolic approaches. The impact of seed biopriming using 12 bacterial isolates, demonstrated that Bac7, Bac9, Bac11, and Bac12 were the most effective for improving plant growth and resilience. Drought stress significantly affected the physiology and biochemistry of maize plants. However, plants inoculated with these bacterial isolates had improved antioxidant potential, chlorophyll content, growth, and reduced rate of water loss. Endogenous metabolic profiling of rhizospheric bacteria showed high accumulation of amino acids, sugars, organic acids, and polyamines, which may facilitate the enhancement of drought tolerance in maize. Taken together, this study provides valuable insights into the potential bacteria to confer drought tolerance in crops species.

## 5.2. Introduction

Maize (*Zea mays L*) is one of the leading staple cereals in the world, with an estimated 197 million hectares of cultivation globally, and is pivotal in ensuring food security (Erenstein et al., 2022). The frequent occurrence of drought as a result of climate change negatively affects food crop production. Drought is a major contributor to soil nutrient depletion and can promote the proliferation of pathogens such as Fusarium species in maize, ultimately leading to a significant decline in agricultural yield (Herrera et al., 2023). Additionally, water deficit conditions also negatively affect plant growth and reproduction and perturb essential molecular, physiological, and biochemical pathways. These effects include the formation of free radicals in cells, protein oxidation, reduced photosynthesis, lipid peroxidation, perturbation of chlorophyll synthesis and enzymatic activities, and reduced plant growth

(Mishra et al., 2020). Taken together, drought is a problematic phenomenon exacerbated by climate change, and when coupled with the application of chemicals, it negatively impacts agricultural production.

Most plants cannot survive under water deficit conditions, but resurrection plants, such as *M. flabellifolia*, have developed the ability to withstand extreme water limitations. *M. flabellifolia* is associated with a diverse and beneficial microbiome in its rhizosphere (Chapter Two, Tebele et al., 2023). The soil microenvironment around these plants supports a wide range of microorganisms, which can be either beneficial or harmful to the plant. Additionally, a recent study by Imminger et al. (2024) demonstrated how soil biocrust microbial communities in desert ecosystems slowly resuscitate after rehydration. Given the potential of microbes in agricultural applications, the role of soil microbes associated with *M. flabellifolia* remains an unexplored area of research.

A healthy fertile and well-functioning soil environment is essential for optimum crop production. The application of plant growth-promoting bacteria (PGPB) as biofertilizers or biostimulants to enhance drought tolerance, plant productivity, and nutrient uptake by the host plant is rapidly expanding. For instance, maize, cumin, wheat, and tomato seeds primed with *Rhizobium phaseoli*-RS-1, *Pseudomonas spp.*, and *Bacillus spp.* respectively, showed improved physiological and agronomic parameters under drought stress (Eke et al., 2019; Lastochkina et al., 2020; Nawaz et al., 2020; Piri et al., 2019). It is also important to use environmentally friendly products, such as biodegradable biological agents. PGPB produce a wide range of metabolites that improve the defense mechanism of plants (Li et al., 2023), however, these avenues have not been explored using microbes associated with resurrection plants.

Although culture-dependent methods for characterizing microbes are valuable, they are limited by the fact that many microbes have not yet been cultured. However, out of millions of bacterial species, only an estimated 30,000 have been successfully cultivated, with many of these applied in biotechnology to enhance human health, food systems, and agricultural productivity (Steen et al., 2019; Vitorino and Bessa, 2017). Therefore, incorporation of technical microbiology such as using microbes is a promising strategy to improve plant resilience against drought stress in agricultural crops (Calvo et al., 2014). Biopriming is commonly used to incorporate beneficial microbes into seeds or plants through various methods namely seed coating, pelleting, direct soil application, and root dipping (Mahmood et al., 2016). Seed biopriming is efficient, promotes uniform germination, and minimise contamination (Nawaz et al., 2019). To the best of our knowledge, the isolation and application of PGPB from the rhizosphere soil of *M. flabellifolia* using biopriming techniques on staple crops has never been explored. Therefore, this study aimed to evaluate the impact of rhizospheric

bacteria isolated from *M. flabellifolia* under desiccated and low-temperature conditions on maize under moderate drought stress.

## 5.3. Materials and methods

### 5.3.1. Collection of rhizosphere soil and pre-culturing

Rhizosphere soil samples of desiccated *M. flabellifolia* were collected in January 2022 from different areas of the Swebeswebe field site in South Africa and all samples were placed in liquid nitrogen, as described in Chapter Three (Figure 3-1). To isolate the bacteria from desiccated and low-temperature conditions, samples were stored in a -80°C freezer at the University of Cape Town. Frozen rhizosphere soil was thawed at room temperature and mixed to form one composite pool of soil samples. One (1) g of soil was weighed into a 50 ml 0.85% saline solution and vigorously mixed for homogenisation. Serial dilutions were performed in four different media, namely, Difco, Luria-Bertani (LB), nutrient agar, and yeast extract-malt extract (YEME) medium, to evaluate which media supported most microbes. All plates, including controls, were supplemented with 50 µg/mL cycloheximide to inhibit fungal growth, and plates were incubated at 28$^{o}$C for 1-5 days based on the type of media. Twelve distinct bacterial colonies (Bac1, Bac2, Bac3, Bac4, Bac5, Bac6, Bac7, Bac8, Bac9, Bac10, Bac11, and Bac12) were recorded, and subculturing was performed to generate pure culture. Furthermore, gram stain was performed to evaluate the gram reaction of the isolated bacteria.

### 5.3.2. Maize seed biopriming and drought stress

Twelve bacterial colonies (Bac1 to Bac12) were cultivated in 5 mL LB broth and incubated for 48 hours at 25$^{o}$C with agitation at 220 rpm for optimal growth. Culturing analysis was conducted in triplicate. The cells were harvested by centrifugation at 10 000 x g for 30 min at 4 °C. The pellet was resuspended in sterile *d*$H_2O$ to obtain a final concentration of $OD_{600}$ = 1 × $10^8$ CFU/mL. Maize seeds (Golden Bantam Sweetcorn) were surface sterilised with 70% ethanol for three min and rinsed in sterile water for two min. Seeds were further sterilised with a mixture of 10% NaOCl (w/v) and 17 µL of Tween-20 for 10 min and washed four times with sterile water (Davoudpour et al., 2020). Sterilised seeds were dried for 24 hours in petri dishes. Finally, three seeds were primed with the 1 × $10^8$ CFU/mL bacterial suspensions (5 mL) and incubated at 25$^{o}$C with agitation at 100 rpm for 24 hours under dark conditions. Maize seeds exhibited a thin coating of bacterial cells after biopriming. The coated seeds were dried in a Petri dish under aseptic conditions with filter paper for 6 hours (Miljaković et al., 2022). Non-primed seeds were treated with sterile distilled water.

Bio-primed maize seeds were germinated in a peat-based compost potting soil in a 3 L (19 cm) pot. Four seeds were germinated for each treatment for a total of 56 maize plants in this experiment. Seeds that were coated with bacterial colony 1 (Bac1) were classified as treatment 1 (T1), application of Bac2 on seeds was named treatment 2 (T2) and this naming system was applied until T12. Non-primed seeds were classified as control. Plants were grown under controlled environmental conditions in the University of Cape Town growth room at 25°/28°C with a 12-hour photoperiod. This experiment comprised two treatments: drought stress (ws) with four primed maize seeds per bacterial isolate and four untreated maize seeds (ws control), as well as well-watered (ww control) untreated maize plants (ww control). The inclusion of well-watered untreated maize samples allowed for an assessment of the impact of drought stress severity on untreated plants. To evaluate the impact of drought on primed maize plants, two-week old maize seedlings at the V5 stage were subjected to drought stress by withholding watering for ten days, and control plants (ww control) were continuously watered. An EM50 data logger with an EC-5 soil volumetric water content (VWC) probe was used to measure the VWC of the soil within the proximity of the maize roots. Plants were assessed when the soil VWC was 10% in all plants and leaves were yellowing, rolling and wilting. After ten days of drought stress, leaf tissue was collected, immediately frozen in liquid nitrogen, and stored at -80°C until further analysis.

### 5.3.3. Physiological characterization of maize plants

Leaf relative water content (RWC) was measured after 10 days of drought stress by collecting one gram of leaves from each plant, and the fresh weight was recorded. Leaves were dried at 65°C for 24 hours, mass was recorded and RWC was calculated as described in Chapter Three (Section 3.3.1). The contents of chlorophyll a and b were analysed according to Senthilkumar et al. (2021), with some modifications. First, the leaf samples were ground using a mixer mill MM400 (Retsch, USA), and 100 mg of fine powder was added to 2 mL of 80% acetone. The samples were vigorously mixed and stored on ice for one hour. The aliquot was centrifuged at 3500 rpm for 10 min at 4 °C, 200 µL supernatant was transferred to a new tube, and the absorbance was measured at 643, 645, 663, and 665 nm. The amount of chlorophyll per millilitre was calculated for all three technical replicates per sample using Equation 2-4 (Tran et al., 2019; Warren, 2008). After rehydration of maize seedlings, chlorophyll fluorescence, leaf area, root dry mass, shoot dry mass, and length were measured after 12 days to assess the survival of treated plants under drought stress. Chlorophyll fluorescence was measured using a portable fluorometer after acclimating plants to dark conditions for 15 minutes, during which the minimum (F0) and maximum (Fm) fluorescence intensities were recorded (Asghari et al., 2020). Photosystem II (Fv/Fm) was calculated using Equation 5 to measure the maximum quantum yield. Maize shoot and root lengths were measured using a measuring tape. Leaf area was calculated by

measuring the leaf width and length. The dry weights of the shoots and roots of maize seedlings were measured by placing the samples in an oven at 65°C for 48 hours to generate dry biomass.

$$Chl\ a(\mu g/mL) = [12.7 \times (A663) - 2.69 \times (A645)] \text{.....(2)}$$

$$Chl\ b(\mu g/mL) = [(22.9 \times A645) - (4.62 \times A663)] \text{.....(3)}$$

$$Chl\ total\ \left(\frac{\mu g}{mL}\right) = [(20.2 \times A645) + (8.02 \times A663)] \text{.....(4)}$$

$$\frac{Fv}{Fm} = (Fm - F0)/Fm \text{.....(5)}$$

### 5.3.4. Enzyme extraction and antioxidant assays

Two distinctive methods were used to measure antioxidant activity: ferric reducing antioxidant power (FRAP) assay (non-enzymatic) and glutathione (GSH) assay. FRAP assay was performed as described by Shin et al. (2021). A 6-hydroxy-2,5,7,8-tetramethylchromane-2-carboxylic acid (Sigma-Aldrich) standard curve was generated at different concentrations (0-120 µM) and 80% methanol was used as a blank. The absorbance was measured at 593 nm, and the results were expressed as µM $g^{-1}$. The GSH assay was performed according to the method described by Rahman et al. (2006). Briefly, the frozen maize leaf powder was homogenised in 0.6% sulfosalicylic acid-triton-X solution and centrifuged at 8000 × g for 10 min at 4 °C. The supernatant was used for the GSH assay and potassium phosphate buffer was used as a blank. A GSH standard curve was prepared with a concentration between 5-100 µM and 2-nitro-5-thiobenzoic acid formation was expressed as a change in absorbance $min^{-1}$. The total GSH concentration in the samples was determined using the standard curve, and the results were reported as mmol $g^{-1}$ fresh weight.

### 5.3.5. Lipid peroxidase activity

Frozen leaf powder (2 g) was homogenised in 1 mL of ice-cold 0.1% trichloroacetic acid. The samples were fractionated by centrifugation at 12 000 rpm for 15 min, and 500 µL of the supernatant was mixed with 2 mL of 0.5% (w/v) thiobarbituric acid (TBA) in 20% (w/v) trichloroacetic acid (TCA). The solution was then heated at 95 °C for 15 min and cooled to room temperature. Solutions were centrifuged at 10 000 rpm for 5 mins. The optical density of the supernatant was measured at 532 and 600 nm to determine the malondialdehyde (MDA) content (Kusvuran, 2015). A standard curve was prepared by serial dilution of MDA stock solution (1-10 µM), the standard was treated with TBA, and OD was measured at 532 and 600 nm.

### 5.3.6. Endogenous metabolite analysis

Microbial metabolites were extracted as described by Purvis et al., (2005). Briefly, twelve bacterial colonies (Bac1 to Bac12) were able to grow in the LB broth. An optical density was measured at 600 nm using a 96-well plate reader (Multiskan Go, Thermo Scientific Inc, USA) to provide sufficient dry cell weight ($OD_{600}$ = 1 x $10^8$ CFU/mL) prior to metabolite extraction (Purvis et al., 2005). Bacterial cells were harvested by centrifugation at 10 000 x g for 10 min at 4$^o$C. A 50% methanol spiked with 2mg/mL ribitol was used to permeabilise cells and metabolites were extracted using an orbital shaker at 1200 rpm for one hour at 4$^o$C. The mixture was centrifuged at 10 000 x g for five min. The supernatant was filtered using 0.22 um pore size and dried in the speedivac system. The derivatization process and data processing were performed as described in Chapter Four (section 4.2.2).

### 5.3.7. Statistical analysis

Statistical analyses including tests of chlorophyll content, MDA, FRAP, RWC, root, and shoot biomass were performed in the RStudio v4.2.1 using ggplot2, ggpubr, rstatix, and patchwork packages. All physiological measurements were carried out in three replications. Differences between the inoculated maize plants and control plants (non-treated) under drought stress were determined by performing pairwise comparison student's t-test. This analysis was used for multiple comparisons with the control. A one-way analysis of variance (ANOVA) was used to measure global statistical differences between the samples. A correlation between all physiological variables was performed using corroplot to determine the analysis accounting for variability among the treatments. Bacterial metabolite data was standardized using sum of squares in the MetaboAnalysist as described in Chapter Four section 4.2. Principal component analysis (PCA) was performed to determine the dimensions of variation in the dataset and ANOVA was used to identify metabolites with significant differences between the bacterial isolates. Heatmaps with hierarchical clustering using Euclidean distance was used to determine similar metabolites abundance in bacterial isolates.

## 5.4. Results

### 5.4.1. Physiological effects of bacterial inoculants on maize under drought stress

#### 5.4.1.1. Relative water content

Water deficit conditions significantly affected the RWC of the maize leaves. Leaf RWC and soil VWC differed significantly ($p < 0.001$) between untreated well-watered (WW) and water-stressed (WS) plants from 80% to 40% RWC (Figure 5-S1A, B). As expected, biopriming with bacterial isolates significantly improved the RWC and VWC of the treated plants (Figure 5-1). All inoculated plants

exhibited significantly higher RWC compared to the control ($P < 0.05$), except for T1, T3, T5, T6, and T9 (Figure 5-1, Table 5-S1). Bacterial inoculation of maize plants improved the RWC of maize leaves by a minimum of 11% compared to untreated samples. Plants inoculated with T2, T4, and T12 exhibited the highest RWC compared to other treatments. The soil moisture of treated maize plants were significantly high compared to control samples with an exception of T1, T4, T7, T10, and T12 (Table 5-S2). This finding indicates that some primed maize seedlings exhibited a lower rate of water loss under drought stress.

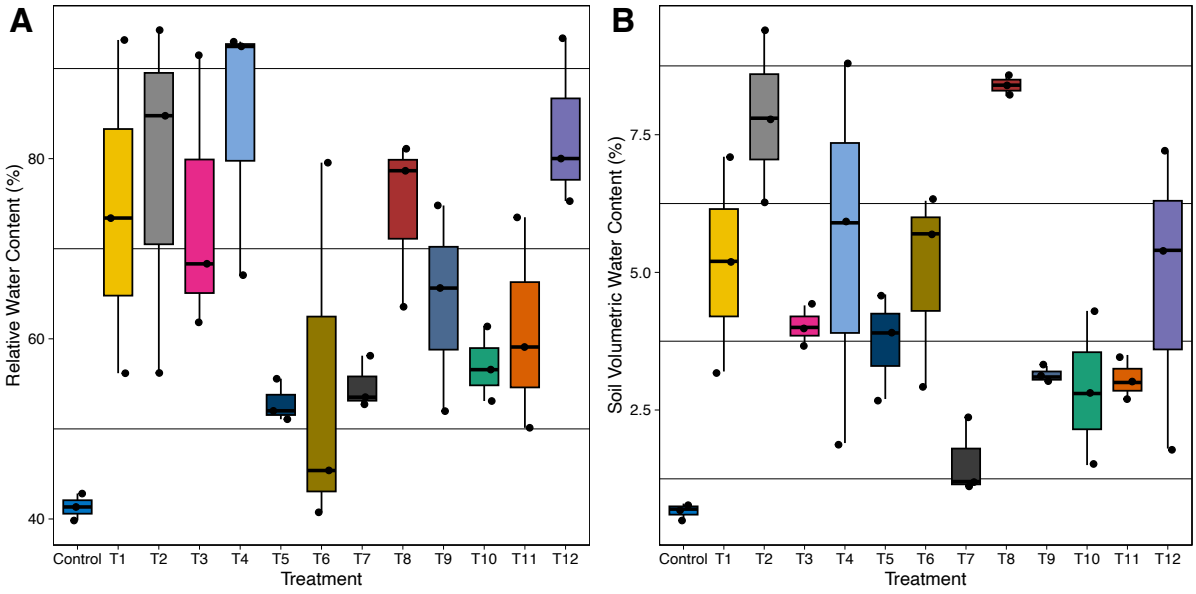


**Figure 5-1.** Effects of biopriming with bacterial inoculants (T1-T12) on the A) leaf relative water content and B) soil moisture of maize plants under drought stress.

#### 5.4.1.2. Chlorophyll content

Drought stress affected the chlorophyll content of maize plants. In control samples, Chl a content of well-watered plants was statistically similar to that of water-stressed plants (Figure 5-S1G), whereas Chl b of WW plants was significantly high ($P = 0.008$) relative to WS plants (Figure 5-S1H). Treatment T4, T7, T8, T9, and T10 exhibited statistically higher Chl a relative to the control, while Chl b content of T7, T8, and T9 was statistically higher than the control (Figure 5-2A, B). Biopriming remarkably improved the total chlorophyll content of plants, for instance, T3, T4, T7, T8, and T9 were significantly higher compared to the control (Figure 5-2C). Elevated total chlorophyll content suggests that the plant maintains efficient photosynthetic activity even under drought stress. Overall, rhizospheric bacteria improved the chlorophyll content of maize plants during drought stress.

The effects of post-drought stress on plant photosynthesis were evaluated by measuring maximum quantum efficiency to determine Fv/Fm. A decline in Fv/Fm values indicates a disruption in PSII (Asghari et al., 2020) and this phenomenon was detected in untreated WW and WS plants (Figure 5-S1J). Inoculated plant T7, T8, T11 and T12 treatments showed significantly higher Fv/Fm values compared to the control (Figure 5-2D). Despite that T11 and T12 plants exhibited lower total chlorophyll content under drought stress, these plants showed an extraordinary recovery upon rehydration. Whereas, T1, T2, T3, and T6 samples exhibited a slow recovery with low Fv/Fm values, indicating that photosynthesis was disrupted by drought stress. Taken together, a couple specific isolates stand out as they perform best across all metrices measured here. Inoculated plant T7, T8 and T9, all mainlined high chlorophyll content during drought stress and exhibited high Fv/Fm values after recovery.

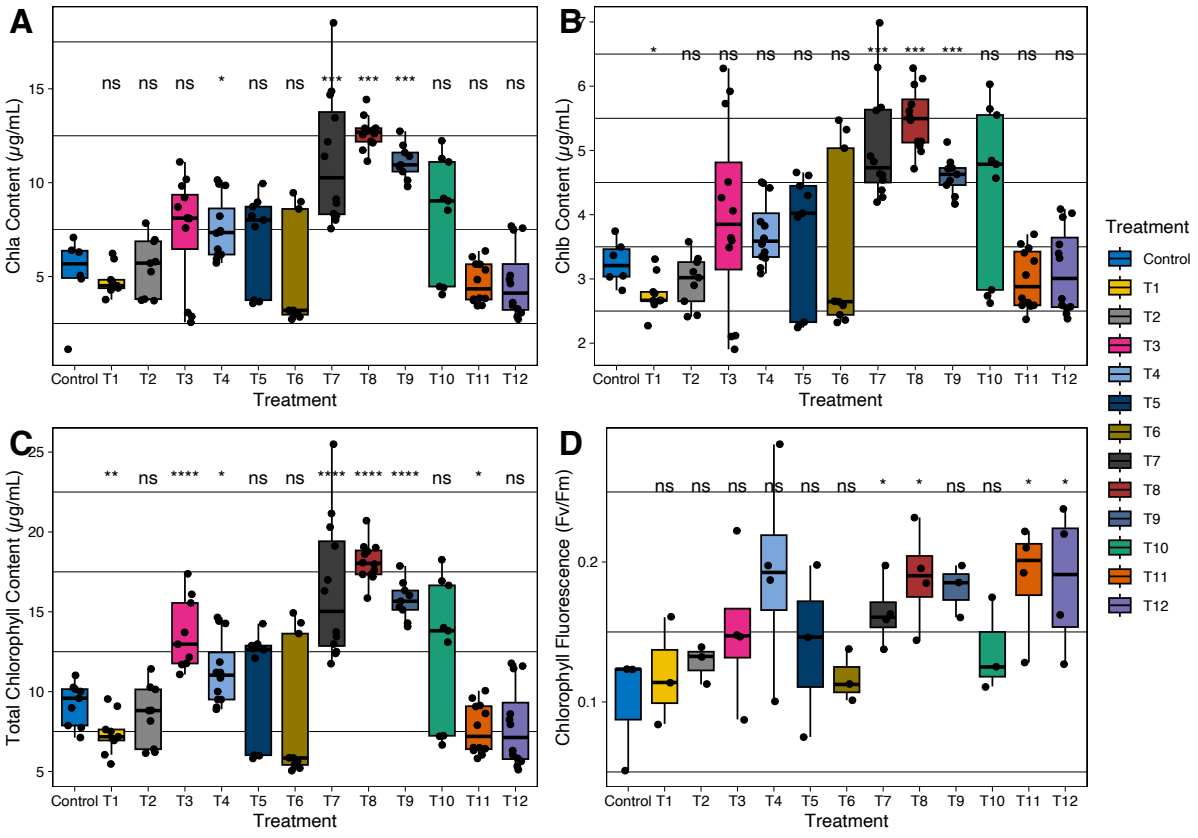


**Figure 5-2.** Effects of biopriming on A) Chlorophyll a, B) Chlorophyll b, and C) total chlorophyll content of maize (T1-12) and control under drought stress. D) Chlorophyll fluorescence (Fv/Fm) of treated maize post rehydration. The asterisk indicates the statistically significant difference level (* = 0.05, ** = 0.01 and *** = 0.001) and between the control and inoculated plants.

### 5.4.1.3. Malondialdehyde

The adverse effects of drought exposure on lipid peroxidation were determined through MDA assay. In general, drought stress leads to significantly increased MDA accumulation in plants. The MDA content of WW and WS plants was insignificantly different (P = 0.07), but the trend showed lower levels of MDA in WW plants relative to WS plants (Figure 5-S1M). The application of bacterial inoculums T1 to T4, T7 and T8 on maize led to a significant reduction of MDA content by approximately 2-fold, particularly T1 and T2 compared to the control. The MDA content of T5-6, T9, and T11 was insignificant compared to the control, however, these bacterial inoculations slightly reduced the lipid peroxidation.

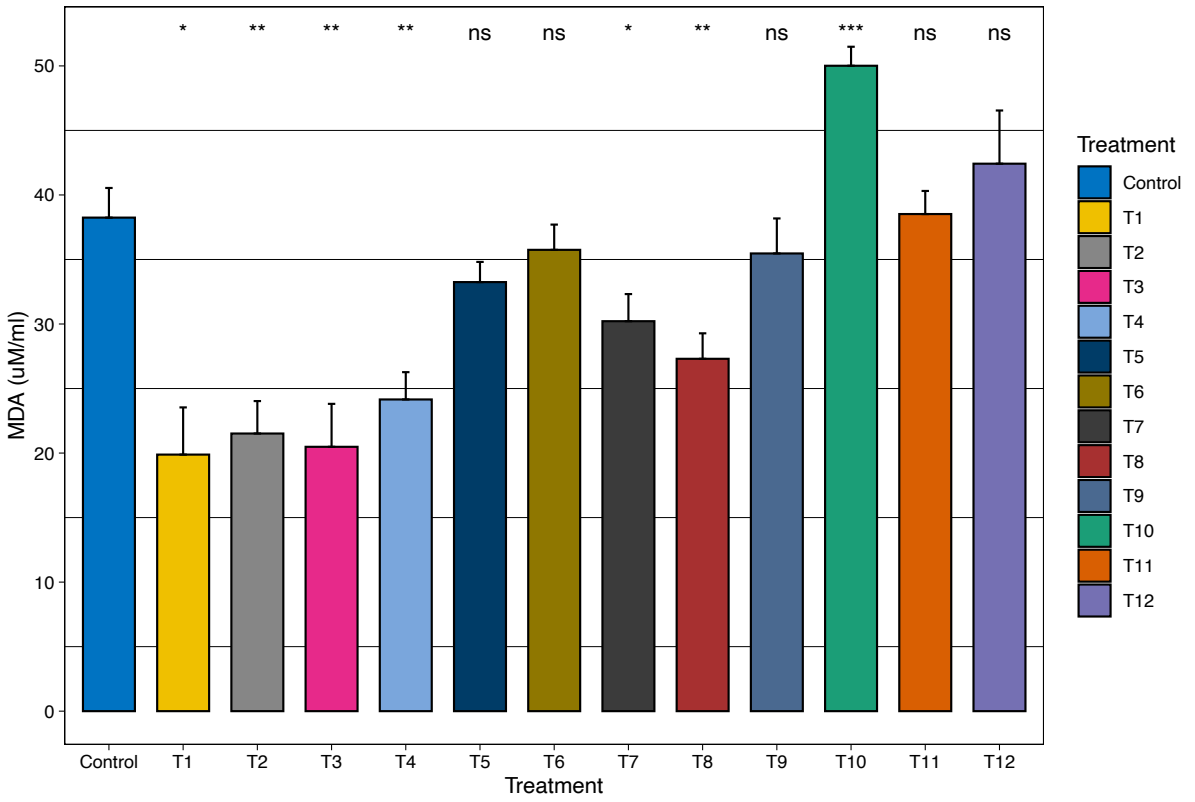


**Figure 5-3.** Effects of biopriming on malondialdehyde (MDA) content of maize under drought stress.

### 5.4.1.4. Antioxidant activities

A non-enzymatic FRAP assay was used to measure the antioxidant potential in the maize plants under drought stress. Water deficit conditions increased the production of reactive oxygen species (ROS) in plants, but biopriming enhanced the antioxidant potential of the plants. The plants inoculated with T2, T5, T6, T7, and T9 to T12 exhibited significantly higher antioxidant potential relative to the control (Figure 5-4A). The highest antioxidant potential was observed in T10 and T11, with a two-fold

enhancement. Additionally, as one method may not be sufficient to provide insight into overall antioxidant activities, an additional non-enzymatic antioxidant assay [glutathione (GSH)] was performed to complement the FRAP assay. GSH is an antioxidant that significantly increase under drought stress (Farrant et al., 2007). Therefore, a significantly elevated GSH level in untreated WS plants was expected, whereas WW plants exhibited lower GSH levels (Figure 5-S1L). A significant reduction of GSH was observed in response to biopriming in T1-3, T6 to T9, and T10 to T12. A maximum decrease of 52.7% of GSH content was found in T8 compared to the control.

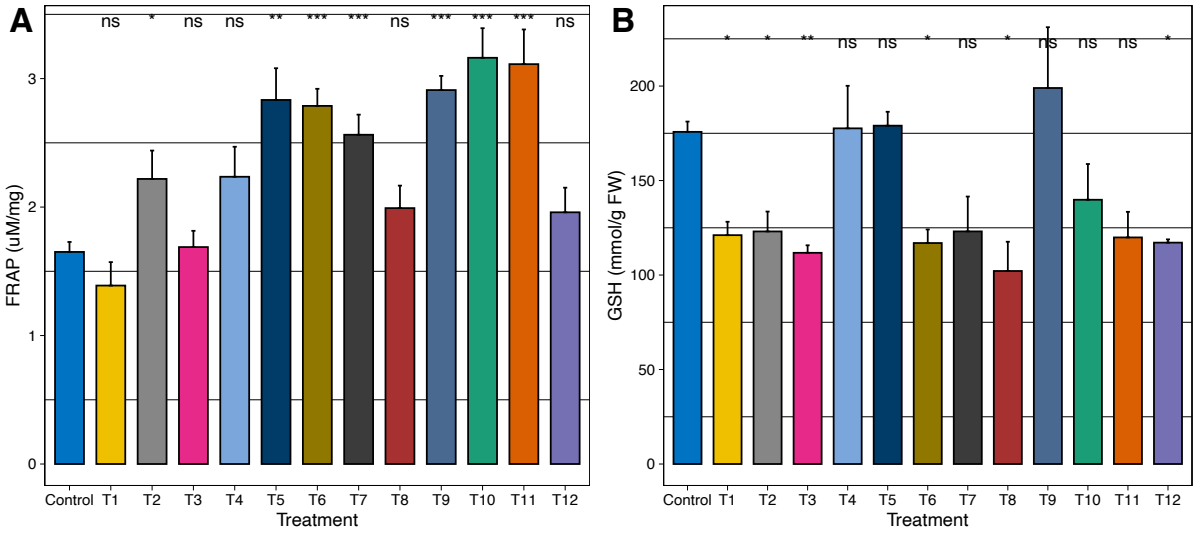


**Figure 5-4.** Antioxidant activities: The effects of biopriming with rhizospheric bacteria on A) the ferric reducing antioxidant power and B) glutathione of maize plants under drought stress.

### 5.4.1.5. Shoot and root measurements

Drought stress significantly affected the growth and biomass of the plants and roots, particularly untreated plants. Plant growth was negatively affected by drought stress and there was a 10% reduction in shoot length of untreated WS plants compared to the untreated WW plants (Figure 5-S1C). The bacterial inoculation significantly improved shoot dry mass of T4, T5, T7, T9, T10, and T11 compared to the control plants (Figure 5-5A, Table 5-S3). Water deficit conditions adversely affected the root morphology and architecture of the plants with a 40% reduction in dry weight in untreated plants compared to the well-watered plants (Figure 5-S1F). Inoculated plants exhibited a significantly high root biomass in T5, T7, T9, and T10 (Figure 5-5B, Table 5-S4). The improvement of the root system of inoculated maize under water deficit conditions is also shown in Figure 5-S2. For many samples, the shoot length of the inoculated plants was statistically insignificant compared to the control. However, the bacterial isolate Bac 9 and Bac11 significantly increased the shoot length of maize plants (T9 and T11) (Figure 5-5C, Table 5-S5). Additionally, there was a 20% reduction in the leaf area of untreated

drought-stress plants compared to the well-watered plants (Figure 5-3D). Biopriming with bacterial inoculum significantly increased the leaf area of inoculated plants T3, T5, T7, T10, and T11 compared to the control (Figure 5-5D, Table 5-S6).

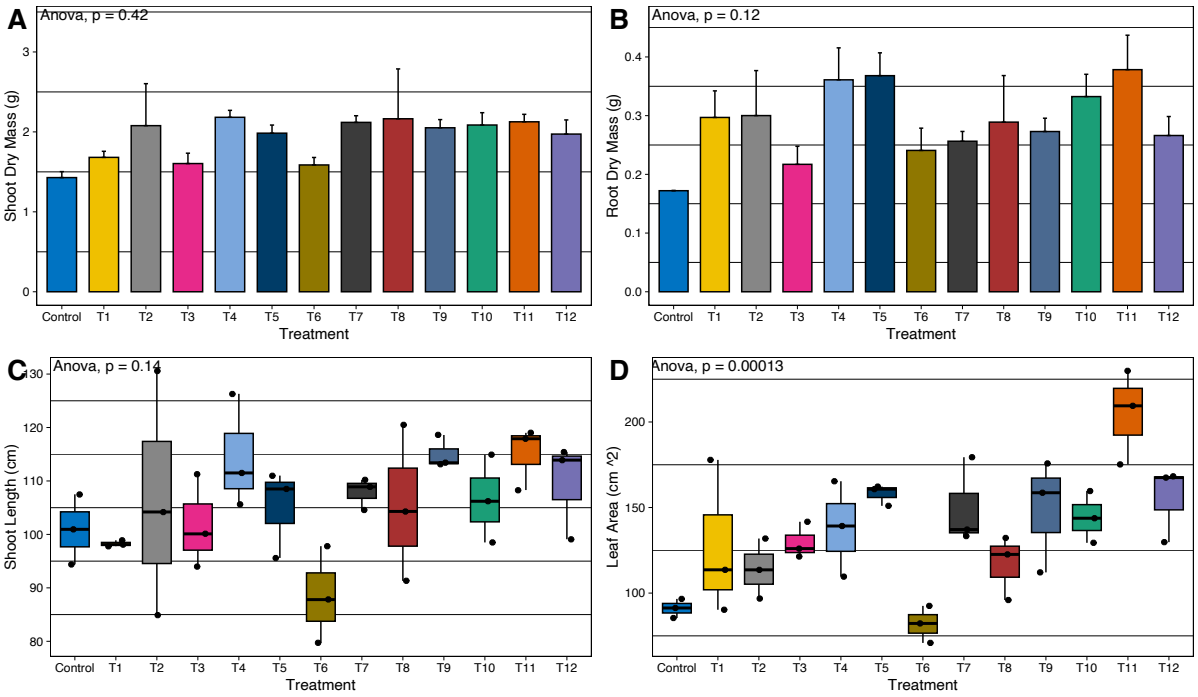


**Figure 5-5.** The impact of bacterial inoculation of maize plants on A) shoot dry mass, B) root dry mass, C) shoot length, and D) leaf area of plants subjected to drought stress.

The phenotypic analysis using corroplot showed that the variables accounting for variability among the treatments were mainly leaf area, root and shoot dry mass (Figure 5-S3). To further discern which bacterial inoculum had the most impact on plant growth and improving the resilience of plants against drought stress. A principal component analysis (PCA) was constructed using mean points of phenotypic variables including shoot length, leaf area, RWC, VWC, and shoot and root dry mass. PC1 explained 55.2 % variation and PC2 accounted for another 26.3 % variation among the treatments and together explained a largely accepted variation of 81.5 % (Figure 5-6). Well-watered (ww) plants controls were clustered with T7 and T9 samples, while untreated WS plants were clustered with T1 and T3 plants. Taken together, this study demonstrated that inoculation with Bac7 and Bac9 were the most impactful treatments (T7 and T9) relative to others by being clustered together with WW plants. These treatments also showed a remarkable improvement of RWC, FRAP, Fv/Fm, Chl a, b and total chlorophyll content in T7 and T9. These inoculated plants exhibited significantly lower levels of MDA and GSH levels under drought stress.

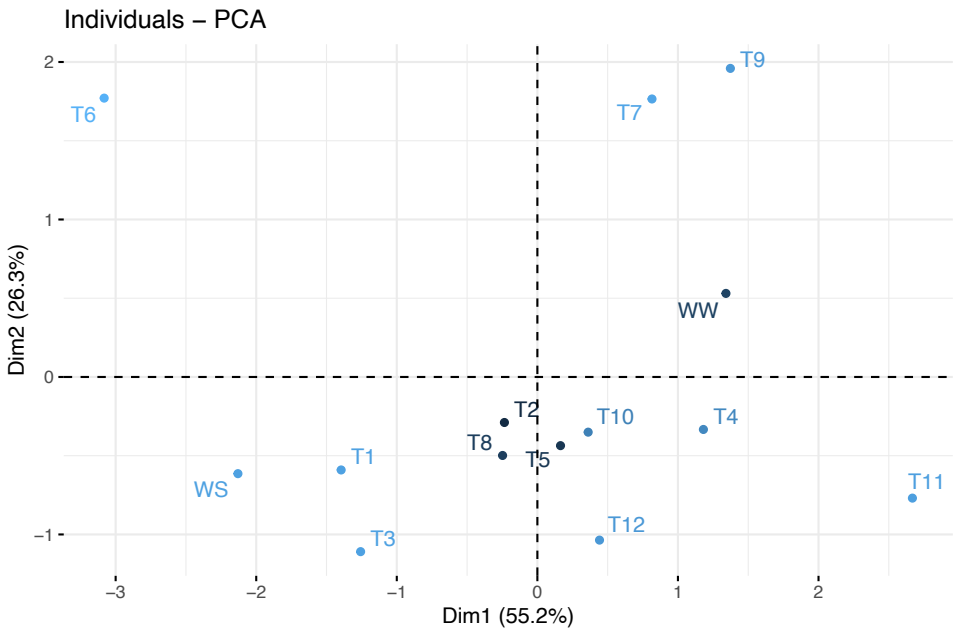


**Figure 5-6.** Principal component analysis (PCA) summarising the most impactful bacterial based on various physiological parameters such as RWC, VWC, shoot length, leaf area, shoot and root dry biomass.

### 5.4.2. Microbial metabolic profiling

The current study investigated how certain rhizospheric bacteria of *M. flabellifolia* tolerate extreme drought stress and low temperature through metabolic analysis. Firstly, the gram stain technique revealed a higher abundance of gram-negative bacteria than gram-positive bacteria in the rhizosphere soil of *M. flabellifolia* (Table 5-S7). Untargeted metabolic profiling was performed using GC-MS and a total of 112 putative metabolites were detected across twelve bacterial species, of which 70 metabolites were significantly different across all twelve bacterial species (Figure 5-S4). PCA shows metabolic similarities and differences between the bacterial samples (Figure 5-7). Significant metabolic variation was observed between the bacterial species with PC1 accounting for 25% of the variation in the dataset and PC2 accounting for another 21.2% of the variation. Furthermore, there was minimal variability between the biological replicates indicating consistency and reproducibility of the data. Bacterial species that displayed similar metabolites were clustered together such as Bac4, Bac8, and Bac12 as well as Bac1, Bac3, and Bac9. This finding indicates that the gram reaction identity of the bacteria did not influence the metabolic profile (Table 5-S7). Therefore, distinct bacterial species have the ability to synthesize common metabolites. A substantial metabolic variation was observed between Bac2 and Bac11 relative to Bac5, Bac6, Bac7, and Bac10.

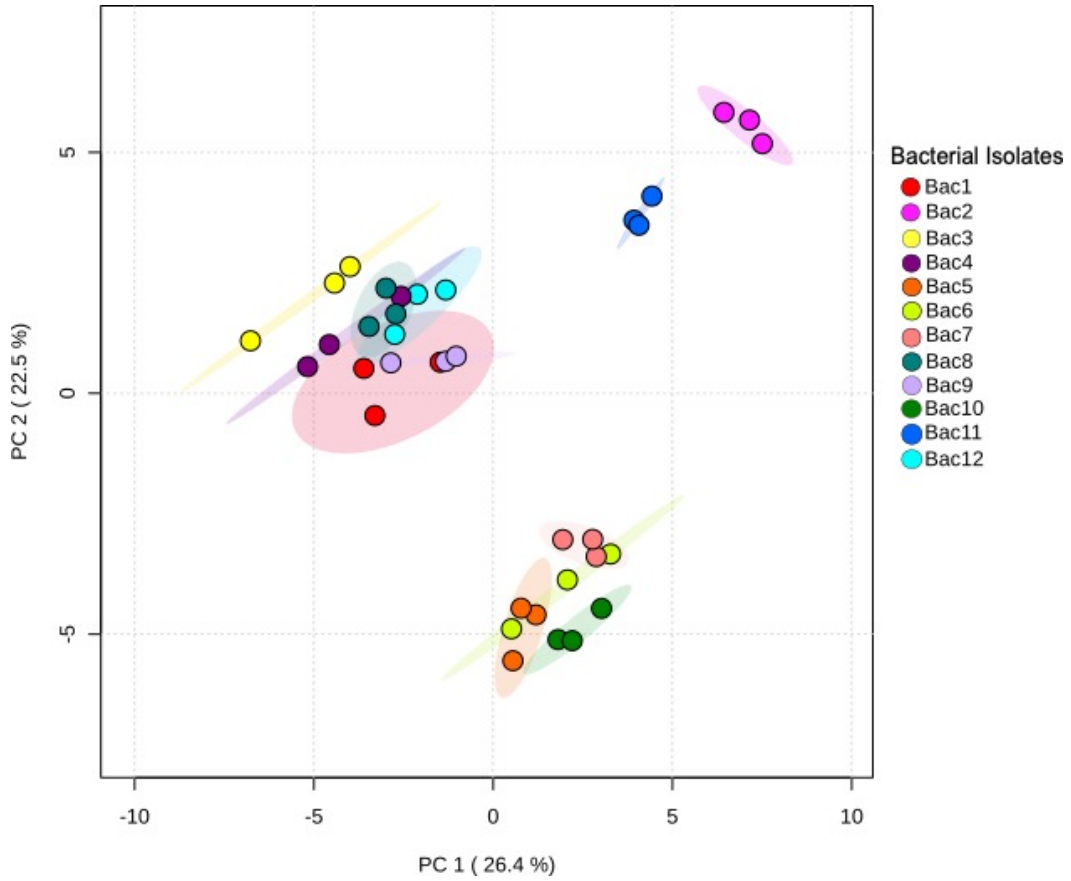


**Figure 5-7.** Principal Component Analysis (PCA) of the endogenous metabolites from 12 bacteria (Bac1-Bac12) isolated from the rhizosphere soil of *Myrothamnus flabellifolia*.

### 5.4.2.1. Differential abundance of metabolites in the rhizospheric bacteria of *M. flabellifolia* isolated under drought stress

The detected metabolites represent diverse chemical categories ranging from free amino acids (37%), organic acids (23,7%), sugars and sugar alcohols (25%), to others (13,8%) such as nucleotides and flavonoids that play important roles in drought tolerance mechanisms of the plant (Bentley et al., 2019; Moore et al., 2005). A heatmap was constructed to visualise differences in the abundance of metabolites across various bacterial species. The amino acid profiles of bacterial species formed two clusters, with the first group including Bac2, Bac5, Bac6, Bac7, Bac10, and Bac11, while the second group consists of Bac1, Bac3, Bac4, Bac8, Bac9, and Bac12 (Figure 5-8A). In the first cluster, there was a significantly elevated content of non-essential amino acids such as glutamic acids, alanine, proline, asparagine, and pyroglutamic acids except for isoleucine (Figure 5-8A). The second cluster showed an abundance of essential amino acids such as leucine, lysine, histidine, methionine, serine, threonine, tryptophan, and phenylalanine. The analysis showed that bacterial isolates Bac2, Bac8, BacT9, Bac11, and Bac12 contained the highest abundance of free amino acids relative to others.

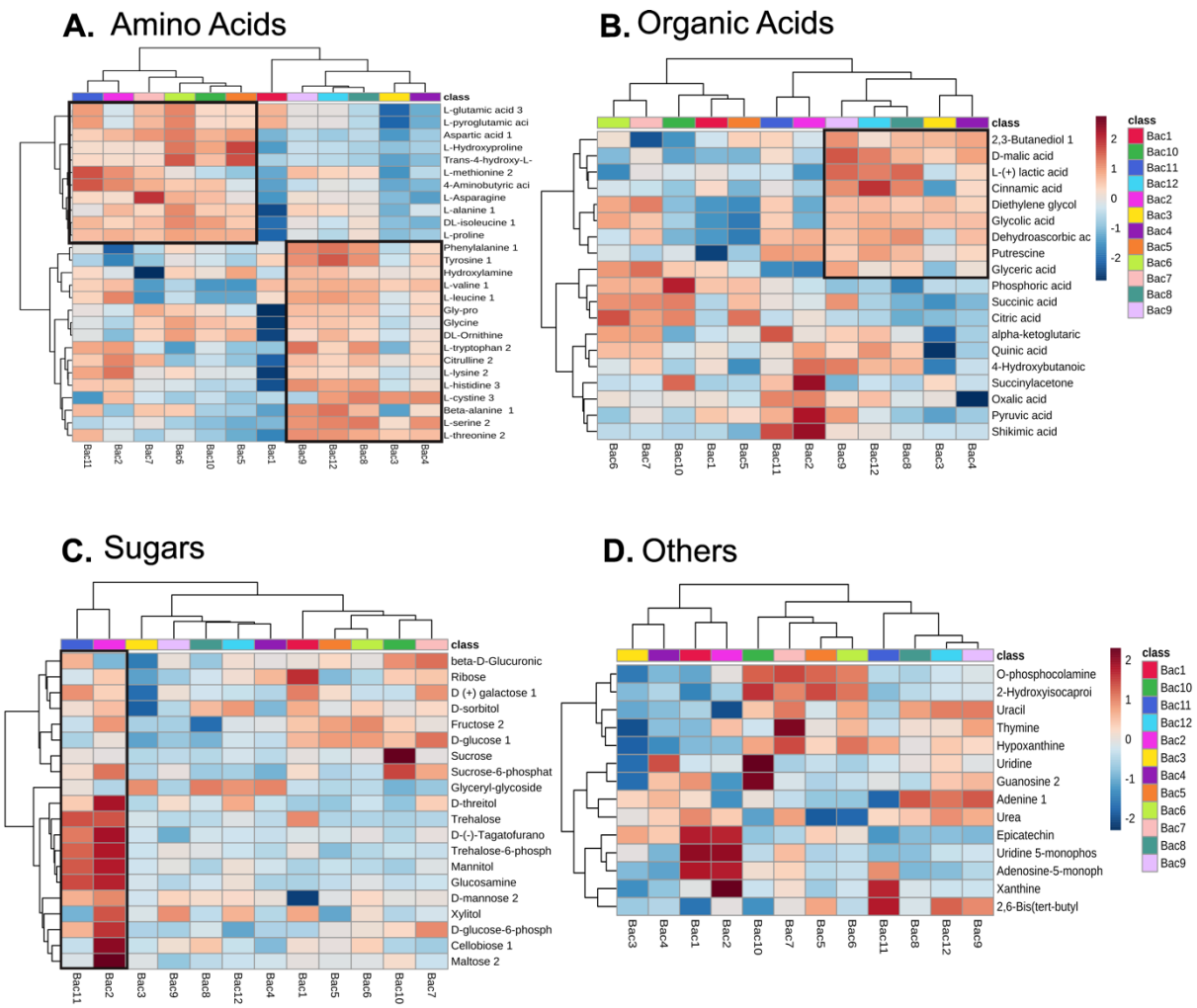


**Figure 5-8.** Heatmaps show the abundance of A) amino acids, B) organic acids, C) sugars, and D) others in bacterial species. Twelve bacterial species (Bac1–Bac12) isolated from the desiccated and frozen rhizosphere of *Myrothamnus flabellifolia* from Swebeswebe Nature Reserve. The black square line indicate the key abundance of metabolites in the clustered bacterial species.

Bacterial organic acids were clustered in two groups similar to amino acids, however, the membership was slightly different with Bac2 and Bac1 clustered in the second group. The analysis further showed that group two had an increased abundance of malic, lactic, cinnamic, glycolic, oxalic acids, 2,3-butanediol, and putrescine relative to group one (Figure 5-8B). Interestingly, Bac2 and Bac11 showed a greater abundance of pyruvic and shikimic acids relative to other bacterial species. Cinnamic acid was predominantly elevated in Bac12 compared to other bacterial species. Across all bacterial species, Bac1, Bac5, and Bac10 exhibited the lowest accumulation of organic acids. The accumulation of sugars and sugar alcohols was significantly high in Bac2 and Bac11 compared to other bacterial species. These includes a high abundance of cellobiose, mannose, maltose, glucosamine, trehalose, threitol,

mannitol, xylitol, glucose-6-phosphate (G6P), tagatofurano, and trehalose-6-phosphate (Figure 5-8C). Interestingly, Bac7 showed elevated G6P, sucrose and sucrose-6-phosphate relative to other bacterial isolates. Finally, many nucleotides and flavonoids such as epicatechin were abundant in Bac1, Bac2, Bac3, and Bac4 bacterial isolates (Figure 5-8D). An elevated content of xanthine was observed in Bac2 and Bac11.

## 5.5. Discussion

Rhizosphere microbiomes are known to contribute to drought tolerance, facilitate nutrient acquisition, and support the growth of the host plant. Under drought stress, plants allocate more resources to the root system and elongation. Consequently, the application of biofertilizers using the biopriming method in agricultural crops is rapidly increasing with promising effects on the host plants (Mishra et al., 2020). Therefore, this study isolated bacteria from desiccated and frozen rhizosphere soil of *M. flabellifolia* using culture-dependent techniques. Findings in this study demonstrated that biopriming maize seeds with rhizospheric bacteria of *M. flabellifolia* improves physiological traits and antioxidant activities compared to uninoculated plants. Furthermore, metabolic profiling of rhizospheric bacteria was performed to investigate the mechanisms of microbes and how they might enhance drought tolerance of the host plant.

Drought stress alters biochemical, physiology and molecular processes in plants. However, biopriming with plant-promoting rhizospheric bacteria is a promising strategy to combat drought stress (Manhood et al., 2016 ). This study demonstrated that inoculation with some of the bacteria isolated from the rhizosphere soil of *M. flabellifolia* enhanced the leaf area, dry weight, and shoot and root growth of maize under drought stress. These findings are in agreement with the results of previous studies on the effect of seed biopriming with PGPR (Mishra et al., 2020; Morcillo et al., 2021; Wang et al., 2022). Under water deficit conditions, reduction of RWC, chlorophyll content, and transpiration rate are physiological biomarkers of drought effects (Asghari et al., 2020). Bioprimed plants in this study responded to water deficit conditions in contrasting ways. Some rhizospheric bacteria (particularly in T8, T9, and T12) improved the plant's ability to maintain water balance, possibly due to enhanced root system properties (Figure 5-S2). Although drought impairs photosynthesis, bacterial inoculation with Bac7, Bac8, Bac9, Bac 11, and Bac 12 improved the chlorophyll content of maize plants. In addition, a remarkable reduction of MDA content in inoculated plants indicates that rhizospheric bacteria have a potent preventative effect against lipid peroxidation, presumably by enhancing antioxidant potential. These findings are consistent with the study by Farrant et al. (2007) who reported that high antioxidant potential in *M. flabellifolia* under desiccated conditions is crucial

to provide significant protection against ROS. Overall, the physiological analysis of maize under drought stress suggests that rhizospheric bacteria of *M. flabellifolia* resilience of plants by increasing biomass, antioxidant activities and reducing the rate of water loss.

The detection of both Gram-positive and Gram-negative bacteria in the rhizosphere soil of *M. flabellifolia* suggests that a diverse microbial community is capable of resuscitating following drought stress. This observation aligns with the metagenomic and metatranscriptomic analyses, which demonstrated the presence of both monoderm and diderm lineages (Chapter Two and Three). Although previous studies have reported an increase of monoderm and reduction of diderm lineages in the rhizosphere microbiome under drought stress (Naylor and Coleman-Deir, 2018; Xu et al., 2018), this study isolated more gram-negative relative to gram-positive bacteria (Table 5-S7). Gram-negative bacteria including Bac3 to Bac5 and Bac7 to Bac10 and they only accumulate osmolytes under abiotic stress conditions. Whereas, gram-positive bacteria (Bac1, Bac2, Bac6, Bac11 and Bac12) tend to constitutively biosynthesize osmolytes under optimal and drought-induced conditions, which enhances their tolerance to osmotic tolerance (Naylor and Coleman-Deir, 2018). This phenomenon was further validated through bacterial metabolic profiling. Despite the gram reaction, the physiological results suggest that Bac7, Bac9, Bac11 and Bac12 were excellent bacterial isolates that alleviated drought stress and improved plant recovery.

The accumulation of osmolytes in bacteria enhances the cellular protection mechanisms and decreases ROS accumulation in the inoculated plants under drought stress (Szablinska-Piernik and Lahuta, 2021; Tran et al., 2023). This study demonstrated a high accumulation of GABA in Bac7 and Bac11 bacterial isolates suggesting that they might be responsible for increased antioxidant capacity in the inoculated plants (T7 and T11) compared to the control. These findings align with a recent study by Zhou et al., (2021), who outlined that seed priming of white clover with GABA exhibited higher antioxidant activities and decreased ROS levels (Zhou et al., 2021). Bac7 exhibited a high content of glutamic acid and glycine relative to other isolates. Interestingly, the accumulation of amino acids in bacterial species correspond with the upregulated genes encoding amino acids in the Chapter Three. These findings are consistent with the results of Talukder et al. (2021), who reported greater growth yield and improved strawberry quality after the foliar application of glutamic acids. In contrast, a significant abundance of aromatic amino acids namely phenylalanine, tyrosine, and tryptophan were detected in Bac9, and Bac12 bacterial isolates, which might have contributed to the enhancement of dry biomass (Feng et al., 2023). The phenomenology of seed biopriming is dynamic and complex. However, this study suggests that the accumulation of various amino acids in bacteria may enhance the performance of inoculated plants under water deficit conditions, potentially acting as osmolytes and precursors too other metabolites.

Sugars are involved in the glycolytic pathway of bacteria, fungi, and plants, and some function as osmoprotectant compounds during drought (Tapia et al., 2015). This study showed sugars were abundant in Bac11 compared to Bac7, Bac9 and Bac12. The concept of constitutive production of osmolytes in gram-positive bacteria was observed in this metabolic class of sugars. On the contrary, it was surprising that a small content of sugars was detected in Bac12, which is a gram-positive bacteria. However, this might be due to within gram-positive phyla, there are various strategies of transcription regulation at the family level (Amon et al., 2010). A significant abundance of trehalose, trehalose-6-phosphate (T6P), galactose, sucrose-6-phosphate (S6P), mannose, glucosamine, and tagatofurano was evident in Bac11. This finding suggests that glucosamine may enhanced the plant-microbiome interaction during the seed biopriming, possibly due to its properties of being a precursor for peptidoglycan, chitosan and lipopolysaccharides, which are elicitors that stimulate ISR in plants (Moye et al., 2014; Saberi et al., 2021). In plants, T6P is essential for trehalose biosynthesis and acts as a signalling molecule in modulating the level of sucrose in the cell (Oliver et al., 2020). On the other hand, in bacteria, trehalose substitutes water under dehydration and is a constitutive part of the cell wall (Tapia et al., 2015). The chromatogram clearly indicates a substantial accumulation of trehalose in bacteria (Figure 5-S6). Remarkably, trehalose was also detected in the rhizosphere soil, suggesting a microbial contribution to the overall trehalose content. This observation is further supported by the expression of bacterial trehalose-related genes under dehydrated conditions (Chapter Three). Moreover, genes responsible for the biosynthesis of glucosamine, mannose, arabinose, cellobiose, and sucrose showed a correlation with the abundance of these metabolites in the rhizosphere metabolome and bacterial metabolites. There were metabolic trade-offs observed on bacterial isolates (Bac9 and Bac12) with a high amino acid content, resulting in a substantially lower accumulation of sugars. Gram-negative bacteria accumulate osmolytes, including various sugars, under drought stress. Interestingly, Bac7 in this study produced glucose-6-phosphate and sucrose-6-phosphate, which could facilitate drought tolerance in both the microbe and host plant.

This study detected an accumulation of organic acids in the bacterial isolates. Interestingly, most organic compounds were also detected in the rhizosphere soil of *M. flabellifolia* (Tebele et al., 2023; Chapter Two), indicating that they may emanate from the microbial community. It is possible that the accumulation of organic acids in the bacteria might supply energy for TCA, and improve the plant's nutrient acquisition. These findings are in agreement with the study by Vanani et al. (2020). Another fascinating finding was the abundance of diethylene glycol in all four of the most impactful bacteria, namely Bac7, Bac9, Bac11 and Bac12. This compound has cryoprotectant and vitrification properties similar to trehalose, suggesting that it enables bacteria to survive lower temperatures (Bhattacharya, 2018). Although cinnamic acid is known to inhibit plant growth (Mehmood et al., 2019), the

accumulation of cinnamic acid in Bac12 might be associated with antibacterial effects that inhibit pathogens (Zhang et al., 2019). Dehydroascorbic acid is an oxidised form of ascorbic acid and was detected in bacterial isolates T9, T11, and T12, but not in rhizosphere soil metabolome (Tebele et al., 2023). It is probable that in the presence of GSH, dehydroascorbate is reduced to ascorbate and contributes to antioxidant activity by donating electrons to neutralise $H_2O_2$ formed during drought stress into $H_2O$ (Pehlivan, 2017). Interestingly, the plants treated with these dehydroascorbic acid-producing bacteria exhibited significantly lower GSH levels under drought stress relative to the control. It was remarkable to detect putrescine in T9, T11 and T12 bacterial isolates. Rhizospheric microbes producing polyamines are known to prevent osmotic stress and enhance root elongation (Aslam et al.,2022). These results are in accord with previous studies indicating that *Arabidopsis* inoculated with *Pseudomonas putida* mitigated drought stress by enhancing the accumulation of putrescine (Liu et al., 2015; Sen et al., 2018). Biopriming revealed a drought defense trade-off phenomenon, in which gram-negative bacteria were predominantly involved in adaptation responses. In contrast to gram-positive bacteria, appear to play a role in regulate both plant growth and defense responses.

It was intriguing to detect a high accumulation of the volatile organic compound (VOC), 2,3-butanediol in T9, T11, and T12, as this is known as an elicitor of ISR response in plants, and enhances root colonisation (Netzker et al., 2020). These findings are consistent with previous studies that reported the secretion of 2,3-butanediol by *Pseudomonas* and *Bacillus spp.* increased drought tolerance in *Arabidopsis thaliana* and *Nicotiana benthamiana* by inducing the stomatal closure (Cho et al., 2008; Wu et al., 2018). These results suggest that the application of rhizospheric bacteria from *M. flabellifolia* on maize may enhanced the drought tolerance by scavenging ROS, leading to lower GSH content. Taken together, biopriming with rhizospheric bacteria improved the adaptability of maize under water deficit conditions.

## 5.6. Conclusion

Taken together, the rhizosphere soil of *M. flabellifolia* harbours many plant growth-promoting and desiccation-tolerant bacteria. Under drought stress, these bacteria produce osmolytes in the rhizosphere soil that limit the production of ROS, protect the root cell membrane, and promote further plant-microbe interaction. These findings demonstrate that biopriming with the rhizospheric bacteria of *M. flabellifolia* improved the plant growth of maize, enhanced drought tolerance by maintaining higher leaf RWC, improved the biosynthesis and/ or retention of chlorophyll, reduced lipid peroxidation in the cell membrane, and enhanced antioxidant activities and ROS scavenging, thereby alleviating drought-induced. The symbiotic relationship between plants and bacteria can contribute

significantly to drought tolerance. In our study, the bacterial isolates T7, T9, T11, and T12 were found to be the most impactful. However, each bacteria has a special role in contributing to the drought tolerance of the plants. Future studies should perform field trials using a consortium of all twelve bacterial isolates on different types of soil and plants. This study has the potential to develop biostimulants that could be applied to drought-sensitive plants.

## 5.7. Supplementary

Table 5-S1. Statistical analysis using pairwise comparison between mean of RWC of inoculated and control plants .

| | .y. | group1 | group2 | n1 | n2 | statistic | df | p |
|---|---|---|---|---|---|---|---|---|
| **1** | RWC | Control | T1 | 3 | 3 | -3.07064433473644 | 2.02611926057689 | 0.09 |
| **2** | RWC | Control | T10 | 3 | 3 | -6.1526852962774 | 2.51025592597087 | 0.014 |
| **3** | RWC | Control | T11 | 3 | 3 | -2.85091651168371 | 2.06432026394094 | 0.1 |
| **4** | RWC | Control | T12 | 3 | 3 | -7.58328611522052 | 2.101790610714 | 0.015 |
| **5** | RWC | Control | T2 | 3 | 3 | -3.23450584234845 | 2.02281790780488 | 0.082 |
| **6** | RWC | Control | T3 | 3 | 3 | -3.6006185759371 | 2.03683233469711 | 0.067 |
| **7** | RWC | Control | T4 | 3 | 3 | -4.98391098604281 | 2.04078298119417 | 0.036 |
| **8** | RWC | Control | T5 | 3 | 3 | -7.13139551081354 | 3.37166843175888 | 0.004 |
| **9** | RWC | Control | T6 | 3 | 3 | -1.13179926146366 | 2.01990712499172 | 0.374 |
| **10** | RWC | Control | T7 | 3 | 3 | -7.12739270388866 | 2.9880837011851 | 0.006 |
| **11** | RWC | Control | T8 | 3 | 3 | -5.96256702083427 | 2.09911679720261 | 0.024 |
| **12** | RWC | Control | T9 | 3 | 3 | -3.40709840867112 | 2.06773009655359 | 0.073 |

Table 5-S2. Statistical analysis using pairwise comparison between mean of VWC of inoculated and control plants.

| | .y. | group1 | group2 | n1 | n2 | statistic | df | p |
|---|---|---|---|---|---|---|---|---|
| **1** | Day10 | Control | T1 | 3 | 3 | -3.98439901868145 | 2.02453895370719 | 0.056 |
| **2** | Day10 | Control | T10 | 3 | 3 | -2.70346533771283 | 2.04753148687206 | 0.111 |
| **3** | Day10 | Control | T11 | 3 | 3 | -9.62140470884728 | 2.56 | 0.004 |
| **4** | Day10 | Control | T12 | 3 | 3 | -2.59974639507036 | 2.01234556140869 | 0.121 |
| **5** | Day10 | Control | T2 | 3 | 3 | -7.96843015410683 | 2.03883129123468 | 0.015 |
| **6** | Day10 | Control | T3 | 3 | 3 | -15.2263229011771 | 2.73060648801128 | 0.001 |
| **7** | Day10 | Control | T4 | 3 | 3 | -2.4306341274739 | 2.0077755885018 | 0.135 |
| **8** | Day10 | Control | T5 | 3 | 3 | -5.45919562769173 | 2.10101852093048 | 0.029 |
| **9** | Day10 | Control | T6 | 3 | 3 | -4.08957493091616 | 2.02833865844152 | 0.054 |
| **10** | Day10 | Control | T7 | 3 | 3 | -2.10834578549618 | 2.17799012065754 | 0.159 |
| **11** | Day10 | Control | T8 | 3 | 3 | -53.2244502579703 | 3.74093264248705 | 1.59e-06 |
| **12** | Day10 | Control | T9 | 3 | 3 | -19.7773319015194 | 4 | 3.86e-05 |

Table 5-S3. Statistical analysis using pairwise comparison between mean of shoot dry mass of inoculated and control maize plants.

| | .y. | group1 | group2 | n1 | n2 | statistic | df | p |
|---|---|---|---|---|---|---|---|---|
| **1** | Shoot_DW | Control | T1 | 3 | 3 | -2.37273627102942 | 3.99879771990278 | 0.077 |
| **2** | Shoot_DW | Control | T10 | 3 | 3 | -3.84031413946604 | 2.89091666985285 | 0.033 |
| **3** | Shoot_DW | Control | T11 | 3 | 3 | -5.82988270638024 | 3.8136079940436 | 0.005 |
| **4** | Shoot_DW | Control | T12 | 3 | 3 | -2.83221485977579 | 2.69016897397797 | 0.075 |
| **5** | Shoot_DW | Control | T2 | 3 | 3 | -1.22482114017663 | 2.08091527756196 | 0.341 |
| **6** | Shoot_DW | Control | T3 | 3 | 3 | -1.1747029852411 | 3.19796650714222 | 0.32 |
| **7** | Shoot_DW | Control | T4 | 3 | 3 | -6.58625668304715 | 3.91334838288304 | 0.003 |
| **8** | Shoot_DW | Control | T5 | 3 | 3 | -4.40799124278492 | 3.67495801283927 | 0.014 |
| **9** | Shoot_DW | Control | T6 | 3 | 3 | -1.31974477528009 | 3.81247550045116 | 0.261 |
| **10** | Shoot_DW | Control | T7 | 3 | 3 | -6.18154069110426 | 3.9555475162467 | 0.004 |
| **11** | Shoot_DW | Control | T8 | 3 | 3 | -1.17181018910129 | 2.05742353183239 | 0.359 |
| **12** | Shoot_DW | Control | T9 | 3 | 3 | -4.91927832340146 | 3.66097475767105 | 0.01 |

Table 5-S4. Statistical analysis using pairwise comparison between mean of root dry mass of inoculated and control maize plants.

| | .y. | group1 | group2 | n1 | n2 | statistic | df | p |
|---|---|---|---|---|---|---|---|---|
| **1** | Root_DW | Control | T1 | 3 | 3 | -2.75631970603011 | 2.00036597128202 | 0.11 |
| **2** | Root_DW | Control | T10 | 3 | 3 | -4.22065964284528 | 2.00051990143331 | 0.052 |
| **3** | Root_DW | Control | T11 | 3 | 3 | -3.51287424304955 | 2.00021772233983 | 0.072 |
| **4** | Root_DW | Control | T12 | 3 | 3 | -2.90665594763232 | 2.00071699585981 | 0.101 |
| **5** | Root_DW | Control | T2 | 3 | 3 | -1.66985370595313 | 2.00012774720348 | 0.237 |
| **6** | Root_DW | Control | T3 | 3 | 3 | -1.46084923893485 | 2.00079349309007 | 0.281 |
| **7** | Root_DW | Control | T4 | 3 | 3 | -3.46913099030379 | 2.0002530130091 | 0.074 |
| **8** | Root_DW | Control | T5 | 3 | 3 | -5.03726258106193 | 2.00049569406323 | 0.037 |
| **9** | Root_DW | Control | T6 | 3 | 3 | -1.80946372041846 | 2.00052162501924 | 0.212 |
| **10** | Root_DW | Control | T7 | 3 | 3 | -5.06078941960201 | 2.00270587592696 | 0.037 |
| **11** | Root_DW | Control | T8 | 3 | 3 | -1.47300284928944 | 2.0001192536733 | 0.279 |
| **12** | Root_DW | Control | T9 | 3 | 3 | -4.44693948146158 | 2.00145974648007 | 0.047 |

Table 5-S5. Statistical analysis using pairwise comparison between mean of shoot length of inoculated and control maize plants.

| | .y. | group1 | group2 | n1 | n2 | statistic | df | p |
|---|---|---|---|---|---|---|---|---|
| **1** | Shoot_Length | Control | T1 | 3 | 3 | 0.706909089185342 | 2.03014416125633 | 0.552 |
| **2** | Shoot_Length | Control | T10 | 3 | 3 | -0.921112102569535 | 3.81284422194213 | 0.411 |
| **3** | Shoot_Length | Control | T11 | 3 | 3 | -2.77660149782188 | 3.95513406380882 | 0.051 |
| **4** | Shoot_Length | Control | T12 | 3 | 3 | -1.32435427756842 | 3.65261697777899 | 0.262 |
| **5** | Shoot_Length | Control | T2 | 3 | 3 | -0.40775282354982 | 2.32390217024765 | 0.718 |
| **6** | Shoot_Length | Control | T3 | 3 | 3 | -0.134457039600201 | 3.70083805335613 | 0.9 |
| **7** | Shoot_Length | Control | T4 | 3 | 3 | -1.87067582504701 | 3.32100729850628 | 0.149 |
| **8** | Shoot_Length | Control | T5 | 3 | 3 | -0.670674318916527 | 3.80165836951768 | 0.541 |
| **9** | Shoot_Length | Control | T6 | 3 | 3 | 1.93825330837208 | 3.64071801533769 | 0.132 |
| **10** | Shoot_Length | Control | T7 | 3 | 3 | -1.67754215786411 | 2.77001681622206 | 0.2 |
| **11** | Shoot_Length | Control | T8 | 3 | 3 | -0.477265251829314 | 2.77088645941752 | 0.668 |
| **12** | Shoot_Length | Control | T9 | 3 | 3 | -3.36765658606766 | 2.84942759166412 | 0.047 |

Table 5-S6. Statistical analysis using pairwise comparison between mean of leaf area of inoculated and control maize plants.

| | .y. | group1 | group2 | n1 | n2 | statistic | df | p |
|---|---|---|---|---|---|---|---|---|
| **1** | Leaf_Area | Control | T1 | 3 | 3 | -1.3693943300405 | 2.06059423897559 | 0.301 |
| **2** | Leaf_Area | Control | T10 | 3 | 3 | -5.70770446275345 | 2.53450029936002 | 0.017 |
| **3** | Leaf_Area | Control | T11 | 3 | 3 | -6.98844225793241 | 2.16301798223721 | 0.016 |
| **4** | Leaf_Area | Control | T12 | 3 | 3 | -4.88980209481859 | 2.25660072651831 | 0.031 |
| **5** | Leaf_Area | Control | T2 | 3 | 3 | -2.16128789224685 | 2.4007943543721 | 0.142 |
| **6** | Leaf_Area | Control | T3 | 3 | 3 | -5.56053322302552 | 3.02342809279209 | 0.011 |
| **7** | Leaf_Area | Control | T4 | 3 | 3 | -2.85917396994869 | 2.16001643515974 | 0.095 |
| **8** | Leaf_Area | Control | T5 | 3 | 3 | -14.0042830296462 | 3.96838029175465 | 0.000159 |
| **9** | Leaf_Area | Control | T6 | 3 | 3 | 1.31189778752865 | 2.9934841435428 | 0.281 |
| **10** | Leaf_Area | Control | T7 | 3 | 3 | -3.89305840736802 | 2.19012850994283 | 0.052 |
| **11** | Leaf_Area | Control | T8 | 3 | 3 | -2.27991536023893 | 2.35012527575864 | 0.131 |
| **12** | Leaf_Area | Control | T9 | 3 | 3 | -2.99214116774972 | 2.11475758008509 | 0.09 |

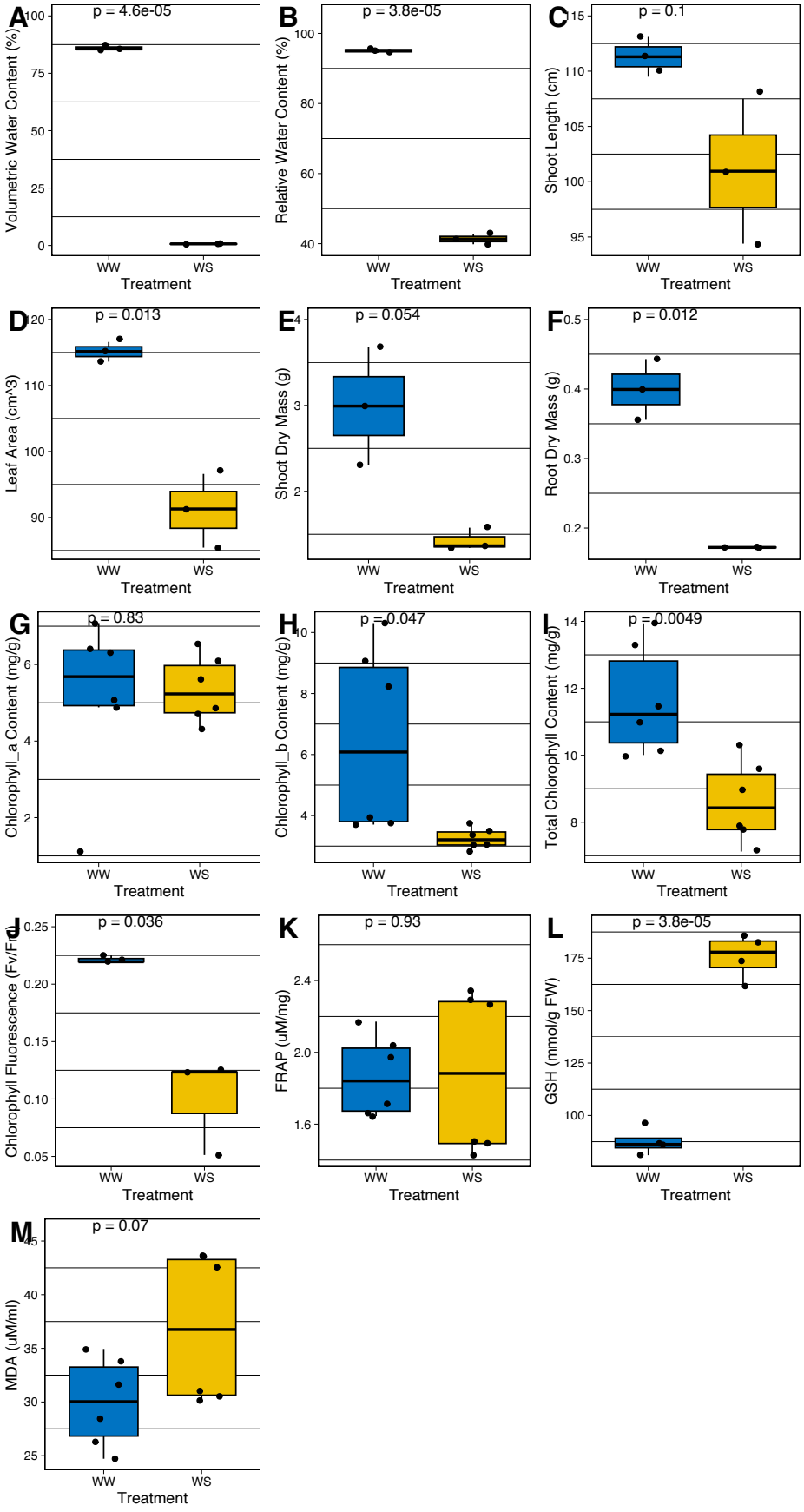


**Figure 5-S1**. The effects of drought on well-watered (WW) and drought stressed (WS) maize plants without the application of bacterial inoculation. A) The volumetric water content of soil adjacent to

the root system, B) leaf relative water content, C) shoot length, D) leaf area, E) shoot dry mass, F) root dry mass, G) chlorophyll a, H) chlorophyll b, I) total chlorophyll, J) chlorophyll fluorescence, K) FRAP assay, L) GSH content and M) MDA content.

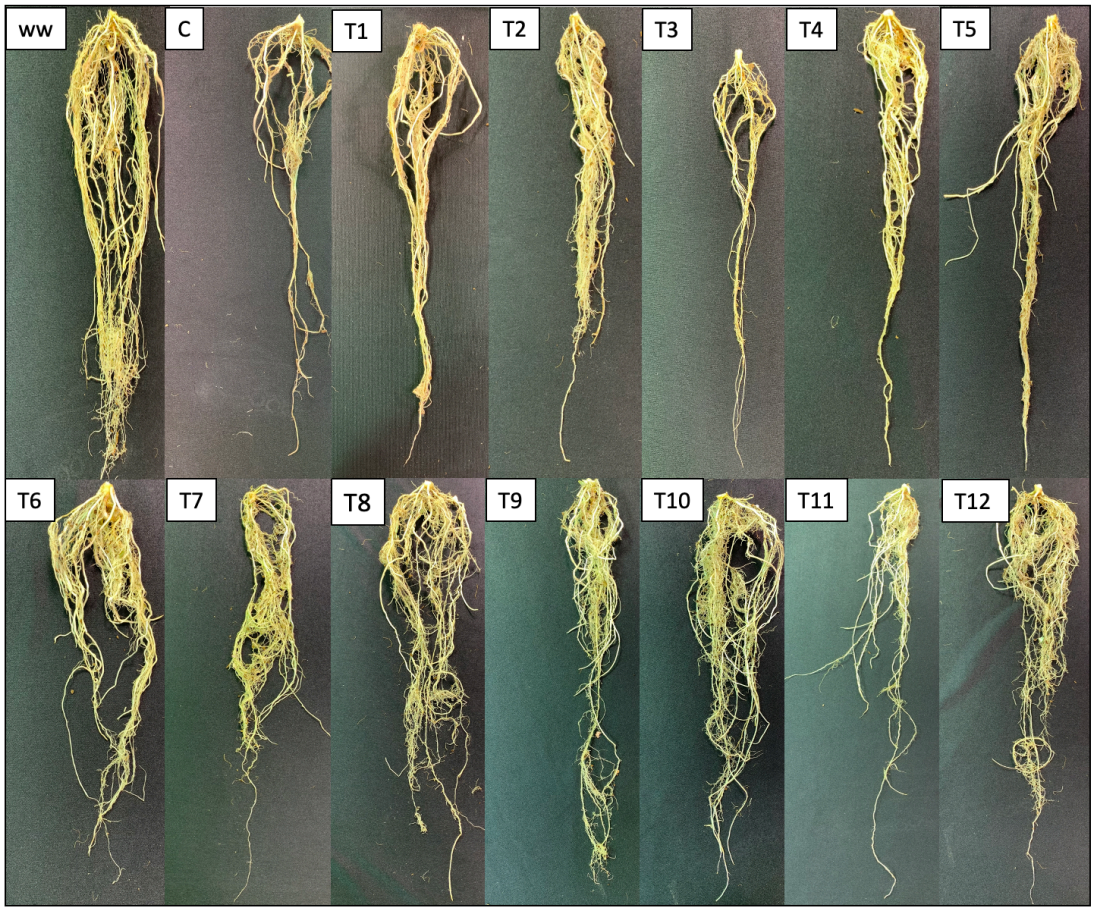


**Figure 5-S2**. The effects of drought stress on the rhizospheric bacterial biopriming on the root morphology of inoculated (T1-T12), uninoculated drought stress (C) and uninoculated well-watered (WW) plants.

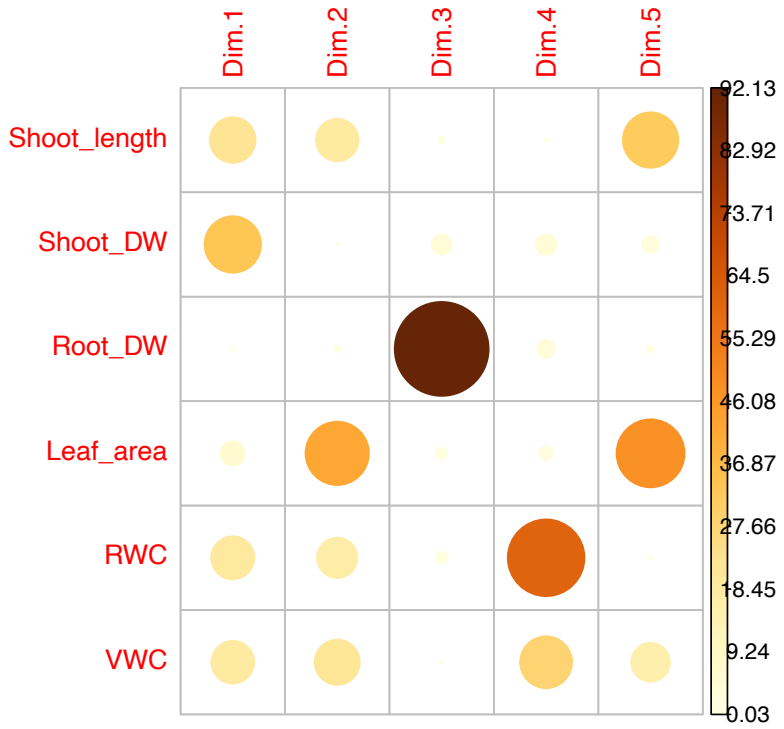


**Figure 5-S3**. Correlation plot showing the contribution of variables accounting for the variability in treated and untreated maize plants.

**Table 5-S7**. Gram-reaction of the isolated rhizospheric bacteria from *Myrothamnus flabellifolia*.

| | **Positive** | **Negative** | **Rod** | **Coccus** |
|---|---|---|---|---|
| **T1** | ✓ | | ✓ | |
| **T2** | ✓ | | | ✓ |
| **T3** | | ✓ | ✓ | |
| **T4** | | ✓ | ✓ | |
| **T5** | | ✓ | ✓ | |
| **T6** | ✓ | | ✓ | |
| **T7** | | ✓ | ✓ | |
| **T8** | | ✓ | ✓ | |
| **T9** | | ✓ | ✓ | |
| **T10** | | ✓ | ✓ | |
| **T11** | ✓ | | ✓ | |
| **T12** | ✓ | | ✓ | |

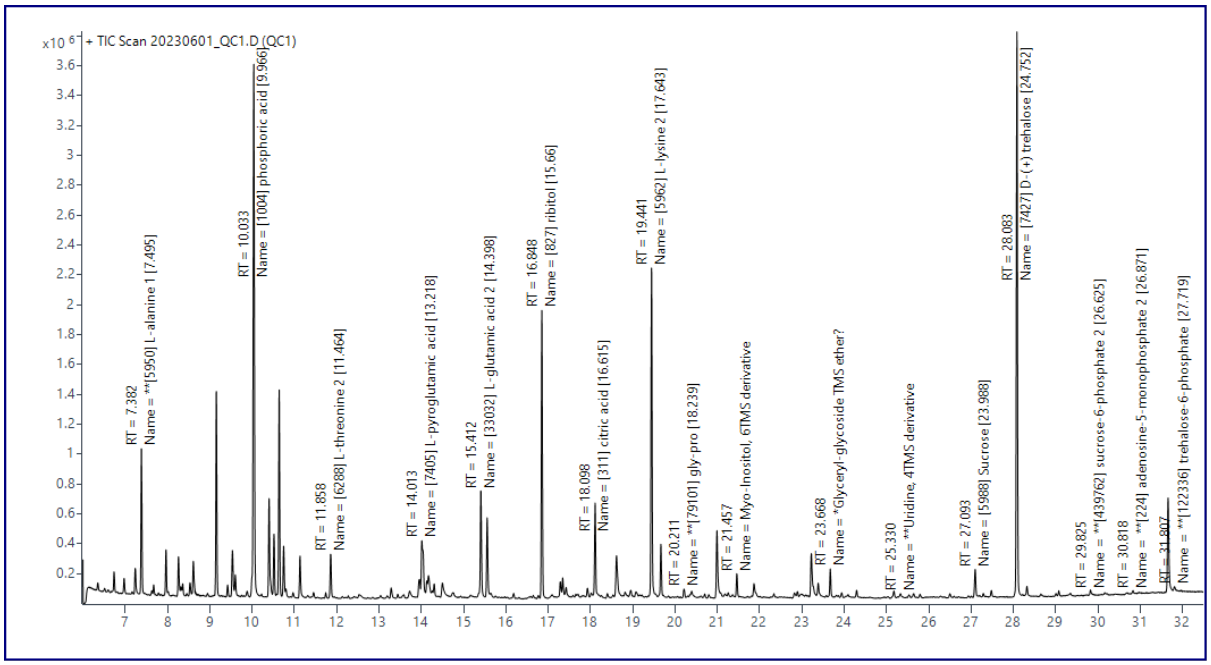


**Figure 5-S4**. Chromatogram of quality control bacterial metabolites analysed using Gas Chromatography-Mass Spectrometry demonstrating amino acids, organic acids, sugars and other compounds.

## 5.8. References


Amon, J., Titgemeyer, F. and Burkovski, A. 2010. Common patterns–unique features: nitrogen metabolism and regulation in Gram-positive bacteria. *Federation of European Microbiological Societies Microbiology Reviews*, 34(4), pp.588-605.

Anke, J., Petereit, F., Engelhardt, C. and Hensel, A. 2008. Procyanidins from Myrothamnus flabellifolia. *Natural Product Research*, 22(14), pp.1237-1248.

Asghari, B., Khademian, R. and Sedaghati, B. 2020. Plant growth-promoting rhizobacteria (PGPR) confer drought resistance and stimulate biosynthesis of secondary metabolites in pennyroyal (Mentha pulegium L.) under water shortage conditions. *Scientia Horticulturae*, 263, p.109132.

Aslam, M.M., IDRIS, A.L., Zhang, Q.I.A.N., Weifeng, X.U., KARANJA, J.K. and Wei, Y.U.A.N. 2022. Rhizosphere microbiomes can regulate plant drought tolerance. *Pedosphere*, 32(1), pp.61-74.

Avonce, N., Mendoza-Vargas, A., Morett, E. and Iturriaga, G. 2006. Insights on the evolution of trehalose biosynthesis. *BMC evolutionary biology*, 6(1), pp.1-15.

Belitsky, B.R., Brill, J., Bremer, E. and Sonenshein, A.L. 2001. Multiple genes for the last step of proline biosynthesis in Bacillus subtilis. *Journal of Bacteriology*, *183*(14), pp.4389-4392.

Bentley, J., Moore, J.P. and Farrant, J.M. 2019. Metabolomics as a complement to phylogenetics for assessing intraspecific boundaries in the desiccation-tolerant medicinal shrub Myrothamnus flabellifolia (Myrothamnaceae). *Phytochemistry*, 159, pp.127-136.

Bhattacharya, S. 2018. Cryoprotectants and their usage in cryopreservation process. Cryopreservation Biotechnology in biomedical and biological sciences, pp.7-19.

Bisht, N. and Chauhan, P.S. 2020. Excessive and disproportionate use of chemicals cause soil contamination and nutritional stress. *Soil Contamination-Threats and Sustainable Solutio*ns, pp.1-10.

Calvo P, Nelson L, Kloepper J. W. (2014). Agricultural uses of plant biostimulants. *Plant and soil*, 383, pp.3-41.

Cho, S.M., Kang, B.R., Han, S.H., Anderson, A.J., Park, J.Y., Lee, Y.H., Cho, B.H., Yang, K.Y., Ryu, C.M. and Kim, Y.C. 2008. 2R, 3R-butanediol, a bacterial volatile produced by Pseudomonas

chlororaphis O6, is involved in induction of systemic tolerance to drought in Arabidopsis thaliana. *Molecular plant-microbe interactions*, 21(8), pp.1067-1075.

Davoudpour, Y., Schmidt, M., Calabrese, F., Richnow, H.H. and Musat, N. 2020. High resolution microscopy to evaluate the efficiency of surface sterilization of Zea Mays seeds. *Public Library of Science one*, 15(11), p.e0242247.

Dhakal, R., Bajpai, V.K. and Baek, K.H. 2012. Production of GABA (γ-aminobutyric acid) by microorganisms: a review. *Brazilian Journal of Microbiology*, 43, pp.1230-1241.

Eke, P., Kumar, A., Sahu, K.P., Wakam, L.N., Sheoran, N., Ashajyothi, M., Patel, A. and Fekam, F.B. 2019. Endophytic bacteria of desert cactus (Euphorbia trigonas Mill) confer drought tolerance and induce growth promotion in tomato (Solanum lycopersicum L.). *Microbiological research*, 228, p.126302.

Farrant, J.M. 2007. Mechanisms of desiccation tolerance in angiosperm resurrection plants. *Plant desiccation tolerance*, pp.51-90.

Erenstein, O., Jaleta, M., Sonder, K., Mottaleb, K. and Prasanna, B.M. 2022. Global maize production, consumption and trade: Trends and R&D implications. *Food Security*, 14(5), pp.1295-1319.

Feng, Z., Xie, X., Wu, P., Chen, M., Qin, Y., Zhou, Y., Zhu, H. and Yao, Q. 2023. Phenylalanine-mediated changes in the soil bacterial community promote nitrogen cycling and plant growth. *Microbiological Research*, 275, p.127447.

Franzoni, G., Cocetta, G. and Ferrante, A. 2021. Effect of glutamic acid foliar applications on lettuce under water stress. *Physiology and Molecular Biology of Plants*, *27*, pp.1059-1072.

Gao, R., Duan, Y., Zhang, J., Ren, Y., Li, H., Liu, X., Zhao, P. and Jing, Y. 2022. Effects of long-term application of organic manure and chemical fertilizer on soil properties and microbial communities in the agro-pastoral ecotone of North China. *Frontiers in Environmental Science*, 10, p.993973.

Hartman, K. and Tringe, S.G. 2019. Interactions between plants and soil shaping the root microbiome under abiotic stress. *Biochemical Journal*, 476(19), pp.2705-2724.

Herrera, M., Cavero, J., Franco-Luesma, S., Álvaro-Fuentes, J., Ariño, A. and Lorán, S. 2023. Mycotoxins and crop yield in maize as affected by irrigation management and tillage practices. *Agronomy*, 13(3), p.798.

Imminger, S., Meier, D.V., Schintlmeister, A., Legin, A., Schnecker, J., Richter, A., Gillor, O., Eichorst, S.A. and Woebken, D., 2024. Survival and rapid resuscitation permit limited productivity in desert microbial communities. *Nature Communications*, 15(1), p.3056.

Klamer, R. 2022. MSc dissertation: Descending below the surface: root metabolomics of the South African resurrection plant *Myrothamnus Flabellifolius* (unpublished). Wageningen University & Research.

Koza, N.A., Adedayo, A.A., Babalola, O.O. and Kappo, A.P. 2022. Microorganisms in plant growth and development: Roles in abiotic stress tolerance and secondary metabolites secretion. *Microorganisms*, 10(8), p.1528.

Isogai, S., Tominaga, M., Kondo, A. and Ishii, J. 2022. Plant flavonoid production in bacteria and yeasts. *Frontiers in Chemical Engineering*, 4, p.880694.

Lastochkina, O., Yakupova, A., Avtushenko, I., Lastochkin, A. and Yuldashev, R. 2023. Effect of Seed Priming with Endophytic Bacillus subtilis on Some Physio-Biochemical Parameters of Two Wheat Varieties Exposed to Drought after Selective Herbicide Application. *Plants*, 12(8), p.1724.

Lephatsi, M., Nephali, L., Meyer, V., Piater, L.A., Buthelezi, N., Dubery, I.A., Opperman, H., Brand, M., Huyser, J. and Tugizimana, F. 2022. Molecular mechanisms associated with microbial biostimulant-mediated growth enhancement, priming and drought stress tolerance in maize plants. *Scientific Reports*, 12(1), p.10450.

Li, Y., Narayanan, M., Shi, X., Chen, X., Li, Z. and Ma, Y. 2023. Biofilms formation in plant growth-promoting bacteria for alleviating agro-environmental stress. *Science of The Total Environment*, p.167774.

Liu, J.H., Wang, W., Wu, H., Gong, X. and Moriguchi, T. 2015. Polyamines function in stress tolerance: from synthesis to regulation. *Frontiers in plant science*, 6, p.827.

Liu, X., Zhang, J., Wang, Q., Chang, T., Shaghaleh, H. and Hamoud, Y.A. 2022. Improvement of photosynthesis by biochar and vermicompost to Enhance Tomato (Solanum lycopersicum L.) yield under greenhouse conditions. *Plants*, 11(23), p.3214.

Mahmood, A., Turgay, O.C., Farooq, M. and Hayat, R. 2016. Seed biopriming with plant growth promoting rhizobacteria: a review. Federation of European Microbiological Societies *Microbiology Reviews*, 92(8), p.fiw112.

Mandal, S.M., Chakraborty, D. and Dey, S. 2010. Phenolic acids act as signaling molecules in plant-microbe symbioses. *Plant signaling & behavior*, 5(4), pp.359-368.

Mehmood, A., Hussain, A., Irshad, M., Hamayun, M., Iqbal, A., Rahman, H., Tawab, A., Ahmad, A. and Ayaz, S. 2019. Cinnamic acid as an inhibitor of growth, flavonoids exudation and endophytic fungus colonization in maize root. *Plant physiology and biochemistry*, 135, pp.61-68.

Menéndez, A.B., Calzadilla, P.I., Sansberro, P.A., Espasandin, F.D., Gazquez, A., Bordenave, C.D., Maiale, S.J., Rodríguez, A.A., Maguire, V.G., Campestre, M.P. and Garriz, A. 2019. Polyamines and legumes: Joint stories of stress, nitrogen fixation and environment. *Frontiers in Plant Science*, 10, p.1415.

Miljaković, D., Marinković, J., Tamindžić, G., Đorđević, V., Tintor, B., Milošević, D., Ignjatov, M. and Nikolić, Z. 2022. Bio-priming of soybean with Bradyrhizobium japonicum and Bacillus megaterium: Strategy to improve seed germination and the initial seedling growth. *Plants*, 11(15), p.1927.

Mishra, S.K., Khan, M.H., Misra, S., Dixit, V.K., Gupta, S., Tiwari, S., Gupta, S.C. and Chauhan, P.S. 2020. Drought tolerant Ochrobactrum sp. inoculation performs multiple roles in maintaining the homeostasis in Zea mays L. subjected to deficit water stress. *Plant Physiology and Biochemistry*, 150, pp.1-14.

Moore, J.P., Farrant, J.M., Lindsey, G.G. and Brandt, W.F. 2005. The South African and Namibian populations of the resurrection plant Myrothamnus flabellifolius are genetically distinct and display variation in their galloylquinic acid composition. *Journal of chemical ecology*, 31, pp.2823-2834.

Morcillo, R.J., Vílchez, J.I., Zhang, S., Kaushal, R., He, D., Zi, H., Liu, R., Niehaus, K., Handa, A.K. and Zhang, H. 2021. Plant transcriptome reprograming and bacterial extracellular metabolites underlying tomato drought resistance triggered by a beneficial soil bacteria. *Metabolites*, 11(6), p.369.

Moye, Z.D., Burne, R.A. and Zeng, L. 2014. Uptake and metabolism of N-acetylglucosamine and glucosamine by Streptococcus mutans. *Applied and Environmental Microbiology*, 80(16), pp.5053-5067.

Naylor, D. and Coleman-Derr, D. 2018. Drought stress and root-associated bacterial communities. *Frontiers in plant science*, 8, p.2223.

Naseem, H., Ahsan, M., Shahid, M.A. and Khan, N. 2018. Exopolysaccharides producing rhizobacteria and their role in plant growth and drought tolerance. *Journal of basic microbiology*, 58(12), pp.1009-1022.

Nawaz, H., Hussain, N., Jamil, M., Yasmeen, A., BUKHARI, A., AURINGZAIB, M. and Usman, M. 2020. Seed biopriming mitigates terminal drought stress at reproductive stage of maize byenhancing gas exchange attributes and nutrient uptake. *Turkish Journal of Agriculture and Forestry*, 44(3), pp.250-261.

Netzker, T., Shepherdson, E.M., Zambri, M.P. and Elliot, M.A. 2020. Bacterial volatile compounds: functions in communication, cooperation, and competition. *Annual Review of Microbiology*, 74, pp.409-430.

Ogbaga, C.C., Stepien, P., Dyson, B.C., Rattray, N.J., Ellis, D.I., Goodacre, R. and Johnson, G.N. 2016. Biochemical analyses of sorghum varieties reveal differential responses to drought. *Public Library of Science one*, 11(5), p.e0154423.

Pehlivan, F.E. 2017. Vitamin C: An antioxidant agent. *Vitamin C*, 2, pp.23-35.

Pieterse, C.M., Zamioudis, C., Berendsen, R.L., Weller, D.M., Van Wees, S.C. and Bakker, P.A. 2014. Induced systemic resistance by beneficial microbes. *Annual review of phytopathology*, 52, pp.347-375.

Piri, R., Moradi, A., Balouchi, H. and Salehi, A. 2019. Improvement of cumin (Cuminum cyminum) seed performance under drought stress by seed coating and biopriming. *Scientia Horticulturae*, 257, p.108667.

Purvis, J.E., Yomano, L.P. and Ingram, L.O. 2005. Enhanced trehalose production improves growth of Escherichia coli under osmotic stress. *Applied and environmental microbiology*, 71(7), pp.3761-3769.

Rahman, I., Kode, A. and Biswas, S.K. 2006. Assay for quantitative determination of glutathione and glutathione disulfide levels using enzymatic recycling method. *Nature protocols*, 1(6), pp.3159-3165.

Kusvuran, A. 2015. The effects of salt stress on the germination and antioxidative enzyme activityof Hungarian vetch (Vicia pannonica Crantz.) varieties. *Legume Research-An International Journal*, 38(1), pp.51-59.

Saberi Riseh, R., Ebrahimi-Zarandi, M., Gholizadeh Vazvani, M. and Skorik, Y.A. 2021. Reducing drought stress in plants by encapsulating plant growth-promoting bacteria with polysaccharides. *International Journal of Molecular Sciences*, 22(23), p.12979.

Sen, S., Ghosh, D. and Mohapatra, S. 2018. Modulation of polyamine biosynthesis in Arabidopsis thaliana by a drought mitigating Pseudomonas putida strain. *Plant Physiology and Biochemistry*, 129, pp.180-188.

Senthilkumar, M., Amaresan, N., Sankaranarayanan, A., Senthilkumar, M., Amaresan, N. and Sankaranarayanan, A. 2021. Determination of Chlorophyll. In: *Plant-Microbe Interactions. Springer Protocols Handbooks*. Humana, New York, NY. https://doi.org/10.1007/978-1-0716-1080-0_37

Shi, J., Wang, X. and Wang, E. 2023. Mycorrhizal symbiosis in plant growth and stress adaptation: From genes to ecosystems. *Annual Review of Plant Biology*, 74, pp.569-607.

Shin, Y.K., Bhandari, S.R., Jo, J.S., Song, J.W. and Lee, J.G. 2021. Effect of drought stress on chlorophyll fluorescence parameters, phytochemical contents, and antioxidant activities in lettuce seedlings. *Horticulturae*, 7(8), p.238.

Steen, A.D., Crits-Christoph, A., Carini, P., DeAngelis, K.M., Fierer, N., Lloyd, K.G. and Thrash, J.C., 2019. High proportions of bacteria and archaea across most biomes remain uncultured. *The International Society for Microbial Ecology journal*, 13(12), pp.3126-3130.

Sun, J., Miller, J.B., Granqvist, E., Wiley-Kalil, A., Gobbato, E., Maillet, F., Cottaz, S., Samain, E., Venkateshwaran, M., Fort, S. and Morris, R.J. 2015. Activation of symbiosis signaling by arbuscular mycorrhizal fungi in legumes and rice. *The Plant Cell*, *27*(3), pp.823-838.

Szablińska-Piernik, J. and Lahuta, L.B. 2021. Metabolite profiling of semi-leafless pea (Pisum sativum L.) under progressive soil drought and subsequent re-watering. *Journal of Plant Physiology*, *256*, p.153314.

Talukder, M.R., Asaduzzaman, M., Tanaka, H. and Asao, T. 2018. Light-emitting diodes and exogenous amino acids application improve growth and yield of strawberry plants cultivated in recycled hydroponics. *Scientia horticulturae*, *239*, pp.93-103.

Tapia, H., Young, L., Fox, D., Bertozzi, C.R. and Koshland, D. 2015. Increasing intracellular trehalose is sufficient to confer desiccation tolerance to Saccharomyces cerevisiae. *Proceedings of the National Academy of Sciences*, 112(19), pp.6122-6127.

Tebele, S.M., Marks, R.A. and Farrant, J.M. 2023. Exploring the root-associated microbiome of the resurrection plant Myrothamnus flabellifolia. *Plant and Soil*, pp.1-16.

Teixeira, W.F., Fagan, E.B., Soares, L.H., Umburanas, R.C., Reichardt, K. and Neto, D.D. 2017. Foliar and seed application of amino acids affects the antioxidant metabolism of the soybean crop. *Frontiers in plant science*, *8*, p.327.

Tran, Q.H., Pham, T.Q., Vu, H.T., Le, D.X., Tran, O.T., Ngo, A.Q., Nguyen, T.D., Hoang, B.T. and Do, S.T. 2019. Research on some factors affecting extraction of chlorophyll from mulberry leaves (Morus alba). In *IOP Conference Series: Materials Science and Engineering* (Vol. 479, No. 1, p. 012004). IOP Publishing.

Vitorino, L.C. and Bessa, L.A. 2017. Technological microbiology: development and applications. *Frontiers in Microbiology*, 8, p.827.

Wang, C.M., Li, T.C., Jhan, Y.L., Weng, J.H. and Chou, C.H. 2013. The impact of microbial biotransformation of catechin in enhancing the allelopathic effects of Rhododendron formosanum. *Public Library of Science One*, 8(12), p.e85162.

Wang, F., Wei, Y., Yan, T., Wang, C., Chao, Y., Jia, M., An, L. and Sheng, H. 2022. Sphingomonas sp. Hbc-6 alters physiological metabolism and recruits beneficial rhizosphere bacteria to improve plant growth and drought tolerance. *Frontiers in Plant Science*, 13, p.1002772.

Warren, C.R. 2008. Rapid measurement of chlorophylls with a microplate reader. *Journal of Plant Nutrition*, 31(7), pp.1321-1332.

Wu, L., Li, X., Ma, L., Borriss, R., Wu, Z. and Gao, X. 2018. Acetoin and 2, 3-butanediol from Bacillus amyloliquefaciens induce stomatal closure in Arabidopsis thaliana and Nicotiana benthamiana. *Journal of experimental botany*, 69(22), pp.5625-5635.

Xu, L., Naylor, D., Dong, Z., Simmons, T., Pierroz, G., Hixson, K.K., Kim, Y.M., Zink, E.M., Engbrecht, K.M., Wang, Y.I. and Gao, C. 2018. Drought delays development of the sorghum root microbiome and enriches for monoderm bacteria. *Proceedings of the National Academy of Sciences*, 115(18), pp.E4284-E4293.

Yang, H., Wang, C., Chen, F., Yue, L., Cao, X., Li, J., Zhao, X., Wu, F., Wang, Z. and Xing, B. 2022. Foliar carbon dot amendment modulates carbohydrate metabolism, rhizospheric properties and drought tolerance in maize seedling. *Science of the total environment*, 809, p.151105.

Yu, Y., Gui, Y., Li, Z., Jiang, C., Guo, J. and Niu, D. 2022. Induced systemic resistance for improving plant immunity by beneficial microbes. *Plants*, 11(3), p.386.

Zhang, Y., Wei, J., Qiu, Y., Niu, C., Song, Z., Yuan, Y. and Yue, T. 2019. Structure-dependent inhibition of Stenotrophomonas maltophilia by polyphenol and its impact on cell membrane. *Frontiers in Microbiology*, 10, p.2646.

Zhi, T., Zhou, Z., Qiu, B., Zhu, Q., Xiong, X. and Ren, C. 2019. Loss of fumarylacetoacetate hydrolase causes light-dependent increases in protochlorophyllide and cell death in Arabidopsis. *The Plant Journal*, 98(4), pp.622-638.

Zhou, M., Hassan, M.J., Peng, Y., Liu, L., Liu, W., Zhang, Y. and Li, Z. 2021. γ-aminobutyric acid (GABA) priming improves seed germination and seedling stress tolerance associated with enhanced antioxidant metabolism, DREB expression, and dehydrin accumulation in white clover under water stress. *Frontiers in Plant Science*, *12*, p.776939.

# Chapter Six

## Discussion and Future Perspectives

## 6.1. General discussion and conclusion

Multiple occurrences of increasingly prolonged drought episodes due to global warming pose serious threats to food security. Drought is the leading factor that adversely affects agricultural crops and reduces productivity and yield. These challenges have led scientists to delve into resurrection plants that can lose approximately 90% RWC and revive upon rehydration. Resurrection plant studies have been increasing in the past four decades and provided insightful knowledge about the adaptation mechanisms used by these plants during desiccation (Tebele et al., 2021). However, the microbiome of resurrection plants and its contribution to desiccation tolerance remains unexplored. A major objective of this study was to identify root-associated microbiome of *M. flabellifolia* and their functions under water deficit conditions. The amplicon metagenomic analysis of three zones namely, bulk soil, rhizosphere and endosphere of *M. flabellifolia* shed light on the diversity of microbial communities that might possess desiccation tolerance traits. The metatranscriptomic analysis of *M. flabellifolia* roots provided insight into the functional role of root-associated bacteria under dehydration and rehydration. The rhizospheric metabolome provides insight into metabolic shifts as a result of drought stress. The outline of the key findings of the thesis is represented in Figure 6-1. Finally, the screening and application of rhizospheric bacteria to maize seeds showed enhancement of seedling resilience under drought.

The tripartite interaction between plant roots, soil and microorganisms is extremely complex and is not fully understood. Root exudates modulate microbial diversity and limit pathogen colonization within its proximity. As a result of the intertwining of microbes and roots, microbial communities also influence the root system. This interaction tends to be more complex especially under water deficit conditions as a result of alteration in biochemical pathways and molecular and physiological mechanisms in both plants and microorganisms. The accumulation of metabolites such as sucrose and procyanidins in the roots of *M. flabellifolia* under drought stress (Klamer, 2022, unpublished), play a significant role in facilitating their desiccation tolerance. However, procyanidins might be secreted into the rhizosphere through apoplastic or symplastic pathways to also inhibit plant pathogens (Akhalwaya et al., 2018; Tea, 2013). Interestingly, the rhizospheric bacteria isolated from desiccated rhizosphere synthesized epicatechin, thus, it is plausible that microbes protect the root membranes

of *M. flabellifolia* and might serve as a source of phenolic antioxidants (**Chapter Five**). Therefore, 16S rRNA and ITS amplicon metagenomic techniques were applied to understand the types of microbiomes in the bulk soil, rhizosphere and endosphere zones of *M. flabellifolia* (**Chapter Two**). Investigation of the microbiome within its ecological habitat and in the desiccated state with the *M. flabellifolia*, have enabled us to identify the nature of bacterial and fungal communities that were desiccation tolerant (**Chapter Two**).

The most prominent bacterial phyla across three zones were *Actinomycetota*, *Acidobacteriota*, *Chloroflexetota*, *Plantomycetota* and *Pseudomonadota,* whereas fungal phyla were *Ascomycota*, *Basidiomycota* and *Mortierellomycota* (Figure 6-1). The microbiomes of *M. flabellifolia* were distinct compared to other desiccation-sensitive plants. For instance, diderm lineages are known to decrease upon water deficit conditions in desiccation-sensitive plants, whereas this study showed high enrichment of both monoderm and diderm lineages in three zones. There was a substantial difference in the microbiome of bulk soil, rhizosphere and endosphere zones. For instance, the bulk soil was significantly enriched with *Cyanophyta* genera such as *Leptolyngbya* and *Coleofascicus*, and *Ascomycota* genera (*Epicoccum* and *Metarhizium*). The rhizosphere soil acted as a central hub for the microbiome, exhibiting significantly higher species richness compared to the endosphere zone.

The rhizosphere zone is composed of a higher diversity of beneficial and drought-tolerant bacterial and fungal communities relative to bulk soil and the endosphere. Higher species richness and microbial dynamics in the rhizosphere suggest that a strong filtering occurs at the soil-to-root interface of *M. flabellifolia*. This phenomenon was detected through alpha and beta-diversity analysis. Additionally, the diversity of the rhizosphere microbiome is likely influenced by root exudates and rhizodeposition, while bulk soil remains unaffected by root activity. This study found the co-occurrence of rhizospheric fungal and bacteria species across the zones and lower exchangeable H ions in the rhizosphere soils suggested that the soil may be less acidic relative to the bulk soil (**Chapter Two**). The identification of microbes with bioremediation traits, such as *Enterobacter cloacae*, *Saccharomyces cerevisiae*, and *Pseudomonas spp*., among others (Ojuederie and Babalola, 2017) in this study indicates that extending the functional role of microbes in the bioremediation of heavy metals would yield valuable insights. The consortium of bacterial and fungal species functions collectively to retain high moisture content and improve nutrients in the rhizosphere soil under desiccation conditions. The diversity of the rhizosphere microbiome has led to delving into the rhizospheric metabolome (**Chapter Four**) and the application of rhizospheric bacteria on maize plants under drought stress (**Chapter Five**).

Plant microbiomes have multiple functions related to abiotic and biotic resilience such as improving soil conditions, and endophytic and anti-pathogen attributes. Although microbial diversity may differ from each plant species, this study forms a baseline for future investigations into resurrection plants microbiomes. Microbial communities associated with plants also suffer from drought stress similar to plants. Metatranscriptomic analysis has provided insights into the establishment of plant-microbe interaction and the mechanisms root-associated bacteria employ during desiccation conditions. A high transcriptional activity resulted from both monoderm and diderm lineages such as *Actinomycetota*, *Bacteroidota*, *Bacillota*, *Cyanophyta* and *Pseudomonadota* in dehydrated roots of *M. flabellifolia* (**Chapter Three**). However, *Pseudomonadota* was dominant compared to other bacterial taxa. Interestingly, these bacterial lineages were also detected in the desiccated rhizosphere soil and endosphere zone (**Chapter Two**). For instance, the significant bacterial taxa including *Streptomyces*, *flavobacterium*, *Novosphingobium*, *Caulobacter*, *Leptolyngbya* and others in the rhizosphere and endosphere as shown in Figure 2-4 were also captured during the transcriptional analysis. It was intriguing to observe the abundance of *Cyanophyta* in the dark environment, considering its typical habitat in soil biocrusts. *Cyanophyta* plays a crucial role in retaining water, ensuring soil stability, and participating in carbon and nitrogen recycling (Lebre et al., 2017). What made this discovery even more interesting was the detection of photosynthetic genes under drought conditions. This suggests that the oxygenic photosynthetic *Cyanophyta* associated with *M. flabellifolia* have developed mechanisms to perform photosynthesis in the absent of light under normal conditions. This adaptation is attributed to cyanobacterial phosphoribulokinase (PRK), which has a single cysteine and is incapable of light or dark redox regulation in the chloroplast (Balsera et al., 2013). Therefore, the identification of bacterial lineages in the metagenomic study aligns with the taxonomic profiles reported in the metatranscriptomics analysis of root-associated bacteria during desiccation. These consistent trends illustrate the microbiome's plasticity and adaptability under harsh environmental stress.

The root-associated microbiome showed a widespread response to rehydration conditions and drought stress. Bacteria expressed genes related to plant-microbe interaction and plant growth promotion, while desiccation was associated with drought-responsive genes (Figure 1-6). It is remarkable to detect the regulation and cell signalling process under drought stress and these involved the upregulation of genes encoding anti-sigma factors. These findings suggest that root-associated bacteria were able to detect extracellular drought stress and employ necessary responses to counteract damage might play a role in survival. Most of the upregulated genes under drought stress were from respiration metabolism. These include ATPase and electron transport, and phosphorylation pathways were two-fold greater in dehydrated samples relative to rehydrated roots

(**Chapter Three**). Therefore, it is plausible that the excessive ATP generated within the bacterial cell was transported into the roots of *M*. *flabellifolia* via ADP/ATP carrier proteins, which were also upregulated under drought stress. These root-associated bacteria may supply fuel cell energy to *M. flabellifolia* roots to utilise it in defense systems against drought stress. Another important finding was the upregulation of genes encoding for NAD(+)/NADH kinases (NADKs) only under drought stress. Remarkably, upregulation of genes encoding protein kinases was also reported in the desiccated leaves of *M. flabellifolia*. These findings demonstrates that root-associated bacteria employ similar mechanisms as the host plant to survive multiple drying and rehydration cycles. For example, NADKs function in antioxidant systems, which modulate ROS homeostasis and they are the only enzymes that catalyse the phosphorylation of NADH to generate NADPH in almost all living organisms. The expressed genes associated with energy generation in bacterial cells might enhance the desiccation tolerance of *M. flabellifolia* by providing energy for ROS scavenging systems.

This study detected a wide spectrum of ROS scavenging systems such as antioxidant enzymes (superoxide dismutase and manganese catalase), molecular chaperones (HSP20, DnaK, HtpG, CsbD), and protective osmolytes which are critical for sustaining homoeostasis within the bacterial cells (Figure 6-1). These expressed genes support the hypothesis of convergent evolution of desiccation tolerance between microbiomes and plants. Convergent adaptive processes for surviving extreme drought stress were further identified through the upregulation of genes (TPS, TS, and TreY) involved in trehalose biosynthesis (Figure 6-1). The abundance of trehalose in the desiccated rhizosphere soil (**Chapter Four**) and bacterial metabolites (**Chapter Five**), aligns with the expressed genes in Chapter Three. Additionally, the expression of indole-pyruvate dehydrogenase genes indicates that bacteria can synthesize IAA, which may enhance the root growth of the *M. flabellifolia* and enable the roots to source water in deeper soil profiles. The accumulation of metabolites in desiccated rhizosphere soil suggests that some may be produced by rhizospheric microbes, which serve as the primary source, with these metabolites being transported into the root system. Additionally, this study observed a high accumulation of organic acids in the rhizosphere, likely originating from the roots, which may aid in rock breakdown and nutrient solubilization (Wu et al., 2017).

Another significant finding was that the quantified metabolites in the desiccated rhizosphere soil and bacterial cells correspond with the expressed genes (Figure 6-1). The alterations in molecular and biochemical processes indicate that microbes also suffer drought stress and employ similar mechanisms to protect their cells, while also contributing to the drought tolerance of the host plant. Although the cultivation of microbes might seem like a conventional technique, this technique makes it possible to explore the functional role of microbes, their metabolic pathways and enables the detection of novel microbes. Culture-dependent methods are crucial for the industrial application of

microbes to improve agricultural outcomes and to perform further investigations of microbes. The application of rhizospheric microbes to improve resilience in agricultural systems is increasing. However, there are challenges in screening and isolating beneficial microbes. This study showed that rhizospheric bacteria isolated from the xeric rhizosphere soil was composed of both gram-negative and gram-positive bacteria (**Chapter Five**). This study served as proof of concept and demonstrated that rhizospheric bacteria associated with desiccation tolerance plants improved the drought tolerance of maize plants. These dynamics may enhance the plant to also adapt under water deficit conditions. This study tested *M. flabellifolia*'s potential to contribute to improve abiotic tolerance, and enhance plant performance such as growth, yield, and the productivity of staple food crops through the application of isolated microbes.

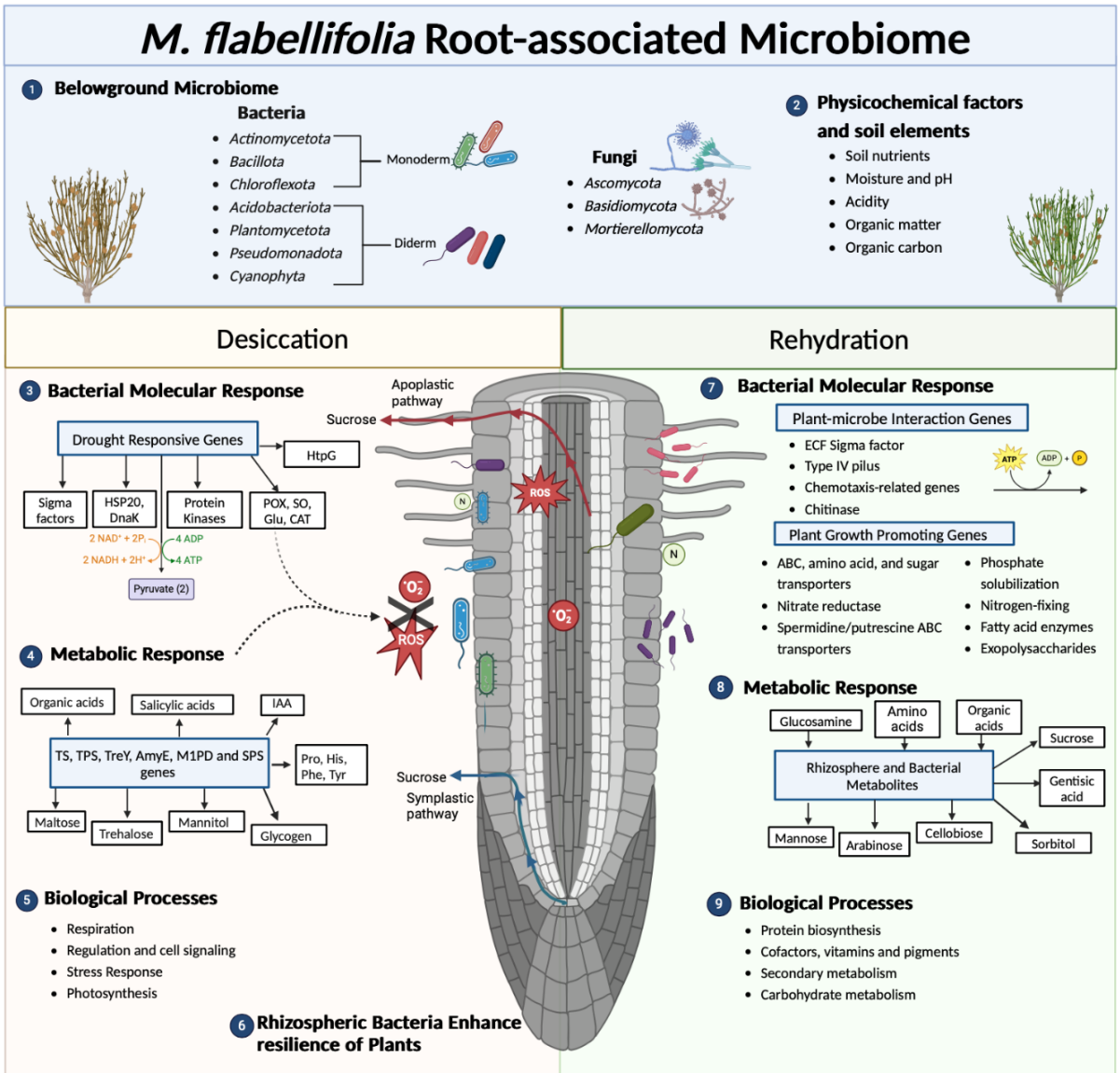


**Figure 6-1.** Summary diagram of key findings of functional role(s) of the root-associated microbiome, bacteria in particular, of *Myrothamnus flabellifolia*. The abundance of sucrose in *M. flabellifolia* roots

under drought stress (Klamer, 2022, unpublished) may be secreted into the rhizosphere soil through the apoplastic or symplastic pathway and may act as a chemoattractant for the microbial community. **1**) The amplicon metagenomic analysis showed the predominant bacterial and fungal phyla in the bulk soil, rhizosphere, and endosphere zones of *M. flabellifolia* under desiccated conditions (<10% RWC). the rhizosphere soil hosts a diversity of bacterial and fungal communities relative to other zones. **2**) The rhizosphere soil of *M. flabellifolia* showed improved physicochemical factors and soil nutrients compared to bulk soil, which might be due to the present microbiome under desiccation stress. **3**) The differentially expressed genes (DEGs) under drought stress in bacterial cells associated with *M. flabellifolia* roots. Here, upregulation of genes encoding cell signalling sigma factors to detect extracellular drought stress and employ drought-responsive genes such as molecular chaperones (DnaK, HSP20), ATP synthase, antioxidant enzyme genes and protein kinases to scavenge ROS and mitigate oxidative stress was evident. **4**) Upregulated genes of phytohormones, primary and secondary metabolites in bacterial cells associated with roots, and significantly abundant metabolites in the rhizosphere soil under dehydration conditions. These metabolites play a crucial role as osmolytes, enhance vitrification, and potentially replace water molecules under drought stress. **5**) Significant biological processes within root-associated bacterial cells under drought stress. **6**) Application of rhizospheric bacteria from *M. flabellifolia* improved drought tolerance in maize plants. **7**) Bacterial molecular responses upon rehydration showing DEGs linked with promoting plant-microbe interaction and plant growth. **8**) Enrichment of metabolites in the rehydrated rhizosphere soil of *M. flabellifolia*. **9**) DEGs under rehydrated conditions were linked with various biological processes such as protein biosynthesis (amino acid transporters), and carbohydrate metabolism (exopolysaccharide synthesis).

## 6.2. The importance and contribution of the study

The study of plant microbiomes has underscored the significance of soil and root microorganisms in improving drought tolerance in host plants. Despite this, the adaptation mechanisms employed by root-associated microbes in resurrection plants remain inadequately explored. This study aimed to address the existing gap in our understanding of resurrection plant microbiomes, and shed light on the limited knowledge in this area. In pursuit of this goal, the resurrection plant *M. flabellifolia* was employed as a model organism, offering insights into both the belowground microbiome and its defense mechanisms and contribution to resilience of the host plant. Notably, this investigation marks the first thesis to explore the root-associated microbiome of *M. flabellifolia* and its functions under conditions of extreme water deficit. The overarching objective of this study extends beyond improving food crops; it also strives to contribute to sustainable agriculture by elucidating promising strategies to address the challenges of food security.

The experiments were executed using field samples, ensuring a thorough examination of the microbiomes within the plant's natural habitat. This distinctive approach sets this study apart, especially when compared to the typical greenhouse or laboratory-controlled experiments. Profiling of bacterial and fungal communities revealed microbes from both the rhizosphere soil and endosphere of *M. flabellifolia* exhibit attributes indicative of desiccation tolerance. Notably, the

rhizosphere zone displayed a rich diversity of microorganisms compared to other zones. For that reason, to harness the potential of the rhizosphere microbiome, the transcriptional activity of root-associated bacteria was explored to understand molecular functions under desiccation stress.

This study also elucidated the role of metabolites in the rhizosphere soil and their ability to alleviate some of the negative effects of drought stress. While rhizospheric osmolytes are known to originate from both microbes and root exudates, this research demonstrated that these metabolites are derived primarily from bacteria. Applying beneficial microorganisms to enhance the plant's drought tolerance emerges as one of the most effective strategies for mitigating the impact of drought, and there is potential for developing a biostimulant that can be employed to fortify crops against the challenges of drought stress. The integration of omics technologies with physiological and biochemical data provide a systems level perspective on the mechanisms of microbial enhancement of resilience.

## 6.3. Challenges and limitations

Variation in rhizosphere soil due to field-based factors presented challenges, as samples were influenced by diverse environmental factors such as plants growing in different micro-niches. This environmental variability may have contributed to unaccounted differences in both rhizosphere microbiomes and metabolomes. Despite these challenges, the primary objective of exploring microbial communities was successfully achieved.

The initial experimental design involved a metatranscriptome analysis of roots and rhizosphere soil. However, the rhizosphere soil, rich in compounds like humic acids and high carbohydrates, inhibited RNA extraction process, resulting in lower RNA yield and poor quality. Consequently, these data were eliminated and only root-associated microbes were used for transcriptome analysis. While breaking down the woody roots of *M. flabellifolia* proved challenging, innovative strategies were implemented to generate a fine powder suitable for RNA extraction. Additionally, the metatranscriptomic study generated extensively huge data files, which cannot be analysed using a personal computer. Therefore, high-performance computing (HPC) was used to achieve pre-processing of the data.

Fungi have spores and cannot be cultivated under the same conditions as bacteria and the absence of fungal culturing facilities limited the isolation of fungi from rhizosphere soil and the evaluation of its impact on maize– a process that was successfully conducted with bacterial isolates.

## 6.4. Future perspective and recommendations

The improvement of plant drought tolerance through the application of beneficial microorganisms necessitates a thorough understanding of the intricate dynamics within plant-microbe interactions.

High-throughput technologies are indispensable tools for unravelling the complex tripartite interactions between plants, microbes, and soil. This study delves into the functional role of the root-associated microbiome, shedding light on the crosstalk between root exudates and the soil microbiome in their natural habitat under water deficit conditions. This thesis establishes a foundation for future investigations into the microbiome of *M. flabellifolia* and its desiccation tolerance. Exploring the microbiome of *M. flabellifolia* across diverse locations is recommended to discern the impact of environmental variations on the microbiome of this plant species. A recent study suggested a higher abundance of *M. flabellifolia* in xeric environments compared to those in mesic habitats (Marks et al., 2022). Therefore, it is crucial to identify microbial differences in *M. flabellifolia* that may positively impact host plant across various habitats. The application of isolated microbes in agricultural set-up should further be investigated to evaluate whether resurrection plant microbiome can have a positive impact in crops. Furthermore, investigating the phyllosphere microbiome could offer valuable insights into the microbial diversity associated with *M. flabellifolia* leaves and how drought influences these microbial communities. To date, there has been no study on leaf microbiome, although Moore et al. (2007) proposed that *M. flabellifolia* leaves are associated with *Bacillus* species producing anti-fungal compounds.

The application of omics technologies in this study has yielded valuable insights into the microbiome and metabolome of *M. flabellifolia*, paving the way for future investigations into other resurrection plant lineages from *Bryophytes*, to *Pteridophytes*, and *Spermatophytes*. While the roots also experience drought stress, the desiccation tolerance mechanisms of resurrection plants remain largely unexplored, as highlighted by Tebele et al. (2021). Upcoming studies should consider delving into the rhizosphere soil metabolome of resurrection plants to unveil the collective defense mechanisms of both roots and microorganisms. For example, this study discovered a significant abundance of osmolytes in the rhizosphere soil that likely counteract the effects of drought. Expanding this knowledge to other resurrection plants could significantly contribute to understanding rhizosphere metabolites, such as trehalose that was secreted by microorganisms. Additionally, employing hydroponics could be instrumental in distinguishing between root exudates and microbial metabolites. While this study focused on the fundamental role of primary metabolites, further investigations into secondary metabolites, such as exopolysaccharides, flavonoids, and carboxylic acids, using liquid chromatography-mass spectrophotometer (LC-MS), would provide valuable insights.

To comprehend the microbial variation across diverse resurrection plants and their roles in desiccation tolerance, similar microbiome analyses should be carried out on other resurrection plants. These forthcoming studies could offer a means to identify beneficial and desiccation-tolerant

microorganisms associated with resurrection plants, allowing their application in agricultural plants to enhance resilience against drought. Examining the impact of isolated endophytes and rhizospheric microorganisms, encompassing both bacteria and fungi from *M. flabellifolia*, on plant pathogens may also provide valuable insights into pathogen inhibition efficacy. Investigating the influence of root-associated microbes on plant salinity, cold, and heat tolerance would further expand our understanding of microbiome resilience against both biotic and abiotic stresses. Given the significance of antioxidant enzymes and the accumulation of osmolytes in microorganisms under drought stress, conducting a metaproteomic analysis of bacteria and fungi associated with resurrection plants would elucidate their functions in plants during drought stress. Furthermore, performing whole-genome or transcriptome sequencing of isolated bacteria and fungi from *M. flabellifolia* and other resurrection plants holds the potential to discover novel species. Considering the diverse industrial applications of microorganisms, this study suggests that rhizospheric bacteria have the potential to formulate biostimulants, improving plant growth and drought tolerance. Future studies would benefit from tracking the persistence and spatial distribution of inoculated microbial isolates in plant tissues over time and using isolate-specific PCR approaches to determine their viability and potential endophytic colonization patterns. The interaction of plants and microbes using advanced multiphoton microscopy (Lee et al., 2022) to visualise live rhizospheric microbes and associated compounds should be further investigated. The primary goal of accumulating this data is to contribute to sustainable agriculture by improving the drought tolerance of plants and reducing the reliance on chemical fertilizers.

## 6.5. References


Akhalwaya, S., Van Vuuren, S. and Patel, M. 2018. An in vitro investigation of indigenous South African medicinal plants used to treat oral infections. *Journal of Ethnopharmacology*, 210, pp.359-371.

Balsera, M., Uberegui, E., Susanti, D., Schmitz, R.A., Mukhopadhyay, B., Schürmann, P. and Buchanan, B.B. 2013. Ferredoxin: thioredoxin reductase (FTR) links the regulation of oxygenic photosynthesis to deeply rooted bacteria. *Planta*, 237, pp.619-635.

Klamer, R. 2022. MSc dissertation: Descending below the surface: root metabolomics of the South African resurrection plant *Myrothamnus Flabellifolius* (unpublished). Wageningen University & Research.

Lebre, P.H., De Maayer, P. and Cowan, D.A. 2017. Xerotolerant bacteria: surviving through a dry spell. *Nature Reviews Microbiology*, 15(5), pp.285-296.

Lee, J., Hestrin, R., Nuccio, E.E., Morrison, K.D., Ramon, C.E., Samo, T.J., Pett-Ridge, J., Ly, S.S., Laurence, T.A. and Weber, P.K. 2022. Label-free multiphoton imaging of microbes in root, mineral, and soil matrices with time-gated coherent Raman and fluorescence lifetime imaging. *Environmental science & technology*, 56(3), pp.1994-2008.

Marks, R.A., Mbobe, M., Greyling, M., Pretorius, J., McLetchie, D.N., VanBuren, R. and Farrant, J.M. 2022. Variability in functional traits along an environmental gradient in the South African resurrection plant Myrothamnus flabellifolia. *Plants*, 11(10), p.1332.

Moore, J.P., Lindsey, G.G., Farrant, J.M. and Brandt, W.F. 2007. An overview of the biology of the desiccation-tolerant resurrection plant Myrothamnus flabellifolia. *Annals of Botany*, 99(2), pp.211-217.

Ojuederie, O.B. and Babalola, O.O. 2017. Microbial and plant-assisted bioremediation of heavy metal polluted environments: a review. *International journal of environmental research and public health*, 14(12), p.1504.

Tea, G., 2013. Anti-infective properties of Epigallocatechin-3-gallate (EGCG), a component of. *British Journal of Pharmacology*, 168(5), pp.1059-1073.

Tebele, S.M., Marks, R.A. and Farrant, J.M. 2021. Two decades of desiccation biology: A systematic review of the best-studied angiosperm resurrection plants. *Plants*, 10(12), p.2784.

Wu, Y.W., Zhang, J.C., Wang, L.J. and Wang, Y.X. 2017. A rock-weathering bacterium isolated from rock surface and its role in ecological restoration on exposed carbonate rocks. *Ecological engineering*, 101, pp.162-169.

## 6.6. Annexures

This annexure comprises of additional figures and tables generated throughout all chapters. It includes figures depicting the pre-processing of amplicon metagenomic and metatranscriptomic sequencing datasets (Chapter Two and Three). Additionally, it presents a list of differentially expressed genes in root-associated bacteria of *M. flabellifolia* under dehydration and rehydration conditions (Chapter Three). Moreover, it contains a compilation of metabolites quantified using GC-MS in Chapter Four and Five. Lastly, it shows the list of enriched KEGG pathways in plants, yeast, and bacteria (Chapter Four).

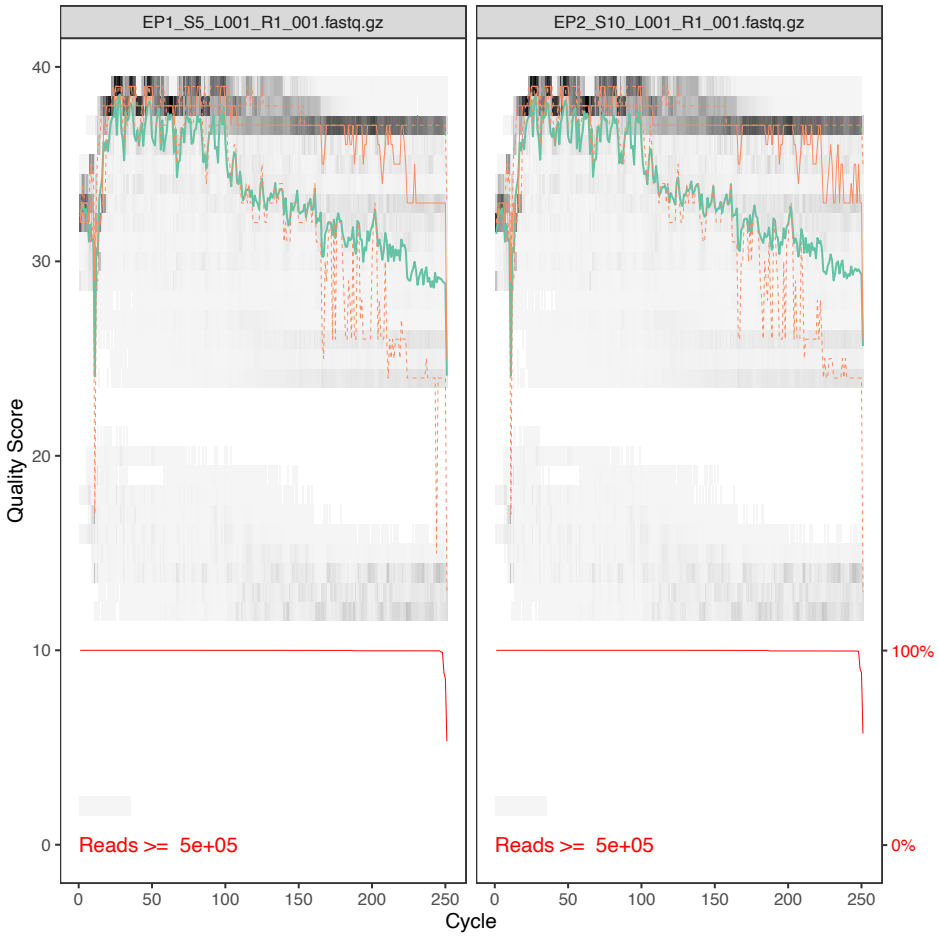


**Figure A1**. An example of amplicon metagenomic sequencing quality of the endosphere sample (EP1) prior trimming (Chapter Two).

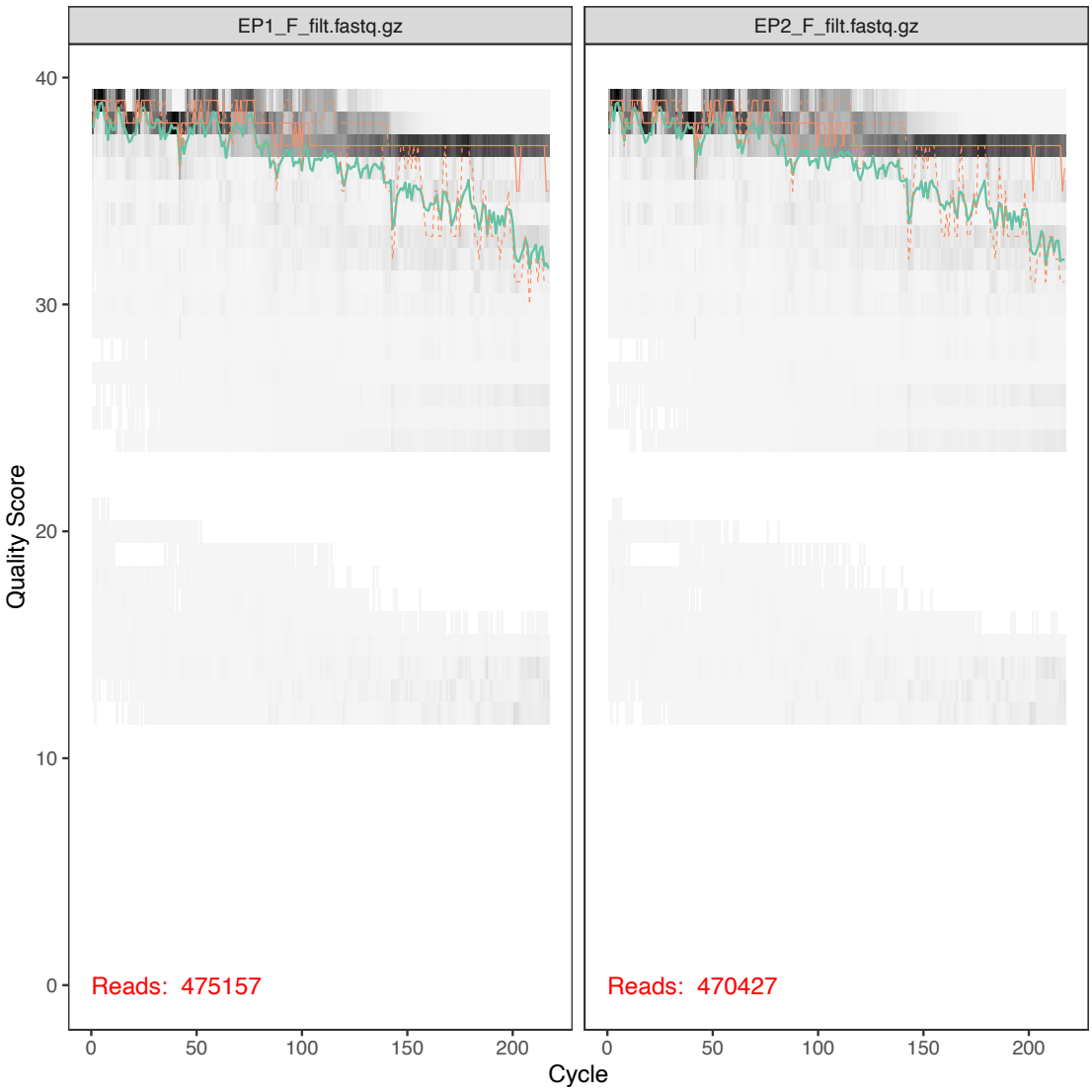


**Figure A2**. An example of amplicon metagenomic sequencing quality of the endosphere sample (EP1 and 2) after trimming with a quality score above 30 (Chapter Two).


**Figure A3.** The mean quality value across each base position in the read in all samples used for metatranscriptomic analysis in Chapter Three.

**Table A1.** The multiQC table of samples for metatranscriptomic analysis in Chapter Three.

| Sample | Number of seq | Total bp | Avg seq length | N50 | N75 | N90 | auN | Min | Max |
|---|---|---|---|---|---|---|---|---|---|
| **DA1_S16_L001.mer** | 57012955 | 7423224700 | 130.20 | 139 | 115 | 98 | 0.00 | 50 | 176 |
| **DA2_S1_L001.merg** | 66872017 | 8525024949 | 127.48 | 135 | 113 | 97 | 0.00 | 50 | 176 |
| **DA3_S4_L001.merg** | 70930303 | 9173718855 | 129.33 | 138 | 114 | 98 | 0.00 | 50 | 176 |
| **DA4_S7_L001.merg** | 71273540 | 9219947494 | 129.36 | 138 | 114 | 98 | 0.00 | 50 | 176 |
| **DA5_S9_L001.merg** | 77121170 | 10156792386 | 131.70 | 141 | 118 | 99 | 0.00 | 50 | 176 |
| **DB10_S15_L001.me** | 66521802 | 8724202580 | 131.15 | 140 | 117 | 99 | 0.00 | 50 | 176 |
| **DB6_S18_L001.mer** | 57453122 | 7747130732 | 134.84 | 144 | 122 | 103 | 0.00 | 50 | 176 |
| **DB8_S11_L001.mer** | 58303669 | 7507396222 | 128.76 | 138 | 113 | 97 | 0.00 | 50 | 176 |
| **DB9_S13_L001.mer** | 76526676 | 9844343287 | 128.64 | 137 | 113 | 98 | 0.00 | 50 | 176 |
| **RA1_S17_L001.mer** | 77393508 | 9955815663 | 128.64 | 137 | 113 | 97 | 0.00 | 50 | 176 |
| **RA2_S2_L001.merg** | 71071378 | 9133706500 | 128.51 | 136 | 113 | 98 | 0.00 | 50 | 176 |
| **RA3_S5_L001.merg** | 69990563 | 9074664676 | 129.66 | 138 | 115 | 99 | 0.00 | 50 | 176 |
| **RA4_S8_L001.merg** | 67746705 | 8755347813 | 129.24 | 137 | 114 | 98 | 0.00 | 50 | 176 |
| **RA5_S10_L001.mer** | 32254771 | 4213211526 | 130.62 | 139 | 117 | 99 | 0.00 | 50 | 176 |
| **RB10_S14_L001.me** | 54926091 | 7228619950 | 131.61 | 141 | 117 | 100 | 0.00 | 50 | 176 |
| **RB6_S12_L001.mer** | 79496814 | 10387886639 | 130.67 | 139 | 116 | 99 | 0.00 | 50 | 176 |
| **RB7_S3_L001.merg** | 70225257 | 9122313920 | 129.90 | 138 | 115 | 99 | 0.00 | 50 | 176 |
| **RB9_S6_L001.merg** | 91412304 | 11812480782 | 129.22 | 138 | 114 | 98 | 0.00 | 50 | 176 |

**Table A2.** The number of raw reads and after quality filtering of metatranscriptome dataset (Chapter Three).

| Sample ID | Number of raw reads | Number of reads (after quality filtering) |
|---|---|---|
| **DA1_S16_ME** | 211,159,901 | 8,675,317 |
| **DA2_S1_ME** | 238,100,967 | 13,116,483 |
| **DA3_S4_ME** | 251,530,275 | 9,689,723 |
| **DA4_S7_ME** | 253,304,707 | 9,209,032 |
| **DA5_S9_ME** | 277,953,302 | 6,331,388 |
| **DB10_S15_ME** | 238,343,834 | 5,541,094 |
| **DB6_S18_ME** | 234,416,140 | 8,688,159 |
| **DB8_S11_ME** | 202,014,880 | 6,071,734 |
| **DB9_S13_ME** | 256,576,694 | 9,075,455 |
| **RA1_S17_ME** | 262,720,156 | 8,318,329 |
| **RA2_S2_ME** | 239,343,770 | 10,133,478 |
| **RA3_S5_ME** | 238,336,179 | 8,291,373 |
| **RA4_S8_ME** | 228,199,428 | 10,320,614 |
| **RA5_S10_ME** | 110,632,749 | 3,492,504 |
| **RB6_S12_ME** | 275,944,580 | 9,320,465 |
| **RB7_S3_ME** | 22,274,741 | 9,246,583 |
| **RB9_S6_ME** | 324,939,822 | 10,369,682 |
| **RB10_S14_ME** | 56,989,461 | 9,913,032 |

**Table A3**. A list of the tops DEGs (166) with a *p*-value < 0.005 of root-associated bacteria under drought stress and rehydration conditions generated from metatranscriptomic analysis (Chapter Three).

| | baseMean | log2FoldChange | lfcSE | stat | pvalue | padj |
|---|---|---|---|---|---|---|
| **CsbD family protein** | 516.532031220293 | -4.06369874572945 | 0.260859491665615 | -15.578113411869 | 1.025365268321132e-54 | 1.044231989258843e-50 |
| **CBS domain-containing protein** | 403.869508795238 | -2.99124752971224 | 0.195860029840211 | -15.2723735013856 | 1.168416527685582e-52 | 5.949576958976622e-49 |
| **cyclase** | 662.937402306407 | -2.64995323329441 | 0.178781130026785 | -14.8223318249381 | 1.050726601226082e-49 | 3.566866568962213e-46 |
| **thiamine pyrophosphate-requiring protein** | 1262.37831722813 | -4.17677789551982 | 0.297182839718699 | -14.0545729338658 | 7.221624071271687e-45 | 1.838625488545577e-41 |
| **type 1 glutamine amidotransferase** | 788.186432128218 | -3.3741406510347 | 0.254113226398536 | -13.2780992900499 | 3.101675186594404e-40 | 6.317492020054474e-37 |
| **DNA starvation/stationary phase protection protein** | 463.339247008704 | -3.82783418445676 | 0.301828986988487 | -12.6821291177138 | 7.428619704106694e-37 | 1.260884384443375e-33 |
| **alpha-1,4-glucan--maltose-1-phosphate maltosyltransferase** | 306.696036044501 | -3.8228572395408 | 0.304360083410843 | -12.5603107894424 | 3.489593596411133e-36 | 4.947440602943327e-33 |
| **isoaspartyl peptidase/L-asparaginase** | 421.910458660202 | -3.80030212024669 | 0.302769831156822 | -12.5517859575465 | 3.886441950466604e-36 | 4.947440602943327e-33 |
| **SigB/SigF/SigG family RNA polymerase sigma factor** | 159.703180856572 | -2.26879442324618 | 0.185084643111682 | -12.2581451655834 | 1.519379375756681e-34 | 1.719262173633415e-31 |
| **NADP-dependent succinic semialdehyde dehydrogenase** | 344.511429830538 | -5.16129277660585 | 0.422301323509827 | -12.2218247712542 | 2.376887912937774e-34 | 2.420622650535 8e-31 |
| **DUF1236 domain-containing protein** | 194.055744695372 | -4.53574713036128 | 0.372753176087596 | -12.1682320133884 | 4.589149333925599e-34 | 4.248717892427748e-31 |
| **DUF2795 domain-containing protein** | 163.782080657688 | -4.62539972818934 | 0.388960550607666 | -11.8916936973767 | 1.307283505690081e-32 | 1.109447935116293e-29 |
| **ornithine decarboxylase** | 120.413557184448 | -4.05932494224794 | 0.347234481057508 | -11.690443097371 | 1.426404747055739e-31 | 1.117423534156634e-28 |
| **DUF1360 domain-containing protein** | 41.2765680997808 | -4.69671507784561 | 0.403011865599656 | -11.6540367139245 | 2.188411688792273e-31 | 1.591913188476608e-28 |
| **glycogen-branching enzyme** | 170.181858126394 | -2.41833412082481 | 0.210537329309697 | -11.4864861673413 | 1.542596827635539e-30 | 1.047320406176592e-27 |
| **DUF3416 domain-containing protein** | 310.735835035113 | -3.80425110012973 | 0.337464151795545 | -11.2730525002092 | 1.782799745402255e-29 | 1.134752037948872e-26 |

| | | | | | | |
|---|---|---|---|---|---|---|
| **catalase HPII** | 916.947054703139 | -3.28378599303666 | 0.29183646812554 | -11.2521441001817 | 2.260296944865579e-29 | 1.354050828618426e-26 |
| **YihY/virulence factor BrkB family protein** | 169.388877706727 | -2.82066776625564 | 0.25116350095551 | -11.2304047185395 | 2.891510349980623e-29 | 1.635952300233348e-26 |
| **hemerythrin** | 110.694382619492 | -2.81917450593066 | 0.252975519601338 | -11.1440605414048 | 7.654784120251 8e-29 | 4.102964288454497e-26 |
| **protein-L-isoaspartate O-methyltransferase** | 110.657471025351 | -1.88694276793074 | 0.171895596870681 | -10.9772606296037 | 4.916056297084487e-28 | 2.503255866475562e-25 |
| **photosystem reaction center subunit H** | 326.150281719706 | -3.10275185681902 | 0.288069440907589 | -10.7708469424717 | 4.726332577004451e-27 | 2.292046236391114e-24 |
| **DUF2382 domain-containing protein** | 161.222457666268 | -3.17708347861482 | 0.303105436855709 | -10.4817766107153 | 1.047570667506647e-25 | 4.849299853584451e-23 |
| **MULTISPECIES: CsbD family protein** | 54.4490407693633 | -3.55016194569992 | 0.341288065675986 | -10.4022446219095 | 2.421605080378876e-25 | 1.072244614720275e-22 |
| **phosphosulfolactate synthase** | 64.1821516856295 | -2.13113309185724 | 0.205570390651083 | -10.3669263122355 | 3.506215607534465e-25 | 1.487804156130354e-22 |
| **transpeptidase** | 137.850686424997 | -5.15208414537641 | 0.499468313997209 | -10.3151371187987 | 6.019532176443 19e-25 | 2.452116627395 9e-22 |
| **CHAD domain-containing protein** | 138.845089018212 | -3.34544947814977 | 0.325794938261261 | -10.2685741405442 | 9.763701730795567e-25 | 3.824366862554 73e-22 |
| **ferritin-like domain-containing protein** | 484.306754557474 | -2.96457665578124 | 0.289365541649709 | -10.2450922071779 | 1.245061082301 86e-24 | 4.696185948948894e-22 |
| **glutamine synthetase type III** | 41.0427238763187 | 3.23330874501099 | 0.319503916271835 | 10.1197781321093 | 4.514377773008 97e-24 | 1.641943687154441e-21 |
| **outer membrane protein assembly factor BamA** | 60.0840791864356 | 3.75691163813742 | 0.373155255882672 | 10.067958521047 | 7.655048142473374e-24 | 2.688241733894491e-21 |
| **YtxH domain-containing protein** | 290.265077972584 | -3.27997972267563 | 0.326239822141682 | -10.0538913402521 | 8.830980186272 61e-24 | 2.997823407233334e-21 |
| **1,4-alpha-glucan branching enzyme** | 224.788343461444 | -2.08891919131605 | 0.208276206398425 | -10.0295623174546 | 1.130164599466671e-23 | 3.712772993860 95e-21 |
| **DUF1942 domain-containing protein** | 115.916789888795 | -4.72786137970939 | 0.475630226 42738 | -9.940203790 70934 | 2.782572953047 63e-23 | 8.855538423074 1e-21 |
| **BON domain-containing protein** | 180.340520537408 | -1.89407895110789 | 0.190757869277158 | -9.929231010 41735 | 3.106419128851 85e-23 | 9.586597699462 81e-21 |
| **Flp family type IVb pilin** | 40.5864945850696 | 3.97840491645073 | 0.403247206625808 | 9.865920584 39844 | 5.849537446453 01e-23 | 1.752108510431 69e-20 |
| **ATP-dependent DNA ligase** | 279.271270572493 | -2.48714442119691 | 0.252222061023437 | -9.860931320 22181 | 6.147649171923 16e-23 | 1.788790261910 44e-20 |
| **DUF4142 domain-containing protein** | 228.846449719044 | -3.18876657939985 | 0.326200898369746 | -9.775468416 35431 | 1.434920204473 29e-22 | 4.059229822876 68e-20 |
| **EvpB family type VI secretion protein** | 48.0552392721002 | 4.08852905102229 | 0.420723124582608 | 9.717861491 63646 | 2.530398313210 06e-22 | 6.964750384 2517e-20 |

| | | | | | | |
|---|---|---|---|---|---|---|
| **LLM class F420-dependent oxidoreductase** | 1085.49075095859 | -1.87862475113902 | 0.1935311656670316 | -9.70709159236551 | 2.81247714251531e-22 | 7.53743874194104e-20 |
| **MULTISPECIES: type 1 glutamine amidotransferase** | 56.953200446054 | -4.07478551252015 | 0.4206948910072462 | -9.68584501259917 | 3.46332561063575e-22 | 9.04372000479859e-20 |
| **thiamine pyrophosphate-requiring protein, partial** | 30.0854111567178 | -5.57746635289528 | 0.5821132857735718 | -9.58141050817292 | 9.57285223160844e-22 | 2.43724817816751e-19 |
| **protease** | 397.633166176134 | -1.78964372929165 | 0.1885439067828 71 | -9.49192026318105 | 2.26816843865273e-21 | 5.63390911688765e-19 |
| **DUF892 domain-containing protein** | 210.730329377073 | -2.32460330053368 | 0.2460071719494919 | -9.44933142442615 | 3.41001759952575e-21 | 8.26848076989767e-19 |
| **beta-phosphoglucomutase family hydrolase** | 58.6451184781587 | -2.09782607496601 | 0.2238260825 31589 | -9.37257200429241 | 7.07861669338984e-21 | 1.67647982338 33e-18 |
| **gas vesicle protein** | 113.095421540787 | -2.73739555547624 | 0.2950292466 10145 | -9.27838709866438 | 1.72063377149531e-20 | 3.98248507475186e-18 |
| **flagellin** | 118.641930502849 | 3.55224035122951 | 0.3831996770 20326 | 9.26994609925283 | 1.86240015721903e-20 | 4.21481848913747e-18 |
| **TonB-dependent receptor** | 366.851887780298 | 2.82756322635568 | 0.3053898413 62403 | 9.25886471449534 | 2.06617331012025e-20 | 4.57432804136187e-18 |
| **transaldolase** | 1728.15776419174 | -1.62495788071571 | 0.1787897010 24383 | -9.08865483529219 | 1.00271904398 98e-19 | 2.17270015829 62e-17 |
| **DUF1206 domain-containing protein** | 72.4035004259753 | -3.56746829249363 | 0.3966610821 75567 | -8.9937441629694 | 2.38948276909247e-19 | 5.06968594175786e-17 |
| **asparaginase** | 66.3552925212656 | -2.588429653 5409 | 0.2880342518 89665 | -8.9865341936 2234 | 2.55149337144 41e-19 | 5.30294050914014e-17 |
| **glutathione-dependent formaldehyde dehydrogenase** | 577.525915541775 | -2.628583947 539 | 0.2926186286 36254 | -8.9829685850 4115 | 2.63557798805221e-19 | 5.36814524606473e-17 |
| **diguanylate cyclase/phosphodiesterase** | 38.9377167162695 | -5.19016815639977 | 0.5808503949 0319 | -8.9354646255 5958 | 4.05470713641997e-19 | 8.09669362300 2e-17 |
| **diaminobutyrate acetyltransferase** | 35.4399024133655 | -6.0287019415778 | 0.6757501229 74697 | -8.9214958852 5275 | 4.60031879925779e-19 | 9.00954743300794e-17 |
| **glycosyltransferase family 9 protein** | 103.534506660548 | -2.2101017455997 | 0.2478915241 7028 | -8.9156002933 0228 | 4.85180650182863e-19 | 9.32279196502317e-17 |
| **D-glycero-beta-D-manno-heptose 1-phosphate adenylyltransferase** | 71.776822127231 | -2.8475471052 2268 | 0.3197008669 21999 | -8.9069108027 0805 | 5.24742433912 87e-19 | 9.89625360549753e-17 |
| **iron-containing redox enzyme family protein** | 55.6362316323349 | -2.8869496783 1853 | 0.3303760411 740234 | -8.7383748019 7328 | 2.36487789724015e-18 | 4.34160282595415e-16 |
| **pyruvate:ferredoxin (flavodoxin) oxidoreductase** | 142.720602313958 | 4.8833850252 7182 | 0.5589120383 41284 | 8.7373051397 5782 | 2.38736997499443e-18 | 4.34160282595415e-16 |
| **HAD family hydrolase** | 342.009157801059 | -1.4791364256 6442 | 0.1712264395 54425 | -8.6384814723 3284 | 5.69650943589951e-18 | 1.01777635254738e-15 |

| | | | | | | |
|---|---|---|---|---|---|---|
| **aconitate hydratase** | 1817.4133181616 | -0.916740312743484 | 0.106499756515305 | -8.60790994026113 | 7.440467418514446e-18 | 1.306443451554433e-15 |
| **FAD-binding dehydrogenase** | 212.1274241866 | -3.69306244355188 | 0.429514542417579 | -8.59822445769821 | 8.095884103896648e-18 | 1.397431927357732e-15 |
| **MULTISPECIES: photosystem reaction center subunit H** | 13.5431526660778 | -3.90313015869204 | 0.454552553889905 | -8.58675223643645 | 8.946227490460654e-18 | 1.518473012714417e-15 |
| **mandelate racemase** | 202.038572417185 | -1.65495843294837 | 0.194040820642967 | -8.52891895357152 | 1.477216306222269e-17 | 2.443291807914446e-15 |
| **rod shape-determining protein RodA** | 26.472248336879 | 2.89285116858321 | 0.339243066917332 | 8.52737005024234 | 1.497123580902251e-17 | 2.443291807914446e-15 |
| **CHAD domain containing protein** | 43.3656171817754 | -4.90195580484296 | 0.574924038735368 | -8.52626690584298 | 1.511462921235538e-17 | 2.443291807914446e-15 |
| **B/F/G family RNA polymerase sigma-70 factor** | 44.857961318501 | -2.25106210504377 | 0.265350161432258 | -8.48336436990805 | 2.187741988966691e-17 | 3.481244439944359e-15 |
| **chromosomal replication initiation protein DnaA** | 71.9502972358721 | 2.07603293327297 | 0.245128454126267 | 8.46916340525524 | 2.471617447347798e-17 | 3.872454166737 2e-15 |
| **carboxylate--amine ligase** | 76.0984320931 77 | -3.27574138391804 | 0.387218981604214 | -8.45966117246355 | 2.681554996403 44e-17 | 4.137720618692 83e-15 |
| **DUF3303 domain-containing protein** | 40.7243890120402 | -2.99760557943986 | 0.354950488079677 | -8.44513722366534 | 3.036885062865 38e-17 | 4.616065295555 38e-15 |
| **DUF3341 domain-containing protein** | 85.4159416015877 | -2.49218444734304 | 0.295563189113039 | -8.43198523747794 | 3.398498633757 15e-17 | 5.089751483262 18e-15 |
| **CoA transferase** | 262.285634744738 | 1.23332911019538 | 0.146376216483356 | 8.42574797891169 | 3.584529642234 2e-17 | 5.290557953117 84e-15 |
| **DUF1501 domain-containing protein** | 719.866905475042 | 2.19080629461261 | 0.260073039609893 | 8.42381162576019 | 3.644300319072 2e-17 | 5.301936349918 76e-15 |
| **DUF2171 domain-containing protein** | 47.9372724671722 | -3.21240703446345 | 0.382219120328471 | -8.40462149487126 | 4.292437231856 32e-17 | 6.156926868904 9e-15 |
| **thiamine pyrophosphate-binding protein, partial** | 65.7457347507556 | -3.94044276625311 | 0.469658391380101 | -8.39001887025597 | 4.860641472547 14e-17 | 6.875107327280 57e-15 |
| **peptidase M13** | 43.6622310945693 | 2.13158169384721 | 0.254520263668404 | 8.37489975503204 | 5.527089821777 776e-17 | 7.710668869177 598e-15 |
| **murein L,D-transpeptidase** | 146.06220782065 | -1.85409541758367 | 0.222095810113067 | -8.34817827783321 | 6.932388192595 82e-17 | 9.540465047756 2e-15 |
| **type VI secretion protein** | 33.4081400050578 | 3.70068958088037 | 0.443527156095733 | 8.34377225840394 | 7.195750540131 64e-17 | 9.770869800093 41e-15 |
| **cation transport regulator ChaB** | 39.5412840191036 | -3.46637868396015 | 0.416329078328197 | -8.32605471104652 | 8.358118738143 98e-17 | 1.119987910911 29e-14 |
| **pyruvate oxidase** | 278.678289127135 | -2.73410595276706 | 0.329238208027489 | -8.30433979442259 | 1.003760026823 04e-16 | 1.327570404307 26e-14 |
| **FAD-binding oxidoreductase** | 785.184572370797 | -1.25136319875499 | 0.151458095079633 | -8.26210839438496 | 1.431216448279 16e-16 | 1.868654911445 51e-14 |

| | | | | | | |
|---|---|---|---|---|---|---|
| **cadmium-translocating P-type ATPase** | 194.12384181169 | -2.71281627657525 | 0.32977962021758 3 | -8.22614894997266 | 1.93328581003965e-16 | 2.49222565689162e-14 |
| **glucose-1-phosphate thymidylyltransferase** | 29.7081351659624 | 2.32131768488134 | 0.28259939453185 | 8.2141636882372 | 2.13647983222362e-16 | 2.71973882642067e-14 |
| **transketolase** | 3131.81921918225 | -1.34112107716616 | 0.16356372126 4874 | -8.19937983065546 | 2.41630327016753e-16 | 3.03797932140 57e-14 |
| **YqaE/Pmp3 family membrane protein** | 379.702033045712 | -2.57643878532846 | 0.31598847730493 | -8.15358460904862 | 3.53292884970602e-16 | 4.38772529334221e-14 |
| **diguanylate cyclase** | 200.487778989657 | 1.18181049415241 | 0.14512751509 3824 | 8.14325590421 9 | 3.84787806615611e-16 | 4.69925293804135e-14 |
| **Cu(2+)-exporting ATPase** | 69.5968962464943 | -1.99419722921899 | 0.24491597893 8903 | -8.14237289808054 | 3.87605309107888e-16 | 4.69925293804135e-14 |
| **cell division protein DivIVA** | 33.9195164044641 | 2.33114901170263 | 0.28685781744 6629 | 8.12649636831439 | 4.41876736612773e-16 | 5.29420315960527e-14 |
| **Na+/galactose cotransporter** | 164.652665915701 | -2.35533017908352 | 0.29151424620 6826 | -8.07964005097864 | 6.49582213624184e-16 | 7.65224800457263e-14 |
| **MULTISPECIES: DUF1942 domain-containing protein** | 19.0730294393167 | -4.23236650260804 | 0.52388124912 7922 | -8.07886617368621 | 6.53717180280655e-16 | 7.65224800457263e-14 |
| **erythromycin esterase** | 27.3030362402419 | -2.37134078387822 | 0.29567447282 3943 | -8.02010657609329 | 1.05653455391558e-15 | 1.22269862466776e-13 |
| **bacterioferritin** | 111.815687062335 | -2.67146886841596 | 0.33362514025 1805 | -8.00739676392389 | 1.17162023664936e-15 | 1.34064949326 26e-13 |
| **thioredoxin domain-containing protein** | 247.829355063113 | -1.46735362385201 | 0.18374513293 3139 | -7.98580947657508 | 1.39603159749818e-15 | 1.57968730988016e-13 |
| **lytic transglycosylase** | 49.7132663948576 | 2.1643449957525 | 0.27160446606 6419 | 7.96873861132762 | 1.60302110572228e-15 | 1.79397438908525e-13 |
| **glycerol acyltransferase** | 64.3233546024883 | -2.58291503049025 | 0.32479598323 9362 | -7.95242294787478 | 1.82898588796 64e-15 | 2.02460785685324e-13 |
| **peptidase C56** | 23.0913296372288 | -4.07524900305555 | 0.51266374527 2008 | -7.94916558980255 | 1.87771926981589e-15 | 2.05620355309732e-13 |
| **DUF3618 domain-containing protein** | 51.5276738300151 | -2.22087904555968 | 0.28073207270 6989 | -7.91102713752873 | 2.55273871060159e-15 | 2.76564798178368e-13 |
| **DJ-1 family protein** | 69.3472103639108 | -2.12639401640374 | 0.26926267474 7668 | -7.89709906282567 | 2.85469482866705e-15 | 3.06023285633108e-13 |
| **prepilin-type cleavage/methylation domain-containing protein** | 265.837697813346 | 2.59132938527149 | 0.32940543380 0455 | 7.86668682229827 | 3.64156747018 82e-15 | 3.86309615795798e-13 |
| **heme-binding protein** | 36.4381698459014 | 1.79647932109137 | 0.22864789747243 | 7.85696846964442 | 3.93541866032547e-15 | 4.13178388007779e-13 |
| **cyclase/dehydrase** | 943.387735051191 | -3.38846191911665 | 0.43217133978 8812 | -7.84055213094992 | 4.48569656254524e-15 | 4.66146263193477e-13 |
| **type VI secretion protein EvpB** | 48.7566554580082 | 4.56485874483361 | 0.58779076616 6025 | 7.76612871040617 | 8.09213233778564e-15 | 8.32427027555646e-13 |
| **aminoglycoside phosphotransferase** | 111.883275416516 | -1.8868749588797 | 0.24310689503 2744 | -7.76150326228122 | 8.39285600897051e-15 | 8.54728455953557e-13 |

| | | | | | | |
|---|---|---|---|---|---|---|
| **heme transporter CcmD** | 17.8575976714713 | -4.8256477334549 | 0.6225618688069 32 | -7.7512741708752 3 | 9.0975021548527 6e-15 | 9.1731645490119 3e-13 |
| **GlsB/YeaQ/YmgE family stress response membrane protein** | 311.911524783052 | -2.6577062940364 | 0.3431290595322 76 | -7.7455004762906 3 | 9.5206096064767 1e-15 | 9.5056753168979 2e-13 |
| **aldo/keto reductase** | 2788.04754810311 | -1.4525226578007 6 | 0.1877748614621 75 | -7.7354479001618 4 | 1.0303969088523 9e-14 | 1.0187924388109 5e-12 |
| **porin** | 90.1904252056352 | 3.4956873353000 5 | 0.4536182485178 92 | 7.7062317195604 8 | 1.2958724114033 3e-14 | 1.2622323686320 1e-12 |
| **maltose alpha-D-glucosyltransferase** | 213.885188396502 | -2.4291744655996 2 | 0.3152442779865 79 | -7.7056893185006 4 | 1.3013888767317 4e-14 | 1.2622323686320 1e-12 |
| **type II/IV secretion system protein** | 66.6826035694689 | 2.1707792244795 1 | 0.2852610523101 23 | 7.6097988382919 3 | 2.7452286094182 5e-14 | 2.6374913356901 4e-12 |
| **D-beta-D-heptose 1-phosphate adenosyltransferase** | 15.7759470131202 | -3.5019997213351 | 0.4606808780706 24 | -7.6017909317222 1 | 2.9206030410189 8e-14 | 2.7797590065175e-12 |
| **zinc-dependent alcohol dehydrogenase** | 32.5901365276498 | 3.900537464418 | 0.5153046765187 32 | 7.5693810713480 1 | 3.7500659754008 7e-14 | 3.5361733234706e-12 |
| **CRTAC1 family protein** | 52.3251897456134 | 2.46779199413 | 0.3273095981246 08 | 7.5396261162818 | 4.7132079572423 5e-14 | 4.4036064070234 9e-12 |
| **thiazole biosynthesis enzyme, partial** | 386.028559367443 | -2.4727147832622 1 | 0.3291513382454 18 | -7.5123947435344 7 | 5.8055416593283 4e-14 | 5.3748760235090 8e-12 |
| **histidine decarboxylase** | 115.682652260169 | -2.2957977572579 4 | 0.3063862829222 63 | -7.4931479809115 3 | 6.7241014720881 8e-14 | 6.1692116569140 6e-12 |
| **Rho termination factor** | 13.9902608086746 | -4.1559658503637 9 | 0.5557928620869 9 | -7.4775444843934 | 7.5724139467439 9e-14 | 6.8854878244322 1e-12 |
| **short-chain dehydrogenase** | 1458.8268506436 | -1.4186317080983 6 | 0.1900506843328 13 | -7.4644914491025 2 | 8.3621944276851 2e-14 | 7.5363352258004 7e-12 |
| **bifunctional 4-hydroxy-3-methylbut-2-enyl diphosphate reductase/30S ribosomal protein S1** | 44.2891510028736 | 2.6736318171135 6 | 0.3597212774189 5 | 7.4325095148589 4 | 1.0655643454537 9e-13 | 9.5190414860538 7e-12 |
| **type IV pili twitching motility protein PilT** | 71.3954579287771 | 2.3550691129232 | 0.3175438150753 24 | 7.4165170320340 2 | 1.2024042511307e-13 | 1.0648073820447 8e-11 |
| **phage holin family protein** | 35.1021382913159 | -2.4963410152 34 | 0.3384790147512 02 | -7.3751721862843 8 | 1.6413278209250 7e-13 | 1.4409726317500 8e-11 |
| **NADH-quinone oxidoreductase subunit D** | 364.047954883411 | -2.0041278359 2295 | 0.2722858974720 25 | -7.3603805945508 4 | 1.8338660990614 1e-13 | 1.5962472096445 6e-11 |
| **cold-shock protein** | 385.799341741302 | 1.3026539938 9439 | 0.1772693028179 22 | 7.3484465340983 4 | 2.0052364423 23e-13 | 1.7306210108997 8e-11 |
| **carboxypeptidase regulatory-like domain-containing protein** | 271.001474866129 | 2.5529959311 4469 | 0.3490325267060 48 | 7.3144928790399 1 | 2.5835520747696e-13 | 2.1933122732421e-11 |

| | | | | | | |
|---|---|---|---|---|---|---|
| **heavy metal translocating P-type ATPase** | 364.617062044242 | -1.62718021560272 | 0.2224611183339726 | -7.31444770100372 | 2.584421374597791e-13 | 2.193312273242 1e-11 |
| **serine protein kinase** | 37.2677616567227 | 2.03251871742712 | 0.2779654249 67549 | 7.3121278218 88436 | 2.629447944883455e-13 | 2.213082468611116e-11 |
| **outer membrane protein assembly factor BamD** | 37.7336775163967 | 3.2576608787 3586 | 0.4459165101 3391 | 7.3055399490 7605 | 2.761555151984 5e-13 | 2.305219480968 04e-11 |
| **glutathione peroxidase** | 524.601621958188 | -1.6849092783 2732 | 0.2311804200 48984 | -7.2882871221 1141 | 3.139204143270 34e-13 | 2.599158942688822e-11 |
| **fumarylacetoacetate hydrolase** | 47.0865879880647 | 1.8430143864 8586 | 0.2530688557 0003 | 7.2826598175 7331 | 3.273018345749 09e-13 | 2.688098292992 64e-11 |
| **esterase family protein** | 23.2490393362756 | 2.5728023621246 | 0.3537087342339 | 7.2737880439 8781 | 3.495442959779 76e-13 | 2.835021287500 045e-11 |
| **MULTISPECIES: 50S ribosomal protein L13** | 22.6428594289224 | 3.2984244392 8696 | 0.4534964158 36387 | 7.2733197531 5318 | 3.507587217449 49e-13 | 2.835021287500 045e-11 |
| **MULTISPECIES: FAD-binding dehydrogenase** | 20.6355605794362 | -4.5125533144432 | 0.6208215223 18991 | -7.2686805341 2066 | 3.630157654910 67e-13 | 2.910986264378 76e-11 |
| **S-(hydroxymethyl)glutathione dehydrogenase** | 110.899475185252 | -1.7340927299 0895 | 0.2395444632 26104 | -7.2391267431 3061 | 4.515828750895555e-13 | 3.592906249931 27e-11 |
| **stress-induced protein** | 76.0655052055939 | -2.4464274574 5614 | 0.3386055200 71969 | -7.2250076045 3098 | 5.010737980291 1e-13 | 3.955763999324 39e-11 |
| **type I glutamate--ammonia ligase** | 459.980036743192 | 2.1808163383 9945 | 0.3024293750 38397 | 7.2109937671 3183 | 5.554499752483307e-13 | 4.351309652252 89e-11 |
| **6-phosphogluconolactonase** | 181.796461253003 | -1.1681427928 1531 | 0.1622052282 33376 | -7.2016346546 7724 | 5.949493107218 59e-13 | 4.604188533379939e-11 |
| **glutamine synthetase** | 327.665708809446 | 1.3486482077 3742 | 0.1872805802 99101 | 7.2012175826 4272 | 5.967722765181 46e-13 | 4.604188533379939e-11 |
| **gfo/Idh/MocA family oxidoreductase** | 791.073948470402 | 1.4445628911 0276 | 0.2009174337 30715 | 7.1898334767 6479 | 6.487039180143 24e-13 | 4.967218572223 96e-11 |
| **acyl-CoA synthetase** | 836.775663771245 | -1.3438799627 1547 | 0.1878301385 64553 | -7.1547621323 4867 | 8.381813473697 46e-13 | 6.370178240010 07e-11 |
| **MULTISPECIES: type I glyceraldehyde-3-phosphate dehydrogenase** | 245.152814381905 | -1.6763304255 5867 | 0.2344226428 30609 | -7.1508895442 7482 | 8.621734665356 47e-13 | 6.485942040631 82e-11 |
| **SELO family protein** | 172.591355076738 | -1.3622085285 7493 | 0.1905118068 93517 | -7.1502577755 5251 | 8.661509402257 73e-13 | 6.485942040631 82e-11 |
| **glutaredoxin** | 341.374528755529 | -1.8793371262 3239 | 0.2629629056 15715 | -7.1467765456 5771 | 8.883931519793 78e-13 | 6.589680751627 22e-11 |
| **cytochrome ubiquinol oxidase subunit I** | 524.800918812107 | -2.2291496084 4302 | 0.3119404354 43223 | -7.1460745551 4933 | 8.929457420704 6e-13 | 6.589680751627 22e-11 |
| **cation-transporting P-type ATPase** | 22.579173341027 | -2.7805965896 4202 | 0.3892488360 88049 | -7.1434936511 9653 | 9.098812606459 56e-13 | 6.666353063610 37e-11 |
| **type VI secretion system-associated protein** | 20.6085134672142 | 3.5494425910 6841 | 0.4982171857 72699 | 7.1242877452 4001 | 1.046202761883327e-12 | 7.610377805013 75e-11 |
| **tonB-system energizer ExbB** | 16.6189935992776 | 4.2351076668 2852 | 0.5949297542 58563 | 7.1186684419 6853 | 1.089747015121 27e-12 | 7.870910356024 85e-11 |

| | | | | | | |
|---|---|---|---|---|---|---|
| **NADPH-dependent FMN reductase** | 62.5313823888599 | -4.02580743540683 | 0.5658818717547 19 | -7.1142187731219 9 | 1.12548505217625e-12 | 8.07178857138238e-11 |
| **SDR family oxidoreductase** | 369.456826133921 | -1.00783859673344 | 0.1418181446479 58 | -7.1065560703479 8 | 1.18974336675981e-12 | 8.47296954341393e-11 |
| **replicative DNA helicase** | 44.0416850216344 | 1.97672580692288 | 0.2784223197071 03 | 7.0997390187768 3 | 1.24992697699013e-12 | 8.83976134282464e-11 |
| **urea ABC transporter substrate-binding protein** | 48.7439393347755 | 4.07887138414549 | 0.5748300908527 69 | 7.0957861271570 3 | 1.28618252821064e-12 | 9.03343646020494e-11 |
| **cytochrome c oxidase subunit 1, partial** | 140.09250237457 | -2.12178127642407 | 0.2991716522683 08 | -7.0921869112157 | 1.32009049676286e-12 | 9.20808330070749e-11 |
| **glutathione-disulfide reductase** | 342.673323808464 | -1.61637300785589 | 0.2283774884006 94 | -7.0776372013511 6 | 1.46632993824928e-12 | 1.01585742116535e-10 |
| **manganese catalase** | 92.1859517750754 | -2.013257247 6614 | 0.2848423863486 87 | -7.0679693196956 | 1.57217294437452e-12 | 1.08182495037 23e-10 |
| **beta-hydroxyacyl-ACP dehydratase** | 34.9067633589608 | 2.20612373517611 | 0.3126266382259 14 | 7.0567362643675 1 | 1.70458703229329e-12 | 1.16506807630032e-10 |
| **DUF3099 domain-containing protein** | 34.3917753570033 | -2.989731707 7319 | 0.4251652253831 8 | -7.0319290695456 1 | 2.03697356145158e-12 | 1.38296924998819e-10 |
| **KamA family radical SAM protein** | 15.5568108992838 | 3.12414247868149 | 0.4445643907425 14 | 7.0274240216665 2 | 2.10381298350516e-12 | 1.41888949827924e-10 |
| **LPS-assembly protein LptD** | 11.7675660422555 | 3.15272058877098 | 0.4494696612042 06 | 7.0143123349511 5 | 2.31082661101361e-12 | 1.54825382937912e-10 |
| **sulfate adenylyltransferase small subunit** | 29.3416987958904 | 2.29351626015834 | 0.3270905224151 64 | 7.0118701184721 6 | 2.35153456408793e-12 | 1.56523058827918e-10 |
| **DUF1552 domain-containing protein** | 137.605654380401 | 2.25677576169787 | 0.3221967999889 51 | 7.0043394651196 5 | 2.48153773845664e-12 | 1.64103768366509e-10 |
| **chemotaxis response regulator protein-glutamate methylesterase** | 18.5505787001929 | 2.9973835763611 | 0.4287487679258 07 | 6.9910021919404 8 | 2.72929496881718e-12 | 1.79323483628607e-10 |
| **sugar ABC transporter** | 44.4410647660159 | 3.72264170148897 | 0.5325878525756 43 | 6.9897232606525 7 | 2.75428988123041e-12 | 1.79805693272118e-10 |
| **ABC transporter permease** | 1092.32420384248 | 1.29787253488249 | 0.1857961446370 65 | 6.9854653734487 4 | 2.83913282245 42e-12 | 1.84163876839959e-10 |
| **NADH:ubiquinone oxidoreductase subunit L** | 1143.15261298054 | -2.14113201335967 | 0.3066586171297 07 | -6.9821354879913 | 2.90726540246192e-12 | 1.86739282886062e-10 |
| **3-hydroxyisobutyrate dehydrogenase** | 124.5581635 17044 | -2.62584889757667 | 0.3761024803583 05 | -6.9817377834761 4 | 2.91550922809151e-12 | 1.86739282886062e-10 |
| **MULTISPECIES: thiamine pyrophosphate-requiring protein** | 29.003995980645 | -3.29997744186781 | 0.4737499981901 72 | -6.9656516189434 1 | 3.26887154847613e-12 | 2.08063674060506e-10 |
| **DUF4230 domain-containing protein** | 13.3930395584318 | -4.23495499117051 | 0.6086991613478 65 | -6.9573859470956 | 3.46644373234559e-12 | 2.19268714100668e-10 |
| **bifunctional acetaldehyde-CoA/alcohol dehydrogenase** | 29.021590148619 | 5.38641681423858 | 0.7755899415854 92 | 6.9449286606624 2 | 3.78651621546156e-12 | 2.38036303322596e-10 |
| **DUF2090 domain-containing protein** | 33.6453943138683 | 2.47221787418027 | 0.3561058813412 02 | 6.9423674354075 7 | 3.85582726371235e-12 | 2.40906410145071e-10 |

| | | | | | | |
|---|---|---|---|---|---|---|
| **50S ribosomal protein L28** | 73.8145404761173 | 2.03593247819182 | 0.293591598601543 | 6.9345733593519 6 | 4.07448929943677e-12 | 2.53015847716244e-10 |
| **glycogen debranching protein** | 105.293143305366 | -1.15772575349972 | 0.167061481693863 | -6.9299382584265 | 4.21024331782953e-12 | 2.59861320901672e-10 |

**Table A4**. A list of compounds with the retention time, matching factor and mass-to-charge ratio used for metabolome analysis in Chapter Four and Five.

| | **Compound** | **Retention time (min)** | **Match factor (%)** | **Mass to charge ratio (m/z)** |
|---|---|---|---|---|
| **1** | [1060] pyruvic acid [6.714] | 6.617 | 94.176 | 174 |
| **2** | [107689] L-(+) lactic acid [6.851] | 6.767 | 97.130 | 219, 117, 191, |
| **3** | [757] glycolic acid [7.049] | 7.003 | 92.830 | 177, 205, 161 |
| **4** | [5950] L-alanine 1 [7.495] | 7.412 | 96.585 | 116, 190, 218 |
| **5** | Hydroxylamine, 3TMS derivative | 7.662 | 95.866 | 133 |
| **6** | [971] oxalic acid [7.883] | 7.822 | 79.511 | 147, 175, 190 |
| **7** | [6287] L-valine 2 [9.151] | 9.182 | 98.123 | 144, 218, 246 |
| **8** | [5951] L-serine 1 [9.706] | 9.862 | 98.061 | 132, 116, 234 |
| **9** | [1004] phosphoric acid [9.966] | 10.063 | 77.546 | 299 |
| **10** | [6106] L-leucine 2 [9.945] | 10.081 | 95.077 | 158, 232, 102 |
| **11** | [753] glycerol [9.941] | 10.087 | 97.955 | 218, 205, 147 |
| **12** | [791] DL-isoleucine 2 [10.225] | 10.431 | 91.628 | 158, 130, 117 |
| **13** | [145742] L-proline 2 [10.321] | 10.548 | 95.485 | 142, 244, 216 |
| **14** | 10.622 256 contaminant | 10.622 | | 256 |
| **15** | [750] glycine [10.456] | 10.671 | 98.284 | 174, 248, 133 |
| **16** | [1110] succinic acid [10.509] | 10.772 | 97.785 | 247, 116, 172 |
| **17** | [5951] L-serine 2 [11.174] | 11.476 | 98.674 | 204 |
| **18** | [6288] L-threonine 2 [11.464] | 11.881 | 98.300 | 218, 117, 203 |
| **19** | [6137] L-methionine 1 [11.835] | 12.388 | 96.237 | 104, |
| **20** | [5960] aspartic acid 1 [12.002] | 12.527 | 94.699 | 160 |
| **21** | [239] Beta- alanine 1 [12.044] | 12.593 | 92.473 | 174 |
| **22** | Threose 2 [12.371]=erythreose | 12.915 | 89.103 | 205 |
| **23** | [970] oxalacetic acid [12.45] | 13.099 | 84.338 | 290 |
| **24** | [92824] D-malic acid [12.794] | 13.470 | 96.535 | 147, 233, 335 |
| **25** | Erythritol, 4TMS derivative | 13.759 | 96.744 | 189 |
| **26** | [169019] D-threitol [12.954] | 13.759 | 96.767 | 217 |
| **27** | [338] salicylic acid [13.075] | 13.869 | 91.247 | 267 |
| **28** | [5960] aspartic acid 2 [13.207] | 13.964 | 93.584 | 232 |
| **29** | [6137] L-methionine 2 [13.188] | 13.988 | 66.184 | 176, 128, 293 |
| **30** | [33032] L-glutamic acid 3 (dehydrated) [13.232] | 14.033 | 85.441 | 348, 230, 128 |
| **31** | [7405] L-pyroglutamic acid [13.218] | 14.039 | 90.677 | 156, 258, 230 |

| | | | | |
|---|---|---|---|---|
| **32** | [5810] trans-4-hydroxy-L-proline 2 [13.267] | 14.068 | 74.740 | 230 |
| **33** | 4-Aminobutanoic acid, 3TMS derivative | 14.157 | 94.433 | 174, 304, 246 |
| **34** | [33032] L-glutamic acid 1 [13.338] | 14.176 | 87.226 | 174 |
| **35** | [994] Phenylalanine 1 [13.545] | 14.491 | 76.645 | 192, 266, 204 |
| **36** | [444539] cinnamic acid [13.562] | 14.512 | 83.323 | 205, 220, 161 |
| **37** | [51] alpha ketoglutaric acid [13.859] | 14.782 | 92.995 | 198, 147, 156 |
| **38** | L-Asparagine, 2TMS derivative | 15.154 | 74.182 | 231 |
| **39** | [6262] L-ornithine 1 [14.349] | 15.373 | 78.180 | 142 |
| **40** | [33032] L-glutamic acid 2 [14.398] | 15.435 | 98.710 | 246 |
| **41** | L-Phenylalanine, 2TMS derivative | 15.581 | 98.650 | 218 |
| **42** | [439240] D-lyxose 1 [14.762] | 15.795 | 91.315 | 307 |
| **43** | [65550] D-lyxose 2 [14.869] | 15.899 | 96.843 | 307 |
| **44** | D-Arabinose, tetrakis(trimethylsilyl) ether, ethyloxime (isomer 2) | 15.997 | 92.425 | 103, 217, 307 |
| **45** | [236] L-asparagine 2 [14.984] | 16.136 | 96.497 | 231 |
| **46** | [993] ribose [15.113] | 16.205 | 97.950 | 217, 160,103, 189 |
| **47** | [6912] xylitol [15.376] | 16.621 | 97.701 | 205 |
| **48** | D-(+)-Arabitol, 5TMS derivative | 16.799 | 92.280 | 217, 103, 422 |
| **49** | [827] ribitol [15.66] | 16.875 | 98.138 | 217, 205, 319 |
| **50** | [9750] citrulline 1 [15.82] | 17.195 | 76.980 | 184 |
| **51** | [3469] gentisic acid [16.123] | 17.586 | 97.189 | 355, 179, 281 |
| **52** | [311] citric acid [16.615] | 18.127 | 97.737 | 273 |
| **53** | [9750] citrulline 2 [16.691] | 18.232 | 92.633 | 157 |
| **54** | [138] 5-aminovaleric acid 2 [14.955] | 18.631 | 79.024 | 174 |
| **55** | [24749] D-glucose 1 [17.426] | 18.980 | 92.585 | 319, 205, 160 |
| **56** | [206] D (+) galactose 1 [17.409] | 19.046 | 97.176 | 319, 364, 160 |
| **57** | [6057] tyrosine 1 [17.354] | 19.076 | 95.883 | 280, 354;100 |
| **58** | [24749] D-glucose 2 [17.629] | 19.122 | 96.292 | 160 |
| **59** | [18950] D-mannose 2 [17.435] | 19.379 | 89.291 | 319, 160, 205, 244 |
| **60** | [6274] L-histidine 3 [17.658] | 19.451 | 60.796 | 254, 154, 356 |
| **61** | [5962] L-lysine 2 [17.643] | 19.478 | 95.236 | 174, 230 |
| **62** | 3-Indoleacetic acid, TMS derivative | 19.539 | 78.733 | 130, 247, 232 |
| **63** | [6251] D-mannitol [17.81] | 19.554 | 98.289 | 217, 307, 157 |
| **64** | [5780] D-sorbitol [17.898] | 19.633 | 94.461 | 319, 437, 451 |
| **65** | Galactitol, 6TMS derivative | 19.696 | 94.466 | 307 |

| | | | | |
|---|---|---|---|---|
| **66** | [6057] tyrosine 2 [17.871] | 19.697 | 97.899 | 280 |
| **67** | [637542] 4-hydroxycinnamic acid [17.854] | 19.754 | 97.649 | 219, 293, 308 |
| **68** | [5785] L-ascorbic acid [17.939] | 19.764 | 86.887 | 332 |
| **69** | [370] gallic acid [18.012] | 19.879 | 97.183 | 281 |
| **70** | Myo-Inositol, 6TMS derivative | 21.489 | 96.562 | 217, 305, 191 |
| **71** | [445858] ferulic acid [19.312] | 21.555 | 93.233 | 338, 117, 218 |
| **72** | L-Tryptophan, TMS derivative | 22.463 | 90.413 | 130, 206, 260 |
| **73** | L-Tryptophan, N(1)-(trimethylsilyl)-, trimethylsilyl ester | 22.838 | 92.966 | 202 |
| **74** | [67678] L-cystine 1 [20.526] | 23.060 | 70.382 | 218, 155, 100 |
| **75** | [67678] L-cystine 2 [20.862] | 23.452 | 86.002 | 218, 411 |
| **76** | [67678] L-cystine 3 [21.104] | 23.750 | 98.209 | 218, 266 |
| **77** | Methyl 12-hydroxystearate, TMS derivative | 24.084 | 91.183 | 187 |
| **78** | [5988] Sucrose [23.988] | 27.132 | 95.970 | 361, 217, 437 |
| **79** | [10712] cellobiose 1 [24.444] | 27.728 | 91.118 | 204, 361, 169 |
| **80** | [10712] cellobiose 2 [24.7] | 28.013 | 82.412 | 204, 480, 319 |
| **81** | [6255] maltose 1 [24.702] | 28.083 | 93.321 | 207, 190, 217 |
| **82** | [7427] D-(+) trehalose [24.752] | 28.127 | 83.412 | 361, 191, 217 |
| **83** | [6255] maltose 2 [24.915] | 28.326 | 82.933 | 361 |
| **84** | [16217663] maltitol [25.37] | 28.965 | 94.454 | 361 |
| **85** | [439242] Raffinose [29.282] | 32.115 | 69.107 | 437, 451, 361 |

**Table A5**. Significant compounds using ANOVA (p-value ≤ 0.05) in the rhizosphere soil of *Myrothamnus flabellifolia* using GC-MS. Most significant metabolites were generated from three conditions namely, partially dry (PD), desiccated (D) and fully rehydrated (FR), therefore these three conditions were used for pathway analysis. These metabolites were used for pathway analysis using KEGG database for model plant *Arabidopsis thaliana*, yeast (*Saccharomyces cerevisiae*) and bacteria (*Escherichia coli*) as described in Chapter Four. Pathway analyses were conducted in MetaboAnalyst platform.

| **Partially Dehydrated** | | | | |
|---|---|---|---|---|
| **Query** | **Match** | **HMDB** | **PubChem** | **KEGG** |
| **Threitol** | D-Threitol | HMDB0004136 | 222285 | C16884 |
| **Glycolic acid** | Glycolic acid | HMDB0000115 | 757 | C03547 |
| **Indole acetic acid** | Indoleacetic acid | HMDB0000197 | 802 | C00954 |
| **Cellobiose** | Cellobiose | HMDB0000055 | 10712 | C06422 |
| **Arabinose** | L-Arabinose | HMDB0000646 | 439195 | C02479 |
| **Erythritol** | Erythritol | HMDB0002994 | 222285 | C00503 |
| **Alpha-ketoglutaric acid** | Oxoglutaric acid | HMDB0000208 | 51 | C00026 |
| **Mannose** | D-Mannose | HMDB0000169 | 18950 | C00936 |
| **Pyruvic acid** | Pyruvic acid | HMDB0000243 | 1060 | C00022 |
| **Desiccated** | | | | |
| **Query** | **Match** | **HMDB** | **PubChem** | **KEGG** |
| **Proline** | L-Proline | HMDB0000162 | 145742 | C00148 |
| **Histidine** | L-Histidine | HMDB0000177 | 6274 | C00135 |
| **Glycolic acid** | Glycolic acid | HMDB0000115 | 757 | C03547 |
| **Oxalic acid** | Oxalic acid | HMDB0002329 | 971 | C00209 |
| **Salicylic acid** | Salicylic acid | HMDB0001895 | 338 | C00805 |
| **Tyrosine** | L-Tyrosine | HMDB0000158 | 6057 | C00082 |
| **Mannitol** | Mannitol | HMDB0000765 | 6251 | C00392 |
| **Glucose** | D-Glucose | HMDB0000122 | 5793 | C00221 |
| **Trehalose** | Trehalose | HMDB0000975 | 7427 | C01083 |
| **Galactose** | D-Galactose | HMDB0000143 | 439357 | C00984 |
| **Ribose** | D-Ribose | HMDB0000283 | 5779 | C00121 |
| **Phenylalanine** | L-Phenylalanine | HMDB0000159 | 6140 | C00079 |
| **Malic acid** | Malic acid | HMDB0000744 | 525 | C03668 |
| **Fully Rehydrated** | | | | |
| **Query** | **Match** | **HMDB** | **PubChem** | **KEGG** |
| **Cystine** | L-Cystine | HMDB0000192 | 67678 | C00491 |
| **Glutamic acid** | L-Glutamic acid | HMDB0000148 | 33032 | C00025 |
| **Myo-inositol** | myo-Inositol | HMDB0000211 | NA | C00137 |
| **Oxaloacetic acid** | Oxalacetic acid | HMDB0000223 | 970 | C00036 |

| | | | | |
|---|---|---|---|---|
| **Tryptophan** | L-Tryptophan | HMDB0000929 | 6305 | C00078 |
| **4-Aminobutanoic acid** | Gamma-Aminobutyric acid | HMDB0000112 | 223130 | C00334 |
| **Leucine** | L-Leucine | HMDB0000687 | 6106 | C00123 |
| **Sucrose** | Sucrose | HMDB0000258 | 5988 | C00089 |
| **Trans-4-hydroxy-proline** | 4-Hydroxyproline | HMDB0000725 | 5810 | C01157 |

**Table A6**. Upregulated KEGG pathways in yeast (*Saccharomyces cerevisiae*) under desiccated conditions using significant metabolites identified in Table A5 (Chapter Four).

| | **Total** | **Expected** | **Hits** | **Raw p** | **-log10(p)** | **Holm adjust** | **FDR** | **Impact** |
|---|---|---|---|---|---|---|---|---|
| **Aminoacyl-tRNA biosynthesis** | 46 | 0.52154 | 4 | 0.0010832 | 2.9653 | 0.079074 | 0.079074 | 0 |
| **Phenylalanine, tyrosine and tryptophan biosynthesis** | 21 | 0.2381 | 2 | 0.021668 | 1.6642 | 1 | 0.54896 | 0.02144 |
| **Ubiquinone and other terpenoid-quinone biosynthesis** | 2 | 0.022676 | 1 | 0.02256 | 1.6467 | 1 | 0.54896 | 0 |
| **Phenylalanine metabolism** | 7 | 0.079365 | 1 | 0.076969 | 1.1137 | 1 | 1 | 0 |
| **Fructose and mannose metabolism** | 14 | 0.15873 | 1 | 0.14857 | 0.82808 | 1 | 1 | 0 |
| **Tyrosine metabolism** | 15 | 0.17007 | 1 | 0.15837 | 0.80032 | 1 | 1 | 0 |
| **Starch and sucrose metabolism** | 15 | 0.17007 | 1 | 0.15837 | 0.80032 | 1 | 1 | 0.01732 |
| **Galactose metabolism** | 17 | 0.19274 | 1 | 0.17769 | 0.75034 | 1 | 1 | 0.15385 |
| **Pentose phosphate pathway** | 18 | 0.20408 | 1 | 0.18719 | 0.72771 | 1 | 1 | 0 |
| **Histidine metabolism** | 18 | 0.20408 | 1 | 0.18719 | 0.72771 | 1 | 1 | 0 |
| **Amino sugar and nucleotide sugar metabolism** | 24 | 0.27211 | 1 | 0.24219 | 0.61585 | 1 | 1 | 0 |
| **Glycolysis / Gluconeogenesis** | 24 | 0.27211 | 1 | 0.24219 | 0.61585 | 1 | 1 | 4E-04 |
| **Arginine and proline metabolism** | 25 | 0.28345 | 1 | 0.25102 | 0.60029 | 1 | 1 | 0 |
| **Glyoxylate and dicarboxylate metabolism** | 26 | 0.29478 | 1 | 0.25976 | 0.58543 | 1 | 1 | 0 |

**Table A7**. Upregulated KEGG pathways in yeast (*Saccharomyces cerevisiae*) under partially dehydrated conditions using significant metabolites identified in Table A5 (Chapter Four).

| | Total | Expected | Hits | Raw p | -log10(p) | Holm adjust | FDR | Impact |
|---|---|---|---|---|---|---|---|---|
| **Citrate cycle (TCA cycle)** | 20 | 0.068027 | 2 | 0.0014471 | 2.8395 | 0.10564 | 0.064118 | 0.1049 |
| **Alanine, aspartate and glutamate metabolism** | 22 | 0.07483 | 2 | 0.0017567 | 2.7553 | 0.12648 | 0.064118 | 0.07194 |
| **C5-Branched dibasic acid metabolism** | 4 | 0.013605 | 1 | 0.013559 | 1.8678 | 0.9627 | 0.32994 | 0 |
| **Taurine and hypotaurine metabolism** | 7 | 0.02381 | 1 | 0.023648 | 1.6262 | 1 | 0.43157 | 0 |
| **Butanoate metabolism** | 14 | 0.047619 | 1 | 0.04692 | 1.3286 | 1 | 0.52772 | 0 |
| **Lysine biosynthesis** | 16 | 0.054422 | 1 | 0.0535 | 1.2716 | 1 | 0.52772 | 0 |
| **Arginine biosynthesis** | 18 | 0.061224 | 1 | 0.06005 | 1.2215 | 1 | 0.52772 | 0 |
| **Pantothenate and CoA biosynthesis** | 20 | 0.068027 | 1 | 0.06657 | 1.1767 | 1 | 0.52772 | 0 |
| **Valine, leucine and isoleucine biosynthesis** | 20 | 0.068027 | 1 | 0.06657 | 1.1767 | 1 | 0.52772 | 0.11374 |
| **Pyruvate metabolism** | 23 | 0.078231 | 1 | 0.076293 | 1.1175 | 1 | 0.52772 | 0.20372 |
| **Glycolysis / Gluconeogenesis** | 24 | 0.081633 | 1 | 0.079519 | 1.0995 | 1 | 0.52772 | 0.09968 |
| **Tryptophan metabolism** | 30 | 0.10204 | 1 | 0.098718 | 1.0056 | 1 | 0.58994 | 0.00775 |
| **Glycine, serine and threonine metabolism** | 32 | 0.10884 | 1 | 0.10506 | 0.97857 | 1 | 0.58994 | 0.0202 |
| **Cysteine and methionine metabolism** | 41 | 0.13946 | 1 | 0.13322 | 0.87544 | 1 | 0.69463 | 0 |

**Table A8**. Upregulated KEGG pathways in yeast (*Saccharomyces cerevisiae*) under fully rehydrated conditions using significant metabolites identified in Table A5 (Chapter Four).

| | Total | Expected | Hits | Raw p | -log10(p) | Holm adjust | FDR | Impact |
|---|---|---|---|---|---|---|---|---|
| **Alanine, aspartate and glutamate metabolism** | 22 | 0.22449 | 3 | 0.0010291 | 2.9875 | 0.075124 | 0.055232 | 0.49641 |
| **Arginine and proline metabolism** | 25 | 0.2551 | 3 | 0.0015132 | 2.8201 | 0.10895 | 0.055232 | 0.1118 |
| **Butanoate metabolism** | 14 | 0.14286 | 2 | 0.0079103 | 2.1018 | 0.56163 | 0.16333 | 0.4 |
| **Aminoacyl-tRNA biosynthesis** | 46 | 0.46939 | 3 | 0.0089493 | 2.0482 | 0.62645 | 0.16333 | 0 |
| **Glyoxylate and dicarboxylate metabolism** | 26 | 0.26531 | 2 | 0.0265 | 1.5768 | 1 | 0.36908 | 0.03313 |
| **Carbapenem biosynthesis** | 3 | 0.030612 | 1 | 0.030335 | 1.5181 | 1 | 0.36908 | 0 |
| **Nitrogen metabolism** | 5 | 0.05102 | 1 | 0.050101 | 1.3002 | 1 | 0.52248 | 0 |
| **Taurine and hypotaurine metabolism** | 7 | 0.071429 | 1 | 0.069508 | 1.158 | 1 | 0.63426 | 0 |
| **Starch and sucrose metabolism** | 15 | 0.15306 | 1 | 0.14366 | 0.84266 | 1 | 0.82398 | 0.05669 |
| **Galactose metabolism** | 17 | 0.17347 | 1 | 0.16136 | 0.79221 | 1 | 0.82398 | 0.02564 |
| **Valine, leucine and isoleucine degradation** | 18 | 0.18367 | 1 | 0.17008 | 0.76934 | 1 | 0.82398 | 0 |
| **Arginine biosynthesis** | 18 | 0.18367 | 1 | 0.17008 | 0.76934 | 1 | 0.82398 | 0.08 |
| **Valine, leucine and isoleucine biosynthesis** | 20 | 0.20408 | 1 | 0.18729 | 0.72748 | 1 | 0.82398 | 0 |
| **Citrate cycle (TCA cycle)** | 20 | 0.20408 | 1 | 0.18729 | 0.72748 | 1 | 0.82398 | 0.11782 |
| **Phenylalanine, tyrosine and tryptophan biosynthesis** | 21 | 0.21429 | 1 | 0.19578 | 0.70824 | 1 | 0.82398 | 0 |

| | | | | | | | | |
|---|---|---|---|---|---|---|---|---|
| **Inositol phosphate metabolism** | 22 | 0.22449 | 1 | 0.20418 | 0.68998 | 1 | 0.82398 | 0.11609 |
| **Porphyrin and chlorophyll metabolism** | 23 | 0.23469 | 1 | 0.21251 | 0.67261 | 1 | 0.82398 | 0 |
| **Pyruvate metabolism** | 23 | 0.23469 | 1 | 0.21251 | 0.67261 | 1 | 0.82398 | 0.00954 |
| **Glycolysis / Gluconeogenesis** | 24 | 0.2449 | 1 | 0.22076 | 0.65607 | 1 | 0.82398 | 0 |
| **Glutathione metabolism** | 26 | 0.26531 | 1 | 0.23703 | 0.62519 | 1 | 0.82398 | 0.02912 |
| **Phosphatidylinositol signaling system** | 26 | 0.26531 | 1 | 0.23703 | 0.62519 | 1 | 0.82398 | 0.04493 |
| **Tryptophan metabolism** | 30 | 0.30612 | 1 | 0.26867 | 0.57077 | 1 | 0.89151 | 0.07752 |
| **Glycine, serine and threonine metabolism** | 32 | 0.32653 | 1 | 0.28405 | 0.5466 | 1 | 0.90156 | 0 |
| **Cysteine and methionine metabolism** | 41 | 0.41837 | 1 | 0.34976 | 0.45624 | 1 | 1 | 0 |

**Table A9**. Upregulated KEGG pathways in bacteria (*Escherichia coli*) under partially dehydrated conditions using significant metabolites identified in Table A5 (Chapter Four).

| | Total | Expected | Hits | Raw p | -log10(p) | Holm adjust | FDR | Impact |
|---|---|---|---|---|---|---|---|---|
| **Citrate cycle (TCA cycle)** | 19 | 0.053371 | 2 | 0.00089078 | 3.0502 | 0.078389 | 0.052846 | 0.0914 |
| **Alanine, aspartate and glutamate metabolism** | 22 | 0.061798 | 2 | 0.0012011 | 2.9204 | 0.10449 | 0.052846 | 0.10448 |
| **Dioxin degradation** | 5 | 0.014045 | 1 | 0.013992 | 1.8541 | 1 | 0.27845 | 0 |
| **Taurine and hypotaurine metabolism** | 8 | 0.022472 | 1 | 0.022325 | 1.6512 | 1 | 0.27845 | 0 |
| **Pentose and glucuronate interconversions** | 9 | 0.025281 | 1 | 0.025092 | 1.6005 | 1 | 0.27845 | 0 |
| **C5-Branched dibasic acid metabolism** | 9 | 0.025281 | 1 | 0.025092 | 1.6005 | 1 | 0.27845 | 0.2 |
| **Ascorbate and aldarate metabolism** | 11 | 0.030899 | 1 | 0.03061 | 1.5141 | 1 | 0.27845 | 0 |
| **Monobactam biosynthesis** | 12 | 0.033708 | 1 | 0.033361 | 1.4768 | 1 | 0.27845 | 0 |
| **Xylene degradation** | 13 | 0.036517 | 1 | 0.036108 | 1.4424 | 1 | 0.27845 | 0 |
| **Terpenoid backbone biosynthesis** | 17 | 0.047753 | 1 | 0.04704 | 1.3275 | 1 | 0.27845 | 0 |
| **Arginine biosynthesis** | 18 | 0.050562 | 1 | 0.04976 | 1.3031 | 1 | 0.27845 | 0 |
| **Lysine degradation** | 19 | 0.053371 | 1 | 0.052475 | 1.28 | 1 | 0.27845 | 0.07447 |
| **Pantothenate and CoA biosynthesis** | 20 | 0.05618 | 1 | 0.055185 | 1.2582 | 1 | 0.27845 | 0 |
| **Phenylalanine metabolism** | 21 | 0.058989 | 1 | 0.05789 | 1.2374 | 1 | 0.27845 | 0 |
| **Tryptophan metabolism** | 22 | 0.061798 | 1 | 0.060589 | 1.2176 | 1 | 0.27845 | 0.08571 |
| **Valine, leucine and isoleucine biosynthesis** | 22 | 0.061798 | 1 | 0.060589 | 1.2176 | 1 | 0.27845 | 0.10727 |
| **Butanoate metabolism** | 23 | 0.064607 | 1 | 0.063283 | 1.1987 | 1 | 0.27845 | 0 |
| **Thiamine metabolism** | 23 | 0.064607 | 1 | 0.063283 | 1.1987 | 1 | 0.27845 | 0 |
| **Glycolysis / Gluconeogenesis** | 23 | 0.064607 | 1 | 0.063283 | 1.1987 | 1 | 0.27845 | 0.10009 |
| **Pyruvate metabolism** | 23 | 0.064607 | 1 | 0.063283 | 1.1987 | 1 | 0.27845 | 0.19301 |
| **Tyrosine metabolism** | 25 | 0.070225 | 1 | 0.068657 | 1.1633 | 1 | 0.2877 | 0 |
| **Glyoxylate and dicarboxylate metabolism** | 28 | 0.078652 | 1 | 0.076678 | 1.1153 | 1 | 0.29338 | 0 |
| **Methane metabolism** | 28 | 0.078652 | 1 | 0.076678 | 1.1153 | 1 | 0.29338 | 0 |
| **Pentose phosphate pathway** | 30 | 0.08427 | 1 | 0.081999 | 1.0862 | 1 | 0.30066 | 0 |
| **Benzoate degradation** | 32 | 0.089888 | 1 | 0.087301 | 1.059 | 1 | 0.3073 | 0.01197 |
| **Glycine, serine and threonine metabolism** | 39 | 0.10955 | 1 | 0.10569 | 0.97595 | 1 | 0.35773 | 0 |

| | | | | | | | | |
|---|---|---|---|---|---|---|---|---|
| **Cysteine and methionine metabolism** | 41 | 0.11517 | 1 | 0.1109 | 0.95505 | 1 | 0.36146 | 0.01739 |

**Table A10.** Upregulated KEGG pathways in bacteria (*Escherichia coli*) under desiccated conditions using significant metabolites identified in Table A5 (Chapter Four).

| | **Total** | **Expected** | **Hits** | **Raw p** | **-log10(p)** | **Holm adjust** | **FDR** | **Impact** |
|---|---|---|---|---|---|---|---|---|
| **Aminoacyl-tRNA biosynthesis** | 45 | 0.37745 | 4 | 0.00029254 | 3.5338 | 0.025159 | 0.025159 | 0 |
| **Phenylalanine, tyrosine and tryptophan biosynthesis** | 23 | 0.19292 | 2 | 0.014447 | 1.8402 | 1 | 0.62122 | 0.00046 |
| **Novobiocin biosynthesis** | 3 | 0.025163 | 1 | 0.024976 | 1.6025 | 1 | 0.71597 | 0 |
| **Tyrosine metabolism** | 10 | 0.083877 | 1 | 0.081109 | 1.0909 | 1 | 1 | 0 |
| **Histidine metabolism** | 12 | 0.10065 | 1 | 0.09661 | 1.015 | 1 | 1 | 0 |
| **Starch and sucrose metabolism** | 22 | 0.18453 | 1 | 0.17068 | 0.76781 | 1 | 1 | 0 |
| **Thiamine metabolism** | 23 | 0.19292 | 1 | 0.17779 | 0.7501 | 1 | 1 | 0 |
| **Pentose phosphate pathway** | 26 | 0.21808 | 1 | 0.19877 | 0.70166 | 1 | 1 | 0 |
| **Arginine and proline metabolism** | 29 | 0.24324 | 1 | 0.21927 | 0.65902 | 1 | 1 | 0 |
| **Glycolysis / Gluconeogenesis** | 29 | 0.24324 | 1 | 0.21927 | 0.65902 | 1 | 1 | 0.00121 |
| **Fructose and mannose metabolism** | 33 | 0.27679 | 1 | 0.24588 | 0.60927 | 1 | 1 | 0 |
| **Phenylalanine metabolism** | 33 | 0.27679 | 1 | 0.24588 | 0.60927 | 1 | 1 | 0.001 |
| **Galactose metabolism** | 39 | 0.32712 | 1 | 0.28429 | 0.54623 | 1 | 1 | 0.09767 |
| **Amino sugar and nucleotide sugar metabolism** | 44 | 0.36906 | 1 | 0.31496 | 0.50174 | 1 | 1 | 0 |

**Table A11**. Upregulated KEGG pathways in bacteria (*Escherichia coli*) under fully rehydrated conditions using significant metabolites identified in Table A5 (Chapter Four).

| | Total | Expected | Hits | Raw p | -log10(p) | Holm adjust | FDR | Impact |
|---|---|---|---|---|---|---|---|---|
| **Alanine, aspartate and glutamate metabolism** | 22 | 0.18453 | 3 | 0.00058136 | 3.2356 | 0.049997 | 0.049997 | 0.49999 |
| **Arginine and proline metabolism** | 29 | 0.24324 | 3 | 0.0013389 | 2.8733 | 0.11381 | 0.057573 | 0.08488 |
| **Aminoacyl-tRNA biosynthesis** | 45 | 0.37745 | 3 | 0.0048554 | 2.3138 | 0.40785 | 0.13919 | 0 |
| **Butanoate metabolism** | 17 | 0.14259 | 2 | 0.0079726 | 2.0984 | 0.66173 | 0.17141 | 0.06349 |
| **Carbapenem biosynthesis** | 3 | 0.025163 | 1 | 0.024976 | 1.6025 | 1 | 0.42958 | 0 |
| **Glyoxylate and dicarboxylate metabolism** | 37 | 0.31034 | 2 | 0.035767 | 1.4465 | 1 | 0.48463 | 0.11022 |
| **Galactose metabolism** | 39 | 0.32712 | 2 | 0.039447 | 1.404 | 1 | 0.48463 | 0.02886 |
| **D-Glutamine and D-glutamate metabolism** | 7 | 0.058714 | 1 | 0.057414 | 1.241 | 1 | 0.6172 | 0.17241 |
| **Inositol phosphate metabolism** | 8 | 0.067102 | 1 | 0.065372 | 1.1846 | 1 | 0.62466 | 1 |
| **Streptomycin biosynthesis** | 9 | 0.075489 | 1 | 0.07327 | 1.1351 | 1 | 0.63012 | 0 |
| **Tryptophan metabolism** | 10 | 0.083877 | 1 | 0.081109 | 1.0909 | 1 | 0.63412 | 0 |
| **Nitrogen metabolism** | 11 | 0.092265 | 1 | 0.088889 | 1.0512 | 1 | 0.63704 | 0 |
| **beta-Alanine metabolism** | 13 | 0.10904 | 1 | 0.10427 | 0.98183 | 1 | 0.68981 | 0 |
| **Arginine biosynthesis** | 16 | 0.1342 | 1 | 0.12692 | 0.89648 | 1 | 0.76448 | 0.10219 |
| **Citrate cycle (TCA cycle)** | 20 | 0.16775 | 1 | 0.15632 | 0.806 | 1 | 0.76448 | 0.08522 |

| | | | | | | | | |
|---|---|---|---|---|---|---|---|---|
| **Valine, leucine and isoleucine biosynthesis** | 22 | 0.18453 | 1 | 0.17068 | 0.76781 | 1 | 0.76448 | 0 |
| **Glutathione metabolism** | 22 | 0.18453 | 1 | 0.17068 | 0.76781 | 1 | 0.76448 | 0.01381 |
| **Starch and sucrose metabolism** | 22 | 0.18453 | 1 | 0.17068 | 0.76781 | 1 | 0.76448 | 0.03022 |
| **Valine, leucine and isoleucine degradation** | 23 | 0.19292 | 1 | 0.17779 | 0.7501 | 1 | 0.76448 | 0 |
| **Phenylalanine, tyrosine and tryptophan biosynthesis** | 23 | 0.19292 | 1 | 0.17779 | 0.7501 | 1 | 0.76448 | 0 |
| **Pyruvate metabolism** | 26 | 0.21808 | 1 | 0.19877 | 0.70166 | 1 | 0.777 | 0.00256 |
| **Methane metabolism** | 26 | 0.21808 | 1 | 0.19877 | 0.70166 | 1 | 0.777 | 0.04762 |
| **Glycolysis / Gluconeogenesis** | 29 | 0.24324 | 1 | 0.21927 | 0.65902 | 1 | 0.81988 | 0 |
| **Glycine, serine and threonine metabolism** | 33 | 0.27679 | 1 | 0.24588 | 0.60927 | 1 | 0.88109 | 0 |
| **Porphyrin and chlorophyll metabolism** | 36 | 0.30196 | 1 | 0.26531 | 0.57624 | 1 | 0.91267 | 0 |
| **Cysteine and methionine metabolism** | 40 | 0.33551 | 1 | 0.29052 | 0.53682 | 1 | 0.96096 | 0 |

**Table A12**. Upregulated KEGG pathways in plant (*Arabidopsis thaliana*) under partially dehydrated conditions using significant metabolites identified in Table A5 (Chapter Four).

| | Total | Expected | Hits | Raw p | -log10(p) | Holm adjust | FDR | Impact |
|---|---|---|---|---|---|---|---|---|
| **Butanoate metabolism** | 17 | 0.045853 | 2 | 0.00073257 | 3.1352 | 0.070326 | 0.039637 | 0 |
| **Citrate cycle (TCA cycle)** | 20 | 0.053945 | 2 | 0.0010207 | 2.9911 | 0.096963 | 0.039637 | 0.06066 |
| **Alanine, aspartate and glutamate metabolism** | 22 | 0.059339 | 2 | 0.0012387 | 2.907 | 0.11643 | 0.039637 | 0.07194 |
| **C5-Branched dibasic acid metabolism** | 6 | 0.016183 | 1 | 0.016102 | 1.7931 | 1 | 0.38644 | 0 |
| **Monobactam biosynthesis** | 8 | 0.021578 | 1 | 0.021425 | 1.6691 | 1 | 0.41137 | 0 |
| **Tyrosine metabolism** | 16 | 0.043156 | 1 | 0.042505 | 1.3716 | 1 | 0.47143 | 0 |
| **Arginine biosynthesis** | 18 | 0.04855 | 1 | 0.047721 | 1.3213 | 1 | 0.47143 | 0 |
| **Carbon fixation in photosynthetic organisms** | 21 | 0.056642 | 1 | 0.055505 | 1.2557 | 1 | 0.47143 | 0.03607 |
| **Thiamine metabolism** | 22 | 0.059339 | 1 | 0.058089 | 1.2359 | 1 | 0.47143 | 0 |
| **Valine, leucine and isoleucine biosynthesis** | 22 | 0.059339 | 1 | 0.058089 | 1.2359 | 1 | 0.47143 | 0.10727 |
| **Pyruvate metabolism** | 22 | 0.059339 | 1 | 0.058089 | 1.2359 | 1 | 0.47143 | 0.16731 |
| **Pantothenate and CoA biosynthesis** | 23 | 0.062036 | 1 | 0.060668 | 1.217 | 1 | 0.47143 | 0 |
| **Glycolysis / Gluconeogenesis** | 26 | 0.070128 | 1 | 0.068373 | 1.1651 | 1 | 0.47143 | 0.12036 |
| **Tryptophan metabolism** | 28 | 0.075523 | 1 | 0.073483 | 1.1338 | 1 | 0.47143 | 0.2037 |
| **Glyoxylate and dicarboxylate metabolism** | 29 | 0.07822 | 1 | 0.07603 | 1.119 | 1 | 0.47143 | 0.04419 |
| **Terpenoid backbone biosynthesis** | 30 | 0.080917 | 1 | 0.078572 | 1.1047 | 1 | 0.47143 | 0 |
| **Glycine, serine and threonine metabolism** | 33 | 0.089009 | 1 | 0.086166 | 1.0647 | 1 | 0.48658 | 0 |
| **Fatty acid degradation** | 37 | 0.099798 | 1 | 0.096218 | 1.0167 | 1 | 0.51316 | 0 |
| **Cysteine and methionine metabolism** | 46 | 0.12407 | 1 | 0.11853 | 0.92616 | 1 | 0.5989 | 0.01139 |

**Table A13**. Upregulated KEGG pathways in plant (*Arabidopsis thaliana*) under desiccated condition using significant metabolites identified in Table A5 (Chapter Four).

| | Total | Expected | Hits | Raw p | -log10(p) | Holm adjust | FDR | Impact |
|---|---|---|---|---|---|---|---|---|
| **Butanoate metabolism** | 17 | 0.045853 | 2 | 0.00073257 | 3.1352 | 0.070326 | 0.039637 | 0 |
| **Citrate cycle (TCA cycle)** | 20 | 0.053945 | 2 | 0.0010207 | 2.9911 | 0.096963 | 0.039637 | 0.06066 |
| **Alanine, aspartate and glutamate metabolism** | 22 | 0.059339 | 2 | 0.0012387 | 2.907 | 0.11643 | 0.039637 | 0.07194 |
| **C5-Branched dibasic acid metabolism** | 6 | 0.016183 | 1 | 0.016102 | 1.7931 | 1 | 0.38644 | 0 |
| **Monobactam biosynthesis** | 8 | 0.021578 | 1 | 0.021425 | 1.6691 | 1 | 0.41137 | 0 |
| **Tyrosine metabolism** | 16 | 0.043156 | 1 | 0.042505 | 1.3716 | 1 | 0.47143 | 0 |
| **Arginine biosynthesis** | 18 | 0.04855 | 1 | 0.047721 | 1.3213 | 1 | 0.47143 | 0 |
| **Carbon fixation in photosynthetic organisms** | 21 | 0.056642 | 1 | 0.055505 | 1.2557 | 1 | 0.47143 | 0.03607 |
| **Thiamine metabolism** | 22 | 0.059339 | 1 | 0.058089 | 1.2359 | 1 | 0.47143 | 0 |
| **Valine, leucine and isoleucine biosynthesis** | 22 | 0.059339 | 1 | 0.058089 | 1.2359 | 1 | 0.47143 | 0.10727 |
| **Pyruvate metabolism** | 22 | 0.059339 | 1 | 0.058089 | 1.2359 | 1 | 0.47143 | 0.16731 |
| **Pantothenate and CoA biosynthesis** | 23 | 0.062036 | 1 | 0.060668 | 1.217 | 1 | 0.47143 | 0 |
| **Glycolysis / Gluconeogenesis** | 26 | 0.070128 | 1 | 0.068373 | 1.1651 | 1 | 0.47143 | 0.12036 |
| **Tryptophan metabolism** | 28 | 0.075523 | 1 | 0.073483 | 1.1338 | 1 | 0.47143 | 0.2037 |
| **Glyoxylate and dicarboxylate metabolism** | 29 | 0.07822 | 1 | 0.07603 | 1.119 | 1 | 0.47143 | 0.04419 |
| **Terpenoid backbone biosynthesis** | 30 | 0.080917 | 1 | 0.078572 | 1.1047 | 1 | 0.47143 | 0 |
| **Glycine, serine and threonine metabolism** | 33 | 0.089009 | 1 | 0.086166 | 1.0647 | 1 | 0.48658 | 0 |
| **Fatty acid degradation** | 37 | 0.099798 | 1 | 0.096218 | 1.0167 | 1 | 0.51316 | 0 |
| **Cysteine and methionine metabolism** | 46 | 0.12407 | 1 | 0.11853 | 0.92616 | 1 | 0.5989 | 0.01139 |

**Table A14**. Upregulated KEGG pathways in plant (*Arabidopsis thaliana*) under fully rehydrated conditions using significant metabolites identified in Table A5 (Chapter Four).

| | Total | Expected | Hits | Raw p | -log10(p) | Holm adjust | FDR | Impact |
|---|---|---|---|---|---|---|---|---|
| **Alanine, aspartate and glutamate metabolism** | 22 | 0.13351 | 3 | 0.00022501 | 3.6478 | 0.021601 | 0.021601 | 0.49641 |
| **Arginine and proline metabolism** | 34 | 0.20634 | 3 | 0.0008427 | 3.0743 | 0.080057 | 0.04045 | 0.12413 |
| **Aminoacyl-tRNA biosynthesis** | 46 | 0.27916 | 3 | 0.0020601 | 2.6861 | 0.19365 | 0.065923 | 0 |
| **Butanoate metabolism** | 17 | 0.10317 | 2 | 0.0042492 | 2.3717 | 0.39518 | 0.10198 | 0.13636 |
| **Galactose metabolism** | 27 | 0.16386 | 2 | 0.010625 | 1.9737 | 0.97753 | 0.1954 | 0.04252 |
| **Glyoxylate and dicarboxylate metabolism** | 29 | 0.17599 | 2 | 0.012213 | 1.9132 | 1 | 0.1954 | 0.07557 |
| **Indole alkaloid biosynthesis** | 4 | 0.024275 | 1 | 0.024079 | 1.6184 | 1 | 0.33023 | 0 |
| **Glucosinolate biosynthesis** | 65 | 0.39447 | 2 | 0.055821 | 1.2532 | 1 | 0.66985 | 0 |
| **Nitrogen metabolism** | 12 | 0.072825 | 1 | 0.070697 | 1.1506 | 1 | 0.68962 | 0 |
| **Ascorbate and aldarate metabolism** | 18 | 0.10924 | 1 | 0.10435 | 0.98151 | 1 | 0.68962 | 0 |
| **Arginine biosynthesis** | 18 | 0.10924 | 1 | 0.10435 | 0.98151 | 1 | 0.68962 | 0.08544 |
| **Citrate cycle (TCA cycle)** | 20 | 0.12138 | 1 | 0.11532 | 0.93808 | 1 | 0.68962 | 0.08327 |
| **Carbon fixation in photosynthetic organisms** | 21 | 0.12744 | 1 | 0.12077 | 0.91805 | 1 | 0.68962 | 0.06468 |
| **Valine, leucine and isoleucine biosynthesis** | 22 | 0.13351 | 1 | 0.12618 | 0.89901 | 1 | 0.68962 | 0 |
| **Phenylalanine, tyrosine and tryptophan biosynthesis** | 22 | 0.13351 | 1 | 0.12618 | 0.89901 | 1 | 0.68962 | 0 |
| **Pyruvate metabolism** | 22 | 0.13351 | 1 | 0.12618 | 0.89901 | 1 | 0.68962 | 0.00962 |
| **Starch and sucrose metabolism** | 22 | 0.13351 | 1 | 0.12618 | 0.89901 | 1 | 0.68962 | 0.0889 |
| **Glycolysis / Gluconeogenesis** | 26 | 0.15779 | 1 | 0.14753 | 0.83111 | 1 | 0.68962 | 0 |
| **Phosphatidylinositol signaling system** | 26 | 0.15779 | 1 | 0.14753 | 0.83111 | 1 | 0.68962 | 0.03285 |
| **Glutathione metabolism** | 26 | 0.15779 | 1 | 0.14753 | 0.83111 | 1 | 0.68962 | 0.05046 |
| **Inositol phosphate metabolism** | 28 | 0.16993 | 1 | 0.15804 | 0.80124 | 1 | 0.68962 | 0.10251 |
| **Tryptophan metabolism** | 28 | 0.16993 | 1 | 0.15804 | 0.80124 | 1 | 0.68962 | 0.12037 |
| **Glycine, serine and threonine metabolism** | 33 | 0.20027 | 1 | 0.18379 | 0.73567 | 1 | 0.76713 | 0 |

| | | | | | | | | |
|---|---|---|---|---|---|---|---|---|
| **Valine, leucine and isoleucine degradation** | 37 | 0.22454 | 1 | 0.20389 | 0.69061 | 1 | 0.81556 | 0 |
| **Cysteine and methionine metabolism** | 46 | 0.27916 | 1 | 0.24751 | 0.60641 | 1 | 0.94858 | 0 |
| **Porphyrin and chlorophyll metabolism** | 48 | 0.2913 | 1 | 0.25691 | 0.59022 | 1 | 0.94858 | 0 |